

PROGRAM & ABSTRACTS

SYMPOSIUM ON

Nonbiological transport and transformation of pollutants on land and water:

Processes and critical data required for predictive description

May 11-13, 1976

National Bureau of Standards
Gaithersburg, Maryland



SPONSORS:

U.S. Environmental Protection Agency
National Bureau of Standards, U.S.
Department of Commerce
National Science Foundation
U.S. Energy Research and Development Administration

“Science is built up with facts as a house is with stones.
But a collection of facts is no more a science than a
heap of stones is a house.”

Jules Henri Poincare
La Science et l'Hypothese, 1908

program

Tuesday, May 11, 1976

POLLUTANT TRANSFORMATION PROCESSES IN LAND AND WATER: SESSION I

Morning

Chairman: Lewis H. Gevantman, NBS

- 9:30 Welcoming Address: E. Ambler, Acting Director, NBS
- 9:35 Opening Remarks: C. Gerber, Associate Assistant Administrator
for R & D, EPA
- 9:45 Environmental Physics and Chemistry of Aquatic Pollutants
J. C. Morris, Harvard University
- For those aquatic pollutants that are not readily oxidized or degraded biologically the ultimate fates are determined by their physical and chemical properties in the aqueous medium. Some physical properties of significance are volatility, aqueous solubility, and adsorptive tendency, for these determine the likelihood that a pollutant will translocate into the air or the sediments. The chemical transformations by which organic pollutants are removed are generally either hydrolytic or oxidative, so that the susceptibilities of pollutants to hydrolysis or oxidation are chemical properties of major interest. Oxidation, in particular, may be either direct reaction with O_2 , catalyzed oxidation, photooxidation or photosensitized oxidation.
- Little is known about the relative importance of the individual physical and chemical properties in regulating the fate of specific aquatic pollutants under environmental conditions. Although there have been some observations of environmental persistence or changes from which mechanisms of transformation may be partially inferred, data are seldom quantitative or sufficiently detailed to predict the ultimate sinks of biologically perdurent materials. Field observations that can be correlated with laboratory data now being accumulated are badly needed.
- 10:30 Coffee Break

Tuesday, May 11, 1976, Morning, continued

11:00 Prediction of Activities of Electrolytes in Natural Waters

Robert Wood, University of Delaware

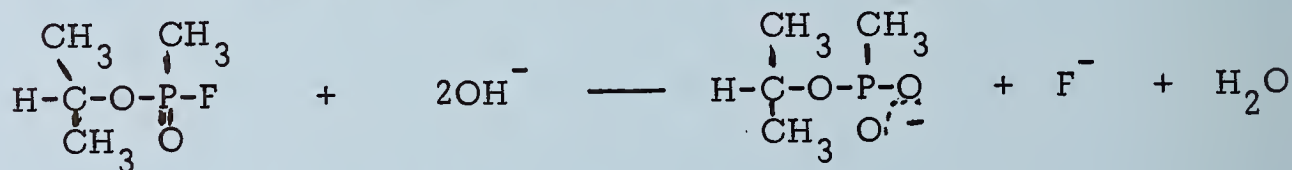
The development of various methods for predicting the properties of mixed electrolytes is reviewed, starting with the ionic strength principle and the mean salt methods of MacInnes, Harned, Lewis and Randall. In the last few years, equations have been developed which allow accurate predictions of the properties of mixtures of strong electrolytes. The accuracy of these equations in predicting the properties of seawater is demonstrated. The possibility of extending these calculations is discussed, together with the limitations of the method.

Possible ways of adjusting the newer equations for mixtures in which there is strong association is discussed. To refine and test these developments in the theory, it will be necessary to develop methods for making accurate measurements of all of the components of natural waters.

11:45 Reaction Rates of Electron Pair Donor Molecules with Pollutants in Water

John O. Edwards, Brown University

Many pollutants (including phosphorus insecticides and sulfur dioxide) react with electron pair donors (also termed nucleophiles, and in most instances these are reductants) to form new compounds less harmful to living systems and to the environment. For example, the anticholinesterases are converted to different chemical compounds which are not poisonous



although there remains an oxygen demand in the organo-phosphorus product. A general introduction into the chemistry of donors' interactions with substrates will be presented along with some aspects of reaction mechanism. The relative rates of donor

Tuesday, May 11, 1976, Morning, continued

reactions with several varieties of organic compounds, tetrahedral phosphorus species, compounds with cyano-groups, and metal complexes will be presented. Correlations of donor reactivity with basicity, electrode potential, polarizability, bonding nature, and the "alpha-effect" will be discussed on an empirical basis. Some generalizations that may be used for prediction of rates with new systems are now possible. The importance and value of hydrogen peroxide for treatment of polluted water will be detailed.

12:30 Lunch

Tuesday, May 11, 1976

POLLUTANT TRANSFORMATION PROCESSES IN LAND AND WATER: SESSION I

Afternoon

Chairman: Gunter Zweig, EPA

2:00 Complexation, Precipitation, and Adsorption of Trace Metals
 in Water

*J. J. Morgan** and Jasenka Vuceta, California Institute of
Technology*

Metals introduced to natural waters are removed by precipitation, adsorption, and incorporation into biotic matter. Distributions of various metals between particulate and aqueous phases depend upon: pH, chemical and physical properties of different adsorbing surfaces, nature and abundance of complexing ligands in the solution phase, competition between metals for available ligands and surface sites, ionic strength, p_e of the redox environment, and temperature. Predictive models must simultaneously consider all significant acid-base, solubility, complexation, redox, and adsorption processes. Adsorption models are briefly reviewed with respect to their treatment of chemical and electrostatic influences on metal ion distributions. Two models, the adsorption-hydrolysis, ion-solvent (AHIS) interaction model and the surface complex formation (SCF) model are considered in detail and applied to the description of complex natural water systems. The dominant role of pH in each of the models is illustrated; the influence of other solution composition variables on the distribution coefficient is examined. Three equilibrium multi-metal, multi-ligand system models are presented in which either AHIS or SCF descriptions of adsorption are employed. These systems models illustrate quantitatively the influences of pH, surface area, organic ligands, and precipitation processes on trace-metal distributions in water.

2:45 Oxidation and Reduction of Pesticides in Soils and Sediments

Jack R. Plimmer, U. S. Department of Agriculture

Several mechanisms may be involved in the transformation of pesticides in soils and aquatic systems. Of these, transformation by microorganisms is predominant, but many purely chemical reactions may accompany biological pathways. The distinction between

** *Speaker*

Tuesday, May 11, 1976, Afternoon, continued

chemical and biological transformations in soils presents many experimental problems. Reactive intermediates may be generated in metabolic processes or arise by the action of free radicals in soil. Some chemical systems may be used as models to provide useful insights into the nature of the processes involved.

Reactions occurring in sediments depend on the availability of oxygen. Anaerobic processes will be favored as oxygen is depleted in sediments rich in organic nutrients. Measurement of redox potential may be a useful guide to potential reaction pathways.

3:30 Coffee Break

3:45 Kinetics of Hydrolysis and Oxidation of Organic Pollutants in the Aquatic Environment

*W. R. Mabey** and T. Mill, Stanford Research Institute*

Oxidation and free radical oxidation can be important degradation pathways for some organic pollutants in aquatic environments. Knowledge of the theoretical and experimental features of these reactions can be meaningfully applied to prediction of degradation rates and to design of experiments that are relevant to environmental conditions.

Three general hydrolysis mechanisms can be described. Depending on the compound, the hydrolysis kinetics may be acid and/or base catalyzed as well as being pH independent in a neutral reaction with water. The observed rate of hydrolysis may be due to any one or a combination of these mechanisms and will be determined by the pH and the temperature of the aquatic environment.

Oxidation of an organic molecule almost never involves a direct reaction with oxygen but usually involves an excited state or intermediate reactive radicals. One of the most common and best understood oxidation processes involves peroxy ($RO_2\cdot$) and alkoxy ($RO\cdot$) radical chains wherein three distinct types of radical processes are initiation, propagation, and termination. The kinetics of these processes can be quite complex and may include photochemical and various catalysis processes. While there is a vast body of data to evaluate these reactions, almost no detailed information is available on chemical oxidation reactions as they occur in aquatic environments.

** *Speaker*

Tuesday, May 11, 1976, Afternoon, continued

4:30 Chemical Degradation of Organic Pollutants in Soil

V. H. Freed, Oregon State University

A number of reaction paths for organic pollutants in soil is theoretically possible. They may be categorized in the two major groups, namely biologically (including extra-cellular enzyme) mediated reactions, and "chemical" reactions. The focus of this presentation is on chemical or non-biological reactions exclusive of the oxidation-reduction reactions. These include such things as hydrolysis, complexation, and physical interactions. Much of the work on degradation of organic pollutants in soil has focused on pesticides. Since these compounds represent a number of classes of organic chemicals, they serve quite adequately as models for many of the organic pollutants. For many compounds, e.g. esters, amides, halogen substituted open-chain compounds, and others subject to nucleophilic attack, hydrolysis is much more rapid in soil than in aqueous solution. This has been attributed to catalytic influences of clay and organic matter, alkaline and alkaline earth ionic species, and overall pH. Other reactions leading to chemical degradation include complexation with some of the transition elements or sorption at specific loci on clay surfaces.

Because of the complexity of the soil system, precise mechanistic interpretation of rate data is often difficult. One must distinguish between biologically mediated reactions and the purely chemical ones. There are a few instances where this has been done, primarily with the organophosphates. Many compounds appear to follow a pseudo first-order kinetics, at least during some stages of degradation. In some compounds it has been found that a hyperbolic rate law more accurately describes the kinetics. However, rate studies have dealt with relatively low concentrations of the pollutant (in the order of 1 to 10 ppm) but in the few instances studied at higher concentration (100 to 1000 ppm) rate behaviors have been different.

5:30 Bus departs for Holiday Inn

Wednesday, May 12, 1976

POLLUTANT TRANSFORMATION PROCESSES IN LAND AND WATER: SESSION II

Morning

Chairman: Richard Zepp, EPA

9:30 The Photochemistry of Xenobiotics

Donald G. Crosby, University of California, Davis

For centuries, chemists have observed the effects of light on chemicals in the laboratory. However, it is only recently that investigation has extended to the sunlight-mediated transformations of foreign compounds--xenobiotics--under environmental conditions. Several characteristic reaction types now are recognized including oxidation, reduction, photonucleophilic displacements, elimination, and isomerization. In addition to the chemical properties of the xenobiotic, the chemical nature of the surrounding micro-environment is an important determinant of its environmental fate. pH and photosensitizers in aquatic environments, interaction with air- and water-borne particles, and atmospheric composition all exert significant influence under laboratory conditions, but more emphasis on field investigations is needed.

10:30 Coffee Break

11:00 Solar Spectral Irradiance Reaching the Ground

Alex E. S. Green, University of Florida

Some of the basic elements of atmospheric radiative transfer which enter into the understanding of components of the solar spectral irradiance reaching the ground will be discussed. The simplest component, the directly transmitted component in most spectral regions can be calculated rather easily in terms of the incident solar flux, the total vertical thickness of each attenuating constituent and the zenith angle of the sun. The diffuse component of sunlight (skylight) which becomes very substantial at short wavelengths is difficult to calculate, and few groups are equipped to treat this component realistically. In a recent series of studies we have attempted to

Wednesday, May 12, 1976, Morning, continued

simplify the various theoretical approaches for ultraviolet radiation and cast their results into forms convenient for scientists concerned with biological consequences of this radiation. The influence of clouds greatly complicates matters and for the purposes of prediction or systematization requires data which are not currently recorded. However, we present approximate formulas based upon analyses and upon data which allow on the average for cloud effects. Our paper concentrates on light transmission and scattering problems in the ultraviolet and particularly the results of spectral irradiance values folded into a response curve of a biological system. The dose rate, daily dose, and annual dose reaching the ground varies with time of day and with the seasons in a fashion which may be represented by analytic functions of latitude, solar declination, and the parameters which characterize the atmospheric model.

11:45 Transmission of Sunlight in Natural Water Bodies

John E. Tyler, Scripps Institution of Oceanography

The basic concepts of radiometry are defined and illustrated and their application to the ocean for the purpose of determining the radiant energy available at various depths is illustrated. The use of radiant energy measurements for describing ocean types is discussed and the application of radiant energy data to the determination of the quantum efficiency of in-situ photosynthesis is discussed.

12:30 Lunch

Wednesday, May 12, 1976

POLLUTANT TRANSFORMATION PROCESSES IN LAND AND WATER: Session II

Afternoon

Chairman: Richard Carrigan, NSF

2:00 Photosensitized Oxidation in Solution

Christopher Foote, University of California, Los Angeles

Photosensitized oxidations proceed by a variety of mechanisms. In the Type I mechanism, there is a sensitizer-substrate interaction to give radicals which react further; in the Type II reaction there is energy transfer from sensitizer to oxygen to give singlet oxygen which reacts with many substrates. Methods of distinguishing these reactions and their complexities are discussed.

2:45 Photolysis of Pesticides on Soil Surfaces

Richard Hautala, University of Georgia

We have examined the photochemical decomposition of Sevin, Parathion, and 2,4-D on three different types of soil surfaces. The effects of anionic and cationic surfactant additives on the "rates" of photodecomposition have been studied. The moisture content of the soils was found to be a critical variable. Crude estimates of the quantum efficiency for photodecomposition indicate that photochemistry on soil surfaces is less efficient than the corresponding photochemistry in aqueous solution for all cases, but the variables described above exert strikingly different effects for each of the pesticides.

3:30 Coffee Break

4:00 The Environmental Photodegradation of Selected Organometallic Complexes

Haines B. Lockhart, Jr., Eastman Kodak

Synthetic chelating agents, such as EDTA, are used in our society. These chelating agents reach the aqueous environment via the discharge of wastes. Due to the concentrations of common metal ions in natural waters and the formation constants for the complexes formed between chelating agents and these metal ions, any study of the environmental fate of chelating agents must be, in fact, a study of these complexes.

Wednesday, May 12, 1976, Afternoon, continued

In our studies, we have investigated the rate of photodegradation of buffered aqueous solutions of various X(N)-carboxyl-¹⁴C-EDTA chelates in the presence of oxygen and simulated sunlight. In addition, photodegradation products of the most photosensitive common metal ion-EDTA chelate, Fe(III)-EDTA, have been identified and their generation studied over the pH range of natural waters.

The environmental implications of chelate photodegradation based on both our results and results recently published by others will be discussed.

4:45 Predictive Modeling of the Behavior of Pollutants in the Aquatic Environment

*R. R. Lassiter***, *G. L. Baughman*, *J. L. Malunchuk*, *EPA*

A prototype model was constructed to classify the behavior and fate of substances with respect to specified environmental conditions, and to evaluate factors and processes important in their behavior and fate. Such models can be called evaluative models. The substance chosen for the prototype was the element mercury.

Forms of mercury represented are mercuric, elemental, and methyl mercury. These forms are assumed to exist in both water and sediment. The water is assumed to be moving over stationary sediments. Factors represented which potentially affect the fate of mercury are flow, water, and sediment depths, suspended particulates, and hydrogen ion concentration. Sorption and volatilization were found to be important processes affecting the fate of mercury as portrayed by the model. The need for measurement of parameters such as the partition coefficient for mercury forms bound to sediments is stressed.

5:30 Reception

6:30 Buffet Dinner

8:00 Bus departs for Holiday Inn

** *Speaker*

Thursday, May 13, 1976

POLLUTANT TRANSPORT PROCESSES IN LAND AND WATER

Morning

Chairman: David R. Lide, Jr., NBS

9:30 Hydrologic Transport Processes for Pollutants in Water
and on Sediments

*Norman H. Crawford** and George Bailey, Hydrocomp, Inc.*

Hydrologic transport processes are described in both surface and groundwater. The variability of hydrologic transport from point to point in a field, and in different climatic zones is described. The development of computer based models for hydrologic transport is discussed, and the current and expected future applications of these models are outlined. The data requirements for analysis of hydrologic transport are discussed.

10:30 Coffee Break

11:00 Vertical Movement and Distribution of Organics in Soils

J. M. Davidson, University of Florida, Gainesville

The mobility and distribution of organic solutes in soils are dependent upon the physical and chemical characteristics of the soil, microbial degradation rate, and interactions between the solute and soil matrix. Chromatography theory has been used to describe solute movement and concentration distributions in soils. The adsorption-desorption of an organic solute in a soil-water system has been shown to follow a Freundlich equation. The velocity at which an adsorbed solute moves through a soil is independent of solute concentration for linear adsorption isotherms ($N = 1$) and concentration dependent for nonlinear adsorption isotherms ($1.0 < N < 1.0$). Adsorbed solutes have greater velocities at high solute concentrations ($C > 1.0 \mu\text{g}/\text{cm}^3$) when N is less than 1.0. The concentration distribution of an adsorption isotherm is nonlinear ($N < 1.0$). The microbial degradation rate and solute velocity determine the depth to which an adsorbed solute front or pulse will move.

** *Speaker*

Thursday, May 13, 1976, Morning, continued

11:45 Adsorption and Transport of Pollutants on Suspended Particles

*B. T. Hargrave and K. Kranck***, *Bedford Institute of Oceanography*

Many pollutants entering water, particularly those of low solubility, become associated with natural suspended material. Particle size and concentration determine the surface area available for adsorption and flocculation into units determined by inorganic grain size. Prediction of transport and dispersal of many aquatic pollutants is thus equivalent to prediction of the dynamics of fine-grained suspended material.

12:30 Lunch

** *Speaker*

Thursday, May 13, 1976

POLLUTANT TRANSPORT PROCESSES IN LAND AND WATER

Afternoon

Chairman: Ralph Franklin, ERDA

2:00 Environmental Transport Modeling of Pollutants in Water and Soil

*M. R. Patterson***, *C. L. Begovich*, *D. R. Jackson*, *Oak Ridge National Laboratory*

A suite of models is discussed which can be applied to calculation of first order effects in transport of several types of pollutants in water and soil. The materials considered include solids in the form of particulates and soluble forms of the heavy metals. The time scale that is currently being emphasized is discussed, along with the physical size of the area covered by these calculations. The role of the hydrologic cycle is introduced along with the importance of bulk flow and particulate transport as suspended sediment. The build-up of lead, cadmium, zinc, and copper in the soil near a lead smelter over a six-year period is presented.

2:45 Prediction of Solubilization of Hydrophobic Organic Compounds in Water

Albert J. Leo, *Pomona College*

The mechanisms by which organic chemicals are dispersed into the environment as pollutants need a great deal of further study. In all environmental subsystems - land, atmosphere, inland waterways, or oceans - water appears to be a major carrier so a pollutant's water solubility and the manner in which it partitions between water and some lipid phase are important parameters to consider when constructing model systems and establishing quantitative relationships.

The partition coefficient P may have greater significance in these studies than water solubility per se. For organic liquids, the solution process can be considered as one of "self-partitioning."

Thursday, May 13, 1976, Afternoon, continued

Normally, most organic solids do not become pollutants until they become dissolved; once this has occurred, they are rarely removed from solution by recrystallization but their availability and mobility may be altered by adsorption to a surface or by solution in an immiscible phase. These latter occurrences can often be modeled by use of the compound's partition coefficient between octanol/water.

The theoretical basis for the partitioning process is discussed and methods by which the $\log P_{(oct)}$ can be predicted from molecular structures are given.

3:30 Coffee Break

4:00 Prediction of Volatilization Rate of Pollutants in Aqueous Systems

*Donald Mackay** and Yoram Cohen, University of Toronto*

In predicting the rate of volatilization of pollutants from aqueous environments the Whitman two film resistance approach is used, yielding a mass flux equation in which the three major parameters are the Henry's Law constant and the gas and liquid phase mass transfer coefficients. These three parameters are discussed in terms of the availability of data representation of environmental conditions, methods of obtaining such data experimentally or theoretically with emphasis on areas of inadequacy. Finally, some complications introduced by surface organic microlayers and the presence of interfering dissolved or particulate materials are outlined. It is concluded that the major areas of uncertainty are the value of the liquid phase mass transfer coefficient and the effects of other dissolved materials in modifying the Henry's Law constant of an evaporating pollutant.

4:45 Patterns of Deposition of Radionuclides in Sediments

*David N. Edgington**, Argonne National Laboratory, and John A. Robbins, The University of Michigan*

Concentration profiles of ^{137}Cs , ^{210}Pb , and $^{239,240}\text{Pu}$ have been measured in sediment cores taken mainly from the southern end of Lake Michigan. Their measurement provides an accurate method for determining the rate of accumulation of sediments. The results indicate that the rate of accumulation of sediments in the lake

Thursday, May 13, 1976, Afternoon, continued

is highly variable. They also indicate that there is a general redistribution of radioactivity in surface sediments from areas where there has been no significant deposition during the last 7000 years to areas where there is considerable sedimentation. Mechanisms such as these will be important in terms of understanding the effects and long-term fate of radionuclides (and other heavy metals) discharged into the lake. The differences in the shapes of the various profiles can be explained in terms of a constant (^{210}Pb) or a variable (^{137}Cs , $^{239,240}\text{Pu}$) flux to the air-water interface with time, sedimentation rate, homogenous mixing due to physical or biological processes, and massive erosion or deposition due to storm activity.

EXTENDED ABSTRACTS

AUTHOR INDEX

CRAWFORD, Norman H. and George Bailey

CROSBY, Donald G.

DAVIDSON, James M.

EDGINGTON, David N. and John A. Robbins

EDWARDS, John O.

FOOTE, Christopher S.

FREED, Virgil H.

GREEN, Alex E. S.

HARGRAVE, B. T. and K. Kranck

HAUTALA, Richard R.

LASSITER, R. R., G. L. Baughman, J. L. Malanchuk

LEO, Albert J.

LOCKHART, Haines B., Jr.

MABEY, W. R. and T. Mill

MACKAY, Donald and Yoram Cohen

MORGAN, J. J. and Jasenka Vuceta

MORRIS, J. Carrell

PATTERSON, M. R., C. L. Begovich, D. R. Jackson

PLIMMER, Jack R.

TYLER, John E.

WOOD, Robert H.

HYDROLOGIC TRANSPORT PROCESSES FOR POLLUTANTS IN WATER AND ON SEDIMENTS

Dr. Norman H. Crawford
Hydrocomp Inc.
1502 Page Mill Road, Palo Alto, California 94304

Dr. George Bailey
Environmental Research Laboratory
EPA, Athens, Georgia 30601

A pollutant is any compound or substance that is undesirable where it is found. Transport processes often create a pollutant simply by moving a compound to a different environment. Nutrients are needed in the root zone in agricultural lands but are pollutants if they are moved into rivers or ground water aquifers.

Hydrologic transport is the movement of compounds in or by water. It may take place along any surface or subsurface path in the hydrologic cycle (Figure 1). The transport processes that are of interest in environmental studies of non-point pollution are:

- (i) the movement of compounds in solution in runoff over the land surface, and the percolation of compounds in solution to ground water aquifers
- (ii) the adsorption of compounds on soil particles, followed by the erosion and movement of the soil as sediment
- (iii) the erosion of particles of compounds.

These processes are represented in the ARM Model¹ (Figure 2), developed for the Environmental Protection Agency to study the movement of pesticides and nutrients in agricultural lands.

Non-point pollution is very closely related to the hydrologic transport processes. Transport processes in nature are extraordinarily variable in time and space. Figure 3 shows the occurrence of overland flow in time for a watershed near Watkinsville, Georgia, in 1973. If overland flow carries sediment to a stream channel how does it move through the channel system? The transport of particles by streamflow is highly selective, and deposition and scour of particles takes place. Figure 4 shows the delivery of sediment particles to a channel system and the transport past a downstream gage. As point sources of pollution are more carefully regulated, diffuse or non-point pollution has become more important in meeting national water quality goals.

To develop public policies for the control of non-point pollution, a method must be available to predict the results of alternate policies. Its accuracy must be sufficient to correctly identify the best policies. Non-point pollution originates on the land surface, and policies to control land surface activities have important economic consequences.

How can alternate public policies be evaluated? How can changes in the hydrologic transport processes be predicted for alternate land uses or land surface activities? The possibilities are:

- (i) field experiments on watersheds where policies are tested and the results are measured
- (ii) computer based experiments with mathematical models of watersheds, on which policies can be tested and results obtained.

Field experiments are without question the best method to investigate a policy alternative for a given watershed. They give straight forward results that are understood by non-specialists. The use of chemical fertilizers is increased when farmers are supplied with samples for small plots in their own fields. Mathematical models must mimic complex transport processes and deal with esoteric topics like parameter estimation, calibration and verification.

The disadvantages of field experiments are the cost and the time needed to produce results. To investigate policies for one non-point pollutant at one location might require five years and 100,000 dollars. Sampling all climates and soils for the major pollutants would require thousands of watersheds throughout the United States and many years of experimentation.

Mathematical models can generate in minutes all of the data that could be measured in a five year field experiment. A model can, if suitable parameters are estimated, generate results for ungaged watersheds. The advantages of mathematical models are not obtained without cost, and models can easily be misused. A summary of requirements for successful model development and application is:

- (i) the physical processes that control watershed response must be identified, and represented in the model by algorithms
- (ii) the model must operate from input data that exists, or from data that can be obtained with reasonable effort
- (iii) the model must calibrate to reproduce historic watershed response, and must be verified by forecasting or predicting other periods of watershed response
- (iv) data series for hydrologic transport processes that are generated by models should be continuous over sufficient time periods to allow statistical analysis for means and extremes.

Success in modeling is relative. If the expected accuracy of model output can be established, and if this accuracy is sufficient to select a correct public policy alternative, then the model is a success. Establishing the expected accuracy of model output requires care, and strict attention to algorithm design, input data, calibration, and verification.

¹Modeling Pesticides and Nutrients on Agricultural Lands, Research Grant R 803116-01-0, Office of Research and Development, Environmental Protection Agency.

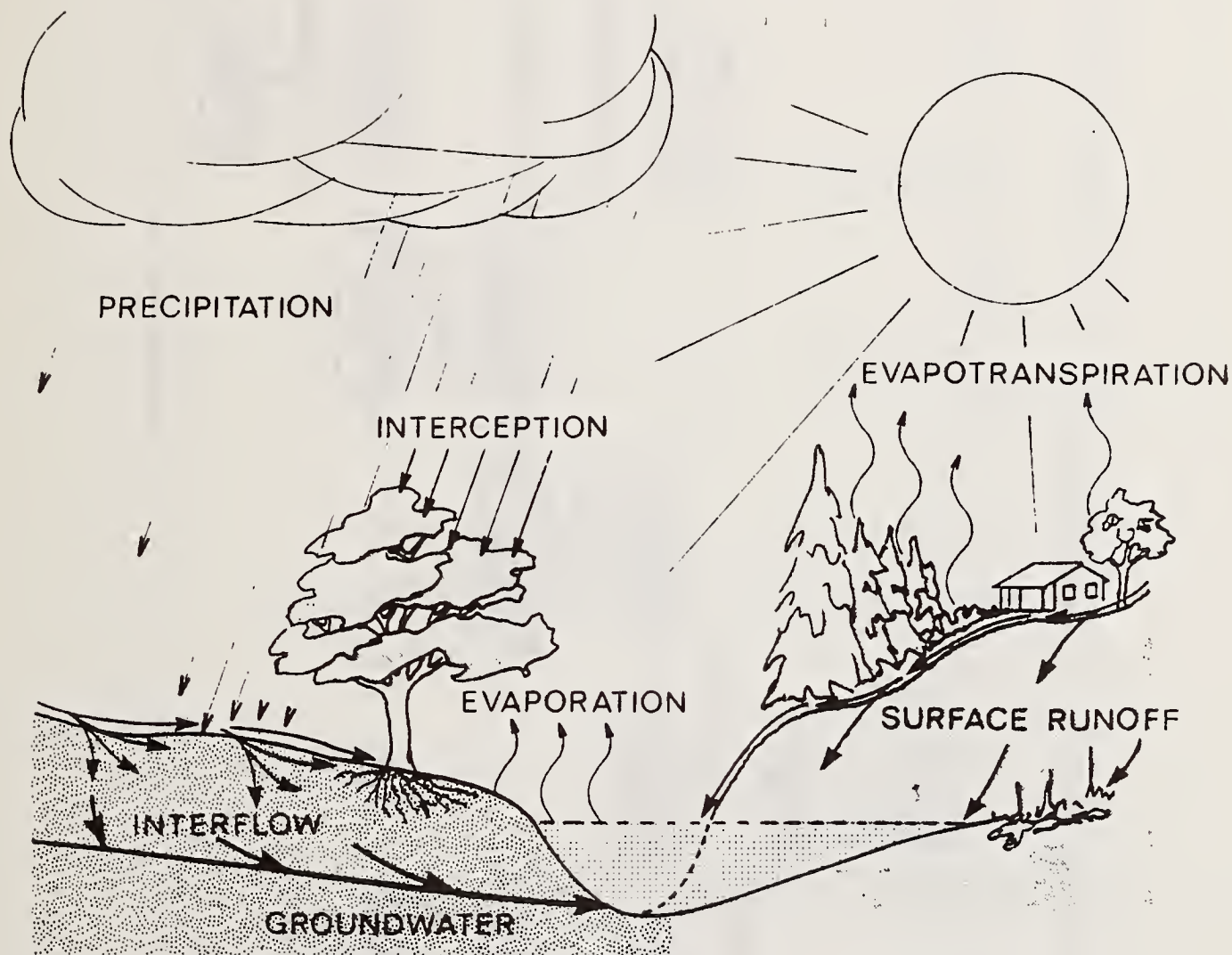
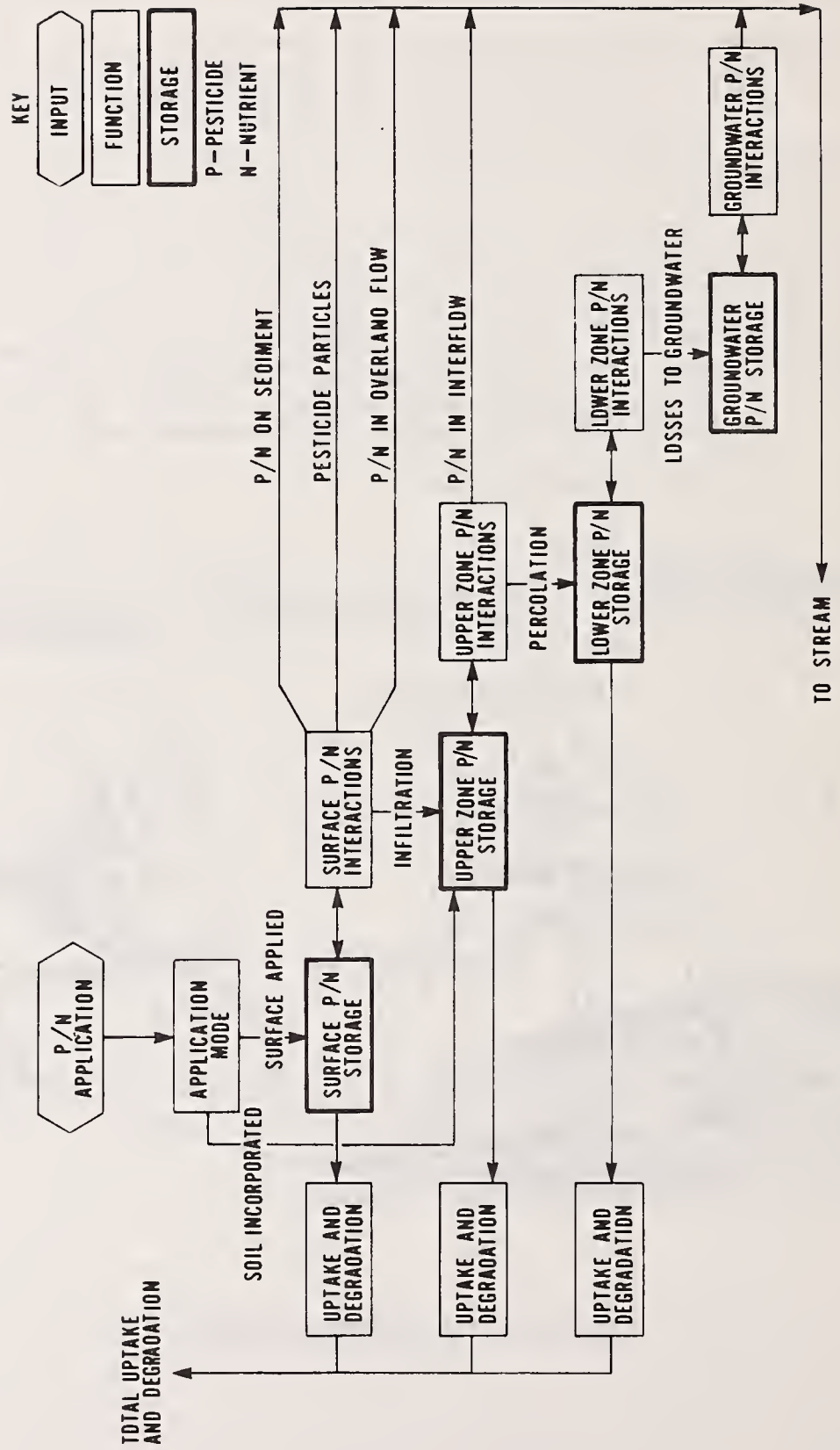


Figure 1. The Hydrologic Cycle

Figure 2
Pesticide and Nutrient movement in the ARM model



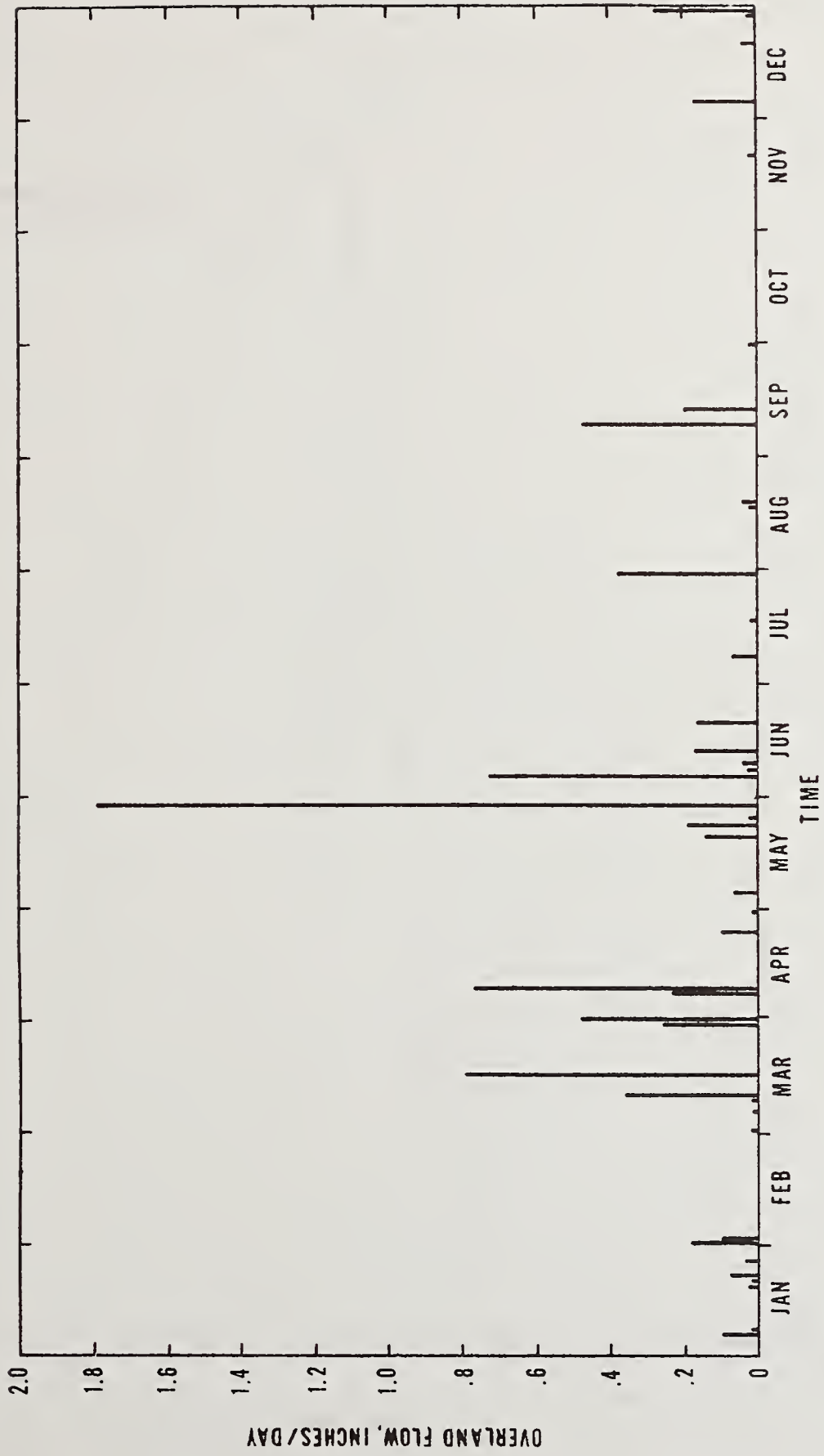


Figure 3. Overland flow in P1 watershed, Watkinsville, Georgia 1973

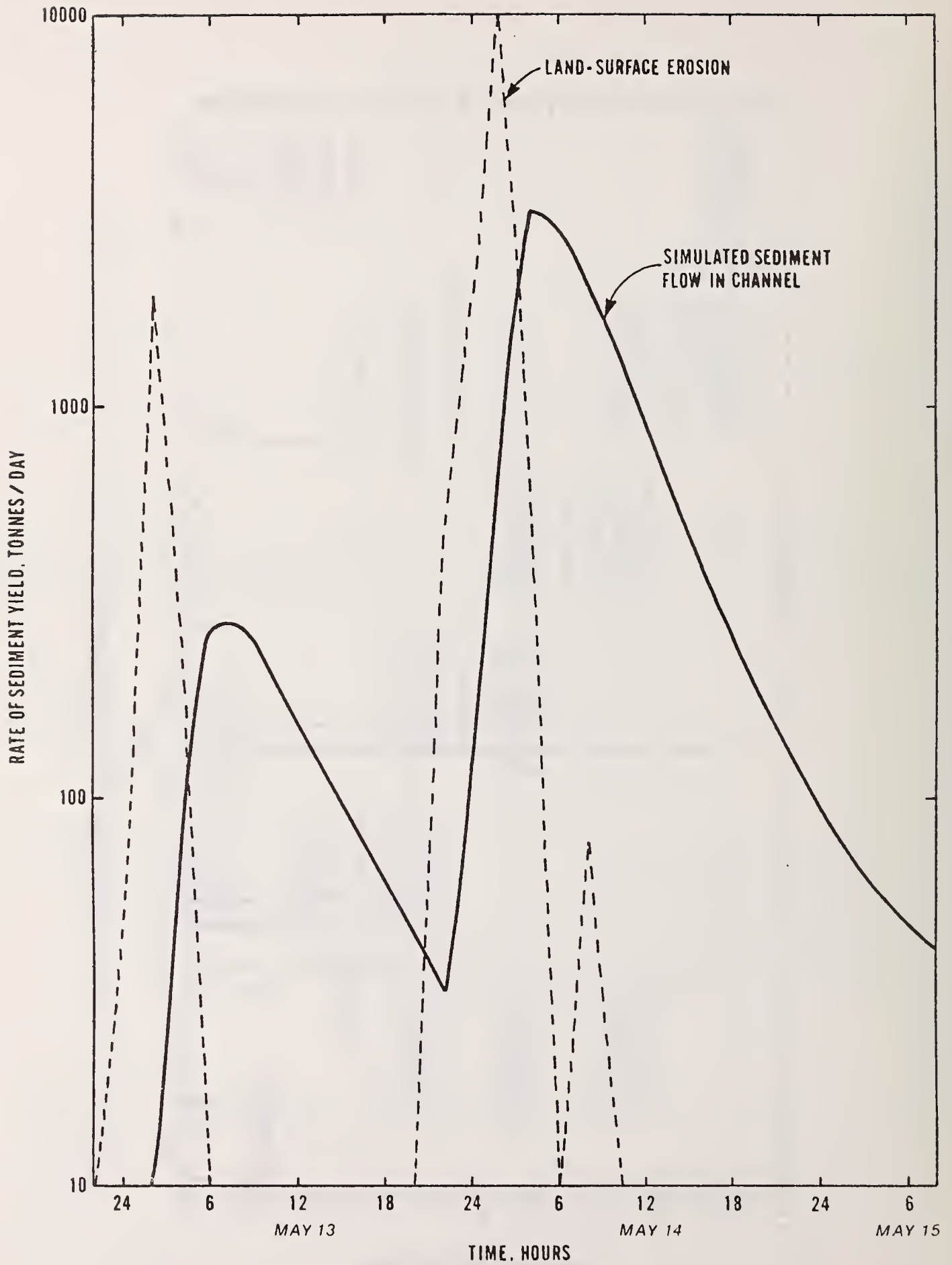


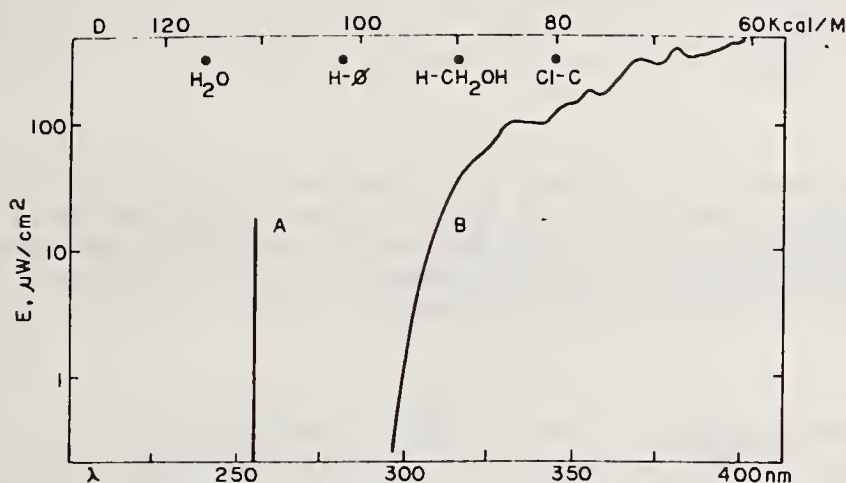
Figure 4. Sediment transport in Four Mile Creek, Iowa—May 1970

notes

THE PHOTOCHEMISTRY OF XENOBIOTICS

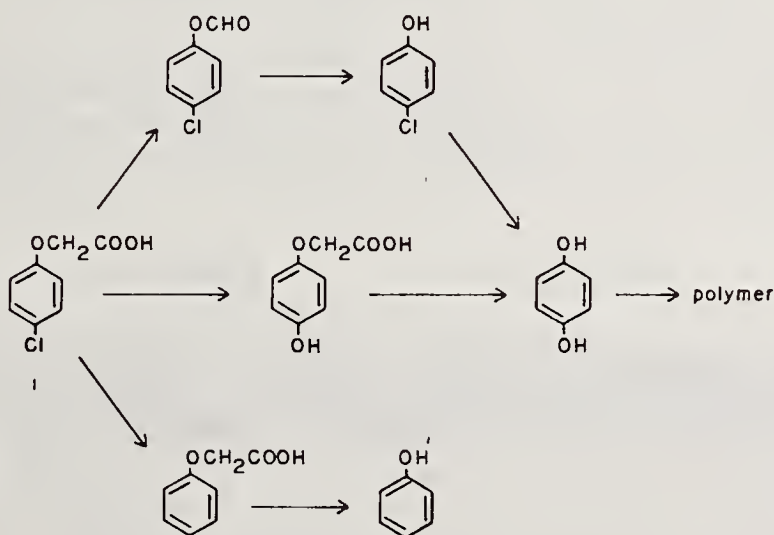
Donald G. Crosby
University of California
Davis, California 95616

For centuries, chemists have observed the effect of light on chemicals in the laboratory. However, it is only in recent years that investigation has extended to the action of sunlight on the foreign chemicals dispersed in the environment--the "xenobiotics." While not so energetic as most common laboratory light sources, the ultraviolet portion of sunlight (Scheme A) nevertheless provides sufficient energy to bring about several important types of photochemical transformations (1).



Scheme A

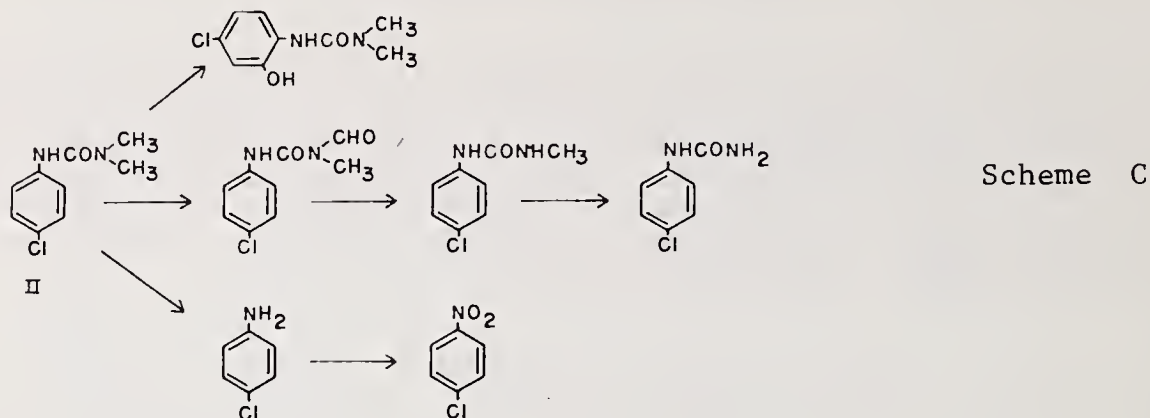
Oxidation, reduction, and photonucleophilic displacements are most often represented, as demonstrated by the growth regulator p-chlorophenoxyacetic acid (I, Scheme B). A free-radical oxidation removes the side-chain, reductive dichlorination replaces the ring Cl with H, and hydroxide ion (from water) replaces the Cl with OH (2).



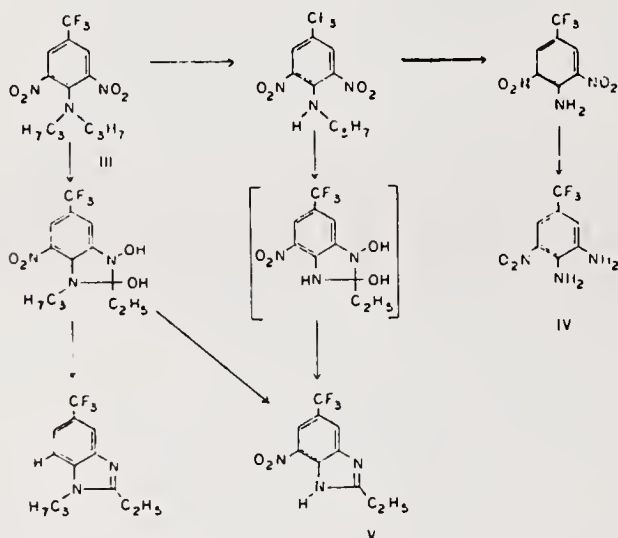
Scheme B

The herbicide monuron (II, Scheme C) provides further examples of oxidation. The N-methyl groups are oxidized to formyls subsequently removed by hydrolysis or loss of CO. Alternatively, the aromatic ring is

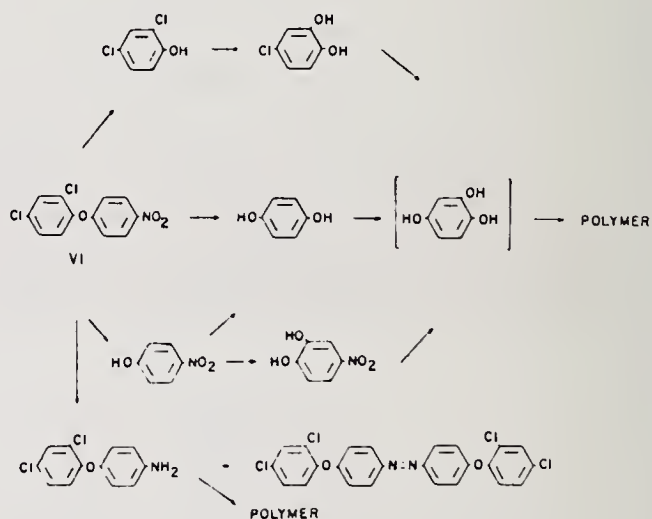
hydroxylated ortho to the urea side-chain. Further, the p-chloroaniline resulting from hydrolysis is oxidized to the corresponding azobenzene or even to p-chloronitrobenzene (3).



The herbicide trifluralin (III, Scheme D) likewise is oxidatively dealkylated but also undergoes reduction of nitro group to the amine IV (4). A similar reduction occurs in nitrofen (VI, Scheme E), although the predominant reaction is photonucleophilic displacement of p-nitrophenate and nitro groups by hydroxide to provide various phenols (5).

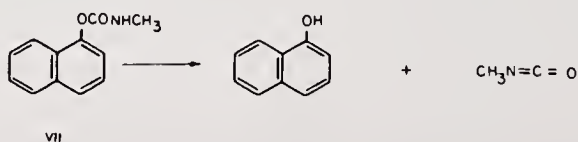


Scheme D



Scheme E

Other common sunlight-energized reactions include elimination (methyl isocyanate from 1-naphthyl N-methylcarbamate, carbaryl, Scheme F VII) and isomerization (dieldrin to the half-cage isomer X, Scheme G) (6,7).



Scheme F

11. R. D. Ross and D. G. Crosby, Chemosphere, in press (1975).
12. C. J. Soderquist, D. G. Crosby, K. W. Moilanen, J. N. Seiber, and J. E. Woodrow, J. Agr. Food Chem. 23, 304 (1975).
13. D. G. Crosby and K. W. Moilanen, unpublished.

notes

VERTICAL MOVEMENT AND DISTRIBUTION OF ORGANICS IN SOILS

J. M. Davidson
Soil Science Department
University of Florida
Gainesville, Florida 32611

The movement of organic solutes through soils occurs as a result of molecular diffusion and mass transport in the soil-water phase. Molecular diffusion is a relatively slow process in comparison to mass transport; therefore, it will not be considered a major transport process in this manuscript. Organic solute movement by mass transport is dependent upon the physical and chemical characteristics of the soil and interactions between the solute and soil matrix. An understanding of how these processes influence the transport of various organic chemicals is required in order to predict and manage the behavior of toxic organic solutes in natural soil-water systems.

Several mathematical models have been proposed to describe the movement and distribution of solutes in porous media (1-5). These models are based on chromatography theory and vary in their conceptual description of the physical characteristics of the soil-water system and interactions between the solute and soil matrix. Because of the general acceptance of chromatography theory and its applicability to a soil-water system, this approach will be used in the following discussion to describe the vertical movement and distribution of organic solutes in soils. Experimental verification of the above models for steady state and transient soil-water conditions is available (5-9).

The movement of organic solutes through soils will be assumed, for discussion purposes, to be described by the following partial differential equation.

$$\frac{\partial C}{\partial t} = D \frac{\partial^2 C}{\partial z^2} - v \frac{\partial C}{\partial z} - \frac{\rho}{\theta} \frac{\partial S}{\partial t} - kC \quad [1]$$

where C is the organic solute concentration ($\mu\text{g}/\text{cm}^3$), t is time (hr), D is dispersion coefficient (cm^2/hr), z is vertical depth

(cm), v is average pore-water velocity (cm/hr) given by dividing Darcy's flux by volumetric soil-water content, ρ is soil bulk density (g/cm^3), θ is volumetric soil-water content (cm^3/cm^3), S is the adsorbed organic solute concentration ($\mu\text{g}/\text{g}$), and k is rate coefficient for microbial degradation (hr^{-1}). The first two terms on the right hand side of equation [1] describe solute transport, while the third and fourth terms describe the adsorption-desorption process and the irreversible loss of an organic solute from the system by microbial degradation, respectively.

The adsorption-desorption of most organic chemicals in a soil-water system has been shown to follow a Freundlich equation (10,11). The relationship assumes adsorption equilibrium exists at all times. Using this relationship to describe adsorption-desorption and the procedure outlined in Hashimoto et al. (1), equation [1] becomes:

$$R \frac{\partial C}{\partial t} = D \frac{\partial^2 C}{\partial z^2} - v \frac{\partial C}{\partial z} - kC \quad [2]$$

where, the retardation term R is:

$$R = 1 + \frac{\rho}{\theta} NK C^{N-1} \quad [3]$$

and K and N are the distribution coefficient (1,10,11) and exponent from the Freundlich equation. The adsorption-desorption of some organic solutes is not instantaneous, but a kinetic process requiring several hours for equilibrium. Kinetic adsorption-desorption equations have also been used (2,4,6) in equation [2].

The simultaneous movement of water and organic solutes through natural field soils is generally a transient process. The direction and rate at which the two phases move depend upon various physical, chemical, and biological processes. The transient nature of the problem, however, makes it difficult

to evaluate specific processes. Therefore, in order to discuss the basic mechanisms influencing the movement and distribution of organic solutes in soils, steady state soil-water conditions will be considered here.

The movement and distribution of organic solutes in soils will be discussed using equations [2] and [3]. The average pore-water velocity, v , in equation [2] is also the velocity at which a nonreactive solute front or pulse moves through a soil (e.g. chloride or tritium). Dividing both sides of equation [2] by R gives a reduced velocity, v/R , which is the velocity of an adsorbed solute front or pulse in a soil. This velocity depends upon the adsorption-desorption characteristics of the organic solute and soil (K , N). The sink term (kC) for microbial degradation does not influence the velocity of an organic solute. The magnitude of k and v/R determine the maximum soil depth to which an organic solute will move and the concentration distribution of the solute in the soil (12,13).

Figure 1 contains four general adsorption isotherms that have been observed for various organic chemicals and adsorbents (14). Isotherms A, B, and C in Figure 1 are described by the Freundlich equation (1,10, 11) and that in Figure 1D by the Langmuir equation (14). Using the adsorption isotherms in Figure 1 and equation [2] and [3], it is possible to describe the relative mobility of different organic solute concentrations in a soil.

The velocity at which an organic solute front or pulse moves through a soil is independent of the solute concentration when $N = 1.0$ in equation (3) (Figure 1A). Thus, the mobility of the organic solute depends upon the soil-water flow rate and distribution coefficient, K . The assumption of a linear adsorption isotherm is frequently made regarding organic chemicals at low concentrations (4,7,11). If the organic solute was introduced into the soil as a pulse, the shape of the pulse in the soil (concentration distribution with soil depth) would be reasonably symmetrical. The distribution of the organic solute in the soil is influenced by the change in soil-water flow direction with time (e.g., evaporation from the soil surface) and dispersion coefficient, D , (mechanical mixing owing to pore size distribution). When water evaporates from the soil surface, a net upward movement of the organic solute occurs. This results in a spreading of the solute concentration distribution and reduction in maximum solute

concentration.

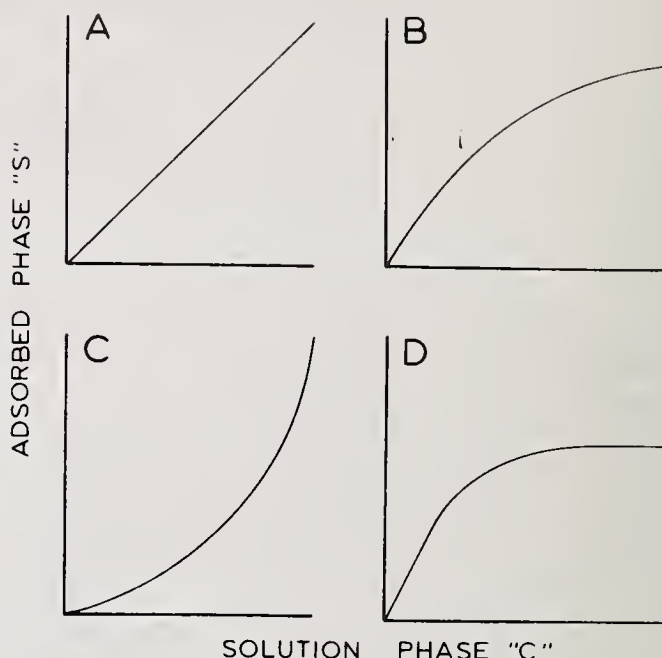


Figure 1. Typical adsorption isotherms for organic solutes in soil-water systems.

If the adsorption isotherm is nonlinear (Figures 1B and 1C), the average velocity, v/R , of the organic solute will depend upon the solute concentration (equation 3) as well as K . Several investigators have observed a deeper penetration of organic solutes with an increase in the chemical concentration (15-17). Organic solute mobility is greater in systems where $N < 1.0$ (Figure 1B) than where $N > 1.0$ (Figure 1C). Note that the retardation term is the same when $C = 1.0$ $\mu\text{g}/\text{cm}^3$ (equation 3). The importance of the adsorption isotherm shape is more pronounced at high than at low organic solute concentrations (< 10 $\mu\text{g}/\text{cm}^3$). For example, if $\rho = 1.5$ g/cm^3 , $\theta = 0.35$ cm^3/cm^3 , $K = 1.0$ cm^3/g and $N = 0.7$, the retardation terms for $C = 10$, and $1,000$ $\mu\text{g}/\text{cm}^3$ using equation [3] are 2.50, and 1.38. For $N = 1.3$ and $C = 10$ and $1,000$ $\mu\text{g}/\text{cm}^3$, the retardation terms are 12.1 and 44.3, respectively. The retardation terms for $N = 1.3$ increase sharply with an increase in solute concentration (equation 3 and Figure 1C). The concentration distribution of a pulse of organic solute will spread over a greater soil depth when $N < 1.0$ than when it is equal to unity. The spread or "tailing" of the solute concentration distribution occurs behind the invading front of the pulse.

A summary of available data on adsorption of organic chemicals in soils and the Freundlich equation parameters that describe the isotherms are given in Hamaker and Thompson (11). There is a tendency for $N = 1.0$ to approximate many adsorption isotherms, but there are also many values significantly lower than unity. The value of N appears to vary between 0.7 and 1.0. Deviations from linearity are more obvious when large concentration ranges are considered. From the previous discussion, it would appear that if the widely used assumption of unity for N was not valid, considerable error would be introduced in calculating organic solute movement and concentration distributions.

The mobility of an organic solute in a soil with an adsorption isotherm described by the Langmuir equation (Figure 1D) is also concentration dependent. At solute concentrations high enough to saturate the adsorption sites, the organic solute mobility is equal to that of a nonadsorbed solute. At lower concentrations the results are similar to the case for $N < 1.0$ in the Freundlich equation.

If the adsorption process was kinetic, and the soil-water flow rate was great enough to prevent equilibrium adsorption, the solute concentration distribution in the soil would be spread over a greater soil distance than occurs for equilibrium adsorption (4,5,6). These types of processes have not been studied in detail for organic solutes and soils. Kinetic adsorption equations may also be nonlinear.

The significance of microbial degradation, k_c , to organic solute mobility is in the depth to which the solute will move (12, 13). If degradation is rapid and the reduced velocity, v/R , is low, the maximum depth to which the organic solute will penetrate the soil profile is small. Organic solutes with large transport velocities move deeper into the soil profile than those with low velocities.

There appears to be no consistent procedure for grouping organic chemicals with regards to their mobility in soils. The adsorption-desorption characteristics for each chemical varies with the soil or adsorbent. The mobility and distribution of a chemical can only be estimated after the adsorption isotherm has been determined. Also, the transient nature of the soil water is important in increasing the soil profile length over which the organic solute is spread. Care should be exercised in making

general statements about the mobility of organic solutes in soils in the absence of adsorption-desorption data.

REFERENCES

1. Hashimoto, I., K. B. Deshpande, and H. C. Thomas. 1969. Peclet Numbers and Retardation Factors for Ion Exchange columns. *Ind. Eng. Chem. Fundamentals* 3: 213-218.
2. Lapidus, L., and N. R. Amundson. 1952. Mathematics of Adsorption in Beds. VI. The Effects of Longitudinal Diffusion in Ion Exchange and Chromatographic Columns. *J. Phys. Chem.* 56:984-988.
3. Lindstrom, F. T., and L. Boersma. 1971. The Theory of Mass Transport of Previously Distributed Chemicals in a Water Saturated Sorbing Porous Medium. *Soil Sci.* 111:192-199.
4. Oddson, J. K., J. Letey, and L. V. Weeks. 1970. Predicted Distribution of Organic Chemicals in Solutions and Adsorbed as A Function of Position and Time for Various Chemicals and Soil Properties. *Soil Sci. Soc. Amer. Proc.* 34: 412-417.
5. van Genuchten, M. Th., and P. J. Wierenga. 1976. Mass Transport Studies in Sorbing Media. I. Analytical Solution. *Soil Sci. Soc. Amer. J.* (in press)
6. Hornsby, A. G., and J. M. Davidson. 1973. Solution and Adsorbed Fluometuron Concentration Distributions in a Water Saturated Soil: Experimental and Predicted Evaluation. *Soil Sci. Soc. Amer. Proc.* 37:823-828.
7. Kay, B. D., and D. E. Elrick. 1967. Adsorption and Movement of Lindane in Soils. *Soil Sci.* 104:314-322.
8. Kirda C., D. R. Nielsen, and J. W. Biggar. 1973. Simultaneous Transport of Chloride and Water During Infiltration. *Soil Sci. Soc. Amer. Proc.* 37:399-345.
9. Wood, A. L., and J. M. Davidson. 1975. Fluometuron and Water Content Distributions During Infiltration: Measured and Calculated. *Soil Sci. Soc. Amer. Proc.* 39:820-825.
10. Bailey, G. W., and J. L. White. 1970. Factors Influencing the Adsorption, Desorption and Movement of Pesticides

in Soils. Residue Review. 32:29-92.

11. Hamaker, J. W., and J. M. Thompson. 1972. Adsorption: Organic Chemicals in The Soil Environment. ed by C. A. I. Goring and J. W. Hamaker. Vol 1. Merce! Dekker, Inc., New York. pp 440.
12. Misra, C., D. R. Nielsen, J. W. Biggar. 1974. Nitrogen Transformations in Soil During Leaching: III. Nitrate Reduction in Soil Columns. Soil Sci. Soc. Amer. Proc. 38:300-304.
13. Cho, C. M. 1971. Convective Transport of Ammonium with Nitrification in Soils. Can. J. Soil Sci. 51:339-350.
14. Weber, W. J., Jr., and P. J. Usinowicz. 1973. Adsorption from Aqueous Solution. Tech. Publication, Research Project 17020 EPA, U.S. Environmental Protection Agency. Cincinnati, Ohio.
15. Ivey, M. J., and H. Andrews. 1965. Leaching of Simazine, Atrazine, Diuron, and DCPA In Soil Columns. Proc. S. Weed Conf. 18:670-684.
16. Birk, L. A., and F. E. B. Roadhouse. 1964. Penetration of and Persistence in Soils of the Herbicide Atrazine. Can. J. Plant. Sci. 44:21-27.
17. Rodgers, E. G. 1962. Leaching of Four Triazines in Three Soils as Influenced by Varying Frequency and Rate of Simulated Rainfall. Proc. S. Weed Conf. 15:268.

notes

PATTERNS OF DEPOSITION OF RADIONUCLIDES IN SEDIMENTS *

David N. Edgington
Radiological and Environmental Research Division
Argonne National Laboratory
Argonne, Illinois 60549

and

John A. Robbins
Great Lakes Research Division
The University of Michigan
Ann Arbor, Michigan 48106

During the last twenty-five years, considerable attention has been given to the study of the distribution of natural and artificial radioactivity in the oceans. From these studies, it has been possible to develop a greater understanding of the physical, chemical and biological processes occurring in the oceans. These studies have centered around either the patterns of deposition of fallout from nuclear testing and the interaction with biotic or abiotic components in the water column (1), or the dispersal of radioactivity from the disposal of radioactive wastes into rivers such as the Columbia (2) or coastal waters such as the Irish Sea (3) or Bombay Harbor (4). These studies show that most of the radioactivity is either in the sediments or dissolved in the water; there is only an extremely small fraction in the biota (5). As a result of these studies, it is possible to predict in general terms the behavior not only of radionuclides, but also many other known or potential pollutants.

In contrast to the extensive data accumulated for the behavior of radionuclides in the oceans, comparatively few historical data are available for the Great Lakes. Recently, Wahlgren and Marshall have reported measurements of $^{239,240}\text{Pu}$, ^{137}Cs , and ^{90}Sr in the water and biota of these lakes (6), and Edgington and Robbins have reported measurements of $^{239,240}\text{Pu}$, ^{137}Cs , and ^{210}Pb in their sediments (7). These results show that while phytoplankton may play a significant role in scavenging plutonium and cesium from the water column, greater than 95% of the known inputs of these radionuclides (from nuclear testing) now reside in the sediments. Wahlgren and Nelson have also shown that the concentrations of plutonium and cesium in suspended matter from the water column are very comparable to those in the surficial sediments (6). Studies of the distribution of trace elements in sediment cores from the lakes have shown that the concentrations of many heavy elements are elevated in the upper few centimeters of the sediment column (8). More recently, Edgington and Robbins have demonstrated that the shape and magnitude of the lead profiles in sediment cores from southern Lake Michigan can be explained in terms of the history of atmospheric lead deposition into the lake from the Chicago-Milwaukee region (9).

Since many pollutants, such as lead, mercury and plutonium are strongly associated with suspended matter or sediment, it is clear that the deposition, resuspension and redistribution of sediments with time may be of primary importance in determining their eventual biological fate. The processes of sedimentation may alter the distribution of a pollutant in such a manner that high concentrations may be contained in local areas which could have adverse effects directly on man, or on the benthic and other components of the aquatic environment.

In this paper, we shall report on the measurement of concentration profiles of ^{137}Cs , ^{210}Pb and $^{239,240}\text{Pu}$ (to be referred to as ^{239}Pu for convenience) in sediment cores taken mainly from southern Lake Michigan. The stations are shown in Figure 1. Since the only significant inputs of these radionuclides have been from atmospheric fallout, it is assumed that the input flux over the lake has been constant and, therefore, variations in the flux at

*Work performed under the auspices of the U.S. Energy Research and Development Administration.

the sediment-water interface are indicative of redistribution of the sediment. The profiles are interpreted in terms of a simple model described by Robbins and Edgington (10), which permits the calculation of sediment rate, a mixing depth which is indicative of the degree of surficial disturbance due to biological or physical disturbances, and the total deposition per unit area. The results are shown in Table 1.

The patterns of post-glacial sedimentation in Lake Michigan as measured by seismic profiling (11) show that the deposition of post-glacial sediments is quite variable. However, the uppermost 1 or 2 centimeters of sediment consist of a highly liquid, reddish-brown flocculent material which contains high concentrations of radionuclides and trace elements, independent of the sedimentation rate or characteristics of the underlying material. Robbins has shown that the chemical composition of this floc is not significantly different than that of underlying fine-grained sediments (12). The relationship between sedimentation rates calculated from the ^{210}Pb or ^{137}Cs profiles, and from the thickness of the Waukegan member, the uppermost stratigraphic layer in southern Lake Michigan is shown in Figure 2. The apparent correlation suggests that the present rate of sedimentation in the lake is not significantly different from the average rate over the last 7000 years.

The cesium or plutonium deposition in the lake is compared with sedimentation rates in Figure 3a and b. Values of the sedimentation rate, mixing depth and the flux normalization factor f , defined as the ratio of the observed deposition in the sediments to that expected to be present if there was direct coupling between the input at the air-water interface and the sediment are given in Table 1. Values of the ratios of f indicate that the scavenging of cesium is very similar to that of plutonium, i.e., $f_{\text{Pu}}/f_{\text{Cs}} \approx 1$, while that of lead is quite different, the values of $f_{\text{Pb}}/f_{\text{Cs}}$ being quite variable. However, it does appear that, in general, the higher values of $f_{\text{Pb}}/f_{\text{Cs}}$ are found at stations well offshore. The similarity in the behavior of cesium and plutonium is surprising considering their very dissimilar chemical properties. Recent experiments by Alberts and Wahlgren (13) using techniques described by Gibbs (14) have shown that: (a) plutonium is primarily associated with reducible hydrous oxides; (b) cesium is associated with the clay minerals; and (c) lead is associated with organic matter. Since Shimp *et al.* have shown that hydrous oxides, like Fe_2O_3 , are strongly correlated with the $<2 \mu\text{m}$ clay fraction and the proportion of organic material increases with increasing distance offshore (8), the similar scavenging of plutonium and cesium, and the inshore-offshore differences in the scavenging of lead are as expected.

The isopleths shown in Figure 3a and b indicate that the total deposition of ^{239}Pu or ^{137}Cs in the sediments is very strongly correlated with the magnitude of the sedimentation rate and that the areal distribution of these nuclides in the sediments is, therefore, very non-uniform. The data indicate that there is considerable resuspension and transport of sediment from the western side of the lake, where there is a 1–2 cm thick layer of floc overlying glacial till or lacustrine clay, to the areas of high deposition, about 12 miles from the eastern shore, where both the rates of sedimentation and radioactivity deposition are highest. This pattern of deposition is interesting. Although the bottom topography indicates an almost continuous slope downward in a westerly direction to the maximum depth of 180 m, the maximum deposition of sediment occurs at a water depth of only 80 m. In addition, no sedimentation or deposition of radioactivity occurs at water depths of less than 50 m, even on the eastern side of the lake where several large rivers discharge. From this and the fact that Wahlgren and Nelson have shown that the residence time of plutonium and cesium in the water column is very short (15), it is concluded that radioactivity which may be released into the nearshore zones from nuclear power plants would be rapidly transported to the region of high sedimentation. In summary, any monitoring scheme for determining the long-term effects of releases from nuclear plants must take into account the sedimentological properties of the receiving body of water, i.e., the final point of deposition may be far removed from the site of release.

Evidence for transport and redeposition of sediments in Lake Michigan can also be deduced from a detailed examination of the profiles of radioactivity in the sediment column. Since the flux to the lake of ^{210}Pb , which is produced in the atmosphere from the decay of terrigenous ^{222}Rn , is constant with time, the ^{210}Pb concentration should decrease

exponentially with depth if the sedimentation rate has been constant, and if there have been no physical and/or biological disturbances of the sediment after deposition. Such a profile, obtained from a core taken from a water depth of 300 m is shown in Figure 4. The line through the points was calculated from a simple exponential model (10). Numerous cores have shown similar profiles for ^{210}Pb . However, in others, the concentration of ^{210}Pb is constant over several centimeters at the top of the core. This is indicative of mixing due to physical processes and/or bioturbation in the lake. The data obtained from the analysis of several cores from Lake Huron show that the depth of mixing coincides with the detection of benthic organisms (12).

The two ^{210}Pb profiles shown in Figures 5 and 6 indicate even greater evidence of redistribution of the sediment after deposition. The profile shown in Figure 5 shows a break at 5 cm which is equivalent to 35 years or 1938. The decreased activity of ^{210}Pb below 5 cm would indicate a much lower sedimentation rate, or even erosion, at that time. On the other hand, the profiles shown in Figure 6, which are for two cores taken at the same station a year apart, are characterized by several breaks. Zones of constant activity correspond to an infinite sedimentation rate, and no elapsed time can be associated with such intervals. These could be due to massive redistributions of sediment or slumping. The zones of constant activity correspond to the dates of 1958, 1940 and 1915, respectively. Similar breaks corresponding to similar dates have been found in many cores from Lake Michigan and Lake Erie. As these dates correspond to the years of major storms in the Great Lakes, these results suggest that storm induced translocation and redeposition of sediments may occur in water over 70 m in depth.

The ^{137}Cs and ^{239}Pu profiles from some cores also indicate that considerable redeposition of sediment is occurring. Since the inputs of these two radionuclides to the lake has been extremely variable (the inputs are dependent upon the intensity of nuclear testing), the profiles in the sediments should reflect this time dependence. Such profiles are shown in Figures 7 and 8. The dashed lines were calculated using the mixing model described by Robbins and Edgington. The maxima in the concentrations of ^{137}Cs or ^{239}Pu correspond to the maximum fallout deposition in 1963, and the horizon of zero activity to 1951 or 1952. In contrast to the profiles shown in Figure 7, the intensity of the maximum in Figure 8 is depressed. This is probably due to the effect of surficial mixing. While the deposition of nuclear fallout in 1972 was more than an order of magnitude lower than in 1963, the concentration of ^{137}Cs or ^{239}Pu in the upper centimeter is less than a factor or two lower. As the estimated inputs of these radionuclides from the watershed are less than new direct inputs of atmospheric fallout (16), these high concentrations of cesium and plutonium can only arise from remobilization and redeposition of surface sediment in the lake.

References

1. Volchok, H. L., V. T. Bowen, T. R. Folsom, W. S. Broecker, E. A. Schnert and E. S. Bien. Oceanic distributions of radionuclides from nuclear explosions, pp. 42-89. In: Radioactivity of the Marine Environment, Nat. Acad. Sci., Washington, D. C.
2. Forster, W. O. (1972) Radioactive and stable nuclides in the Columbia River and adjacent northeast Pacific Ocean, pp. 663-700. In: The Columbia River Estuary and Adjacent Ocean Waters, A. T. Pruter and P. L. Alverson (eds.), University of Washington Press, Seattle and London.
3. Preston, A., D. F. Jefferies and R. J. Pentreath. (1972) The possible contributions of radioecology to marine productivity studies. Symp. Zool. Soc. Lond. No. 29, pp. 271-284.
4. Pillai, K. C. and E. Mathew. (1975) Plutonium in aquatic environment - its behavior, distribution and significance. IAEA-SM-199/27 (in press).
5. Preston, A. D., D. F. Jefferies and N. T. Mitchell. (1971) Experience gained from the controlled introduction of liquid radioactive wastes to coastal waters, pp. 629-644. In: Nuclear Techniques in Environmental Pollution, Proc. Symp. IAEA, Vienna.

6. Wahlgren, M. A. and J. S. Marshall. (1975) The behavior of plutonium and other long-lived radionuclides in Lake Michigan: I. Biological transport, seasonal cycling, and residence times in the water column. IAEA-SM-198/39 (in press).
7. Edgington, D. N. and J. A. Robbins. (1975) The behavior of plutonium and other long-lived radionuclides in Lake Michigan: II. Patterns of deposition in the sediments. IAEA-SM-198/40 (in press).
8. Shimp, N. F., J. A. Schleicher, R. R. Ruch, D. B. Heck and H. V. Leland. (1971) Trace element and organic carbon accumulation in the most recent sediments of southern Lake Michigan. Ill. State Geol. Survey, Environ. Geol. Notes No. 41.
9. Edgington, D. N. and J. A. Robbins. (1976) Records of lead deposition in Lake Michigan sediments since 1800. Environ. Sci. and Technol. (in press).
10. Robbins, J. A. and D. N. Edgington. (1975) Determination of recent sedimentation rates in Lake Michigan using Pb-210 and Cs-137. Geochim. Cosmochim. Acta 39, p. 285-304.
11. Lineback, J. A. and D. L. Gross. (1972) Depositional patterns, facies and trace element accumulation in the Waukegan member of the Late Pleistocene-Lake Michigan formation in southern Lake Michigan. Ill. State Geol. Survey, Environ. Geol. Notes EGN-58.
12. Robbins, J. A., unpublished data.
13. Alberts, J. J. and M. A. Wahlgren, unpublished data.
14. Gibbs, R. J. (1973) Mechanisms of trace metal transport in a river. Science 180, p. 71-73.
15. Wahlgren, M. A. and D. M. Nelson. (1974) Studies of plutonium cycling and sedimentation in the Great Lakes. Proc. 17th Conf. Great Lakes Res., pp. 218.
16. Edgington, D. N., J. C. Ritchie and J. A. Robbins. (1975) Comments on the paper, "Use of rivers to predict accumulation in sediments of radionuclides discharged from nuclear power plants," by P. Plato. Health Physics 29, pp. 429-431.

TABLE 1. Summary of measured and calculated parameters from the distribution of ^{210}Pb , ^{137}Cs and ^{239}Pu in Lake Michigan sediment cores.

Station	Sedimentation Rate		Mixing Depth (cm)	Flux Normalization Factor			Flux Ratios		
	(cm/yr)	(mg/cm ² /yr)		fPb	fCs	fPu	Pb/Cs	Pb/Pu	Cs/Pu
72-54	0.02	5.9	1.0	0.91	0.59	0.58	1.54	1.55	1.01
72-17	0.066	15.0	0	0.90	0.24	0.30	3.75	3.00	0.80
73-8	0.10	14.5	2.0	2.43	0.88	0.48	2.76	5.06	2.08
73-7	0.18	32.1	0	3.32	1.15	0.95	2.88	3.49	1.21
73-6	0.23	43.4	0	3.80	1.04	0.65	3.65	5.84	1.60
73-5	0.20	40.4	0	2.94	1.03	0.80	2.85	3.67	1.29
73-4	0.18	41.5	1.6	2.75	1.41	--	1.95	--	--
73-3	0.30	87.9	7.0	5.05	3.78	--	1.34	--	--
72-29	0.24	85.0	3.0	4.51	2.39	2.18	1.89	2.07	1.10



Figure 1. Sampling locations in Lake Michigan.

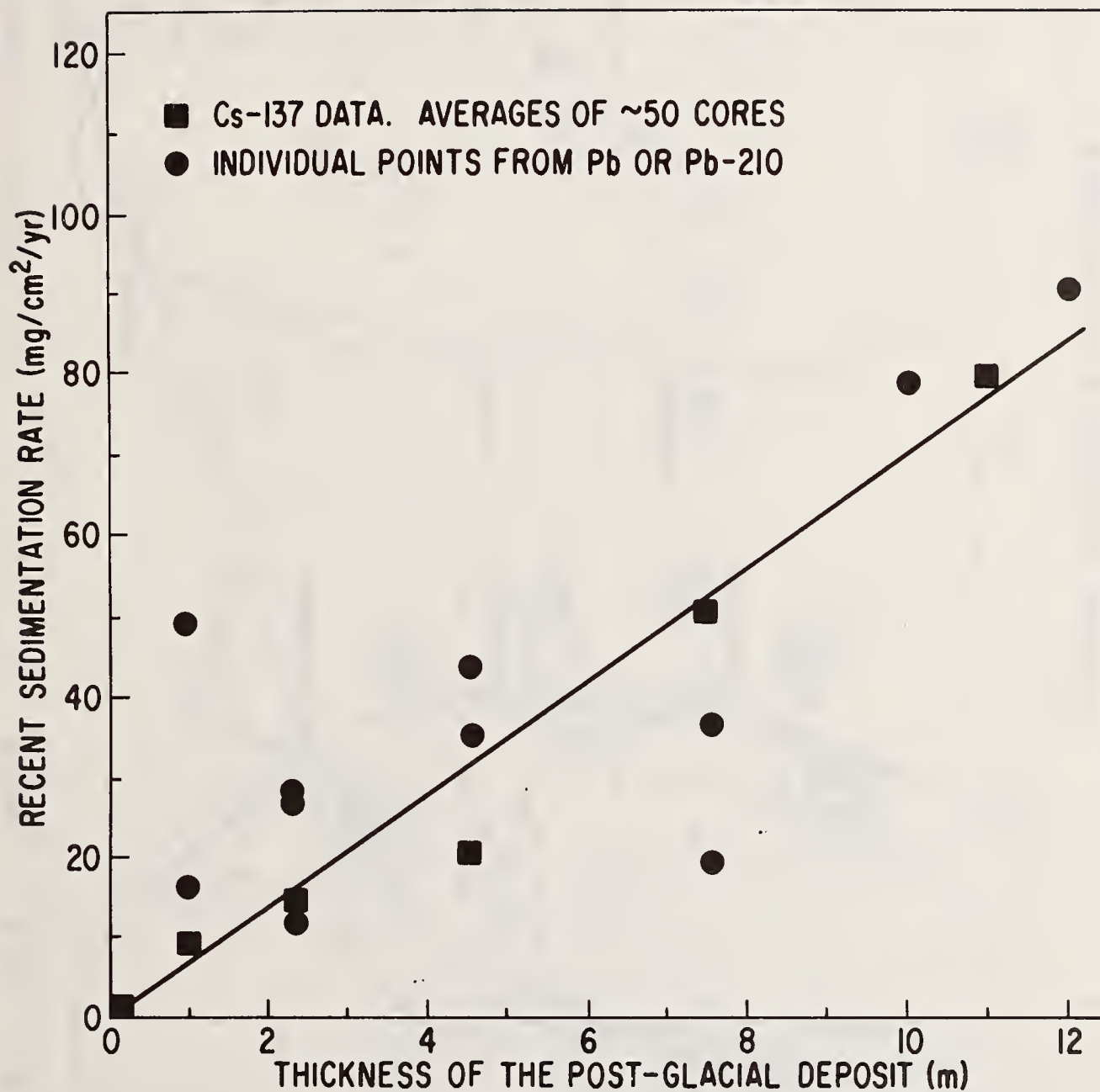


Figure 2. Correspondence between the thickness of post-glacial deposits in Lake Michigan and modern sedimentation rates inferred from radioactivity measurements.

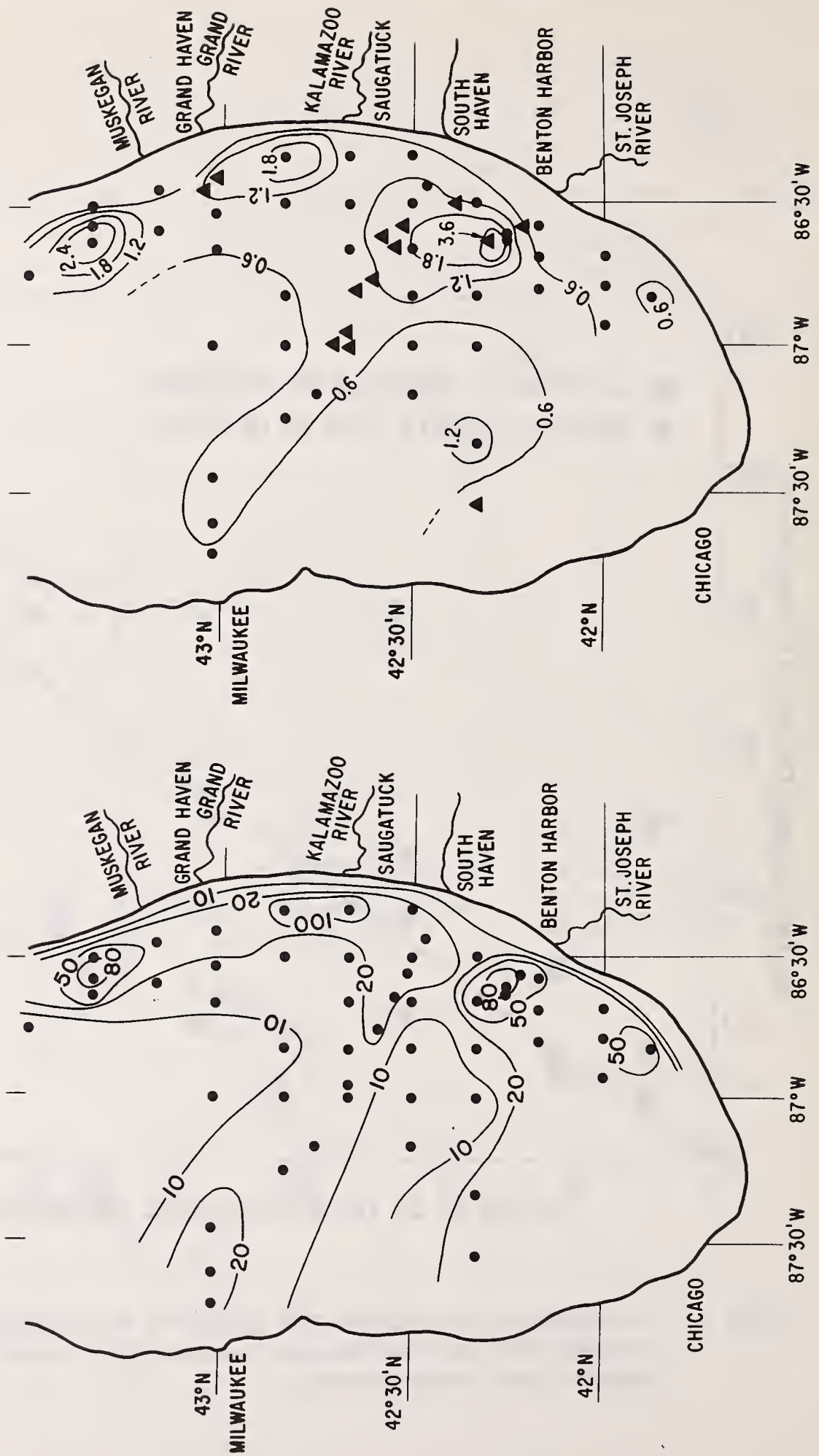


Figure 3. Comparison of the mass sedimentation rate and total deposition of ^{137}Cs or ^{239}Pu in southern Lake Michigan. (a) Mass sedimentation rate in $\text{mg}/\text{cm}^2/\text{yr}$. (b) Total deposition expressed in terms of fCs or fPu (see text).

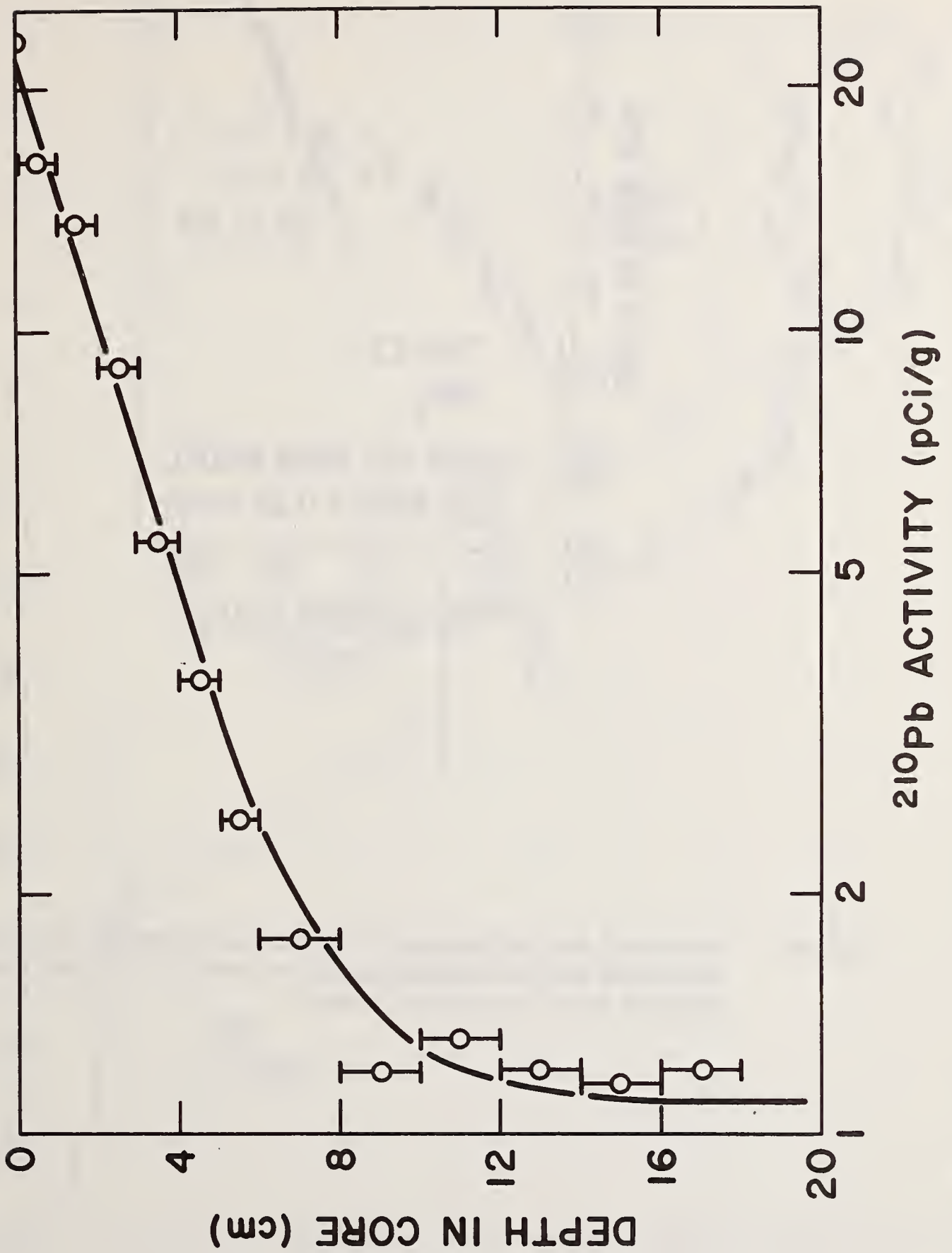


Figure 4. Measured and calculated ^{210}Pb profile at Station 72-103.

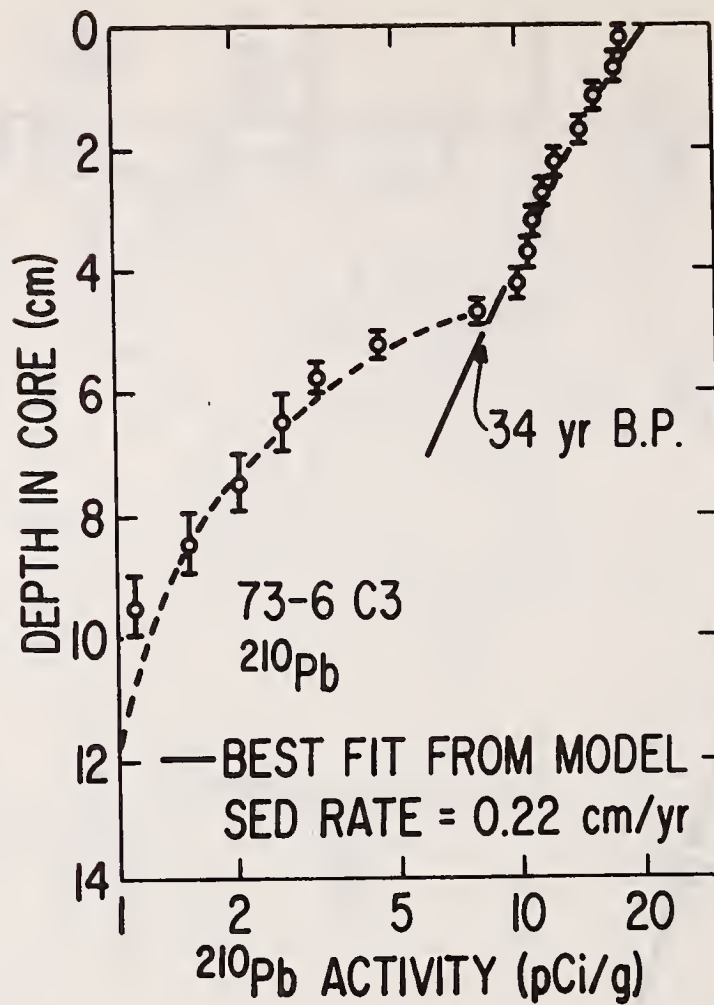


Figure 5. Measured and calculated ^{210}Pb profile at Station 73-6. Note the sharp break at approximately 34 years B.P. (1940) corresponding to an "erosional" event.

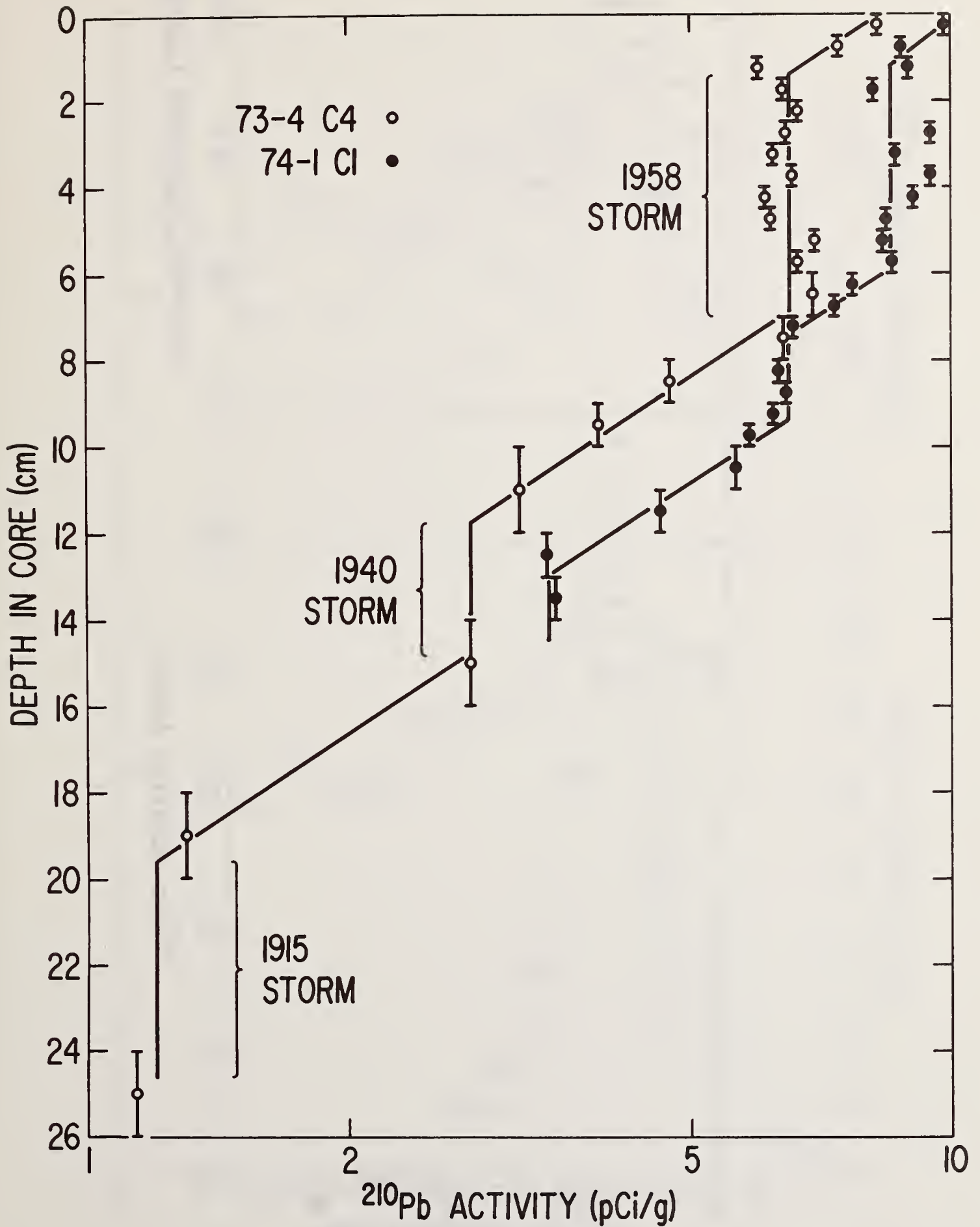


Figure 6. Measured profiles of ^{210}Pb at Stations 73-4 and 74-1. Note the periods of "infinite" sedimentation rate corresponding to the years 1958, 1940, and 1915, interspersed with an apparent constant sedimentation rate.

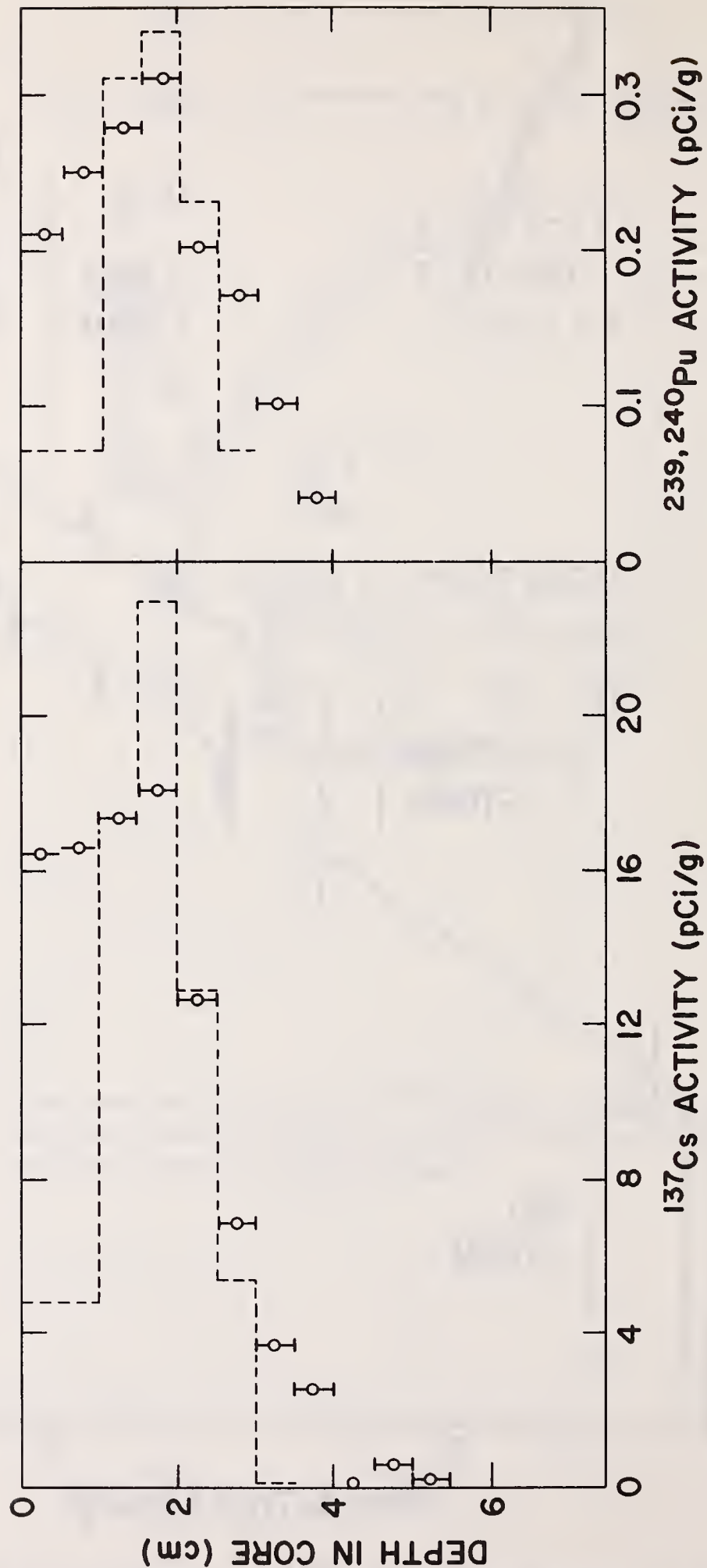


Figure 7. Measured and calculated ^{137}Cs and ^{239}Pu profiles at Station 73-5. Note the difference between the calculated and observed concentrations near the surface. The sedimentation rate is 0.17 cm/yr and there is no surficial mixing.

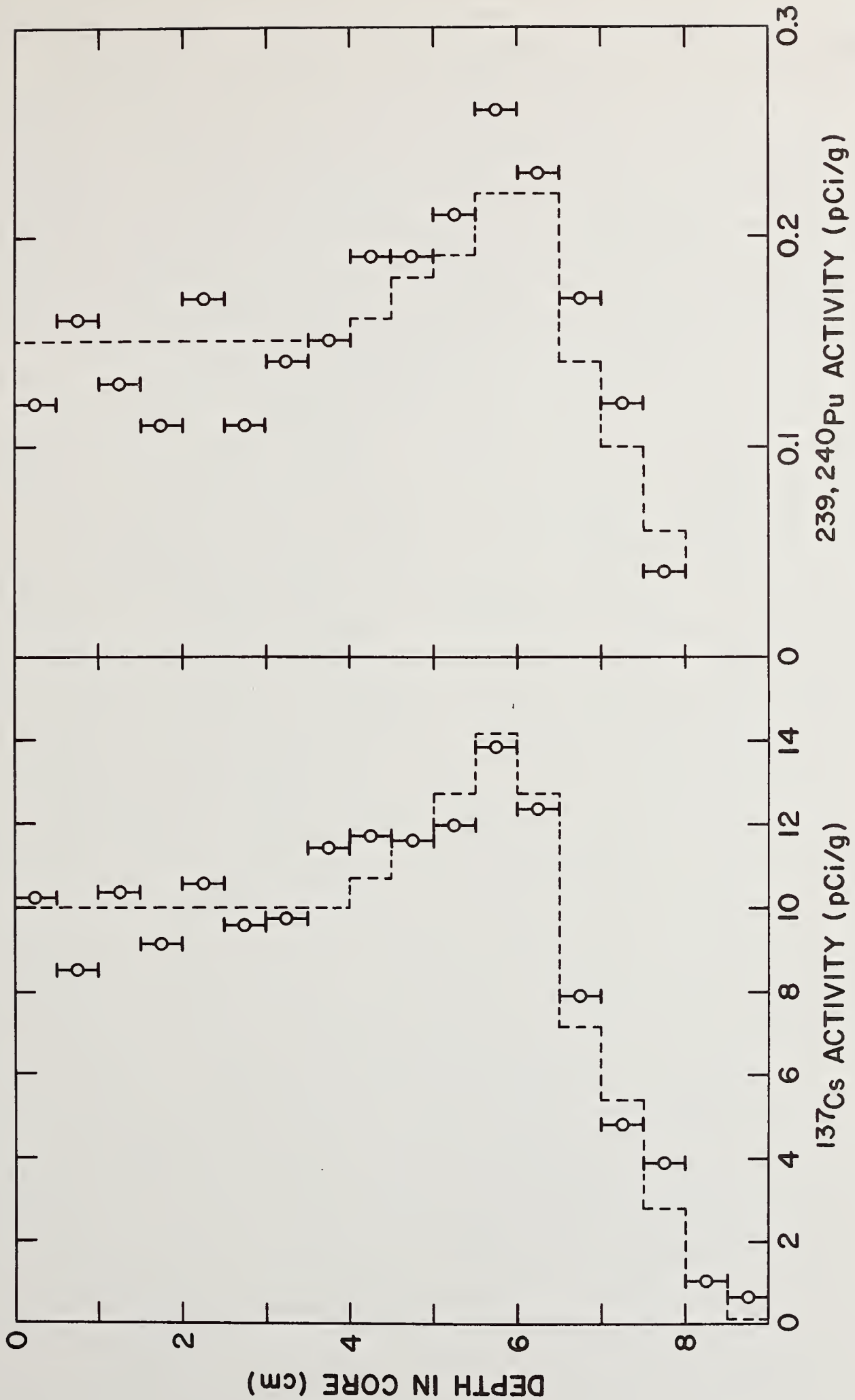


Figure 8. Measured and calculated ^{137}Cs and ^{239}Pu profiles at Station 74-1. The sedimentation rate is 0.5 cm/yr and there is mixing to a depth equivalent to 12 years of deposition.

notes

REACTION RATES OF ELECTRON PAIR DONOR MOLECULES WITH POLLUTANTS IN WATER

John O. Edwards, Department of Chemistry,
Brown University, Providence, R.I. 02912

Pollutants in water often are compounds which react with electron pair donors; the latter have also been termed bases and nucleophiles in several contexts. Further, there is a close relationship of donor reactivity to reducing capability. It is possible to convert pollutants to less harmful compounds by reacting them with donors, thus advantage should be taken of donor reactivity in pollution control whenever possible. It is necessary to have some knowledge of the pollutant and of donor reactivity scales in order to choose the proper anti-pollutant. Fortunately, enough data are now available in the literature to make feasible the estimation of a rate for the reaction



where D is a donor and R-X is a pollutant (hereafter substrate). Even if the exact molecule R-X has not been studied, a range of compounds useful as models have been investigated. It is now possible to predict which donors are very reactive towards model substrates of a general class thus enabling a chemist to confine his study to those donors which are already known to be reactive.

For example, the phosphorus anti-cholinesterases (which include some insecticides and nerve gases) react rapidly with oxygen anions such as hydroperoxide HOO^- , hydroxide OH^- and hypochlorite OCl^- and are unreactive towards donors like iodide ion I^- and thio-rea $\text{SC}(\text{NH}_2)_2$. Minor differences between orders of reactivity of donors towards two tetrahedral phosphorus substrates are to be expected but anything like a complete inversion is not to be expected. In fact, it has been found that hydroperoxide ion is about one hundred fold more reactive than hydroxide for a large number (at least 16) of phosphorus compounds.

Reactivity orders for donor reactions with a number of diverse substrates have been obtained in recent years. Among these are tetrahedral carbon (as in methyl bromide) trigonal carbon (as in esters, carbonium ions, aromatic compounds and olefins), digonal carbon (as in benzonitrile and cyanogen halides), tetrahedral phosphorus, a mixed bag of sulfur compounds, electrophilic oxygen (in peroxides and hypohalites), square planar metal complexes (such as PtCl_4^{2-}) and trigonal nitrogen (as in NH_2Cl). Lesser complete sets of data have been reported for boron, fluorine and other halogens, silicon and some octahedral metal complexes. Thus there are sufficient data on compounds that could be acceptable models for almost any pollutant that interacts with donors.

Treatment of donor reactivity is usually accomplished by the technique of linear free energy relationships. These are empirical plots of log rate constant towards one substrate against log rate constant towards another substrate (or rate constant against equilibrium constant, or equilibrium constant against equilibrium constant) with each point on the plot representing two constants for a particular donor. A number of the relationships including those devised by Brönsted, Hammett, Swain and Scott, Edwards and Ritchie will be shown. The correlations of donor reactivity with basicity to protons, with electrode potential, with polarizability and with other scales will be pointed out. The emphasis will be on the experimental observations that are useful in predicting reactivities. (The

fundamental basis of reactivity is still to a significant degree unknown so that the practical applications of donor reactivity in pollution treatment are better treated at the semi-empirical level.)

The qualitative terminology (Hard and Soft Acids and Bases) of Pearson will be used to describe the fact that some substrates react with donors following the reactivity order $I^- > Br^- > Cl^- > F^-$ (using halide ions as representative donors) whereas for other substrates the order is $F^- > Cl^- > Br^- > I^-$. More quantitative treatments of the same behavior will also be described, and it will be demonstrated that no less than three parameters are necessary in order to explain donor reactivity. The nature of the alpha-effect and its importance in pollution control will be delineated.

Towards a wide variety of compounds, the hydroperoxide ion is a very reactive donor indeed. Although it is much less basic to protons than is hydroxide ion, it reacts more rapidly in any bimolecular displacement situation (with the probable exception of general base catalysis). In his analysis of donor attack at trigonal carbon centers, Ritchie has found that OOH^- is 2000 fold more reactive than OH^- . The factor is 700 in case of cyanogen chloride (a digonal carbon substrate) and is 35 in the case of benzyl bromide (a tetrahedral carbon substrate). Oxidation of sulfur dioxide by peroxide is very rapid and at least in some pH ranges the attack is by peroxide first acting as a donor, with a subsequent intramolecular redox process. Peroxide can, of course, act as an electrophile (an electron pair acceptor, an oxidizing reagent) and it shows considerable selectivity in control of sewage order, etc.

A number of books contain discussions of donor reactivity. These include texts and monographs in the areas of physical-organic chemistry (Hammett, Ingold, Gould, March, Hine, Kosower), inorganic mechanisms (Basolo and Pearson, Langford and Gray, Edwards), proton reactions (Bell), hard and soft acids and bases (Pearson), enzyme catalysis (Jencks, Bender), bioorganic mechanisms (Bruice and Benkovic, Hudson), linear free energy relationships (Wells, Leffler and Grunwald), and solvent-donor interactions (Amis, Coetzee and Ritchie).

Some important references (in no particular order) are below:

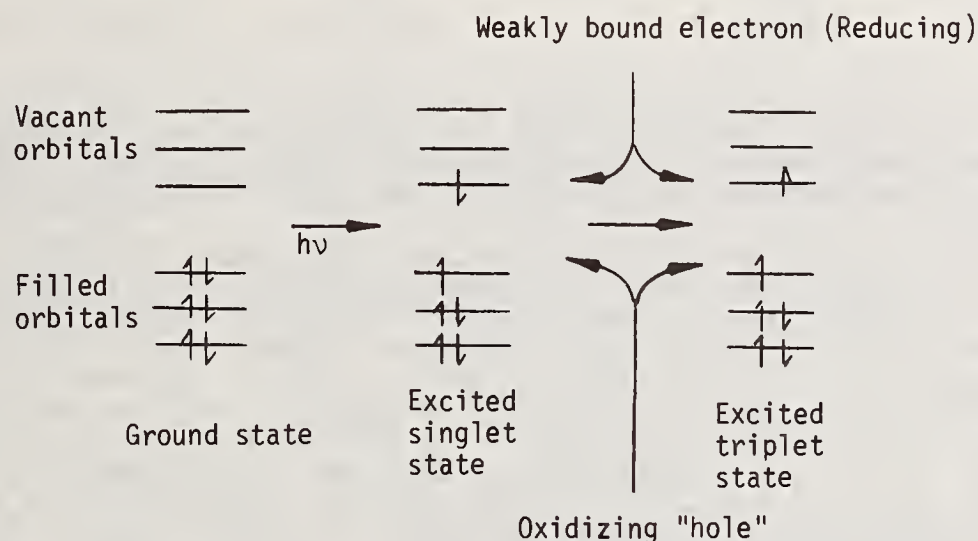
- (1) J. F. Bunnett, *Ann. Rev. Phys. Chem.*, 14, 271 (1963).
- (2) R. F. Hudson, *Chimica*, 16, 173 (1962).
- (3) K. M. Ibne-Rasa, *J. Chem. Educ.*, 44, 89 (1967).
- (4) J. O. Edwards, *J. Amer. Chem. Soc.*, 76, 1540 (1954); *ibid*, 78, 141 (1953); *ibid*, *J. Chem. Educ.*, 45, 386 (1968).
- (5) J. O. Edwards and R. G. Pearson, *J. Amer. Chem. Soc.*, 84, 16 (1962).
- (6) R. E. Davis, in "Survey of Progress in Chemistry," Vol. II, Academic Press, New York (1964).
- (7) C. G. Swain and C. B. Scott, *J. Amer. Chem. Soc.*, 75, 141 (1953).
- (8) C. D. Ritchie, *Accounts Chem. Res.*, 5, 348 (1972); *ibid*, *J. Amer. Chem. Soc.*, 97, 1170 (1975).
- (9) W. P. Jencks and J. Carriuolo, *J. Amer. Chem. Soc.*, 82, 1778 (1960).
- (10) N. J. Fina and J. O. Edwards, *Int'l J. Chem. Kinetics*, 5, 1 (1973).

- (11) J. E. McIsaac, L. R. Subbaraman, J. Subbaraman, H. A. Mulhausen and E. J. Behrman, *J. Org. Chem.*, 37, 1037 (1972).
- (12) L. Larsson, *Svensk Kemisk Tidskrift*, 70, 405 (1958).
- (13) R. G. Pearson, H. Sobel and J. Songstand, *J. Amer. Chem. Soc.*, 90, 319 (1968).
- (14) V. Belluco, *Coord. Chem. Rev.*, 1, 111 (1966).

PHOTOSENSITIZED OXIDATION IN SOLUTION

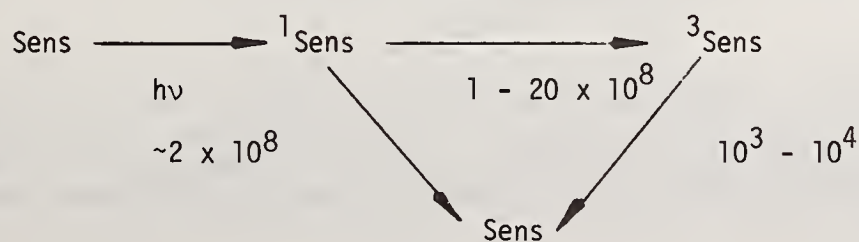
Christopher S. Foote
 Department of Chemistry, University of California
 Los Angeles, California 90024

Organic molecules are converted to chemically reactive electronically excited states on absorption of light. Only light that is absorbed can cause photochemical reactions. Absorption of light promotes an electron to a higher orbital without change of spin; thus, the first state formed is the singlet, in which there are no unpaired spins. The singlet in many cases undergoes a spin inversion very rapidly to give the triplet state (which has two unpaired electrons). Usually the triplet state lasts much longer than the singlet. Both states involve electrons promoted to higher orbitals; as these orbitals bind the electrons less strongly than do those of the ground state, one would expect that electrons in these orbitals would be more readily removed by oxidizing agents than would those in the ground state. By the same token, the holes left by the promoted electron are in orbitals that bind electrons comparatively strongly; thus, one would expect that the excited molecule that results would be more readily reduced than the molecule in the ground state. Both expectations are realized: Excited singlet and triplet molecules are both oxidized and reduced more readily than ground-state molecules.



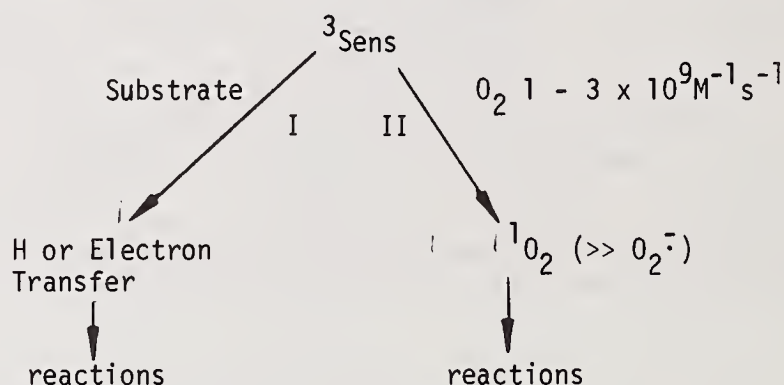
Photosensitized oxygenations of organic compounds have been studied for many years. (1-3) Recent studies have led to greatly increased understanding in this area. It is now possible to recognize several distinct mechanistic pathways, and to make a beginning in predicting which mechanism will occur in a given case. (4,5)

With few exceptions, sensitized oxidations proceed via the sensitizer triplet state, at least in part because the lifetime of the triplet is much longer than that of the singlet. (1-5) The most effective sensitizers are those that give a long-lived triplet state with high quantum yield. Many dyes, such as methylene blue or eosin, natural pigments (chlorophyll, hematoporphyrin, flavins), and aromatic hydrocarbons (rubrene, anthracene), are effective sensitizers. Most of these compounds absorb visible or near ultraviolet light. Typical rates for various sensitizer processes (in $M^{-1}sec^{-1}$) are given below. (5)



Mechanistic Classification

There are two broad classes of reaction open to the sensitizer triplet. (6) The first is one in which the sensitizer interacts with another molecule directly, usually with hydrogen atom or electron transfer. The radicals thus formed undergo further reaction with oxygen or other organic molecules. This reaction has been classed Type I by Gollnick. (1) The second class of reaction, Type II, is one in which the sensitizer triplet interacts with oxygen. The most common of the Type II interactions has been shown to be energy transfer to give singlet molecular oxygen, which reacts further with various acceptors in solution. (7,8) Less efficiently, in the studied cases, electron transfer to oxygen occurs with the formation of the superoxide ion ($O_2^{\cdot-}$); this reaction occurs in less than 1 percent of the deactivating collisions of oxygen with the sensitizer triplet. (9) These reactions are shown below.



The rates of reaction, k_I and k_{II} , of the two processes are now well enough known that many of the factors governing them can be stated definitively. The rate of the Type I process depends on the sensitizer and the substrate and varies over a wide range. (5)

In general, the types of molecular structure that favor Type I (substrate-sensitizer) chemistry are those that are readily oxidized (phenols, amines, etc.) or readily reduced (quinones, etc.). Compounds that are not so readily oxidized or reduced (olefins, dienes, aromatic compounds) more often favor Type II reactions; however, Type II reactions of amines (10), phenols (11), and other substrates are also known. The rates for the Type II process depend mainly on the oxygen concentration in solution, since the rate constant (k_{II}) with few exceptions falls in the range $1 - 3 \times 10^9 \text{ M}^{-1} \text{ s}^{-1}$ for all sensitizers. (1,5) Thus, for example, oxygen is much less soluble in water than in most organic solvents, so that in studies carried out in water saturated with air, the product $k_{II}[O_2]$ is much smaller than in organic solvents saturated with oxygen, as shown in Table 1. Unfortunately, biologists have tended to favor studies under the former set of conditions, whereas most mechanistic chemical studies have been carried out under the latter.

TABLE 1. Rates of Type II Process^a

Condition	$k_{II}[O_2], \text{ s}^{-1}$
Water saturated with air	$\sim 5 \times 10^5$
Organic solvent saturated with oxygen	$\sim 2 \times 10^7$

^aAssuming $k_{II} \sim 2 \times 10^9 \text{ M}^{-1} \text{ s}^{-1}$

The significant competition that determines whether Type I or Type II reaction occurs is thus between substrate and oxygen for triplet sensitizer. Table 2 shows that, for benzophenone in oxygen-saturated ethanol, the Type I process (with solvent ethanol) competes effectively with the Type II process; however, with eosin under the same condi-

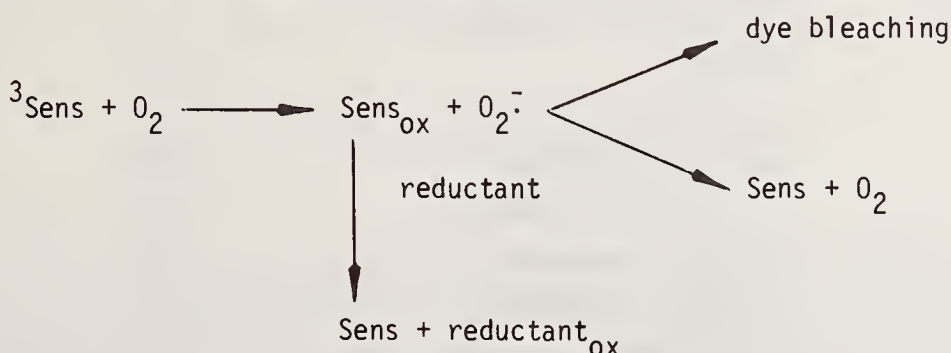
tions, the Type II process predominates and would continue to predominate even at very low oxygen concentration. It is probable that the same is true for bilirubin. Thus, changes in sensitizer, substrate, or concentrations of substrate and oxygen may change the mechanism of the photooxidation from Type I to Type II. It is also important to recognize that binding of dye to macromolecular substrates is likely to favor Type I mechanisms. (12,13)

TABLE 2. Competitive Rates of Type I and Type II Processes for Triplet-State Sensitizer in Ethanol

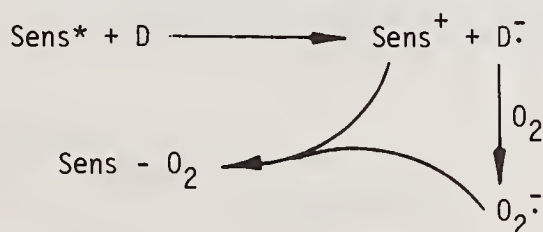
Sensitizer	Rates of Reaction by Type, sec ⁻¹	
	k _I [S]	k _{II} [O ₂]
(C ₆ H ₅) ₂ C=O	~10 ⁷	~2 x 10 ⁷
Eosin	~10 ³	~2 x 10 ⁷

Products of the Reaction

Type I chemistry usually involves the production of free radicals or radical ions. These radicals have a very wide variety of possible reactions, such as reaction with or electron transfer to oxygen, electron or hydrogen abstraction from other substrates, initiation of chain autoxidation, and recombination. Many apparently simple reactions of this type are found to involve complex sequences of reactions when scrutinized carefully. For example, the oxidized dye formed by electron donation to oxygen or another oxidizing species (including another dye molecule) can oxidize the substrate, regenerating dye and giving a new reactive species capable of further reaction or recombination with reduced primary oxidant. (9,14)

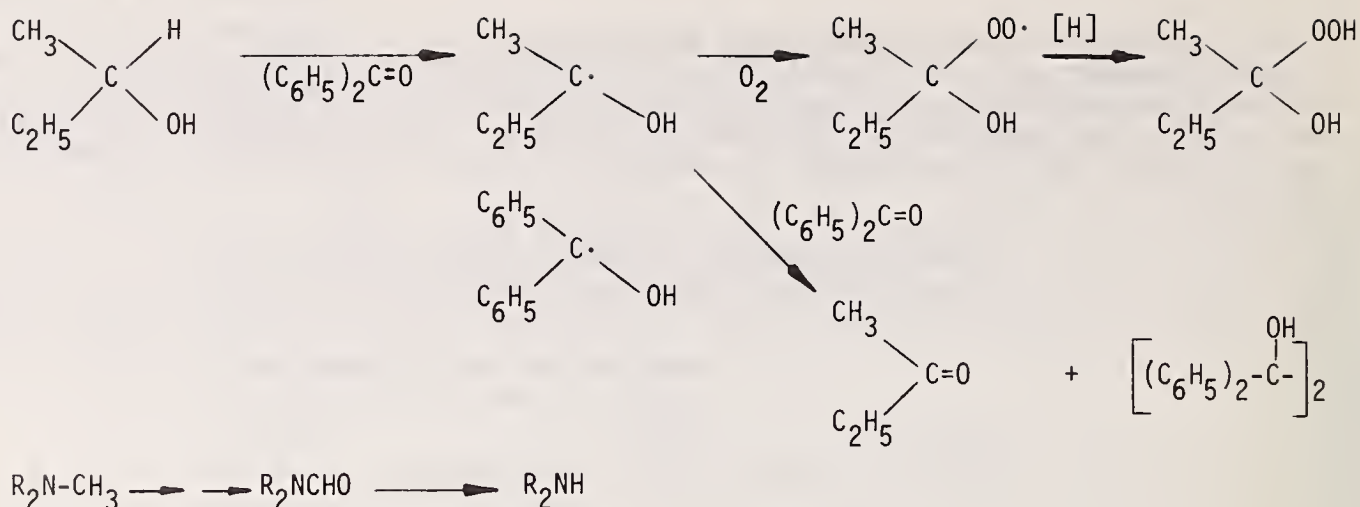


Alternatively, an electron donor can react with a sensitizer, giving a radical pair which can react further, as shown below. This reaction occurs well with singlet sensitizers which are electron poor. (15)



Shown below are two examples of Type I reactions: the oxidation of alcohols by benzophenone, which can lead either to ketone or hydroxyhydroperoxide, depending on the conditions (16), and the oxidation of amines, which may proceed either by hydrogen or

electron transfer. (17)



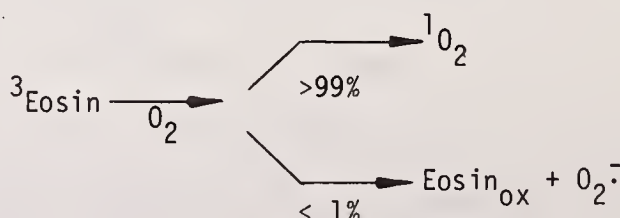
The type II reaction produces singlet molecular oxygen as the primary reactive species. (7,8) There are two excited states of singlet oxygen. The lower energy state, $^1\Delta_g$, is now believed to be the only singlet oxygen species that is reactive. The lifetime of $^1\Delta_g$ oxygen has recently been determined by direct methods and is moderately subject to influence by solvent. The lifetime is shortest in hydroxylic solvents: In water, the lifetime is about 10^{-6} s. (18-19) In aprotic solvents, and particularly in those with no hydrogens whatever, the lifetime is longer and reaches several hundred microseconds.

There is thus a second competition, between the decay rate of singlet oxygen and the product $k_A[A]$; if $k_A[A] \ll k_d$, the main result of a Type II reaction is simply the quenching of triplet sensitizer, and one may observe no reaction at all. Rates for some typical substrates are given in Table 3.

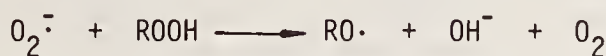
TABLE 3. Rates of Reaction of Some Typical Substrates with $^1\text{O}_2$

Acceptor	$k_A, \text{M}^{-1}\text{s}^{-1}$
2,5-Dimethylfuran	1.4×10^8
2,3-Dimethyl-2-butene	5×10^7
2-Methyl-2-pentene	1×10^6
1-Methylcyclohexene	2×10^5
Cyclohexene	3×10^3
<u>trans</u> -4-Methyl-2-pentene	3×10^3

Certain dyes that are less efficient oxidizers can also transfer an electron to oxygen, giving an oxidized dye molecule and superoxide ion. (9,20) For example, eosin reduces oxygen on a small fraction (<1%) of quenching collisions; the other collisions give singlet oxygen.



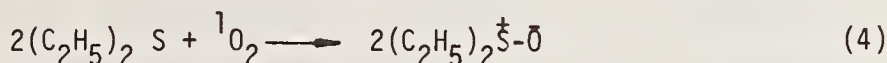
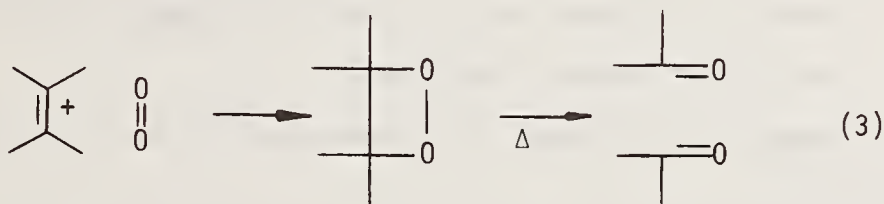
Both oxidized dye and superoxide can react further. Superoxide reacts with alkyl hydroperoxides and H_2O_2 to give reactive radical species capable of inducing autoxidation. (21)



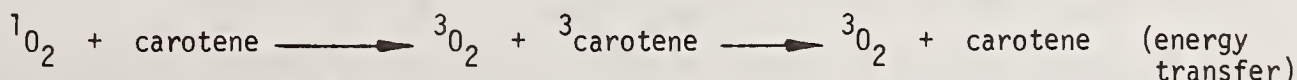
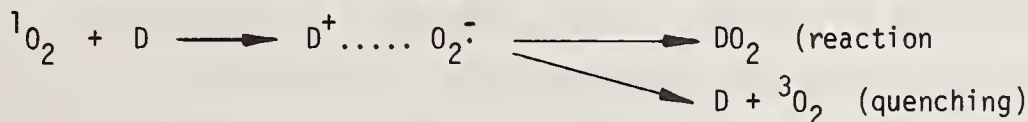
Two classes of reaction of singlet oxygen are particularly important: addition to olefins, giving allylic hydroperoxides, analogous to the Alder "ene" reaction of Eq. (1), and additions to diene systems to produce endoperoxides, analogous to the Diels-Alder reaction of Eq. (2). (2,22)



To these should be added two other classes of somewhat less generality, a 2 + 2 cycloaddition to electron-rich olefins (e.g., enamines and vinyl ethers) and a very few other olefins to produce dioxetanes [Eq. (3)], which are sometimes of moderate stability but readily cleave into two carbonyl-containing fragments (23-25), and oxidation of certain heteroatoms, notably sulfur and phosphorus [Eq. (4)], a reaction exemplified by the oxidation of diethyl sulfide to diethyl sulfoxide, in which two moles of sulfoxide are formed for each mole of oxygen consumed. (26)



Under ordinary conditions (dye sensitizer, oxygen-saturated in organic solvent, dilute substrate), Type I mechanisms do not occur for these types of substrate. Certain phenols and amines have also been shown to react with singlet oxygen; these reactions may well involve hydrogen or electron abstraction by singlet oxygen, and the overall chemistry resembles that observed in Type I cases. (10,11) Amines and phenols can also quench singlet oxygen; the mechanism of this quenching may also involve electron transfer. (10,11) Carotenes and other highly conjugated compounds with low triplet energies appear to quench by an energy transfer mechanism. (27,28)



REFERENCES

- (1) K. Gollnick, Adv. Photochem., 6, 1 (1968).
- (2) K. Gollnick and G. O. Schenck, in "1,4-Cycloaddition Reactions," J. Hamer, Ed., Academic Press, Inc., New York, 1967, pp 255-344.
- (3) R. Livingston, in "Autoxidation and Antioxidants," W. O. Lundberg, Ed., Vol. I, Interscience Publishers, New York, 1961, pp 249-298.
- (4) C. S. Foote, Science, 162, 936 (1968).
- (5) C. S. Foote, in "Free Radicals in Biology," W. A. Pryor, Ed., Vol. II, Academic Press, New York, 1976, pp 85-133.
- (6) G. O. Schenck and E. Koch, Z. Elektrochem, 64, 170 (1960).
- (7) C. S. Foote, Accounts Chem. Res., 1, 104 (1968).
- (8) D. R. Kearns, Chem. Rev., 71, 395 (1971).
- (9) A. G. Kepka and L. I. Grossweiner, Photochem. Photobiol., 14, 621 (1972).
- (10) W. F. Smith, Jr., J. Amer. Chem. Soc., 94, 186 (1972).
- (11) I. Saito, S. Kato, and T. Matsuura, Tetrahedron Lett., 239 (1970).
- (12) J. S. Bellin, Photochem. Photobiol., 4, 33 (1965).
- (13) K. J. Youtsey and L. I. Grossweiner, Photochem. Photobiol., 6, 721 (1967).
- (14) P. B. Merkel, R. Nilsson, and D. R. Kearns, J. Amer. Chem. Soc., 94, 1030 (1972).
- (15) C. S. Foote and T. Parker, unpublished.
- (16) G. O. Schenck, H.-D. Becker, K.-H. Schulte-Elte, and C. H. Krauch, Chem. Ber., 96, 509 (1963).
- (17) R. F. Bartholemew and R. S. Davidson, J. Chem. Soc. D, 1174 (1970).
- (18) D. R. Adams and F. Wilkinson, J. Chem. Soc., Faraday Trans. 2, 68, 586 (1972).
- (19) P. B. Merkel and D. R. Kearns, J. Amer. Chem. Soc., 94, 1029 (1972).
- (20) V. Kasche and L. Lindqvist, Photochem. Photobiol., 4, 923 (1965).
- (21) J. W. Peters and C. S. Foote, J. Amer. Chem. Soc., 98, 873 (1976).
- (22) A. Nickon, V. T. Chuang, P. J. L. Daniels, R. W. Denny, J. B. DiGiorgio, J. Tsunetsugu, H. G. Vilhuber, and E. Werstiuk, J. Amer. Chem. Soc., 94, 5517 (1972).
- (23) P. D. Bartlett and A. P. Schaap, J. Amer. Chem. Soc., 92, 3223 (1970).
- (24) C. S. Foote and J. W.-P. Lin, Tetrahedron Lett., 29, 3267 (1968).
- (25) S. Mazur and C. S. Foote, J. Amer. Chem. Soc., 92, 3225 (1970).
- (26) C. S. Foote and J. W. Peters, in XXIIIrd International Congress of Pure and Applied Chemistry, "Special Lectures", Vol. 4, Butterworths & Co. Ltd., England, 1971 pp 129-154.
- (27) C. S. Foote and R. W. Denny, J. Amer. Chem. Soc., 90, 6233 (1968).

(28) C. S. Foote, Y. C. Chang, and R. W. Denny, J. Amer. Chem. Soc., 92, 5216 (1970).

CHEMICAL DEGRADATION OF ORGANIC POLLUTANTS IN THE ENVIRONMENT

V. H. Freed
Oregon State University
Corvallis, Oregon 97331

Soil becomes the ultimate residence of a great deal of the organic pollutants that may be released into the environment. It also receives quantities of a wide variety of organic compounds that arise out of natural systems. The synthetic chemicals may be industrial effluents, waste products, or chemicals that have been used as pesticides. Detailed studies have shown that a variety of things can happen to the chemical once it reaches the soil. The chemical may be further transported by leaching or soil erosion or even by evaporation from the soil surface. Almost certainly, any chemical in intimate contact with the soil will be sorbed to a greater or lesser degree by one of the fractions.

Once in the soil, the organic pollutant is subject to a number of physical, chemical, and biological processes. It may undergo complexation, be subject to chemical reactions, or be modified and degraded by a series of biochemical reactions mediated by organisms or extra-cellular enzymes. This presentation is primarily concerned with certain of the physical and chemical reactions in soil leading to degradation, excluding the redox reaction which is the subject of another presentation.

Among the pollutants, the pesticides and their degradation have been the most extensively studied in soils. Consequently, many of the examples used are those of pesticides, but this poses no serious limitations. Many organic groupings are represented among the pesticides, thus providing appropriate models for a number of organic compounds from other sources.

In considering the non-biologically mediated reactions of organic pollutants in soil, we are left with the photochemical and the chemical. For obvious reasons the photochemical reactions are probably of little significance in degradation of organic pollutants once the chemical has entered the soil. Indeed, once sorbed even at the surface of the soil, photochemical degradation is probably slow. The importance of chemical reaction including coordination or complexation may be of variable importance depending on the nature of the pollutant under consideration. With some compounds, investigators have found the rate of chemical reaction in soil under environmental conditions to be slow compared to the biologically mediated reactions. Thus, for example, while the chlorotriazines are hydrolyzed by soil, the chemical hydrolysis catalyzed by benzoxyazinone is more related to plants since the catalyst is presumed to be a constituent thereof. On the other hand, certain of the organophosphorus insecticides have been shown to undergo hydrolysis that is catalyzed by clays. The relative importance then of the purely chemical hydrolysis of an organic pollutant in soil must be determined for the individual compound as there is not yet sufficient data to allow a generalization.

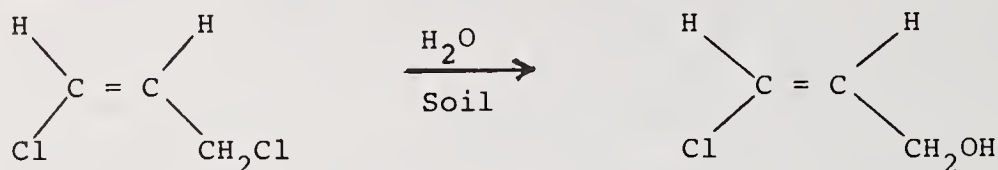
Coordination

A number of organic pollutants have been shown to react with various cations to form coordination complexes. In some instances, this occurs in solution, in other instances, the coordination occurs at exchange sites on the clay colloid that are occupied by the appropriate element. An example of the first instance is the compound aminotriazole that forms coordination complexes with certain of the transition elements such as nickel, cobalt, and copper. The alkyl amines on the other hand, coordinate with the element located on a reactive site of clay complexes.

Certain elements present in the soil or added as an amendment may serve as a catalyst in the degradation of pollutants. It has been found that magnesium oxide catalyzes the dehydrochlorination of DDT to DDE.

Hydrolysis and Other Nucleophilic Reactions

Perhaps the most extensively studied chemical reaction leading to degradation of organic pollutants is that of hydrolysis. A number of compounds are sufficiently reactive to undergo hydrolysis including the halogen substituted alkanes and alkenes, esters, amides, anhydrides, and epoxides. The soil fumigant, 1,3-dichloropropene is hydrolyzed in soil to either cis- or trans- 3-chloroallyl alcohol as shown in the following reaction:



The organophosphorus insecticides have perhaps been the most extensively studied group of organic pollutants as regards hydrolysis in soil. Parathion (o,o-diethyl paranitrophenyl phosphorethiolate) has been shown to undergo slow hydrolysis even on dry soil.



That the soil is important in the hydrolysis of the organophosphorus chemicals is illustrated by the much more rapid rate of hydrolysis of malathion in soil than in aqueous solution.

Other types of compounds shown to undergo hydrolysis included the n-methyl carbamates in which the half-life of the 4-N-methyl benzothienyl carbamate was shown to be something under 8 days at 20°C. The esters of carboxylic acids such as the esters of 2,4-D undergo rapid hydrolysis in soil.

Factors Influencing Rates of Hydrolysis

As would be expected in so complex a system as the soil, a number of factors are operative in determining the rate of hydrolysis. At a given moisture content the most important factors appear to be temperature and pH of the soil. Other rate determining factors include the soil type, the nature of the clays present, the ions, e.g. alkali and alkaline earth cations, salt concentration, and the concentration of the pollutant.

Only limited studies have been performed in measuring actual reaction rates and determination of the apparent orders of the hydrolysis reaction in soil. Obviously, with the complexity of reactions, it is difficult to separate the biologically mediated reactions from the chemical reactions except by heat or radiation sterilization of the soil. However, with some of the compounds studied the pseudo first-order kinetics appears to describe rates reasonably well. With a few compounds, notably the chlorinated picolinic acid, picloram, a hyperbolic law appears to best describe the observed rates.

Chemical reactions, notably hydrolysis, coordination, oxidation and reduction, play a role in degradation of organic pollutants in soil. Though the rates are not always comparable to the biologically mediated reactions, nonetheless, the chemical reactions probably play an important role in degradation. There has not been sufficient study of the purely chemical reactions in degradation of organic pollutants to give an intimate understanding of their importance with all classes of compounds. This is an area warranting much more research in the future.

Solar Spectral Irradiance Reaching the Ground

Alex E. S. Green

Interdisciplinary Center for Aeronomy
and (other) Atmospheric Sciences

1. Introduction

I will present some illustrative results of intensive calculations carried out to assist scientists concerned with the biological consequence of ultraviolet radiation. These results are given in the form of practical "engineering formulas" which give ground based UV spectral irradiances, dose rates, daily doses, and annual doses for various atmospheric models, locations and time of year. While the results are specialized to the 280-340 nm spectral region, the formulas can also be applied to other spectral regions with an appropriate readjustment of parameters.

2. Elementary Concepts of Atmospheric Transmission

The calculation of solar radiation reaching the ground has many aspects which are familiar to radiation physicists, photobiologists, and many other scientists. Essentially the sun is the radiation source, the atmosphere is the propagating medium, which absorbs, diffuses, or in some cases reemits radiation, and people, animals, plants, or instruments serve as detectors.

Let us first consider the simplest aspect of the atmospheric radiative transfer, namely the law of attenuation, variously attributed to Beer, Lambert or Bouguer. Suppose we have a collimated beam of monoenergetic incident light particles with the intensity I (photons/cm²sec). We introduce into this beam a thin (Δw) layer of substance having n molecules/cm³. If these molecules interact with the incident beam, the transmitted beam intensity will be reduced by the effective area blocked out by the $n\Delta w A$ molecules in the beam. If the reduction in intensity is ΔI , we may define an area associated with each molecule by means of

$$\frac{\Delta I}{I} = - \frac{\sigma n \Delta w A}{A} = -\sigma n \Delta w \quad (1)$$

The number of molecules per cubic centimeter may be calculated using $n = \rho N_a / M_a$, where ρ is the density (in gr/cm³), N_a is Avogadro's number, and M_a is the gram molecular weight.

The characteristic area σ obtained from such an experiment depends upon the properties of the target molecules, and the nature of the incident light or particles. Our assumption of a thin layer permits us to ignore the overlap of the areas associated with different molecules.

In many types of absorbing processes we may assume that σ is independent of the distance of penetration. This is usually true for light quanta, when spectrally separated at high resolution, and gamma rays and neutrons passing through solids. However, it is not true for infrared radiation measured at low resolution or for charged particles such as electrons and protons, which interact with many scatterers via the long-range coulomb forces. In these latter cases the quality of the beam degrades and hence the value of σ varies with depth. In the former case, i.e. when σ is constant, we may integrate Eq. (1) to obtain

$$I = I_0 e^{-\sigma n w} \quad (2)$$

where I_0 is the incident intensity and I is the intensity at any depth w in the absorber.

In atmospheric problems the number densities are altitude dependent, hence, we must calculate the total thickness of a column of air above an observer. We may do so using

$$w(y) = \int_y^\infty \rho(y) dy \quad (3)$$

where y is the altitude variable and $\rho(y) = n(y)/n_0$ is the relative density. To allow for the extra thickness, when the look angle departs from the zenith (see Fig. 1a), we usually divide w by μ where $\mu = \cos\theta$. This may be called the flat earth approximation. Accordingly the formula for transmission is

$$T = I/I_0 = e^{-n_0 \sigma w / \mu} = e^{-k w / \mu} = e^{-\tau / \mu} \quad (4)$$

where $k = n_0 \sigma$ is the attenuation coefficient and $\tau = k w$ is the optical depth.

When we have several attenuators along a path, the total transmission is simply the product of the transmission function for each attenuator or the optical depth is the sum of the component optical depths. Figure 1b (Green, Sawada, Shettle (GSS), 1974) illustrates the simplest model which can, with some degree of realism, be applied to the problem of attenuation of solar ultraviolet radiation by ozone, air molecules and atmospheric aerosols.

3. The Transmitted Solar UV Irradiance at the Ground

Using the foregoing formulas, the downward component of the transmitted solar irradiance is given by

$$B_t(\theta, \lambda) = \mu H(\lambda) \exp - A_t(\theta, \lambda) \quad (5)$$

where

$$A_t(\theta, \lambda) = \sum_i w_i(\lambda) k_i(\lambda) / \mu_i \quad (6)$$

Here $H(\lambda)$ is the extraterrestrial solar flux, θ is the solar zenith angle, $i = 1, 2, 3$ denote air, particulates and ozone respectively, $w_i(y)$ denote the altitude dependent vertical thickness, $k(\lambda)$ the wavelength dependent attenuating coefficient. To allow approximately for the fact that the earth is round, we use a generalization of $\mu = \cos\theta$ given by

$$\mu_i = [(\mu^2 + t_i) / (1 + t_i)]^{1/2} \quad (7)$$

where t_i are species dependent dimensionless parameters, which keeps μ_i from going to zero at 90° .¹ To a reasonable approximation the extra terrestrial solar irradiance in low resolution in any narrow spectral region may be approximated by a linear relationship.

$$H(\lambda) = K \left[1 + \frac{\lambda - \lambda_0}{d} \right] \quad (8)$$

The parameters K , d and λ_0 for the 280-340 nm region are given in Table 1. Note that this formula yields 1 watt/m² nm at $\lambda = 330$ nm (see Fig. 2), which might be compared with the integrated solar constant of 1.37 kw/m². If we now specify the optical depths of the three components at a standard wavelength and their wavelength dependencies, we can simply calculate the downward transmitted component of the sun's UV irradiance using Eqs. (5) and (6). The spectral dependence of the optical depth for ozone, air and a representative aerosol model in the UV region of interest are illustrated in Fig. 3. These are based upon analytic representations of the attenuation coefficients given by

$$k_1 = k_a (\lambda_0/\lambda)^{\nu_a}, \quad k_2 = k_p (\lambda_0/\lambda)^{\nu_p}, \quad \text{and } k_3 = k_{oz} \exp -[(\lambda-\lambda_0)/d_0] \quad (9)$$

and the thickness vs. altitude functions

$$w_1 = w_{10} \left[\frac{(1+\alpha)}{\alpha+e} \right]^{y/h_1} \quad (10)$$

$$w_2 = w_{20} \frac{(1+\alpha_2)}{(\alpha_2+e)} \left(\frac{y}{h_2} \right) + w'_{20} \frac{(1+\alpha')}{(\alpha'+e)} \left(\frac{y}{h'_2} \right) \quad (11)$$

$$w_3 = w_{30} / \left[1+e^{(y-y_3)/h_3} \right] + w'_{30} e^{-y/h'_3} \quad (12)$$

Suitable constants for a standard atmosphere are given in Table 1. Figure 4 illustrates the downward transmitted irradiance as a function of the solar zenith angle computed using these equations and parameters.

4. The Diffuse Spectral Irradiance

Prior to 1974, almost all UV spectral irradiance calculations considered only the directly transmitted solar irradiance (i.e. sunlight), but ignored the diffusely scattered irradiance (i.e. skylight). The available UV skylight calculations (Dave and Furukawa, 1966) consider only the case of a purely molecular cloud-free atmosphere. To deal with the turbid atmosphere prevailing over most population centers, we proceeded along several parallel paths. One path (Green, Sawada, Shettle, 1974) was addressed towards developing an analytic representation of the diffuse spectral irradiance in the middle ultraviolet which could serve as a synthesis of the 10-year UV measurement program of Bener(1972). The second path (Shettle and Green, 1974) used a simple and fast multiple scattering calculational technique to obtain the UV skylight component. When completed, this was found to conform reasonably well to our analytic synthesis as well as to the more elaborate multiple scattering calculations of Dave and Braslau (1975). A third path (Mo, Kezwer and Green, 1975) utilized a simple two-stream approximation to analytically represent multistream solutions of the radiative transfer equation. A fourth path (Chai and Green, 1976) involved measurements of the ratio of the diffuse to transmitted components which follows a fairly simple systematics.

According to GSS, the downward scattered irradiance may be represented by the empirical formulas

$$B_s(\theta, \lambda) = H(\lambda) \exp - D_s(\theta, \lambda) \quad (13)$$

where

$$D_s(\theta, \lambda) = L_{ap}/\mu_{ap} + L_{oz}/\tilde{\mu}_{oz} \quad (14)$$

$$L_{oz} = K_{oz} e^{\kappa k_{oz} w_3 - (\lambda - \lambda_o) / \delta} \quad (15)$$

$$L_{ap} = \ell_o \left[1 + \ell_1 y + \ell_2 (w_2 k_p - \ell_3)^2 \right] \quad (16)$$

where μ_{ap} has the form of Eq. (7) but with

$$t_2 \rightarrow s_2 = t_{20} (1 + t_{21} y) \quad (y \text{ in Km}) \quad (17)$$

and where (with a minor change from GSS)

$$\tilde{\mu}_{oz} = \left[\left(1 - \frac{\sin^p \theta}{q} \right) \frac{\lambda - \lambda_o}{\delta p} \right] \times \left(\frac{\mu^2 + s_3}{1 + s_3} \right)^{1/2} \quad (18)$$

The constants for this equation are also given in Table 1, Figure 5 illustrates the diffuse spectral irradiance based upon these analytic representations of the systematic experimental results of Bener.

The global flux $G(\theta, \lambda)$ can now be obtained by addition i.e.

$$G(\theta, \lambda) = B_t(\theta, \lambda) + B_s(\theta, \lambda) \quad (19)$$

While these formulas are simply empirical representations of experimental data or of ab-initio multiple scattering calculations they can serve the valuable purpose of providing approximate estimates of skylight in a form almost as convenient as that of Beer's law for the transmitted component of sunlight.

5. Irradiances or Dose-Rates

For many purposes we are not interested in the spectral irradiance at the ground but rather the irradiance as measured with a detector or biological system with a given response function (Green, Mo and Miller (GMM) 1974). The specification of the relative efficiency $\epsilon(\lambda)$ of a detector enables us to translate a spectral irradiance into an irradiance or dose rate. For example

$$\phi_t(\theta) = \int \epsilon(\lambda) B_t(\theta, \lambda) d\lambda \quad (20)$$

is the transmitted irradiance associated with a transmitted spectral irradiance $B_t(\theta, \lambda)$. The units of $\phi_t(\theta)$ is effective-watts/m², or (W/m²)_e, a unit which is defined relative to the specific efficiency curve chosen.

For illustration let us choose an analytic representation of the relative erythema spectrum measured by Coblentz and Stair (1934) as the standard $\epsilon(\lambda)$. In the 280-340 nm region this $\epsilon(\lambda)$ can be accurately represented by (see Fig. 6)

$$\epsilon(\lambda) = 4 \exp\left(\frac{\lambda - \lambda_p}{\lambda_f}\right) / \left[1 + \exp\left(\frac{\lambda - \lambda_p}{\lambda_f}\right) \right]^2 \quad (21)$$

Figure 7 illustrates the results of a numerical calculation of the integral defined by Eq. (21) and the correspond scattered dose rate for a standard atmospheric condition. It should be noted that the erythema dose rate associated with the diffuse flux in this instance is larger than that associated with the transmitted flux.

It is noteworthy that these numerical results can be represented quite accurately by simple analytic functions of angle. For example the global dose rate $\phi_g = \phi_t + \phi_s$ may be

represented accurately by

$$\phi_g(\theta) = \mu \phi_g(0) e^{\kappa} e^{-\kappa/\mu_g(\theta)}, \quad \left(\mu = [(\mu^2 + g)/(1 + g)]^{\frac{1}{2}} \right) \quad (22)$$

where μ_g is defined by Eq. 7 (with $t \rightarrow g$). The quantity $\phi_g(0)$ equals the value of $\phi_g(\theta)$ at $\theta = 0$ and the parameters κ and g can be obtained by fitting Eq. 22 to the numerical results of the integrations. We have found that these parameters are smooth slowly varying functions of ozone concentrations (see GMM).

6. Daily Dose

The daily dose corresponding to the global irradiance or dose rate may be defined by

$$\Delta = \int \phi_g(\theta) dT \quad (23)$$

where $\phi_g(\theta)$ may now be represented by Eq. (22), and the integration with respect to the time of day (T) is from sunrise to sunset. The relationship between the time of day (measured from noon) and latitude (L) and solar declination (D) is given by

$$\mu = \cos\theta = \sin L \sin D + \cos L \cos D \cos T \quad (24)$$

where T the hour angle is measured from the local noon. Using this equation the quantities $\phi_g(\theta)$ and μ_g become implicit functions of time.

We have evaluated many integrals of this form of Eq. (23) and have found it possible to represent the results of such numerical integration quite accurately (1% - 3%) with the formula

$$\Delta = 2c_t \bar{\phi}_g \left[\sin L \sin D \cos^{-1}(-\tan L \tan D) + \sqrt{\cos^2 L \cos^2 D - \sin^2 L \sin^2 D} \right] \quad (25)$$

where $c_t = 13751$ sec/rad converts the hour angle T (in radian) to time (in sec) and

$$\bar{\phi}_g = \phi_g(0) e^{\bar{\kappa}} \left[\frac{\rho + 1}{\bar{\kappa}/\mu_g(L-D)} \right] \quad (26)$$

The best-fit values of $\bar{\kappa}$, and \bar{g} for different amounts of ozone are smooth functions (see GMM) and ρ may be taken as a constant. The results of such a fit to numerical outputs are illustrated in Fig. 8 which shows the latitudinal and monthly variation of the daily erythema dose for standard atmospheric conditions.

6. Annual Doses

The analytic representation of daily dose as a function of solar declination and latitude and the parameters which characterize the ozone distribution and turbidity may be used to calculate the annual dose for any location in terms of the climatological data. Mo and Green (1974) have found that for a cloudless sky the annual erythema dose can be accurately represented as a function of latitude by the analytic expression

$$D_a(L) = B / \left[1 + e^{(L-L_0)/L_f} \right] \quad (27)$$

where $D_a(L)$ represents the annual erythema dose in effective joules/m² or (joules/m²)_e at the latitude L (in degrees). The adjustable parameters B, L_o, L_f are obtained by NLLS fitting the numerically calculated results of annual erythema doses. The points in Fig. 9 are the annual erythema doses calculated with the experimentally determined worldwide ozone distribution, which depends on the geographic latitudes and seasons of the year (12) and with an assumed ground albedo of 0.05. The solid curve in Fig. 9 represents the fit to these points with Eq. (27) and the parameters

$B = 24.1 \times 10^5$ (Joules/m²)_e, $L_o = 30$, $L_f = 15$. Calculations with a 5%, 10% and 20% reduction of the ozone distribution are also exhibited in Fig. 9. These modified curves can be represented accurately by Eq. (27) with the constant B replaced by

$$B' = B e^{\alpha f} \quad (28)$$

where $\alpha = 1.53$ and $f = -\Delta w_{oz} / w_{oz}$ is the fractional depletion of the ozone column thickness (w_{oz}).

If we chose other types of response curves e.g. the DNA absorption spectrum we will obtain results which also can be fit by these equations but with altered parameters.

Calculations on the influence of cloud cover, cloud and smog thickness, ground albedo and local ground elevations (i.e. altitude) upon the annual dose may be approximately accommodated by generalizing Eq. (27) to the form

$$D_a = B e^{\alpha f} \left(\frac{1 - \Gamma e^{\theta} C_{\ell}}{(L - L_o) / L_f} \right) \cdot \left(\frac{e^{h/H - \tau_s / \tau_{so}}}{1 - r_o A} \right) \quad (29)$$

where $H = 8$ Km, $\tau_{so} = 4.2$, $\Gamma = 0.056$, $r_o = 1/3$

$$\theta = \sqrt{\tau_c / \tau_{co}} - 1 \text{ with } \tau_{co} = 15.$$

The denominator of the first factor allows for the latitude dependence of the annual erythema dose. The numerator of the first factor allows for the cloud cover (C_{ℓ}) and cloud thickness (τ_c) and is based upon the work of Buttner (see Cutchis (1973) and Nack and Green (1974)). Values of C_{ℓ} (measured in tenths from 0-10) for many metropolitan areas can be obtained from the Climatic Atlas (NOAA, 1969; see also MG). Unfortunately data does not appear to be available on cloud thickness. The denominator $(1 - r_o A)$ in the second factor corrects for the ground albedo (A) where r_o is an approximate air-ground-air reflection coefficient for the solar radiation in the 300^o- 320 nm interval (2). Values of A can be as large as 0.75 for snow conditions. The factor $e^{h/H}$ represents the influence of local ground altitude, (h) as suggested by the results of Bener (1972). The factor $e^{-\tau_s / \tau_{so}}$, where τ_s is the smog optical depth at ~305 nm, is a correction suggested by the results of Nack and Green (1974).

The same correction factors shown in Eq. (29) may be used in daily dose rate or spectral irradiance calculations as an approximate basis for allowing for cloud cover, smog, etc. In most cases the uncertainty in climatological data is the primary limitation on the accuracy of the predicted results.

7. An Application of Dose Calculations

Our approximate methodology for assigning dose may be used for a variety of applications. For example one might attempt to correlate the calculated annual doses with reported skin cancer incidence rates (Green and Mo, 1974, Green et al 1976). Figure 10 illustrates such a correlation for two sets of non-melanoma skin cancer data (1) older data in the literature from the United States, United Kingdom, Canada and Australia (points) and (2) recent data from the recent Third National Cancer Survey (circles). Also shown

are best fit curves satisfying the functional form

$$R = R_0 e^{D/Do} \quad (30)$$

While the values of R_0 differ for the two sets of data it is interesting to note that the same e folding dose $Do \sim 0.33$ can be used for both. This is important since such a non-linear dose response curve implies a varying relationship between an percentage increase in dose and the corresponding percentage increase in incidence rate i.e.

$$\beta = (dR/R) / (dD/D) = D/Do \quad (31)$$

For example for Northern U.S.A. ($D \sim .4$) $\beta \sim 1.2$; for Central U.S.A. ($D \sim .7$) $\beta \sim 2.1$ whereas for Southern U.S.A. ($\beta \sim 1$) $\beta \sim 3$.

A number of other applications of our spectral irradiance, dose rate and dose calculations to other biological systems have been made (Nachtwey Ed. 1975 Vol 5 CIAP)

8. Summary and Conclusion

The subject of atmospheric radiative transfer is now undergoing very rapid development and the literature is expanding at a fast pace (see Coulson, Fraser, 1975). Theoretical work in this field usually requires the use of large computers to solve the complex integrodifferential equation of radiative transfer. The influence of clouds, smog, and other climatological variables upon calculated irradiances has just been explored and much work remains. Experimental work is fraught with many technical problems and it is quite difficult even under clear sky conditions to measure spectral irradiance or integrated irradiance with accuracies better than 5%. It is very difficult to characterize the influence of clouds upon spectral irradiance measurements in any organized way.

For these various reasons there tends to be a large gap between atmospheric radiative transfer specialists and persons who need to know atmospheric radiation levels for various applied problems. The formulas presented in this report were developed for the purpose of bridging the gap in the important spectral region extending from 280 nm - 340 nm. From a number of exploratory calculations however, we have become convinced that these formulas can be adapted to serve in a much larger context mostly by a simple readjustment of the parameters.

The author would like to thank his many collaborators for their assistance in these endeavors and the National Science Foundation and the Department of Transportation for their support.

REFERENCES

1. Bener, P. (1972), European Research Office, U.S. Army, London, Contract No. DAJA37-68-C-1017, 59 pp.
2. Chai, A.T., and A.E.S. Green (1976), to be published in Appl. Opt.
3. Coblentz, W.W. and R. Stair (1934), U.S. Bureau of Standards Journal of Research 12, 13-14.
4. Coulson, K.L., and R.S. Fraser (1975), R. Geophys. and Space Physics, 13.
5. Cutchis, P. (1974) Science, 184, 13-19.
6. Dave, J.V., and P.M. Furukawa (1966), Meteor. Monographs, 7, 1-10.
7. Dave, J.V., and N. Braslau, J. Appl. Meteor. (1975), 14, 388-395.
8. Green, A.E.S., T. Sawada and E.P. Shettle (1974), Photochem. Photobiol., 19, 251-259.
9. Green, A.E.S., T. Mo and J.H. Miller (1974), Photochem. Photobio., 20, 473-482.
10. Green, A.E.S., G. B. Findley Jr., W.M. Wilson, K.F. Klenk and T. Mo (1976), submitted for publication.
11. Mo, T., G.P. Kezwer and A.E.S. Green (1975), J.G.R., 80, 2672-2676.
12. Mo, T. and A.E.S. Green (1974) Photochem. Photobio., 20, 483-496.
13. Nack, M.L. and A.E.S. Green, (1974) Appl Opt., 13, 2405-2415.
14. Nachtwey, D.S. (1975) Editor, CIAP Monograph 5, DOT-TST-75-55, Final Report.
15. Shettle, E.P. and A.E.S. Green (1974), Appl. Opt. 13, 1567-1581.
16. U.S. Department of Commerce (1968), Climatic Atlas of the United States, 72

Table 1

Constants Associated with Transmitted and Diffuse Flux

<u>Air (1)</u>	<u>Particulates (2)</u>	<u>Ozone (3)</u>	<u>Diffuse</u>
$w_{10} = 8.423 \text{ Km}$	$w_2 = 1.404 \text{ Km}$	$w_3 = 0.32 \text{ cm}$	$L_{ap} = 0.873$
$k_a = 0.145 \text{ Km}^{-1}$	$k_p = 0.260 \text{ Km}$	$k_{oz} = 10 \text{ cm}^{-1}$	$K_{oz} = 1.32$
$v_a = 4.27$	$v_p = 0.58$	$t_3 = 0.0074$	$\kappa = 0.277$
$t_1 = 0.0018$	$w_{20} = 1.40 \text{ Km}$		$\delta = 7.70 \text{ nm}$
$\lambda_o = 300 \text{ nm}$	$h_2 = 1.0 \text{ Km}$	$d_o = 8 \text{ nm}$	$p = 3.887$
$h_1 = 6.42 \text{ Km}$	$\alpha_2 = 0.4$	$w_{30} = 0.304 \text{ cm}$	$q = 1.269$
$\alpha = 0.312$	$w_{20}' = 0.0045 \text{ Km}$		$s_2 = 0.06$
	$h_2' = 2.5 \text{ Km}$		$s_3 = 0.12$
$K = 0.552 \frac{\text{Watts}}{\text{m}^2 \text{-nm}}$	$\alpha' = 2981$	$y_3 = 23.2 \text{ Km}$	$l_o = 0.872$
$d = 37 \text{ nm}$	$t_2 = 0.0003$	$h_3 = 4.63 \text{ Km}$	$l_1 = 0.179$
		$w_{30}' = 0.0177 \text{ cm}$	$l_2 = 0.0487$
		$h_3' = 5.78 \text{ Km}$	$l_3 = 0.538$
			$t_{20} = 0.06$
			$t_{21} = 1.867$

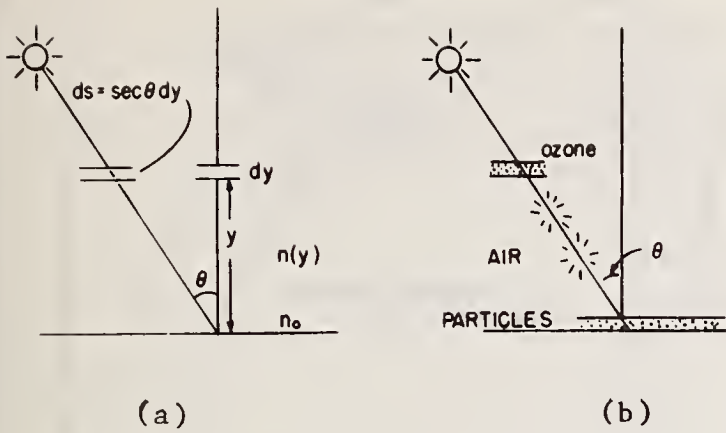


Fig. 1 Schematic illustration of the direct solar irradiance reaching the Earth's surface. (a) geometry (b) transmission through ozone, air and aerosol layers (adapted from GSS)

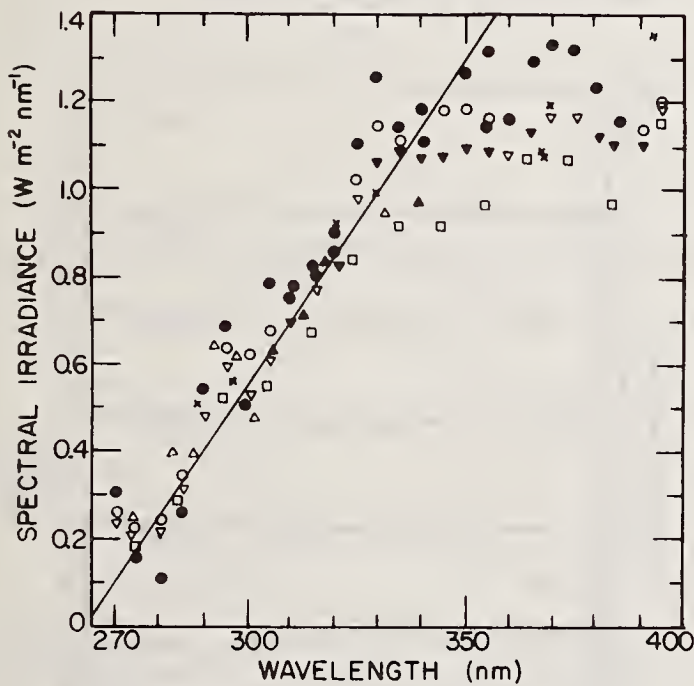


Fig. 2 Plot of reduced measurement points from pertinent references (see GSS). The straight line represents Eq. (8) (adapted from GSS).

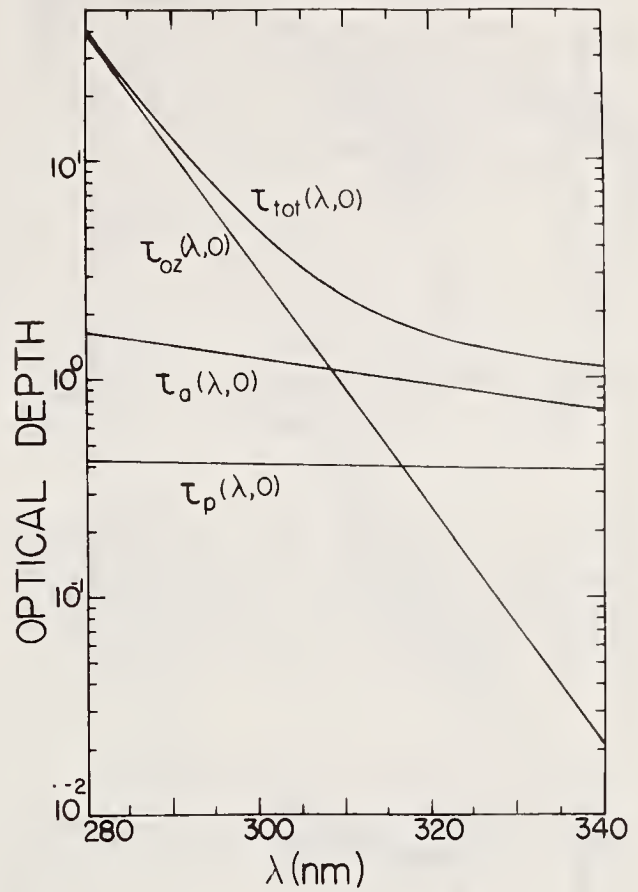


Fig. 3 Optical depths of atmospheric constituents as a function of wavelength (adapted from SG).

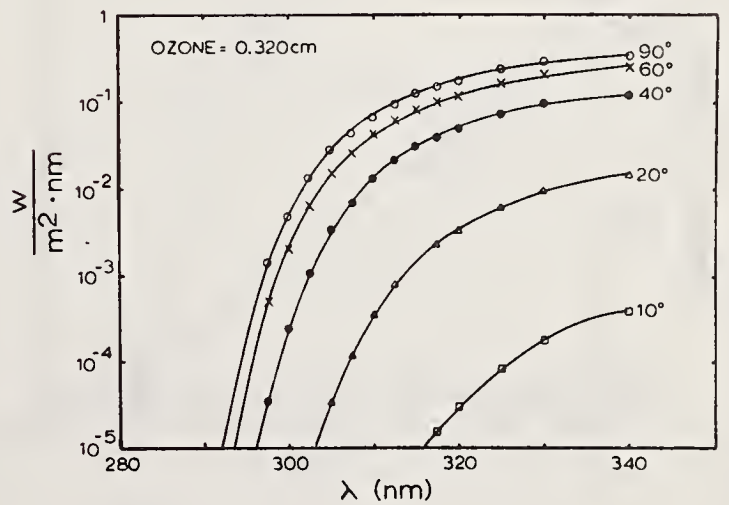


Fig. 4 Solar Direct-Beam ultraviolet energy spectra at several solar elevation angles. Atmospheric ozone content = 0.320 cm STP.

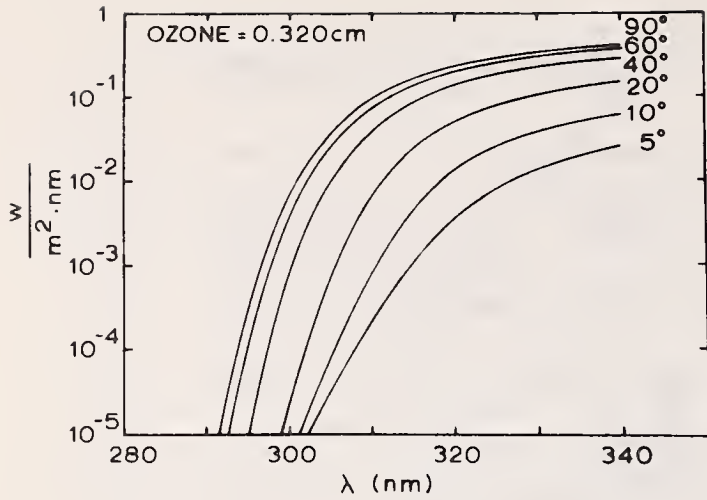


Fig. 5 Diffuse Sky ultraviolet energy spectra at several solar elevation angles. Atmospheric ozone content = 0.320 cm STP.

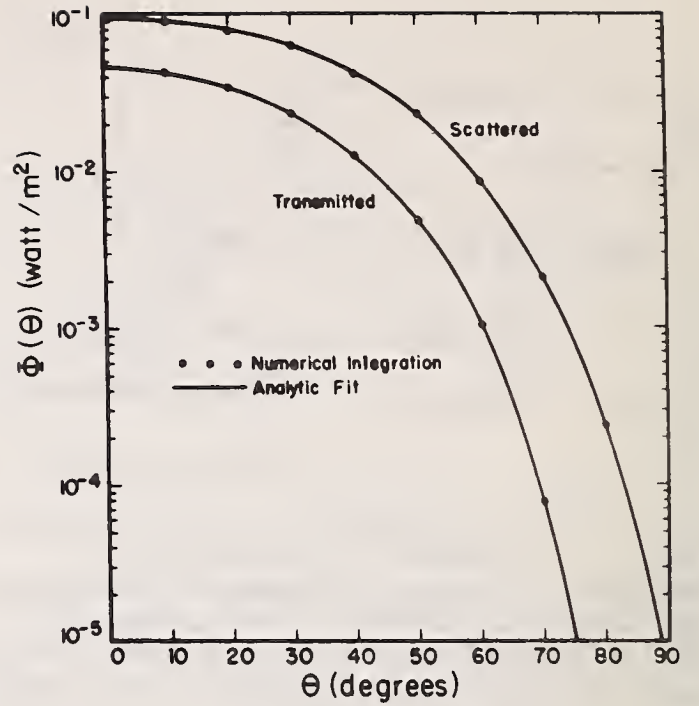


Fig. 7 Transmitted and scattered UV Dose Integrals vs. the zenith angle of the sun, ozone content = 0.320 cm STP.

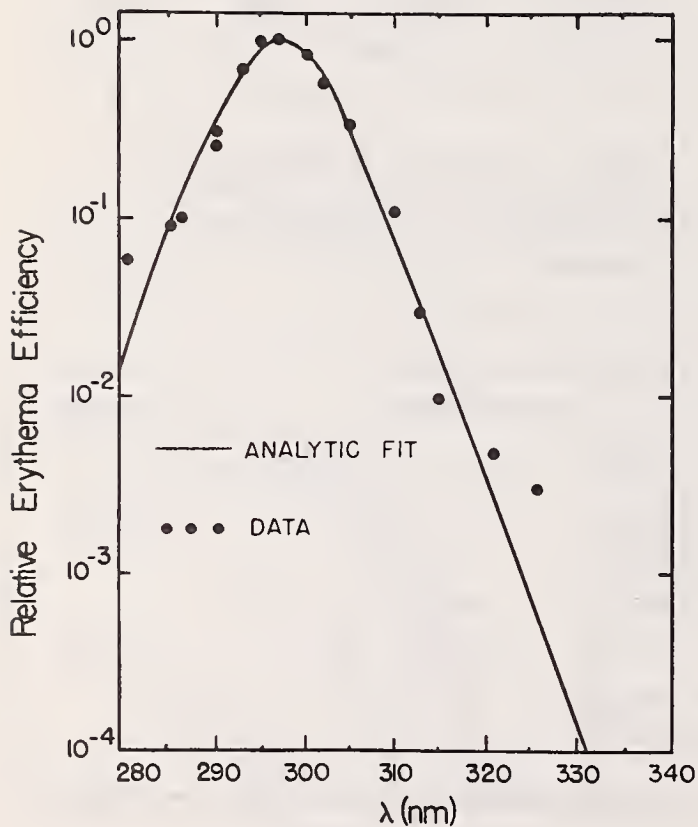


Fig. 6 The spectral efficiency for erythema, data and analytic fit (adapted from GMM).

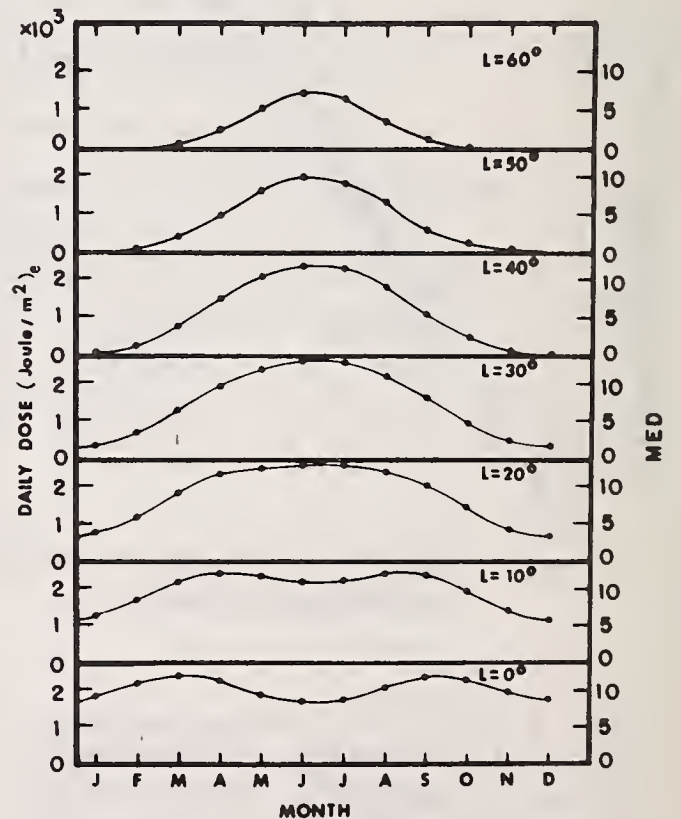


Fig. 8 Daily erythema dose (erythema-spectrum-weighted) under standard atmospheric conditions (ozone content=0.320 cm STP) at various latitudes vs. months of the year (from MG).

Fig. 9 Annual erythema dose as a function of latitude for several percentage ozone reductions from equation (27)

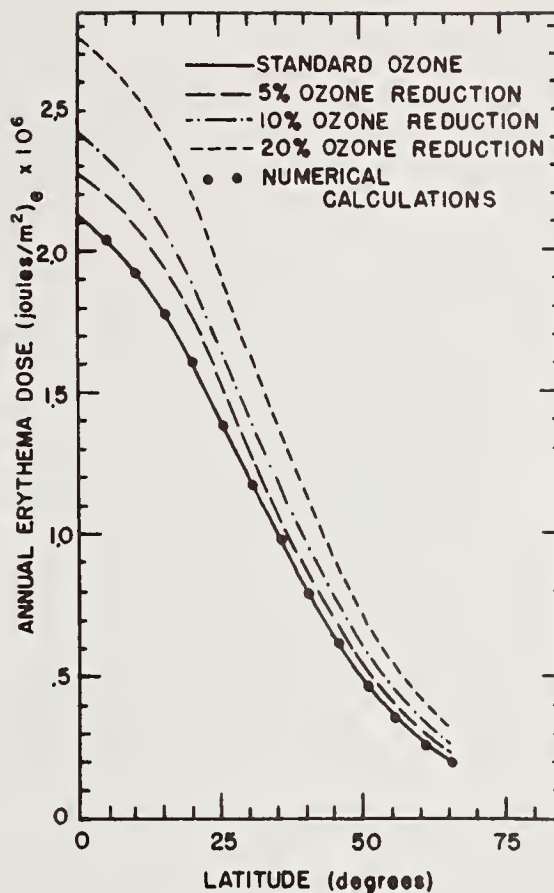
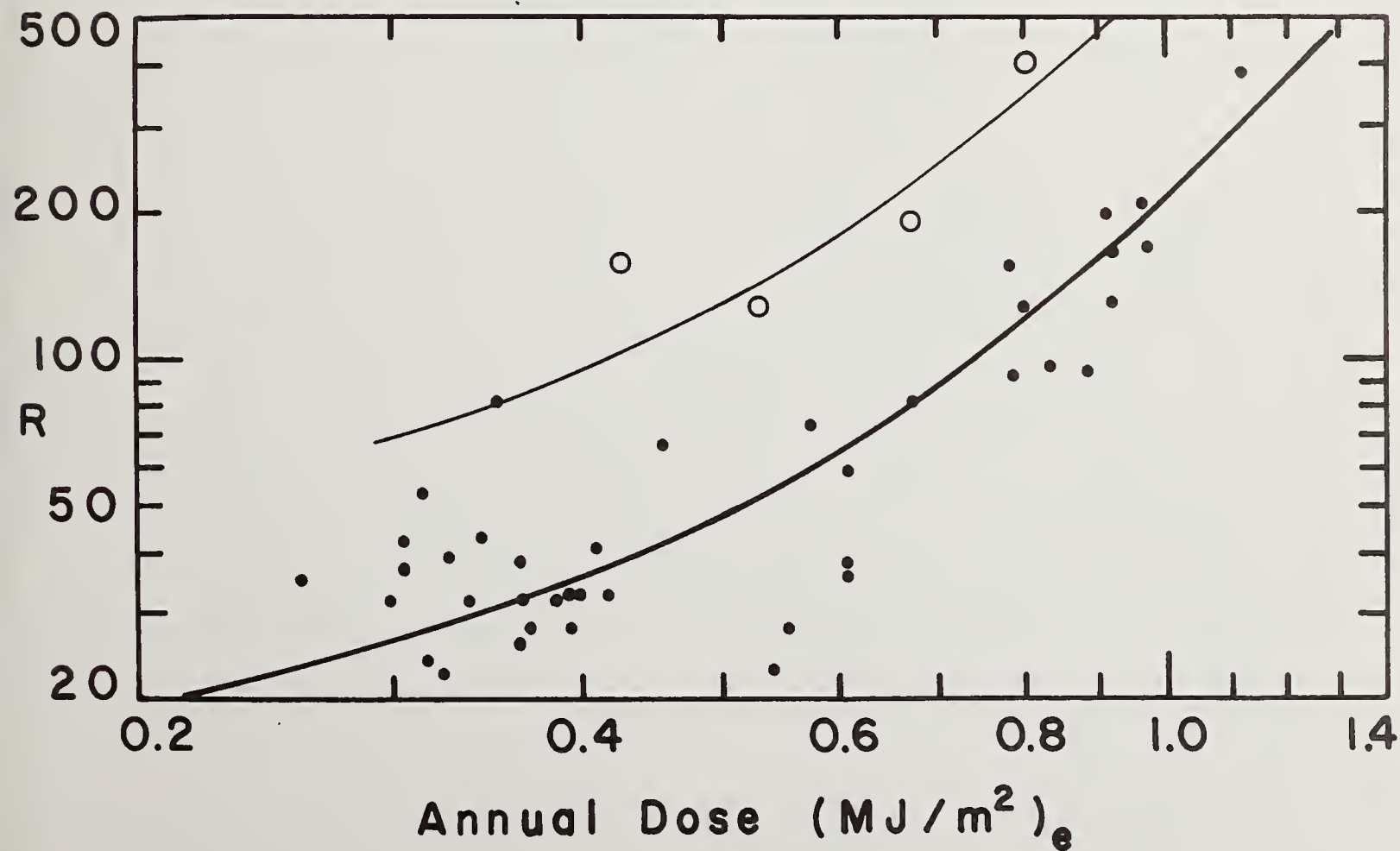


Fig. 10 (below) Age-adjusted non-melanoma skin cancer rate (R) per hundred thousand for the world, (•), and the Third National Cancer Survey (TNCS) (O). The curves are analytic fits with Eq. (30).



ADSORPTION AND TRANSPORT OF POLLUTANTS ON SUSPENDED PARTICLES

by

B. T. Hargrave
Marine Ecology Laboratory

K. Kranck
Atlantic Oceanographic Laboratory
Bedford Institute of Oceanography
Dartmouth, Nova Scotia, Canada

INTRODUCTION

The environmental impact of any pollutant depends largely on its concentration, physical-chemical state and interactions which occur with components of the environment into which it is added. These factors determine the fate and biological effect of all types of pollutants added to air, soil or water. Relationships between the nature of a pollutant and its environmental fate have been documented for transfer and transport processes occurring in water. These will be considered here and an attempt made to identify nonbiological rate-controlling factors determining uptake and transport of common aquatic pollutants.

NATURE OF POLLUTANT

Organic pesticides, hydrocarbons, heavy metals, radionuclides and particulate organic effluents (pulp mill wastes) comprise a partial list of compounds usually considered deleterious in aquatic systems. Unlike other substances, such as inorganic ions (phosphates, nitrates) which readily dissolve, these compounds either emulsify, precipitate, or have a low solubility and remain in colloidal form or adsorb to particulate matter.

Association of pollutants with particulate matter in water greatly alters their subsequent fate. Compounds in solution are only available for uptake by organisms by absorption through membranes. Once precipitated or adsorbed, however, ingestion of concentrated amounts becomes possible. Also, dispersal then follows sedimentation patterns of natural suspended material and the behavior of non-soluble pollutants becomes directly related to the dynamics of naturally occurring particles.

When a compound is added to water, it will either dissolve and enter into true solution, or remain insoluble and form a colloidal or particulate suspension. The initial state which a pollutant assumes determines its subsequent fate (Fig. 1). Compounds of low solubility such as hydrophobic hydrocarbons, may be solubilized to some extent by association with surface active humic-like organic matter (Boehm and Quinn 1973). Such compounds usually form emulsions. Also, if concentrations approach or exceed compound solubility, accumulation occurs at the air-water interface where evaporation occurs. Chlorinated hydrocarbons show this behavior (Oloffs

et al. 1972) and empirical equations have been derived to calculate potential evaporation rates for hydrocarbons of known vapor pressure and solubility (MacKay and Wolkoff 1973).

Pollutants which do not dissolve, such as wood fiber, become an integral part of the total suspended material and flocculate in a manner similar to naturally occurring suspended particles (Kranck 1974). On the other hand, dissolved metals may be precipitated by changes in electrolyte balance during passage through an estuary (Lowman *et al.* 1966). For example, high molecular weight organic material containing mercury may precipitate at salinity gradients (Lindberg *et al.* 1975). Precipitation and coprecipitation in metallic coatings on particles is also a major mechanism for trace metal transport in rivers (Gibbs 1973).

ADSORPTION-DESORPTION PROCESSES

Pollutants like radionuclides and nutrients which dissolve or like hydrocarbons which form colloidal suspensions have apparent solubilities which are greatly affected by adsorption-desorption reactions with suspended particulate matter. Carritt and Goodgal (1954) review studies which have indicated that suspended solids and colloidal gels can rapidly adsorb nutrients like phosphate. They proposed a mechanism for uptake by rapid adsorption and a slower diffusion controlled reaction. Soluble radiophosphorus and zinc, for example, are rapidly adsorbed by salt marsh sediment (Pomeroy *et al.* 1966). Tritremmel *et al.* (1966) demonstrated that equilibrium concentrations between individual sediment particles and water are reached quickly. Uptake to saturation levels, which varied inversely with particle size, was largely complete within 10 minutes, 50% of maximum values being reached after one minute. Desorption rates were slower. Desorption stabilized after an hour but final equilibrium concentrations were different for different nuclides. Aston and Duursma (1973) have demonstrated similar differences for other isotopes indicating that adsorption depends on properties of both the isotope and the adsorbing surface.

Adsorption-desorption processes also greatly affect the distribution of organic hydrocarbons in water. The hydrophobic nature of many of these substances results in colloidal suspensions and accumulation

at interfaces making determinations of true solubilities difficult (Bigger and Riggs 1974). Qualitative and quantitative differences exist in pesticides associated with various size classes of microparticulate matter in natural water (Pfister *et al.* 1969) and it is possible that most hydrophobic compounds are bound to such particles. Cox (1971) points out that most particulate surface area in natural waters is accounted for by suspended matter < 2 μ diameter and it seems likely that hydrophobic compounds will usually be bound to these particles.

Adsorption-desorption processes of pesticides in soil have been extensively reviewed (Bailey and White 1970, Weber 1972). Particle surface area, charge and organic content determine adsorptive capacity in conjunction with water solubility and charge distribution. Huang (1971, 1974) has indicated the extensive adsorptive capacity of clay particles and colloidal humic material for chlorinated hydrocarbons. Pierce (1973) and Pierce *et al.* (1974) also considered the partitioning of *p,p'*-DDT between sea water and suspended particles of various types. Adsorption to suspended clay and sediment occurred by physical adsorption-desorption equilibria whereas adsorption to humic acid occurred by lipophilic binding and capillary adsorption within the humic polymer. Poirrier *et al.* (1972) also noted high adsorptive capacity of colored colloidal material for DDT. Physical rather than chemical adsorption through the formation of weak hydrogen bonds appear to be the primary mechanism for uptake.

Numerous empirical plots can be used to describe adsorbed concentrations as a function of the concentration remaining in solution. Compounds of relatively high solubility (like nitrophenol) may form saturated monolayers, so that uptake becomes asymptotic above certain concentrations. Langmuir isotherms describe uptake of these compounds (Weber and Gould 1966). Adsorption of less soluble compounds, present below saturation levels, however, is usually logarithmically related to concentration, and uptake follows a Freundlich plot

$$X = K C^n \quad (1)$$

where X is the amount adsorbed per unit weight of adsorbent, C is the equilibrium concentration in solution, and n and K are constants (slope and intercept) which represent the extent (capacity) and nature of adsorption respectively.

Pierce *et al.* (1974) observed that uptake from dilute concentrations of DDT by various particles was described by Freundlich isotherms with $n = 1$. Data for uptake experiments described by Hargrave and Phillips (1974) show a similar slope constant. The experiments were repeated using various particles exposed to lindane, aldrin and dieldrin (Fig. 2). The slope constants for Freundlich plots were between 0.80 and 1.70 with a mean value (1.04) similar to published values derived for other compounds (Table 1). This indicates physical binding with absolute values of n determined by the degree of competition of solvent for sites on the adsorbing surface (Khan 1974).

Values of K are an indirect measure of the extent of adsorption. Increased temperature results in decreased values of K indicating the exothermic nature of adsorption which may be proportional to relative free energy changes (Khan 1974). K values are also inversely related to particle diameter by the equation

$$K = a d^{-b} \quad (2)$$

where D is the spherical equivalent of particle diameter (μ) and a and b are constants (Hargrave and Phillips 1974). Haque (1974) attributed high values of K for humic acid to its organic nature, large surface area, and numerous reaction sites. Organic matter in lake sediment and soil is a major determinant for adsorption of non-ionic pesticides (Lotse *et al.* 1968, Wershaw *et al.* 1969). The importance of organic content is further substantiated by a reduction of marine sediment adsorption capacity for DDT by removal of humic material (Pierce *et al.* 1974). Similarly, DDT uptake by sediment of various grain sizes was reduced an order of magnitude after ashing (Hargrave and Phillips 1974).

These observations suggest that a general expression for equilibrium concentrations of hydrophobic compounds on particles of various sizes may be of the form

$$X = \frac{C^n}{AD^b} \quad (3)$$

by combining equations (1) and (2). Further expansion to standardize for an effect of organic content on adsorption would be to express uptake per unit organic carbon (or

a related index of organic matter) as suggested by Goring (1967) and Hamaker and Thompson (1972). Thus,

$$\frac{X}{c} = \frac{C^n}{a D^b} \quad (4)$$

Uptake per unit organic matter is directly related to the concentration of a hydrophobic compound in solution and particle surface area available for adsorption. Organic content is often inversely related to particle diameter, however, and thus comparisons of K values and particle size (Hargrave and Phillips 1974) may include effects of this variable. This would explain why over 90% of the variation in uptake by particles ranging in size from bacterial cells to sand grains can be accounted for by only considering differences in median particle diameter and DDT concentration.

Desorption of hydrophobic compounds from particles depends on the nature of the binding, compound solubility, and the length of time available for desorption. For example, DDT adsorbed to humic acid is not desorbed as readily as that on clay or sediment (Pierce *et al.* 1974). Compound solubility is also critical in determining loss rates through desorption. Little DDT is lost from sand on rinsing (Hargrave and Phillips 1974), but lindane and dieldrin are readily lost in proportion to their solubilities (Boucher and Lee 1972). Thus, just as compound solubility determines the concentration available for adsorption to particle surfaces, it also determines desorption rates when concentrations in solution are reduced.

FLOCCULATION PROCESSES

Initially pollutants retain the physical state in which they were introduced and in this state are acted on by physical forces. For example, pollutants associated with coarse-grained sediment dumped from a barge onto mud bottom may never become resuspended for further transport. Fine-grained particulate effluent may disperse widely before flocculating.

Once particles are suspended in a turbulent environment they interact and flocculate with each other and the naturally occurring particles thereby changing their size and hence their transport behavior. The exact mechanism of particle interaction and

aggregate formation is poorly understood and only partly predictable at the present time.

Attraction due to molecular forces within the particles and/or adhesion due to organic coatings on surfaces is believed responsible for flocculation. Some mineral species appear to flocculate more readily than others (Whitehouse 1958). Observations with natural suspended particulate matter show that organic matter forms an integral part of flocs. This is not surprising since all surfaces in contact with sea water appear to become coated with organic material. The action of bacteria adhering to particle surfaces may be important in binding flocs. This would diminish the importance of mineralogy in controlling flocculation.

Sediment flocculates in sea water into aggregates the size of which are dependent on the grain size of inorganic particles (Kranck 1975). There is a logarithmic relationship between the modal size of the single deflocculated constituent grains. Flocculation occurs until all particles have approximately the same dynamic transport speed and no longer come into contact with each other. Since particle size and density rather than composition appear to be the controlling factor, the distinct flocculation behavior reported for minerals such as montmorillonite may be a product of their distinct grain size rather than their surface chemistry. Pollutant particles such as organic pulp mill effluent also become incorporated in the natural floc distribution, lose their individual physical characteristics and are transported as part of the natural sediment load (Kranck 1974).

The extent to which suspended particulate matter in fresh water is flocculated is not known. According to classical concepts massive flocculation takes place as unflocculated river sediment comes into contact with saline estuarine water. Some workers, however, have documented the importance of flocculation in lacustrine sedimentation (Sherman 1953). If bacteria are indeed a significant factor in particle flocculation, then flocculation should be as prevalent in fresh water as in the sea.

Microscopic observations of fresh water particulate matter show that a high proportion of the particles consist of aggregates. The grain size spectra show smooth nearly symmetrical distributions similar to those

of marine particulate matter (Fig. 3). Since all natural particulate matter contains particles from multiple sources with discrete grain sizes, the size distributions should be irregular multimodal if no interparticle reaction has taken place.

TRANSPORT PROCESSES

Once pollutants become associated with particles their fate is essentially dependent on the transport and dispersal of the particles themselves; they can be sedimented or transported and dispersed. Both can be transitional in that sediment can be eroded and resuspended or sedimented many times.

The transport and dispersal of particles is dependent on the transport rate of the water and on the relationship of the transport rate of particles to that of the water. Dissolved pollutants can be expected to disperse at the same rate as the parcel of water into which they were introduced. But particles usually have specific gravities greater than that of the water and gravity and inertia will give them a slower net motion. Only very small particles and particles with densities close to that of water will behave as dissolved substances. Progressively larger and heavier particles will have transport histories increasingly different from that of the water they are suspended in, and particle size and density are of primary importance in prediction of their transport behavior.

Models to predict transport rate of suspended sediment in relation to dynamic water transport are presently imperfect. The movement of large sand and silt particles transported as bedload with a rapid exponential decrease in concentrations away from the bottom is best understood. Their behavior has been studied in numerous laboratory and theoretical investigations (Sternberg 1967, Sundborg 1956). The fine-grained suspended load, composed mostly of cohesive material less than 16 microns, shows physical behavior different from that of the bedload and are easily distinguished from the bedload in grain size analysis of bottom sediments (Visher 1969). Suspension of the material is largely dependent on levels of microturbulence and the highest concentrations are often encountered near the surface and near the bottom of a water body as well as in association with density layers within the water column (Heathershaw and Simpson 1974, Drake and Gorsline 1973).

At present the best guide to where particles of a given size will be deposited seems to be an empirical study of geological conditions along an aquatic pathway. For example, whether or not a pollutant associated with particles of a certain size can become deposited in a lake along a waterway or trapped in the turbidity maximum of an estuary may be determined by comparison of natural sediment grain size and that of the polluted material.

SUMMARY

In conclusion it can be shown that pollutants entering the aquatic environment readily become associated with natural suspended particles. Dissolved compounds are adsorbed onto particles and substances in particulate form flocculate with other particles. The division between true solutions and colloidal suspension may be difficult to determine and is of no practical significance if both forms ultimately become associated with other particles.

Particle size and concentration are of prime importance in predicting transport and dispersal of pollutants. While the organic nature and surface charge of suspended particles affect adsorption, particle size and number (i.e. total surface area) may be the most important factor determining adsorption of non-soluble pollutants in water. Transport of particles after adsorption and flocculation is dependent on the relationship between grain size and the turbulence of the hydraulic environment.

REFERENCES

- Aston, S.R. and E.K. Duursma. 1973. Concentration effects on ¹³⁷Cs, ⁶⁵Zn, ⁶⁰Co and ¹⁰⁶Ru sorption by marine sediments with geochemical implications. *Neth. J. Sea Res.* 6: 225-240.
- Bailey, A.W. and J.L. White. 1970. Factors influencing the adsorption, desorption, and movement of pesticides in soil. *Residue Rev.* 32: 29-92.
- Biggar, S.W. and R.L. Riasas. 1974. Apparent solubility of organochlorine insecticides in water at various temperatures. *Hilgardia* 42: 383-391.

- Boehm, R.D. and J.G. Quinn. 1973. Solubilization of hydrocarbons by the dissolved organic matter in seawater. *Geochim. Cosmochim. Acta* 37: 2459-2477.
- Boucher, F.R. and G.F. Lee. 1972. Adsorption of lindane and dieldrin pesticides on unconsolidated aquifer sands. *Environ. Sci. Technol.* 6: 538-543.
- Carritt, D.E. and S. Goodgal. 1954. Sorption reactions and some ecological implications. *Deep-Sea Res.* 1: 224-243.
- Cox, J.L. 1971. DDT residues in seawater and particulate matter in the California current system. *Fish. Bull.* 69: 443-450.
- Drake, D.E. and D.S. Gorsline. 1973. Distribution and transport of suspended particulate matter in Huenene, Redondo, Newport and La Jolla submarine canyons, California. *Geological Society of America Bulletin*, 8: 3949-3968.
- Gibbs, R.J. 1973. Mechanisms of trace metal transport in rivers. *Science* 180: 71-73.
- Goring, C.A.I. 1967. Physical aspects of soil in relation to the action of soil fungicides. *Ann. Rev. of Phytopathology* 5: 285-315.
- Hamaker, J.W. and J.M. Thompson. 1972. Adsorption. *In: C.A.I. Goring and J.W. Hamaker (eds.), Organic Chemicals in the Soil Environment, Vol. 1.* Marcel Dekker, Inc., N.Y.
- Haque, R. 1974. Role of adsorption in studying the dynamics of pesticides. Plenum Press, N.Y.
- Hargrave, B.T. and G.A. Phillips. 1974. Adsorption of ¹⁴C-DDT to particle surfaces. *In: Proceedings of the International Conference on Transport of Persistent Chemicals in Aquatic Ecosystems.* N.R.C. Ottawa, Canada.
- Heathershaw, D.C. and J.H. Simpson. 1974. Fine structure of light attenuation and its relation to temperature in the Irish Sea. *Estuarine and Coastal Marine Science* 2: 91-103.
- Huang, J.C. 1971. Effect of selected factors on pesticide sorption and desorption in the aquatic system. *J. Water Poll. Control Fed.* 43: 1739-1748.
- Huang, J.C. 1974. Water-sediment distribution of chlorinated hydrocarbon pesticides in various environmental conditions. *In: Proceedings of the International Conference on Transport of Persistent Chemicals in Aquatic Ecosystems.* N.R.C. Ottawa, Canada.
- Kan, S.U. 1974. Adsorption of 2,4-D from aqueous solution by fulvic acid-clay complex. *Environ. Sci. Technol.* 8: 236-238.
- Kranck, K. 1974. The role of flocculation in the transport of particulate pollutants in the marine environment. *In: Proceedings of the International Conference on the Transport of Persistent Chemicals in Aquatic Ecosystems.* N.R.C. Ottawa, Canada.
- Kranck, K. 1975. Sediment deposition from flocculated suspensions. *Sedimentology*, 22: 111-123.
- Lindberg, S.E., A.W. Andrew, and R.C. Harriss. 1975. Geochemistry of mercury in the estuarine environment, pp. 64-107. *In: L.E. Cronin (ed.), Estuarine Research, Vol. I, Chemistry, Biology and the Estuarine System.* Academic Press.
- Lotse, E.G., D.A. Gratz, G. Chesters, G.F. Lee and L.W. Newland. 1968. Lindane adsorption by lake sediments. *Environ. Sci. Technol.* 2: 353-357.
- Lowman, F.G., D.K. Phelps, R. McClin, V. Roman de Vega, I. Oliver de Padovani and R.J. Garcia. 1966. Interactions of the environmental and biological factors on the distribution of trace elements in the marine environment, IAEA, Vienna, SM-72/15.
- MacKay, D. and A.W. Wolkoff. 1973. Rate of evaporation of low-solubility contaminants from water bodies to atmosphere. *Environ. Sci. Technol.* 1: 611-614.
- Oloffs, P.C., L.J. Albright, and S.Y. Szeto. 1972. Fate and behavior of five chlorinated hydrocarbons in three natural waters. *Can. J. Microbiol.* 18: 1393-1398.

- Pfister, R.M., P.R. Dugan, and J.I. Frea. 1969. Microparticulates: Isolation from water and identification of associated chlorinated pesticides. *Science* 166: 878-879.
- Pierce, R.H., Jr. 1973. A study of the mechanism of the adsorption of chlorinated hydrocarbons in marine sediments. Ph.D. Dissertation, Univ. of Rhode Island. 99 pp.
- Pierce, R.H., Jr., C.E. Olney and G.T. Felbeck, Jr. 1974. *p,p'*-DDT adsorption to suspended particulate matter in seawater. *Geochim. Cosmochim. Acta* 38: 1061-1073.
- Poirrier, M.A., B.R. Bordelon and J.L. Laseter. 1972. Adsorption and concentration of dissolved carbon-14 DDT by colouring colloids in surface water. *Environ. Sci. Technol.* 6: 1033-1035.
- Pomeroy, L.R., E.P. Odum, R.E. Johannes and B. Roffman. 1966. Flux of ³²P and ⁶⁵Zn through a salt-marsh ecosystem. IAEA: Vienna SM 72/10: 177-188.
- Sundborg, A. 1956. The River Klarälven: a study of fluvial processes. *Geograf. Ann.*, 38: 127-136.
- Sherman, Irving. 1953. Flocculent structure of sediment in Lake Mead. *Transactions, m. Geophys. Union.* Vol. 34: 394-406.
- Sternberg, R.W. 1967. Measurements of sediment movement and ripple migration in a shallow marine environment. *Marine Geology*, 5: 195-205.
- Tritremmel, C., A. Knollmayer, E. Wanderer, H.G. Heintschel and P. Stipantis. 1966. Behaviour of radioisotopes released to a stream, IAEA Vienna, SM-72/5, 89-105.
- Vishner, G.S. 1969. Grain-size distribution and depositional processes. *J. Sed. Pet.*, 39: 1074-1106.
- Weber, J.B. 1972. Interaction of organic pesticides with particulate matter in aquatic and soil systems. Fate of organic pesticides in the aquatic environment. *Adv. Chem. Ser.* 111. Amer. Chem. Soc., Washington, D.C.
- Weber, W.J., Jr. and J.P. Gould. 1966. Sorption of organic pesticides from aqueous solution, pp. 280-304. In: R.F. Gould (ed.), *Organic Pesticides in the Environment.* Amer. Chem. Soc. Washington, D.C. *Advan. Chem. Ser.* 60.
- Wershaw, R.L., P.J. Bucar, and M.S. Goldberg. 1969. Interaction of pesticides with natural organic material. *Environ. Sci. Technol.* 3: 271-273.
- Whitehouse, V.G., L.M. Jeffrey, and J.D. Debrecht. 1960. Differential settling tendencies of clay minerals in saline waters, in *Clay and Clay Minerals. Proc. 7th Nat. Conf. on Clays and Clay Minerals: Nat. Acad. Sci.-Nat. Res. Council:* 1-76.

Table 1 - Comparison of Freundlich adsorption constants (n = slope, K = intercept) for uptake of different compounds by particles of various size and type.

Compound	Surface	Temperature (C)	n	K	Reference
Lindane	lake sediment	23	0.92	0.30	Lotse <u>et al</u> (1968)
Arochlor 1254	illite clay soil	26	1.10 0.81	63 26	Haque <u>et al</u> (1974)
2,4-D	fulvic acid-clay	5	0.76	6.6	Khan (1974)
		25	0.83	5.2	
	illite	0	0.69	12.9	
		25	0.72	10.5	
	montmorillonite	0	0.93	0.87	
		25	1.00	0.65	
sand	0	0.67	0.11		
	25	0.83	0.04		
2,4-D	alumina	0	0.97	0.87	Haque (1974)
		25	1.01	0.83	
	silic gel	0	0.90	3.8	
		25	0.95	1.3	
humic acid	0	0.86	102.3		
	25	0.93	79.4		
humic acid	25	1.00	245		
-DDT	marine sediment	25	1.00	48	Pierce <u>et al</u> (1974)
	kaolinite clay	25	1.00	6	
p,p'-DDT	2 μ silt	10	1.15	320	
	12 μ silt	10	1.68	86	
	46 μ sand	10	1.02	8	
	270 μ sand	10	0.86	0.32	Hargrave and Phillips (1974)
	605 μ sand	10	0.83	0.07	
	1500 μ sand	10	0.80	0.02	
	250 μ sand (ashed)	10	1.16	0.02	
	2 μ silt	10	1.24	242	
	20 μ pollen grains	10	1.17	604	
	Aldrin	90 μ sand	10	1.10	1.5
294 μ sand		10	0.93	0.20	
855 μ sand		10	0.80	0.04	
Lindane	10 μ silt	10	1.05	37.2	
	428 μ sand	10	0.94	0.003	Hargrave (unpublished)
Dieldrin	10 μ silt	10	1.11	405	
	428 μ sand	10	0.92	0.04	Hargrave (unpublished)
	855 μ sand	10	0.86	0.006	

ADSORPTION AND TRANSPORT PROCESSES OF POLLUTANTS ON SUSPENDED PARTICLES

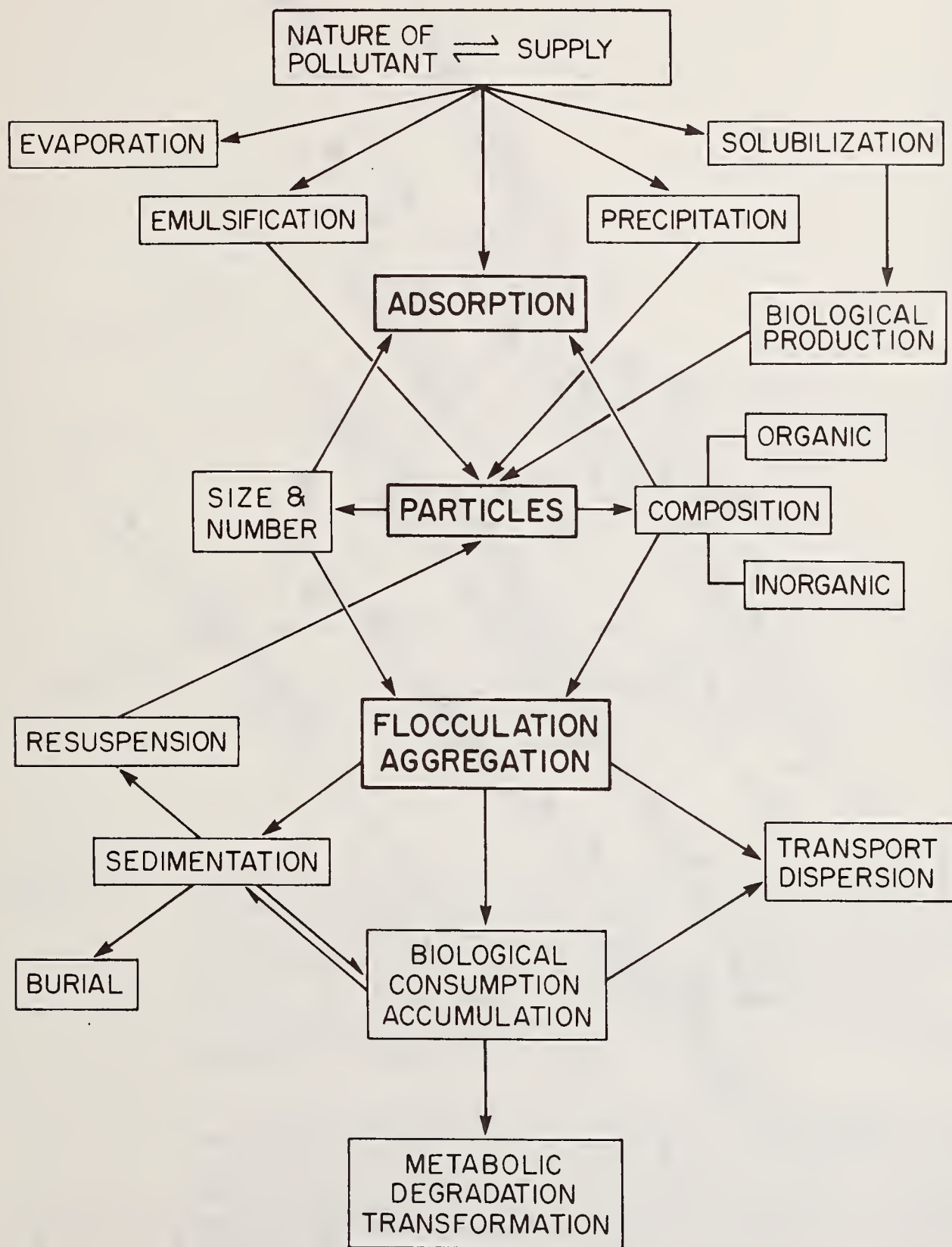


Figure 1. Schematic outline of major processes which affect adsorption and transport of nonsoluble pollutants in water.

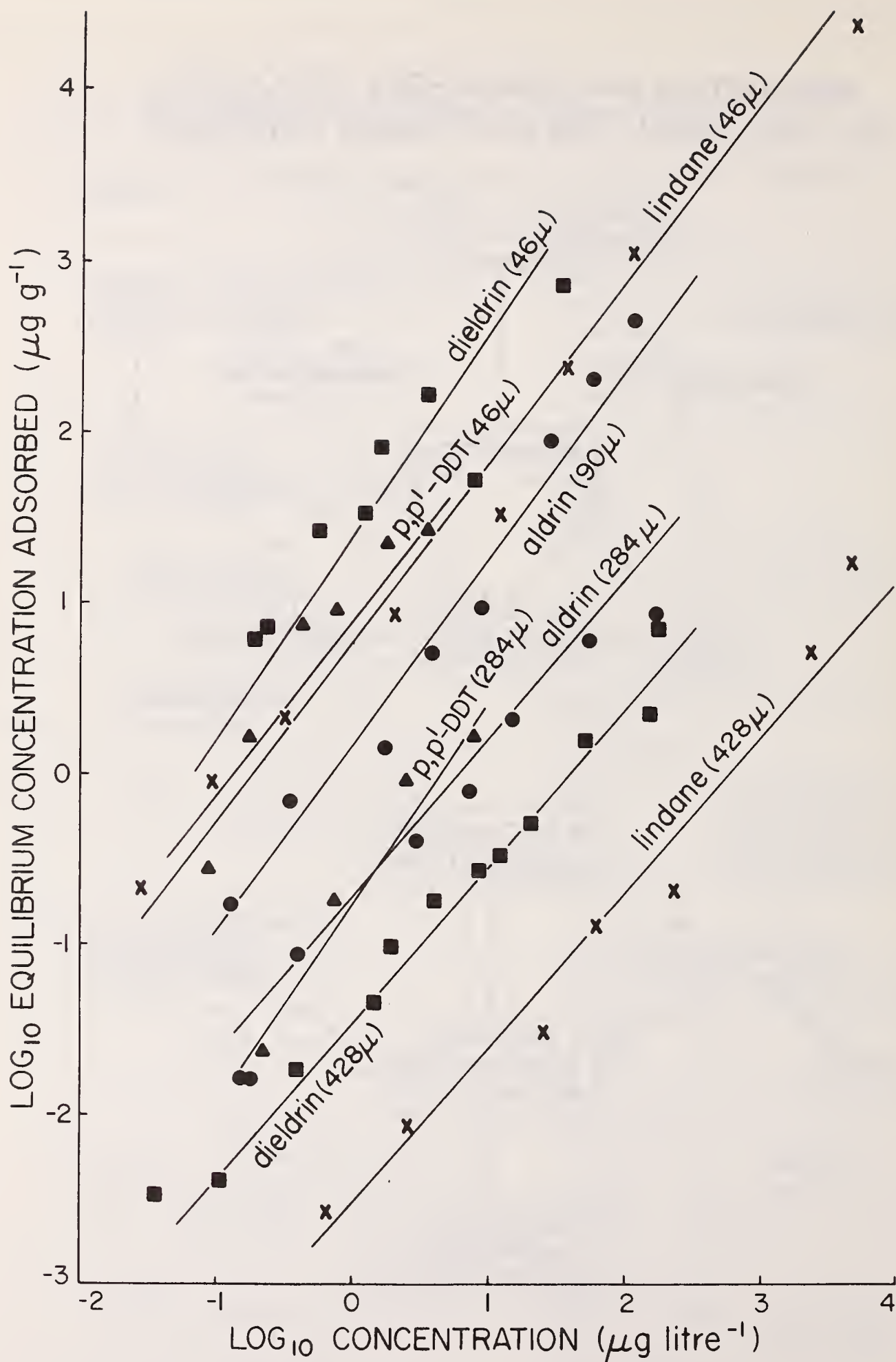


Figure 2.

Freundlich isotherm diagrams for *p,p'*-DDT, lindane, aldrin and dieldrin on sand particles of various sizes. Adsorption measured after equilibrium concentrations on particle surfaces were reached (24-36 hr). No correction for desorption was applied to the data.

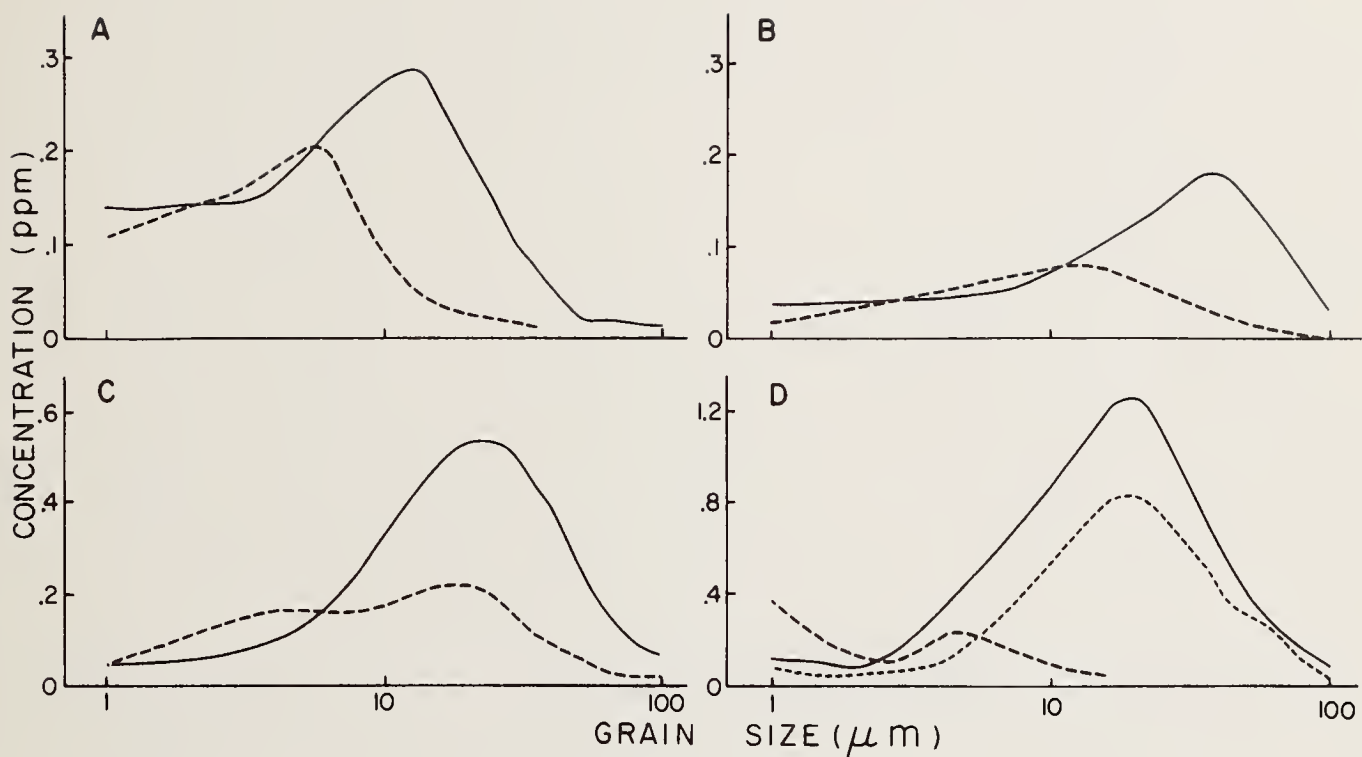


Figure 3. A to C. Suspended particulate matter grain size spectra illustrating smooth unimodal distributions typical for natural material. Solid line shows natural distribution and dashed line shows distribution of deflocculated inorganic grains. A: Fresh water, Lake of Two Mountains, Que. B: Fresh water, Miramichi River, N.B. C: Sea water, Petpeswick Inlet, N.S.

D. Effluent particles artificially flocculated with natural sediment distribution to produce smooth unimodal distribution. Dashed line shows effluent particles, short dashed line shows natural sediment distribution. Solid line shows total distribution resulting from 15 hours of gentle agitation.

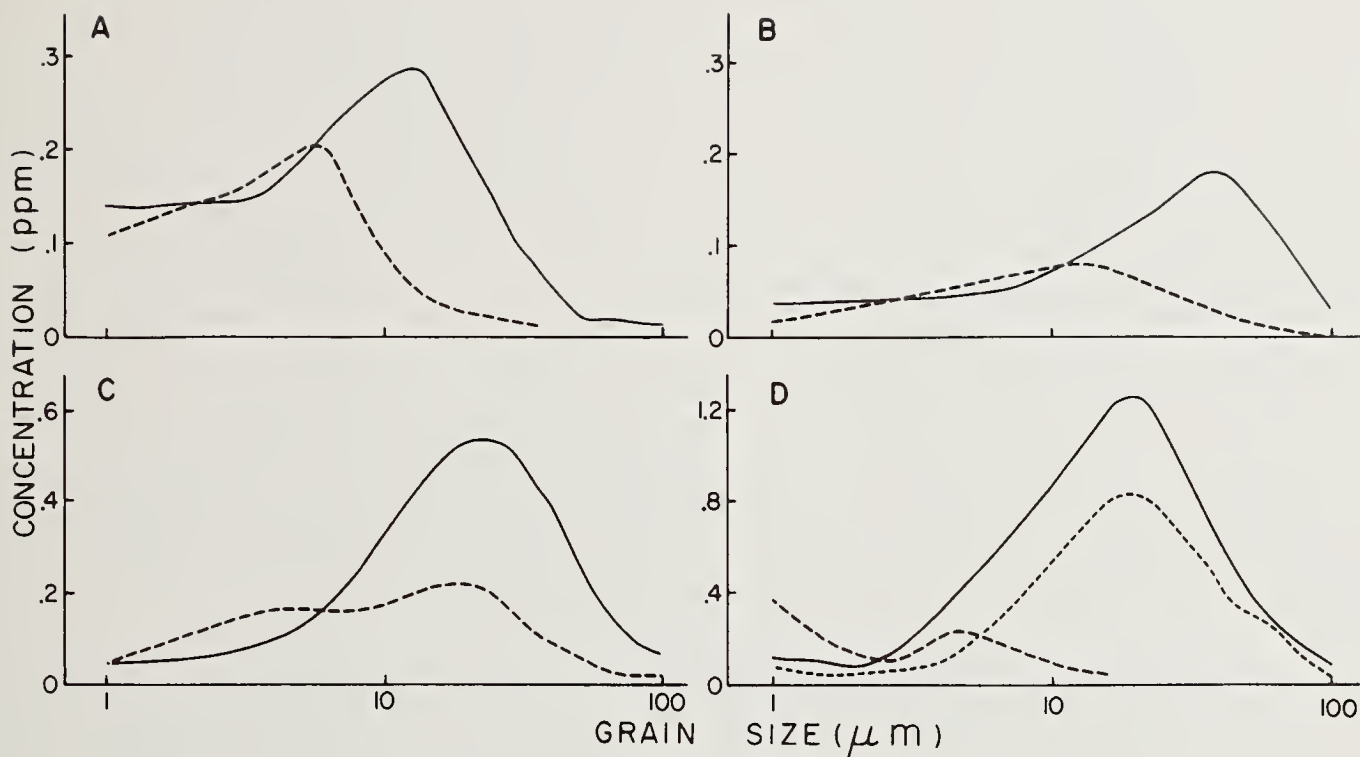


Figure 3. A to C. Suspended particulate matter grain size spectra illustrating smooth unimodal distributions typical for natural material. Solid line shows natural distribution and dashed line shows distribution of deflocculated inorganic grains. A: Fresh water, Lake of Two Mountains, Que. B: Fresh water, Miramichi River, N.B. C: Sea water, Petpeswick Inlet, N.S.

D. Effluent particles artificially flocculated with natural sediment distribution to produce smooth unimodal distribution. Dashed line shows effluent particles, short dashed line shows natural sediment distribution. Solid line shows total distribution resulting from 15 hours of gentle agitation.

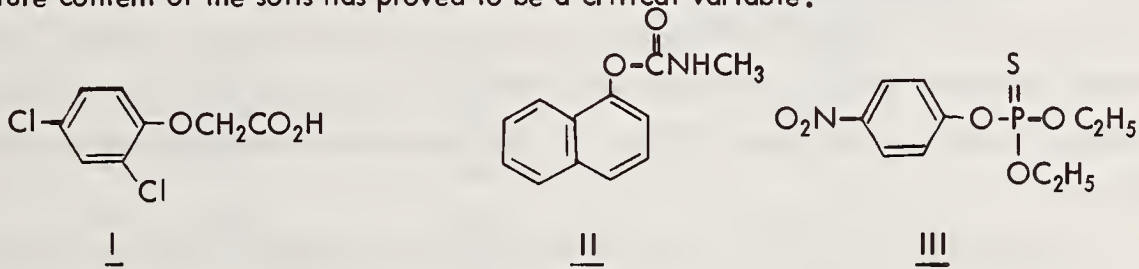
notes

PHOTOLYSIS OF PESTICIDES ON SOIL SURFACES⁽¹⁾

Richard R. Hautala
 Department of Chemistry
 University of Georgia
 Athens, Georgia 30602

Introduction

The role of photochemical decomposition in the degradation of pesticides on soil surfaces is at best very nebulous. A number of studies indicate that pesticide photochemistry is quite sensitive to the precise nature of the surface and that studies using silica or glass as soil models may be very misleading.^{2,3} The analytical problems encountered in monitoring this aspect of decomposition in the "field" are great and any definitive conclusions are lacking.⁽²⁾ As a result it is necessary to approach the problem with controlled laboratory studies by simulating selected variables expected under environmental conditions. We have examined the photochemical decomposition of 2,4-D (I), Sevin (II) and Parathion (III) on three types of arable soils. Our interest was in determining the extent to which surfactant additives (simulating pesticidal formulations) may influence the photochemistry. The moisture content of the soils has proved to be a critical variable.



Experimental Conditions

The soils used in our studies are typical arable types differing widely in pH, organic content, nature of exchangeable cations present, etc. Pertinent characteristics are given in Table I. The

Table I. Soil Characteristics

<u>Type</u>	<u>Name</u>	<u>Slurry pH</u>	<u>% Carbon</u>	<u>Bulk Density</u>	<u>% Pore Space</u>
I	Etowah	4.4	0.13	1.70	35.8
II	Holston	6.3	0.60	1.90	28.3
III	Conasauga Siltloam	7.6	2.79	1.57	40.8

surfactants studied were of the anionic (sodium dodecyl sulfate, SDS) and cationic (hexadecyltrimethylammonium bromide, HDTBr) types. The moisture content of the soils was varied and can be categorized as follows:

- (1) Dry: soil which has been dried with no additional water added.
- (2) Saturated: dried soil to which a quantity of water has been added to fill the "pore space". This quantity depends on the individual soil and amounts to roughly 1 ml. per gram soil. It has been found that when detergents are co-applied an additional quantity of water is required to give the visual appearance of saturation. The additional quantity is probably used in hydration of the surfactant head group.
- (3) Wet-quantities of water (up to 4 ml) are added to saturated soils to form slurries.

The general procedure involves preparation of a uniform soil surface by spreading an aqueous slurry containing one gram soil on a 10x15 cm surface (Figure 1) and allowing the surface to dry completely. The pesticide (5 mg) and, in certain cases, detergent (100 mg) are dissolved in 5 ml acetone or methanol and spread uniformly on the thin soil film. The solvents are evaporated completely. This corresponds to a coverage of 2.9 lbs. pesticide per acre and 58 lbs surfactant per acre. For those experiments involving water saturated or wet soils, an appropriate amount of water is uniformly added to surface. The vessel is then sealed and photolyzed (Figure 1). An identical vessel is simultaneously prepared and stored in the dark for an equivalent time period.

The samples are photolyzed on custom built glass tray with cooling water circulating on the under side to avoid evaporative losses and to maintain the initial moisture content. The trays are tightly covered with Pyrex glass on top and are placed about 6 inches under a horizontal water-cooled Pyrex-jacketted medium pressure Hg arc (450 w). The radiant density is reasonably uniform over the entire surface.

After photolysis the soil films are exhaustively extracted and the extract is prepared for analysis by gas chromatography (2,4-D and Parathion) or high pressure liquid chromatography (Sevin). In the case of 2,4-D the extract is treated with $\text{BF}_3\text{-CH}_3\text{OH}$ to esterify the carboxylic acids. Appropriate controls have indicated that the procedures employed allow near quantitative recovery of the pesticides and expected decomposition products.

The output of the lamp as constructed and filtered by Pyrex provides radiation with approximately the following photon flux on the plate surface.

λ (nm)	total incident light (Einsteins-sec ⁻¹)
297	0.58×10^{-7}
303	1.4×10^{-7}
313	4.4×10^{-7}
314	1.1×10^{-7}

Longer wavelength light is not absorbed by the pesticides used and shorter wavelength light is totally filtered by the Pyrex. For Sevin and 2,4 D the quantity applied is such that only a small fraction of the incident intensity is absorbed. Consequently, it is expected that the extent of photolysis should

fall off exponentially with time. Experiments at various time intervals have confirmed this expectation. The bulk of our experiments have been run at exposure times of 18-150 hrs, but in order to facilitate comparison the results have been calculated and are reported in terms of the time required for 50% photodecomposition.

Very crude quantum yields can be calculated by assuming that extinction data in solution is applicable to soil surfaces.

Results

The photolysis of 2,4-D was carried out on the acid rather than the various esters actually used as pesticides because it was found that hydrolysis of the ester to the acid occurred very rapidly on the soils studied. Representative results are given in Table 2.

Several factors are apparent from these results. The dry and water saturated soils behave similarly. The anionic surfactant decreases the extent of photolysis on dry or saturated soils. In the presence of either detergent excess water dramatically increases the rate of photolysis. In the absence
 Table 2. Effects of soil types, detergents and soil water content on the time required for 50% photodecomposition of 2,4-D.

<u>Soil</u>	<u>Detergent</u>	<u>Water Content</u>	<u>Time required for 50% Photodecomposition</u>
I	none	wet	144 hr
I	HDTBr	wet	49
I	SDS	wet	19
I	HDTBr	satd.	55
I	SDS	satd.	175
I	SDS	dry	145
II	none	wet	149
II	HDTBr	wet	35
II	SDS	wet	<14
II	HDTBr	satd.	64
III	none	wet	440
III	HDTBr	wet	<4
III	SDS	wet	<10
III	HDTBr	satd.	55
III	SDS	satd.	139
III	none	dry	58 ($\phi \sim 0.004$)
III	SDS	dry	175

of detergent excess water actually decreases the rate of photolysis. For purposes of comparison to solution photodecomposition a crude quantum yield of 0.004 can be estimated for the experiment designated in Table 2. In aqueous solution the quantum efficiency for photodecomposition of 2,4-D is approximately 0.1.

Studies using the pesticide Sevin were carried out only on dry and water saturated soils. Problems with hydrolysis to a -naphthol precluded studies with wet slurries. Representative results for this system are presented in Table 3. Note that in three cases decomposition in the dark was the most significant process. In all other cases, decomposition in the absence of light did not interfere to any significant extent. These analyses were done on samples exposed for 72 hours. However the results are reported in the same manner as those for 2,4-D in order to facilitate comparison. In general the photolysis of Sevin on soils is very inefficient. A crude approximation of the quantum yield for the most favorable case in Table 3 is ca. 0.0004. In solution the quantum yields are approximately 0.01 to 0.03.

Table 3. Effects of soil types, detergents and soil water content on the time required for 50% photodecomposition of Sevin.

<u>Soil</u>	<u>Detergent</u>	<u>Water Content</u>	<u>Time required for 50% Photodecomposition</u>
I	none	dry	97 hr
I	none	satd.	<u>long</u> (no loss in 72 hr)
I	HDTBr	dry	251
I	HDTBr	satd.	274
I	SDS	dry	274
I	SDS	satd.	251
II	none	dry	251
II	none	satd.	1700
II	HDTBr	dry	440
II	HDTBr	satd.	(a)
II	SDS	dry	251
II	SDS	satd.	251
III	none	dry	105
III	none	satd.	(b)
III	HDTBr	dry	381
III	HDTBr	satd.	72 (c)
III	SDS	dry	251
III	SDS	satd.	440

(a) about 22% is decomposed under either the dark or photolytic conditions in 72 hr.

(b) about 17% is decomposed under either the dark or photolytic conditions in 72 hr.

(c) in the dark control 36% is decomposed to give an unknown material, 31% appears as a -naphthol and 32% Sevin remains; in the photolysis only 30% Sevin remains in 72 hr.

Our studies with the pesticide Parathion are in preliminary stages. Representative data for photolysis on Soil III are given in Table 4.

Table 4. Effects of detergents and soil water content on the time required for 50% photodecomposition of Parathion on Soil III.

<u>Detergent</u>	<u>Water content</u>	<u>Time required for 50% Photodecomposition</u>
none	dry	150 hr
none	satd.	60
HDTBr	dry	173
HDTBr	satd.	159
SDS	dry	254
SDS	satd.	83

Analysis of the extracts revealed no p-nitrophenol or paraoxon. Controls showed that 100% of either could be recovered from the soil with the workup procedure employed. Studies are currently in progress to determine how rapidly either would photodecompose under the photolysis conditions.

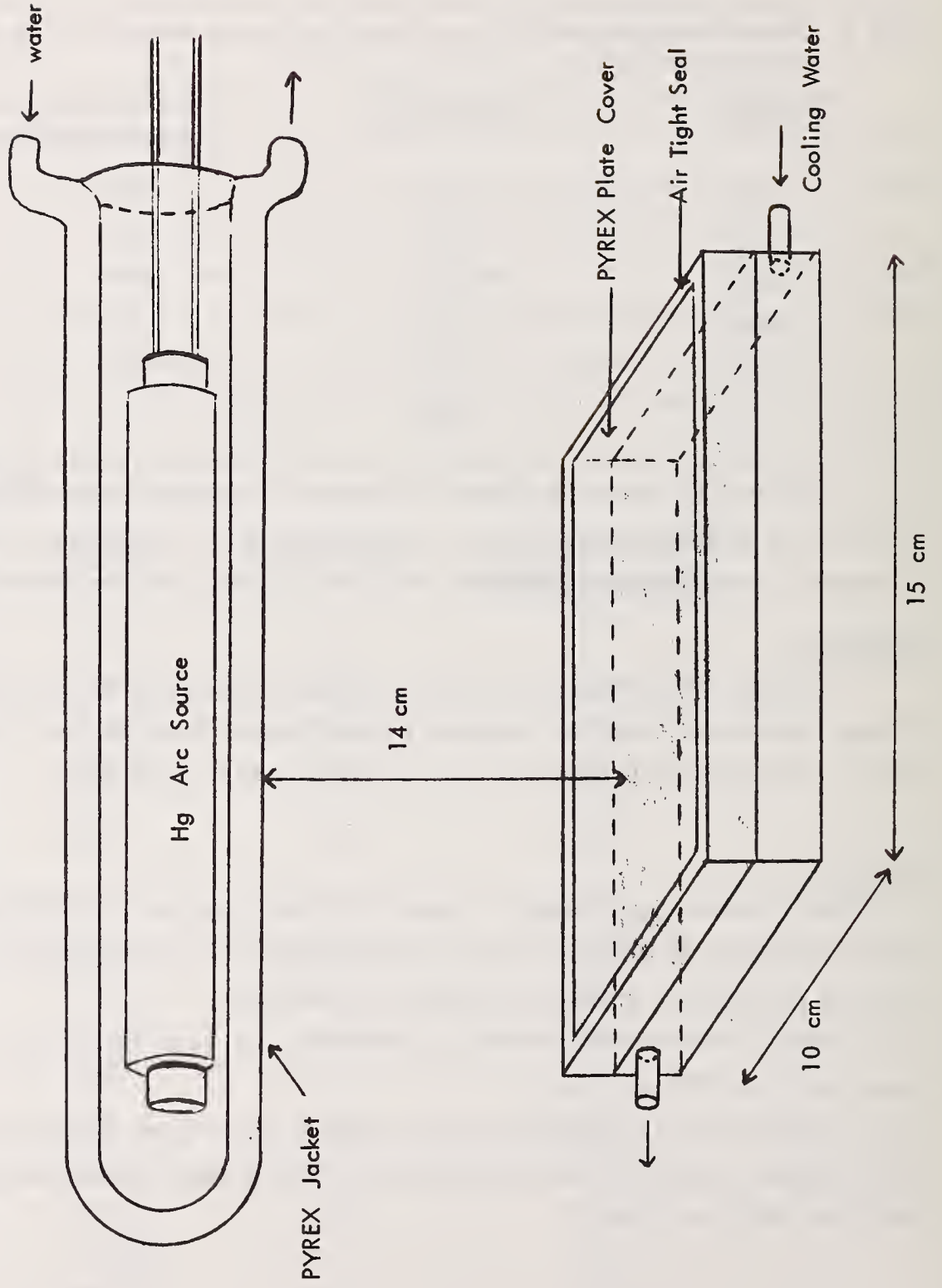
Conclusions

It is clear each of the factors (soil type, detergents, moisture content) studied exerts a different effect on each pesticide. Mechanistic explanations for these effects are currently being pursued. Photolysis on these soils occurs at a much slower rate than in solution.

References

1. Address: Department of Chemistry, University of Georgia, Athens, GA. 30602; the experimental work was carried out by Dr. Ram D. Laura; Financial support from the United States Environmental Protection Agency (grant R-802959) is gratefully acknowledged.
2. J.D.Rosen in "Environmental Toxicology of Pesticides", ed. by F. Matsumura, et. al., Academic Press, New York, 1972, pp. 435-447.
3. J.R.Plimmer in "Fate of Pesticides in the Environment", Proceedings of the Second International IUPAC Congress of Pesticide Chemistry, Vol. VI, ed. by A.S.Tahori, Gordon and Breach Pub., New York, 1972, pp. 47-76.

Figure 1. APPARATUS FOR PHOTOLYSIS ON SOIL SURFACES



notes



Predictive Modeling of the Behavior of Pollutants in the Aquatic Environment

Lassiter, R.R., Baughman, G.L., Malanchuk, J.L.
Environmental Research Laboratory
Athens, Georgia

Introduction

Predictive models differ mainly in their scope and applicability. Models used to predict chemical and physical phenomena for controlled laboratory conditions are at one extreme of predictive scope and applicability. At the other extreme are models used to predict future events and conditions of some natural system, e.g., models of weather, hydrology, or water quality. Between these extremes, models can be used to classify the behavior and fate of substances with respect to specified environmental conditions and to evaluate factors and processes important in their behavior and fate. Models intended for these purposes can be called evaluative models. A model for mercury was chosen to illustrate some of the problems of construction, conceptual difficulties, and data needs for evaluative models.

Evaluative models are usefully applied wherever detailed relationships can be described mathematically, but where the overall complexity is too great for net results to be clear. Much is known of the chemistry and physics of mercury, yet the factors influencing its behavior are too complex for its fate in a given environment to be apparent. Therefore, it is a useful subject to illustrate the concepts of an evaluative model.

The mathematical model used was structured to explore the possibility of predicting the fate of mercuric ion and its complexes (Hg_T), ionic methyl mercuric species (CH_3HgX_T), and elemental mercury (Hg^0) in aquatic systems. A schematic representation of the major features of the system is given in Figure 1. The aquatic system that is represented consists of a body of moving water in contact with the atmosphere and the underlying sediments.

Model Description

A set of differential equations is used to represent the forms of mercury in the system. Each equation is similar to the following:

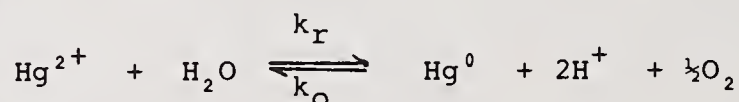
$$\frac{\partial [\text{Hg}]}{\partial t} = \frac{D \partial^2 [\text{Hg}]}{\partial x^2} - \frac{V \partial [\text{Hg}]}{\partial x} + S([\text{Hg}])$$

in which the first term on the right represents dispersion, the second advection, and the third the algebraic sum of the sources and sinks relating to this form of mercury. The source-sink terms, S , are written as functions of environmental descriptors, e.g., pH, concentration of suspended particulate material, or depth of sediment and water. Although a great deal is known about the chemistry of mercury, none of the source or sink terms can be written without conjecture. Nevertheless, an attempt was made to structure each term to reflect as much as is understood about the chemistry of the process.

An example from the mercury model will illustrate some of the uncertainties accompanying the writing of source or sink terms. Oxidation and reduction of elemental mercury and mercuric ion, respectively, is described by the following equilibrium expression (Parks, G.A., pers. comm.)

$$K_{\text{red}}^{\text{ox}} = \frac{[\text{Hg}^0] [\text{H}^+]^2 \text{PO}_2^{\frac{1}{2}}}{[\text{Hg}^{2+}]} = 10^{-19.6}$$

However, observations from several types of experiments show that the reactions do not proceed rapidly to completion, i.e., solutions containing mercuric ion continue to produce elemental mercury for days (1,2,3). Because of these observations the reactions are better represented by rate terms rather than by algebraic equilibrium expressions. Equilibrium expressions do not necessarily reflect mechanisms, and rate expressions cannot properly be obtained from them. In spite of this fact, the following reactions, given by Parks (4), were used to represent oxidation and reduction pathways:



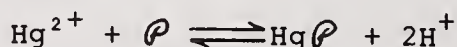
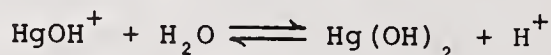
The rate expression for oxidation was taken to be

$$k_o [\text{Hg}^0] [\text{H}^+]^2 [\text{O}_2]^{\frac{1}{2}}$$

The rate expression for reduction was

$$k_r [\text{Hg}^{2+}].$$

For the environment reduction cannot be as simply represented as this term. It is complicated in most natural waters by the presence of suspended particulate material which is probably encased by a layer of organic material (5). Mercuric ion complexes strongly (6) with sulfhydryl-containing compounds and will therefore be expected to bind strongly to suspended particulates. The question facing the modeler is whether reduction of mercuric ion bound to particulates can be represented by a simple proportion as assumed for dissolved. If not, the bound mercuric ion concentration must be computed. The following equations are used as an approximation for computing the bound mercuric ion, also taking into account hydrolysis.



Here, ρ , is a symbol for suspended particles treated as though they are a dissolved constituent. The three equilibria are

$$\frac{[\text{HgOH}^+][\text{H}^+]}{[\text{Hg}^{2+}]} = K_1$$

$$\frac{[\text{Hg}(\text{OH})_2][\text{H}^+]}{[\text{HgOH}^+]} = K_2$$

$$\frac{[\text{Hg}\rho][\text{H}^+]^2}{[\text{Hg}^{2+}][\rho]} = K_p$$

Assuming that $[\text{Hg}^{2+}] \ll [\rho]$ and is so low that the reactions do not affect $[\text{H}^+]$, there are four unknowns $[\text{Hg}^{2+}]$, $[\text{HgOH}^+]$, $[\text{Hg}(\text{OH})_2]$, $[\text{Hg}\rho]$. A mass balance equation for Hg_T provides the other information necessary for solution:

$$[\text{Hg}_T^{2+}] = [\text{Hg}^{2+}] + [\text{HgOH}^+] + [\text{Hg}(\text{OH})_2] + [\text{Hg}\rho].$$

The bound fraction, β , is

$$\beta = \frac{K_p[\rho]}{[\text{H}^+]^2 + K_1[\text{H}^+] + K_2K_1 + K_p[\rho]}$$

and the free mercuric ion fraction, δ , is

$$\delta = \left[1 + \frac{K_1}{[\text{H}^+]} + \frac{K_2K_1 + K_p[\rho]}{[\text{H}^+]^2} \right]^{-1}$$

Depending upon whether reduction of only free mercuric ion or of both bound and free can be described by the constant proportion, the reduction term is either

$$k_r \delta [\text{Hg}_T^{2+}]$$

or

$$k_r (\beta + \delta) [\text{Hg}_T^{2+}].$$

Each term in the model was subject to similar uncertainties. The question of how to express accepted chemical, biochemical or other equations in the context of a complex natural system is the basic difficulty facing the "environmental modeler".

Some of these questions might be theoretically answerable, but most will be solved only through observation and experiment. For the example above, results may be obtained by testing each case, reduction of bound mercury and

reduction of both bound and soluble. If the results are different, that difference may be used to design a critical experiment to detect which hypothesis, if either, is correct.

Results and Discussion

Two kinds of quantities were checked for their importance to the environmental behavior of mercury. One kind is solely a property of the environment, e.g., pH, suspended sediment load. The other is best considered as an interaction of mercury and the environment, e.g., volatilization rate, strength of binding to particulates. Their importance was judged on the basis of the sensitivity of the forms of mercury to variation in these quantities. Several computations were made before arriving at a set of initial values that is reasonably compatible with the rates and equilibria assumed for the system. The initial values selected are

for water:

Mercuric	$2 \times 10^{-10}M$
Methyl	$2 \times 10^{-16}M$
Elemental	$8.5 \times 10^{-12}M$

and for sediment:

Mercuric	$2.2 \times 10^{-9}M$
Methyl	$2.6 \times 10^{-14}M$
Elemental	$2 \times 10^{-11}M$

These values are not defensible as being "realistic", nevertheless, they are useful in two ways. First, they provide a starting point from which further computations can be made. Second, discrepancies from expected values may point to deficiencies in the current representation.

Physically, one kilometer of a very slowly moving body of water is represented. Each data point is taken after a 20-day simulation and the sampling point chosen is that of the lower end of the one-kilometer reach. This procedure was adopted so that the points would indicate conditions at a distance from a low level source.

It has been speculated that solids in aquatic systems control the fate of mercury. In assessing this possibility, the equilibrium constant, K_p , for binding of mercuric ion to sediment was varied over five orders of magnitude, while the concentration of suspended particulates was held constant at 10 mg/l. A marked dependence of all forms of mercury on K_p is apparent. Methyl mercury concentration is much higher in the sediments for low values of K_p (Figure 2). The opposite is noticed in the water (Figure 3). These observations result mostly from the model assumptions that both the methylation and reduction processes occur for bound mercuric mercury, and that there is no settling of suspended particulates.

An alternative way to evaluate the importance of suspended particulates in the system is to vary the particulate load itself. In this analysis K_p was held constant at 1.5×10^{-2} (equivalent to a partition coefficient of 1.5×10^2 at pH 7) and suspended sediment was varied over a range of five orders of magnitude (Figures 4-6). Elemental (Figure 4) and mercuric mercury in the sediments decrease as expected with increasing suspended sediment load. Surprisingly, however, methyl increases in the sediment (Figure 5). In the model methyl mercury is formed microbially from mercuric mercury that is bound to particulate material. A greater suspended particulate load results in greater production of methyl mercury. The greater quantity of methyl mercury in sediments results from the greater production rate and resulting greater concentration (Figure 6) in the water, followed by sediment water exchange and binding of methyl mercury to the sediment particles.

At $K_p = 1.5 \times 10^{-2}$ and 10 mg/l of suspended particulates, all forms were remarkably insensitive to changes in pH. Preliminary computations indicate, however, that a major change in the concentration of all forms occurs between pH 4 and 5.

Certain aspects of the physical geometry of the system could result in variation in the concentrations of the mercury forms. For this simple model only depths of water and sediment may be varied. The depths of water and sediment were each varied three orders of magnitude. Mercuric mercury concentration in the water was completely insensitive to sediment depth, but was a rather strong function of water depth. Elemental mercury in the water (Figure 7) was positively correlated with variation of both water and sediment depth but was more strongly a function of water depth. Elemental mercury in a sediment, however, was affected markedly by sediment depth (Figure 8) and nearly unaffected by water depth, especially for the situations with deeper sediments.

Conclusions

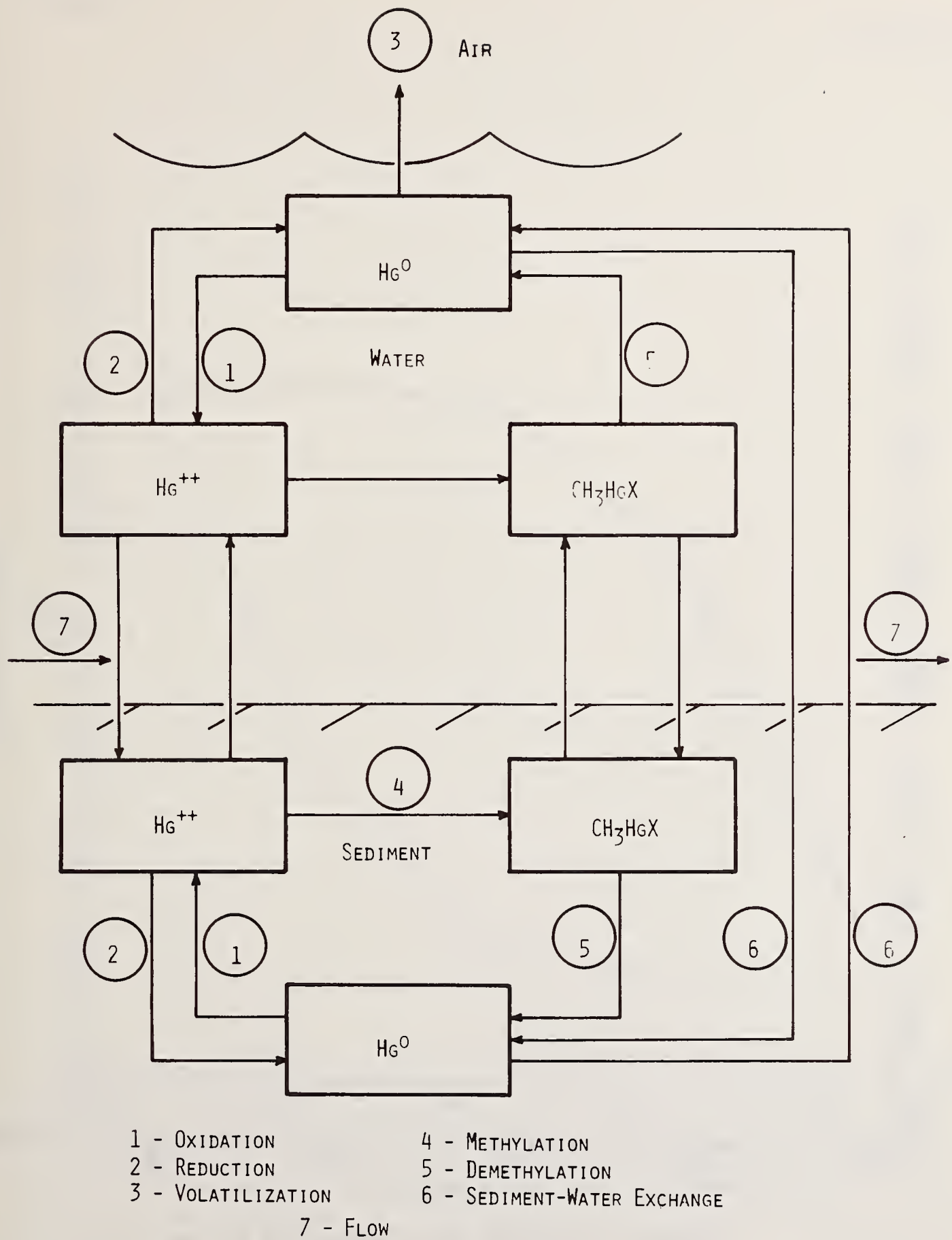
As a result of both constructing and using an evaluative model for mercury, two deficiencies can be identified. The uncertainty about the way that the transformation processes operate is the most basic deficiency. The processes cannot be described mathematically and used in a model unless they are understood. Second, uncertainty about the value of such parameters as the equilibrium coefficient for binding of forms to particulate materials, limits the confidence that can be placed in results obtained from the model.

The behavior of a substance in the environment is assumed to result solely from the interaction of certain quantities considered to be properties of the substance and others considered properties of the environment. Many of the properties of elements have been studied, catalogued, and are widely available. Some quantities such as a partition coefficient of mercuric mercury between particulate material and water are, by nature of the measurement, quantities that chemists naturally would measure. Unfortunately, by nature of the material, these quantities are more likely to be considered properties of the environment. Chemists usually prefer to work with defined chemicals rather than "particulate material", and therefore measurements of this sort often are not made.

Literature Cited

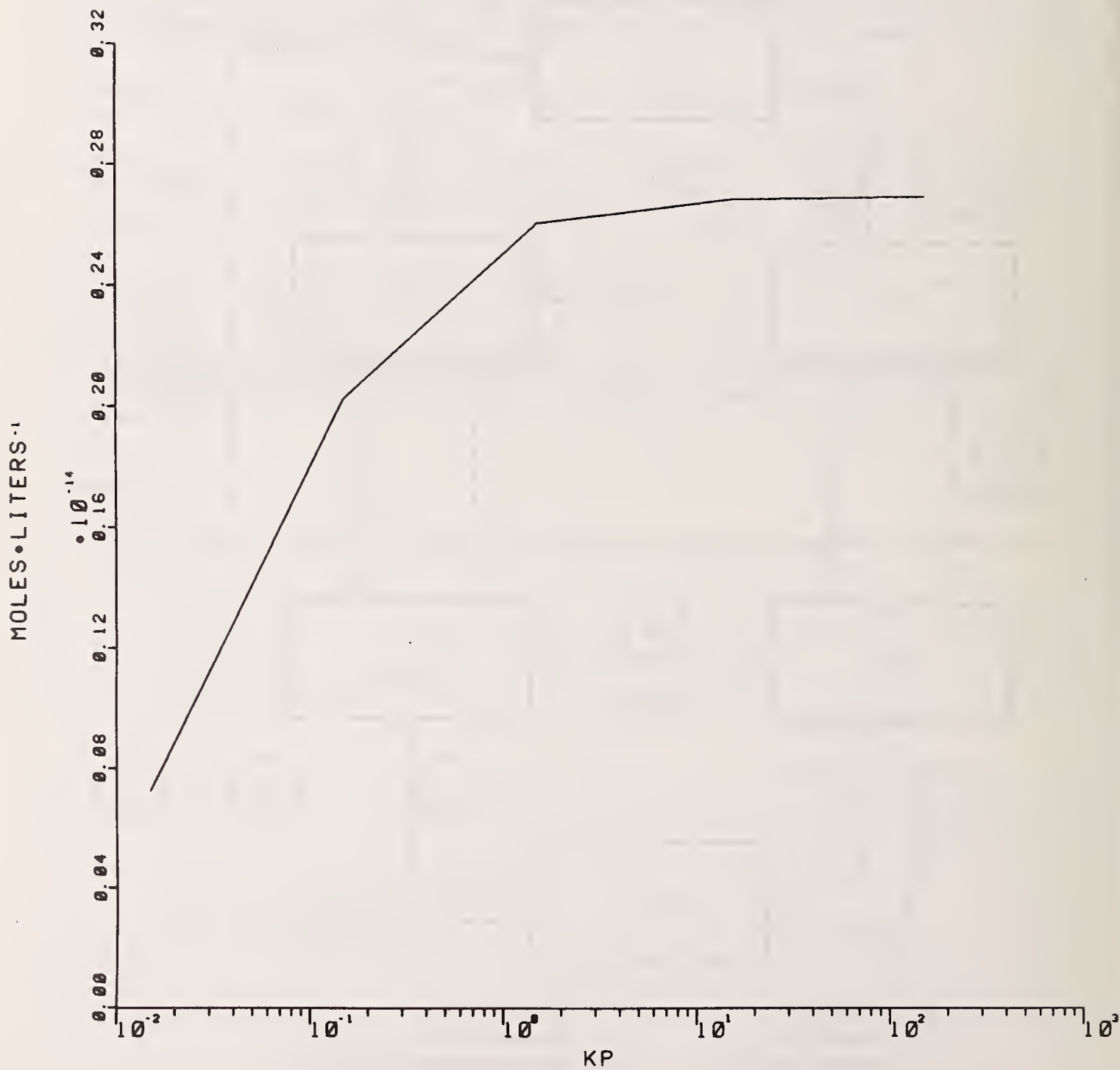
1. Bisogni, J.J., Lawrence, A.W., Kinetics of Microbially Mediated Methylation of Mercury in Aerobic and Anaerobic Aquatic Environments. Technical Report 63. Cornell University Water Resources and Marine Sciences Center. Ithaca, New York. 180p. (1973).
2. Holm, H.W., Cox, M.F., Mercury in Aquatic Systems: Methylation, Oxidation-Reduction and Bioaccumulation. Report No. EPA-660/3-74-01 Bioaccumulation. Report No. EPA-660/3-74-021. U.S. Environmental Protection Agency. Corvallis, Oregon. 38p. (1974).
3. Baier, R.W., Wojnowich, L., Petrie, L., Mercury Loss From Culture Media. Anal. Chem. 44,2464 (1975).
4. Parks, G.A., Dickson, F.W., Leckie, J.O., McCarty, P.L., Trace Elements in Water: Origin, Fate and Control: I. Mercury. Report of Progress, Mar 1, 1972 to Feb 1, 1973. Submitted to National Science Foundation. Stanford University. Stanford, California. 247p. (1973).
5. Neihof, R.A., Loeb, G.W., The Surface Charge of Particulate Matter in Seawater. Limnol. Oceanogr. 17,7 (1972).
6. Baughman, G.L., Gordon, J.A., Wolfe, N.L., Zepp, R.G., Chemistry of Organomercurials in Aquatic Systems. Report No. EPA-660/3-73-012. U.S. Environmental Protection Agency. Corvallis, Oregon. 97p. (1973).

FIGURE 1



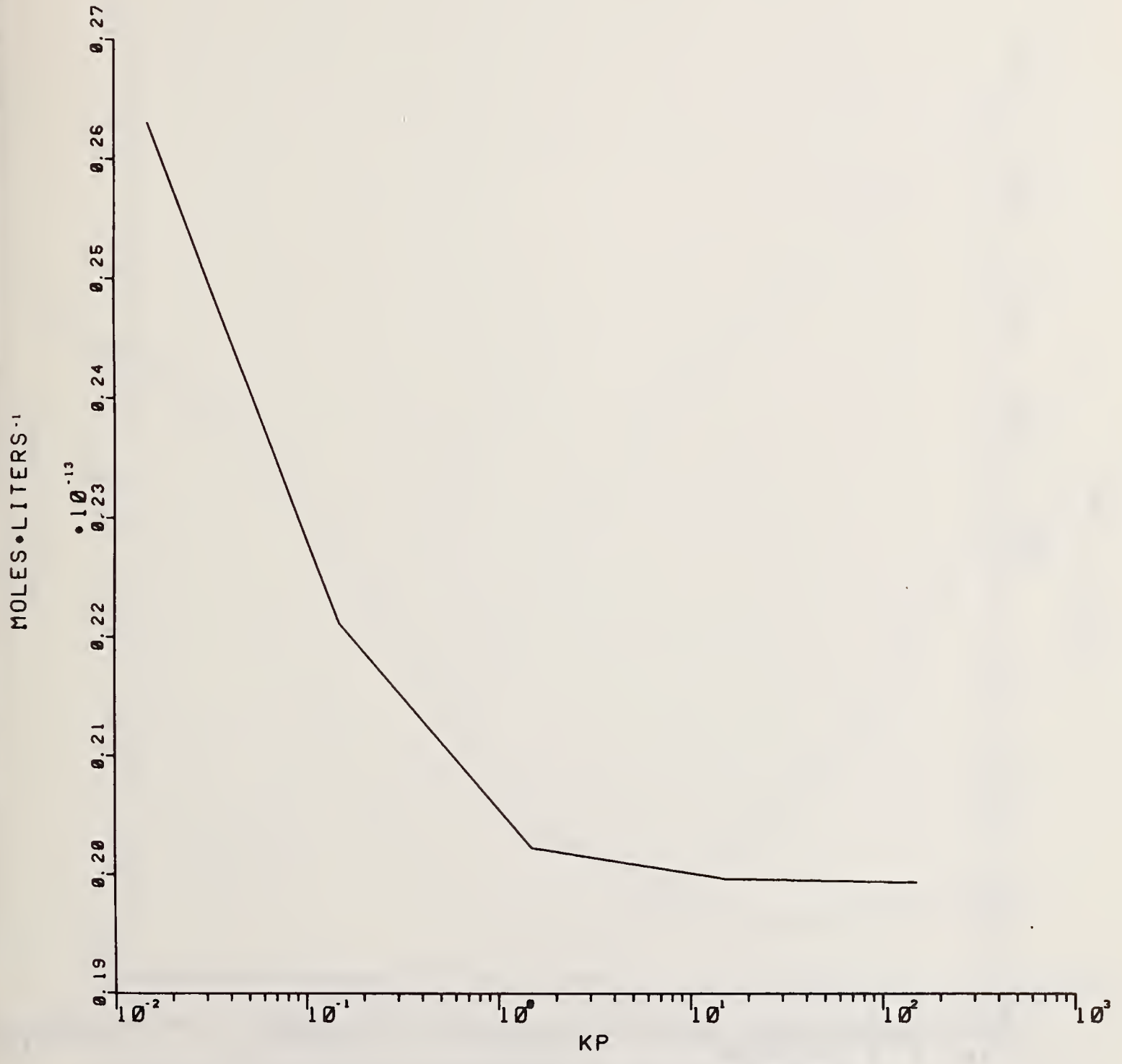
SCHEMATIC REPRESENTATION OF THE COMPONENTS, TRANSFORMATIONS, EXCHANGES AND TRANSPORT PATHWAYS REPRESENTED IN THE MODEL.

FIGURE 2



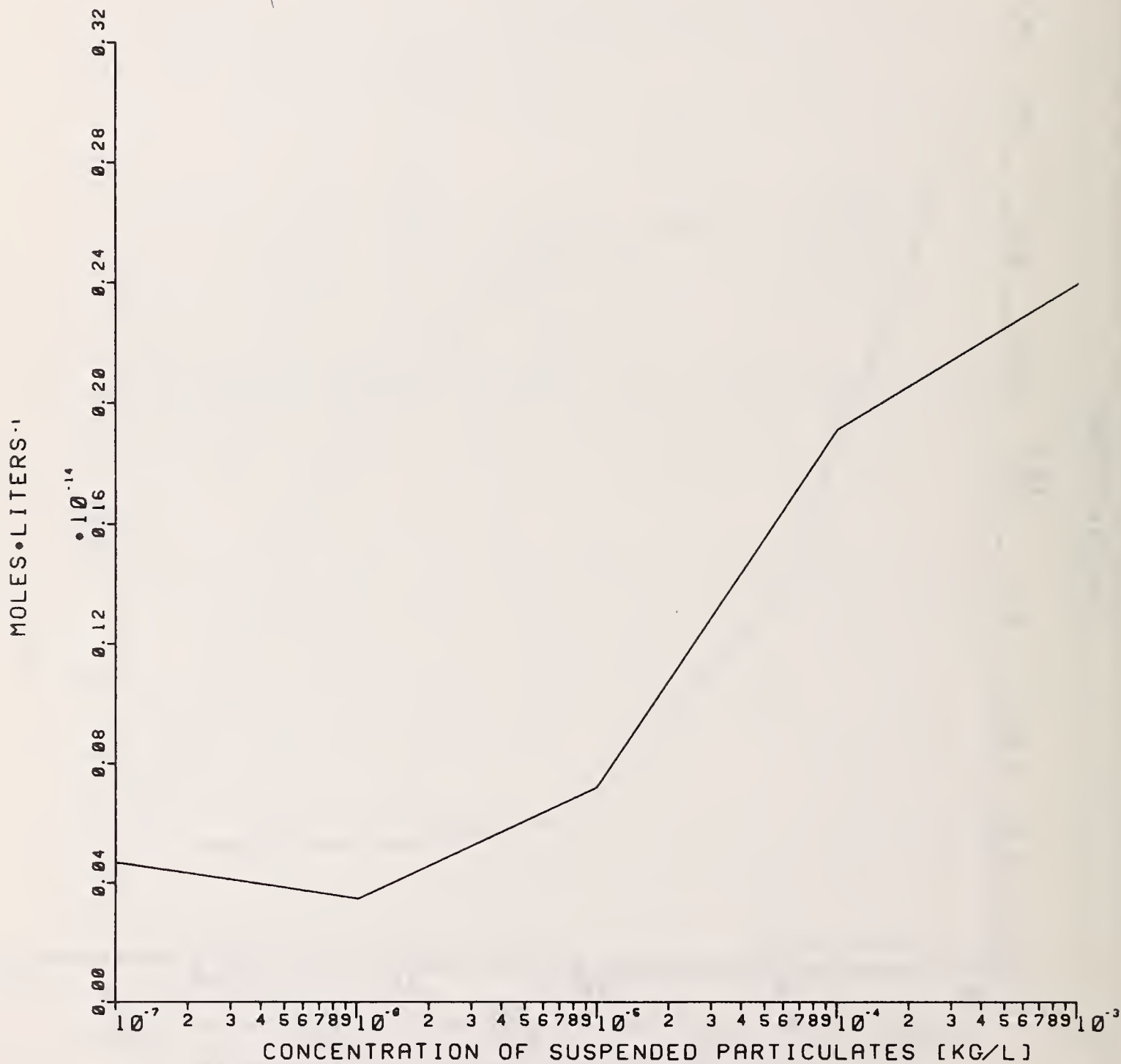
CH₃HGX IN WATER AS A FUNCTION OF KP

FIGURE 3



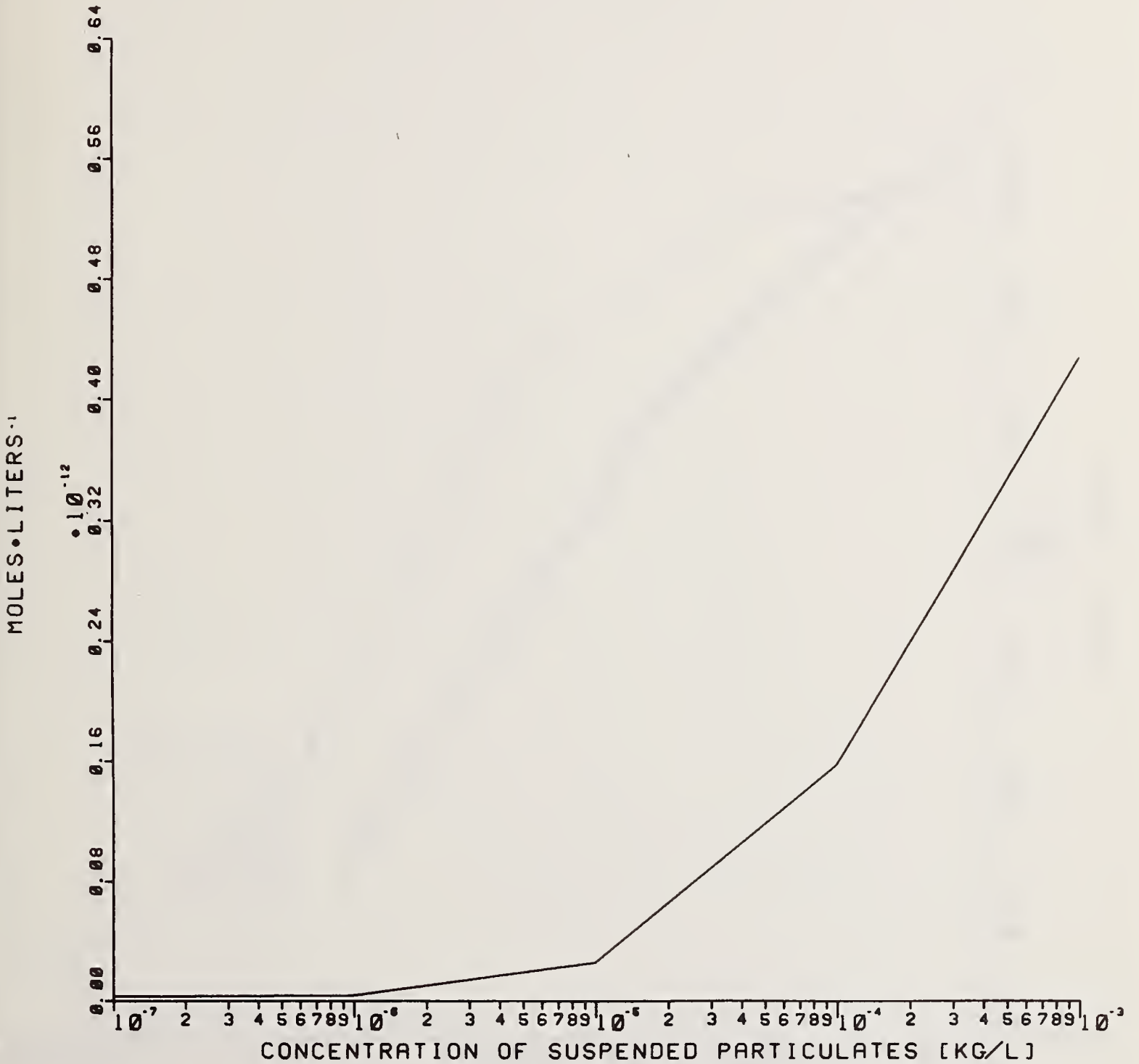
CH₃HGX IN SEDIMENT AS A FUNCTION OF KP

FIGURE 4



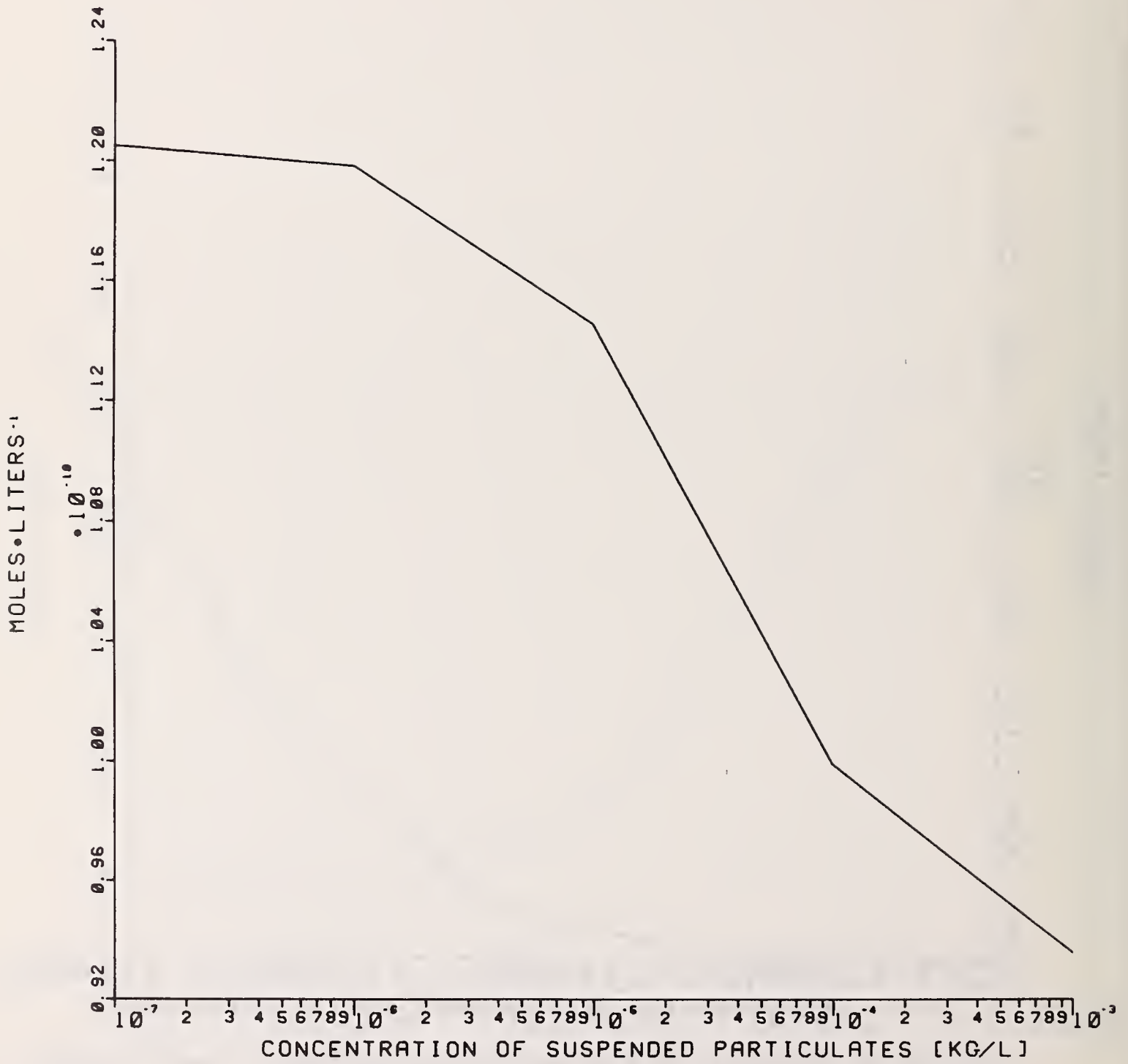
CH3HGX IN WATER AS A FUNCTION OF SUSPENDED PARTICULATES

FIGURE 5



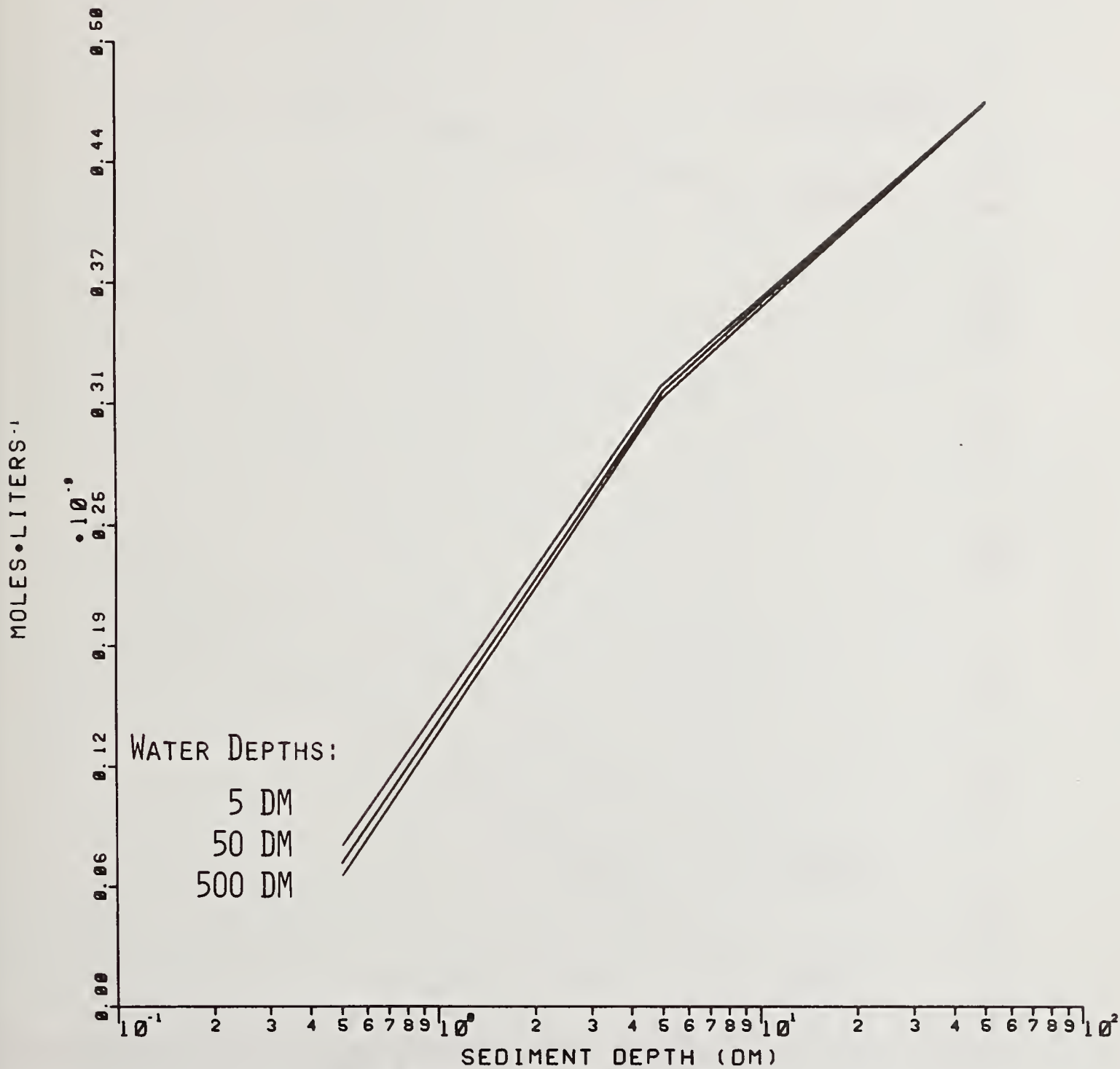
CH3HGX IN SEDIMENT AS A FUNCTION OF SUSPENDED PARTICULATES

FIGURE 6



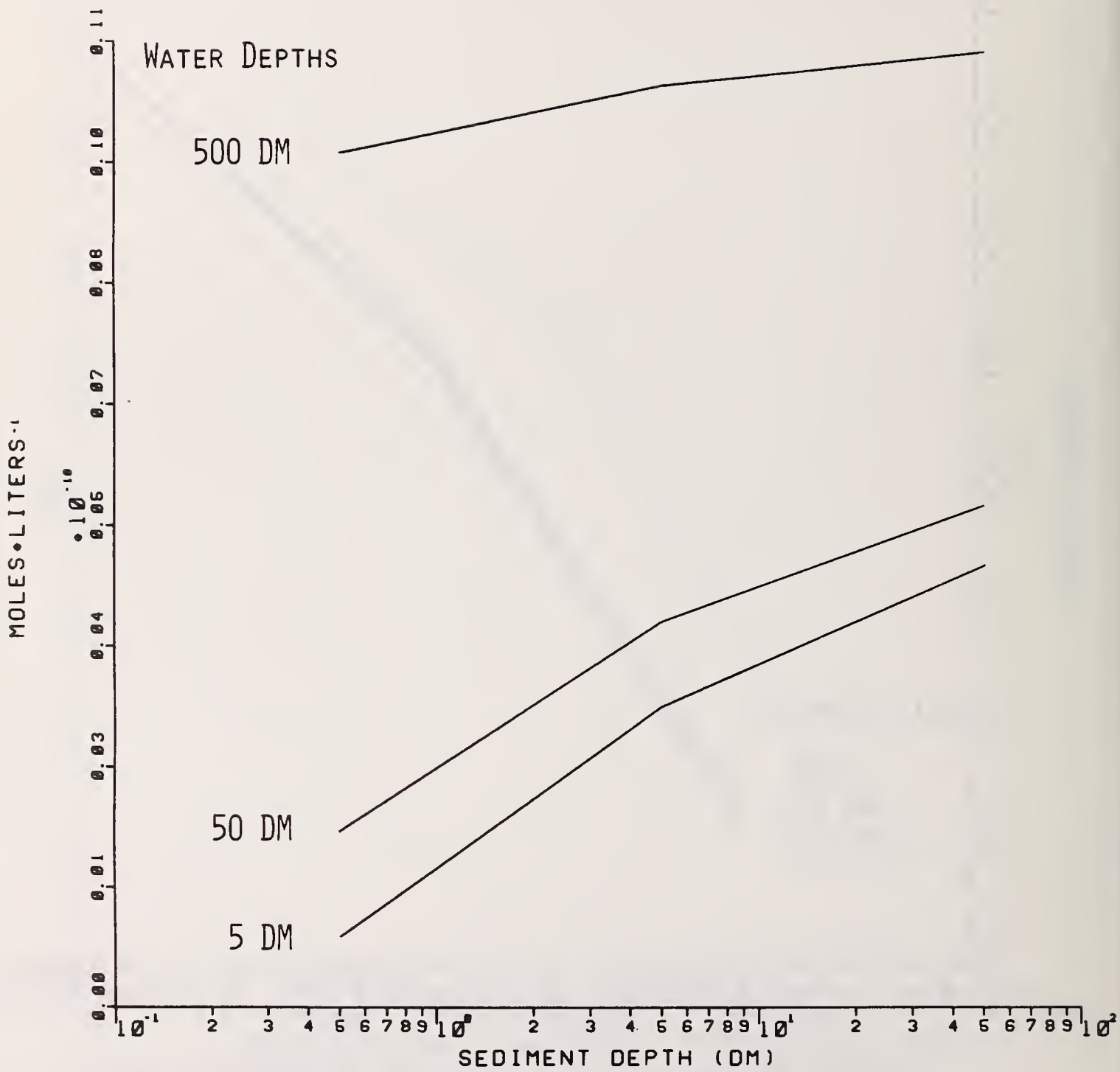
HG[0] IN SEDIMENT AS A FUNCTION OF SUSPENDED PARTICULATES

FIGURE 7



Hg(0) IN SEDIMENT AS A FUNCTION OF SEDIMENT DEPTH
FOR VARYING DEPTHS OF WATER

FIGURE 8



HG(0) IN WATER AS A FUNCTION OF DEPTH OF SEDIMENT FOR VARYING DEPTHS OF WATER

PREDICTION OF SOLUBILIZATION OF HYDROPHOBIC ORGANIC COMPOUNDS IN WATER

Albert J. Leo
Department of Chemistry, Pomona College
Claremont, California 91711

I. INTRODUCTION

The role played by the partition coefficient (model system, octanol/water) in bioaccumulation and, therefore, in biological transport, is fairly well established.¹ In fact, it would appear to be the dominant variable. In *non*-biological transport (NBT) many more factors must be considered, as is evident from the topics of this symposium. But again, partitioning between phases or the closely allied phenomenon of adsorption to a hydrophobic surface^{2,3} is assuredly going to play an important role.

A. Solubility

1. Of Solids: Studying the solubility of solid, hydrophobic organic chemicals, even in simplified model environments, is likely to prove more difficult than it is rewarding for the demands imposed by either the kinetic or the equilibrium approach in most cases make even a gross approximation difficult. There are some exceptions; a sizable quantity of insecticide and fungicide, for example, is currently being applied in the form of a wettable powder. In all probability, some of it may begin its dispersion into the environment without ever passing into solute form. Rates of solution and ultimate solubility of the crystalline form of the active material would be of far less value than the same parameters measured on the highly dispersed solid phase. Even in this example, however, it is probable that a "random walk" *partitioning* process - solution in water/adsorption on hydrophobic surface/solution in water/solution in lipid phase/etc. - will ultimately be responsible for any sizable movement of the pollutant away from its source.

2. Of Liquids: The process of dissolving an organic liquid in water is closely analogous to its partitioning between a lipid phase and water. In fact, when the organic liquid is not miscible with water, it can be considered a process of self-partitioning. Hansch *et al.*⁴ have shown that the solubility of a wide variety of nonpolar and partially polar organic liquids is related to their $\log P_{(\text{oct})}$ values by this relationship:

$$\log 1/S = a \log P + b \quad (1)$$

	Slope <i>a</i>	Intercept <i>b</i>	<i>n</i>	<i>r</i>	<i>s</i>
All Solute Types	1.339	-0.978	156	0.935	0.472
All Except Alkanes	1.214	-0.850	140	0.955	0.344
Alkanes	1.142	-0.644	16	0.953	0.198

where *n* = number of data points, *r* = coefficient of correlation, and *s* = standard deviation.

There is one very important difference between solubility and partitioning measurements, especially as they apply to certain of the very hydrophobic compounds. Since the chlorinated hydrocarbon insecticides (including DDT) and also the polychlorinated biphenyls (PCBs) are involved, this difference may indeed be critical.

Solubility measurements are made in pure water and, even at saturation, the effects of one solute molecule on another are almost nil. However, when a solute such as pentachlorophenol is distributed between mutually saturated water and octanol phases, the 10^{-3} M octanol in the polar phase is considerably above the concentration of the phenol which can be expected to dissolve in pure water. Although small, this amount of octanol can help solubilize certain types of structures giving them a lower apparent hydrophobic character than would be predicted.

What is remarkable, however, is that *transport* phenomena in many biological systems and measurements of *bioaccumulation* in trout¹ are predicted much better by using $\log P_{(oct)}$ than by using a solubility parameter. This will be covered in greater detail later.

B. Altered Solubility

Of course many pollutants are not accidental contaminants but, like insecticides and herbicides, are purposely used and applied. They are considered pollutants as soon as they "escape" from their intended target area. A rather frightening observation is that frequently, in aerial application, less than half the material applied actually strikes the target area! Be that as it may, the solubility and initial partition behavior of many of these are markedly altered to increase functionality. For instance, most lipophilic insecticides and herbicides are applied as emulsions which are much more rapidly dispersed into the aqueous phase of the environment. The chlorinated hydrocarbons used in machine cutting oils are another example of a potential pollutant whose properties are significantly altered through emulsification.

Yapel has measured the $\log P_{(oct)}$ for 15 trifluoromethane sulfonanilide preemergence herbicides in the presence and absence of 0.1% Tween-80 (polyoxyethylene-20-sorbitan-mono-oleate). This work showed that T-80 did cause a lowering of observed lipophilicity of each member of the series but it was not evident how to relate the amount of lowering to the structural features of the herbicide-surfactant combination. Nor was there any attempt to determine how long this effect could be expected to persist in actual environmental conditions. There is a clear and obvious need for further carefully planned research in this area.

II. STRUCTURAL BASIS FOR SOLUBILITY AND PARTITIONING OF ORGANIC LIQUIDS

Reference to the close relationship between solubility and partitioning of organic liquids was made earlier. Recent attempts⁶⁻⁹ to put one or both on a sound structural basis appear to be making progress.

Briefly stated, both solution and partitioning are equilibrium processes which depend very largely, in the case of apolar solutes, on the *size* of the cavity needed to accommodate the molecule and upon the *amount* of solvent structure (clustering) it induces in the surrounding water molecules (Figure 1a,b). If the solute contains a permanent localized dipole or formal charge, solvent clustering around that part of the cavity will be reduced and the reduced entropy decreases hydrophobicity. Hydrogen bonding groups in the solute likewise reduce this entropy effect and also reduce the net energy needed for cavity formation. Each of these effects will be elaborated on and their relationship to the rules governing the calculation of $\log P$ values pointed out.

A. Charge Separation Effects and Hydrogen Bonding

The addition of a "polar" or "hydrophilic" group to an otherwise apolar solute increases its water solubility and decreases its partition coefficient (oil/water by common usage). There appear to be two separate mechanisms - one depending upon a dipole and the other on hydrogen bonding - for the decrease in partition coefficient when a -Cl or an -OH is added to an alkane; but both must operate to some extent through their cluster breaking properties.

In Figure 1c, the water molecules in the section of the cavity wall near the -Cl orient themselves according to the *localized* charge separation present in the C-Cl bond. This solvent orientation is *structure-breaking* as far as water clustering is concerned. Of course, the dipole-dipole bond adds more stability than just London forces operating between water and hydrocarbon.

Much the same argument holds in Figure 1d where the polar group is -OH. Even though water clustering is dependent upon hydrogen bonds, the hydrogen bonds between solvent and solute ($HB_{\nu-\mu}$) must be considered as *structure-breaking* rather than structure-reinforcing as will be seen later.

B. Proximity Effects

1. Dipole Screening: A chlorine atom is larger than a hydrogen so, as expected, CCl_4 has a higher $\log P$ than does CH_4 . $\log P(CCl_4) = 2.83$ and $\log P(CH_4) = 1.09$; $\pi(Cl) = 1.74/4 = +0.44$. As is seen in Figure 2a and 2b, both CCl_4 and CH_4 appear to expose an uninterpreted hydrophobic surface to the aqueous phase. However, in the case of methyl chloride (Figure 2c, $\log P = 0.91$), the charge separation in the C-Cl bond is exposed and the combination of a smaller structured water "sweater" and the solute-solvent dipole-dipole attraction reduces $\pi(Cl)$ from +0.44 to -0.18. This effect will be taken into account in the calculation procedures which follow as a multiple-halogenation correction.

The *diffuse* dipole in *aromatic* halides apparently cannot act in the structure-breaking (hydrophilic) manner because $\pi-Cl/C_6H_5 = +0.71$ (*vs* +0.44 for alkane). It should be noted that, because it does not measure *localized* charge separation, dipole moment is *NOT* an indicator of the hydrophilicity imparted by cluster breaking. For example, in the di-chloro-benzene isomers, the ortho and para forms are essentially equally hydrophobic: $\log P$ -ortho = 3.38, $\mu = 1.58D$; $\log P$ -para = 3.39, $\mu = 0.0D$.

2. Cluster-Breaking Overlap: If two cluster-breaking (hydrophilic) groups are placed in close proximity (separated by no more than two carbon atoms), their effects overlap and thus are not additive; see Figure 3. This was first incorporated into a calculation scheme by Nys and Rekker.¹⁰ At present, it seems adequately accounted for by assigning one of two correction values, depending on whether one or two methylene groups separate a wide variety of hydrogen bonding groups.

III. CALCULATION PROCEDURE

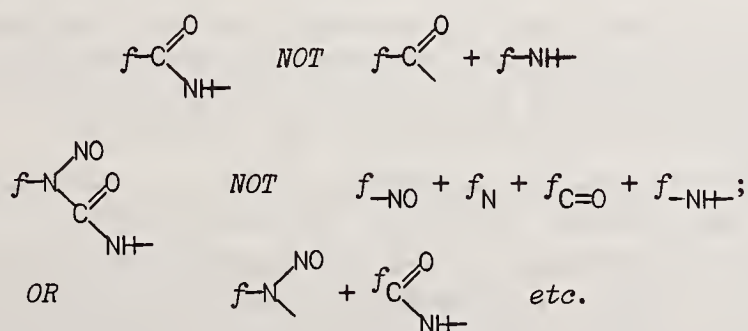
Partition coefficients can best be calculated in the form of their logarithms. All of the following are based on the octanol/water system but conversion to other solvent systems is possible by means of suitable regression equations.^{11 12} The original system of $\log P$ calculation,¹³ based on the addition of a π constant to the known $\log P$ of a parent compound, is the simplest and most dependable to use when the data are available. However, even when using the largest list of $\log P$ values available at the present time - over 10,000 structure-sorted values¹⁴ - one soon learns that a large number of environmentally interesting molecules are absent and not even any close analogs have their $\log P$'s reported. Therefore, the calculation method presented here will be based on the summation of hydrophobic "fragment constants" and certain other "factors" arising out of the constitutive nature of this parameter.

In a manner similar to Nys and Rekker's original proposal,¹⁰ $\log P$ is calculated as:

$$\log P = \sum_1^n a_n f_n + bPe_1 + cPe_2 \quad (2)$$

where f is either a fragment or a factor and there are a number of each of n types of them; b is the number of hydrogen-bonding groups separated by only one methylene group and c is the number separated by two. It will be noted in Table I that $Pe_1 = +0.80$ and $Pe_2 = +0.40$.

Hydrophilic fragments cannot join one another; *i.e.*, the entire sequence of atoms must be considered as a single fragment. For example, it is:



The various polar fragments can be expected to interact in a different way with an aromatic fragment than with an aliphatic one. In every case, the aliphatic attachment is considered the "ground" state value and it is enhanced if the joined fragment is aromatic instead - doubly enhanced if two aromatic fragments join it. The enhancement is not uniform, however, and it is necessary to give separate listings for each type as will be noted in Table I as f , f^ϕ , and $f^{\phi\phi}$, respectively.

The need for constitutive factors in such calculations has been established previously.¹⁵ These factors for chain and ring bonds, for chain and group branching, and for normal and conjugated multiple bonds are also given in Table I. The empirical formulae which allow for the extra hydrophobicity caused by multiple halogenation in aliphatic systems also appear.

Fujita¹³ showed that the polar effect exerted by one aromatic substituent upon another often changes the hydrogen bonding of either group which in turn affects π or $\log P$. For anilines and phenols this can be expressed in terms of Hammett's electronic parameter, σ :

$$\Delta\pi_{X/\text{aniline vs benzene}} = 0.905\sigma_X + 0.16 \quad \begin{matrix} n & r & s \\ 11 & 0.974 & 0.08 \end{matrix} \quad (3)$$

$$\Delta\pi_{X/\text{phenol vs benzene}} = 0.823\sigma_X + 0.06 \quad \begin{matrix} n & r & s \\ 24 & 0.954 & 0.10 \end{matrix} \quad (4)$$

This provides an equally good method for correcting aromatic *fragment* values for electronic interaction effects because it is evident that: $\Delta\pi_X = \Delta f_X$. Even though it is a more precise correction, we presently need one which does *not* require knowledge of the various σ values. Thus we must compromise. In fact, we are experimenting with quite a number of compromises at the present time, several of which appear in Table I under the heading "Special Aromatic Fragment Types." The needs filled by these special values are:

- (1) f^{1R} = fragment attached to α -carbon of aromatic ring side chain; this carbon has a slight aromatic character and therefore fragments attached to it have enhanced lipophilicity. It appears that this special type may be replaced by a constant correction of +0.15.
- (2) f^{1X} = fragment attached either meta or para to $-\text{NO}_2$ group or in 3- or 4-position in pyridine. This may also apply when fragment in this relationship with any substituent having $\sigma_p \geq 0.5$.
- (3) f^{2X} = fragment attached either ortho to $-\text{NO}_2$ or in 2-position of pyridine ring; can possibly be combined with f^{1X} .

In aliphatic systems, there can be a very large hydrophobic enhancement caused by halogenating the carbon atom adjacent to a hydrogen bonding group. The variation in group susceptibility to this polar effect is large (over 2.5 log units for the α -trifluoro-derivatives) and no predictive "rule" has been devised. The type of functional groups for which this effect has been studied appears in Figure 4. At present we have no alternative but to choose that hydrogen bonding substituent from these graphs which most closely resemble the one in question and then read off the $\Sigma\pi$ values for either mono-, di-, or tri-halogenation.

IV. CONCLUSIONS

Further research will likely bear out the early findings that hydrophobicity, as measured by $\log P_{(\text{oct})}$, is the most important parameter in bioaccumulation and biotransport; its role in non-biological transport may not be so dominant but should, none the less, be important. Some possibilities which may follow these findings are:

- (1) The measurement of partition coefficients might be established as one requirement for registering a chemical (herbicide, insecticide, etc.).
- (2) Projects could be encouraged or contracts proposed for partition coefficient measurement of basic classes of unregistered chemicals, taking care to avoid duplication of effort. As more measured values become available, the calculation procedures can be refined so that the number of structures for which neither measured nor calculated values are available will be rapidly reduced.

- (3) The basic knowledge of the partitioning process can be applied to the design of chemical structures, or at least can direct a choice among various alternatives to one which should minimize any pollution problem.

To summarize: Partitioning is recognized as a vital physical process in the elaboration of transport phenomena of drugs and xenobiotics in living organisms and it seems safe to assume it will have no less important a role in that delicate "super-organism", the earth's total biosphere. Perhaps someday a partition coefficient will be measured and reported for every new compound as routinely as a boiling point or index of refraction. It may have greater ultimate significance.

REFERENCES

1. D. R. Branson *et al.*, Proceeding of Symposium, "Structure-Activity Correlations in Studies of Toxicity and Bioconcentration with Aquatic Organisms," Canada Centre for Inland Waters, Burlington, Ontario, 1975.
2. W. Dunn III and C. Hansch, *J. Pharm. Sci.*, 61, 1 (1972).
3. W. Dunn III and C. Hansch, *Chem.-Biol. Interactions*, 9, 75 (1974).
4. C. Hansch, J. Quinlan, and G. Lawrence, *J. Org. Chem.*, 33, 347 (1968).
5. "Biological Correlations - The Hansch Approach," *Advances in Chemistry Series #114*, A.C.S. 1972, p 183.
6. M. Harris, T. Higuchi, and J. Rytting, *J. Phys. Chem.*, 77, 2694 (1973).
7. R. Hermann, *J. Phys. Chem.*, 79, 163 (1975).
8. G. Amidon, S. Yalkowsky, and S. Leung, *J. Pharm. Sci.*, 63, 1858 (1974).
9. A. Leo, C. Hansch, and P. Jow, *J. Med. Chem.*, 19, 000 (1976).
10. G. Nys and R. Rekker, *Chim. Therap.*, 1973, 521.
11. A. Leo, C. Hansch, and D. Elkins, *Chem. Rev.*, 71, 525 (1971).
12. P. Seiler, *Europ. J. Med. Chem.*, 9, 473 (1974).
13. T. Fujita, J. Iwasa, and C. Hansch, *J. Am. Chem. Soc.*, 86, 5175 (1964).
14. Can be purchased from Pomona College Medicinal Chemistry Project, Claremont, Ca. 91711.
15. A. Leo, P. Jow, C. Silipo, and C. Hansch, *J. Med. Chem.*, 18, 865 (1975).

TABLE I. FRAGMENT CONSTANTS

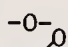
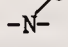

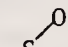
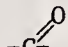
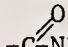
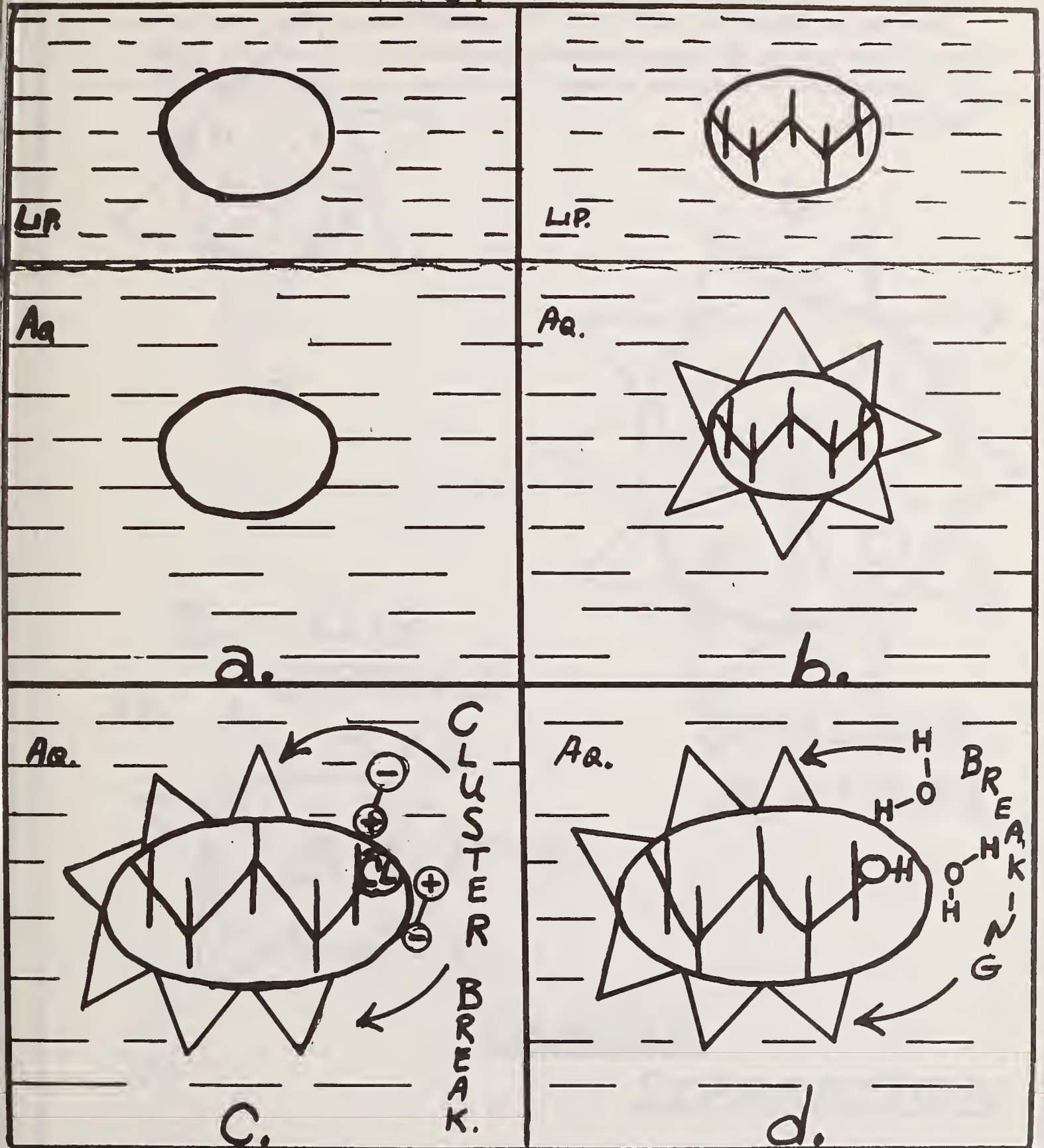
	f	f^ϕ	$f^{\phi\phi}$	S.F.T. ¹		In Aromatic Ring		
No Carbon					-N=	-1.08		
No H	-Br	0.20	1.09		$f^{1R} = 0.48$	-N-	-0.52	
	-Cl	0.06	0.94			-N+=	-6.59	
	-F	-0.38	0.37			-NH-	-0.67	
	-SO ₂ F		0.30				-0.08	
	-I	0.59	1.35				-3.46	
	-N<	-2.18	-0.93	-1.13	$f^{1R} = -1.76$	-S-	0.38	
		-7.37	-6.71				-2.08	
	-NO		0.11			-Se-	0.45	
	-NO ₂	-1.16	-0.03		$f^{X2} = +0.09$	<u>C</u>	0.13	
	-SO ₂ N<		-2.09			<u>C</u>	0.225	
	-O-	-1.82	-0.61	0.53	$\begin{cases} f^{X1} = -0.22 \\ f^{X2} = +0.17 \end{cases}$	<u>C</u>	0.44	
	-SO-	-3.01	-2.12	-1.62		CH	0.355	
	-SO ₂ -	-2.40	-2.17	-1.28		-CO ₂ -	-1.40	
	-OPO ₃ <		-2.22				-1.10	
	-S-	-0.79	0.03	0.77			-2.00	
	With H	-NH-	-2.15	-1.03	-0.09	$f^{X1} = -0.37$		
-SO ₂ NH-				-1.10	$f^{1/\phi} = -1.72$			
=NNH-		-3.06	-0.62			<u>Double Bonds</u>		
-OH		-1.64	-0.44		$\begin{cases} f^{X1} = +0.32 \\ f^{1R} = -1.34 \end{cases}$	Normal	-0.55	
-SH		-0.23	0.62			Conjugated to ϕ	-0.40	
-NH ₂		-1.54	-1.00		$\begin{cases} f^{1R} = -1.35 \\ f^{X1} = -0.23 \end{cases}$	Conjugated to -C=O	-0.08	
-SO ₂ NH ₂			-1.59		$f^{X1} = -1.04$	Conjugated to -O-	+0.15	
With Carbon						<u>Triple Bonds</u>		
	-CN	-1.27	-0.34		$f^{1R} = -0.88$	Normal	-1.42	
	-CON<	-3.04	-2.80	-1.93	$f^{1/\phi} = -2.20$			
	No H	-SCN	-0.48	0.64		$f^{1R} = -0.45$	<u>Factors</u>	
		-CO-	-1.90	-1.09	-0.50	$\begin{cases} f^{1R} = -1.77 \\ f^{X1} = -0.83 \end{cases}$	Chain Bonds =	-0.12 (n-1)
		-CO ₂ -	-1.49	-0.56	-0.09	$\begin{cases} f^{1R} = -1.38 \\ f^{X1} = -0.36 \end{cases}$	Ring Bonds =	-0.09 (n-1)
		-CO ₂ -	-5.19	-4.13			Ring Cluster =	-0.45
	With H	-CONH-	-2.71	-1.81	-1.06	$f^{1/\phi} = -1.51$	Chain Branch =	-0.13
		>C=NOH	-1.25	-0.38			Group Branch =	-0.22
		-OCONH-		-1.51		$f^{1/\phi} = -0.91$	<u>Halogenation²</u>	
-C=O(H)			-0.42			Multiple:		
-CO ₂ H		-1.11	-0.03		$f^{1R} = -1.03$	gem- 2 = 0.30; 3 = 0.53; 4 = 0.70		
					vic- 2(n-1) × 0.14			

Fig. 1

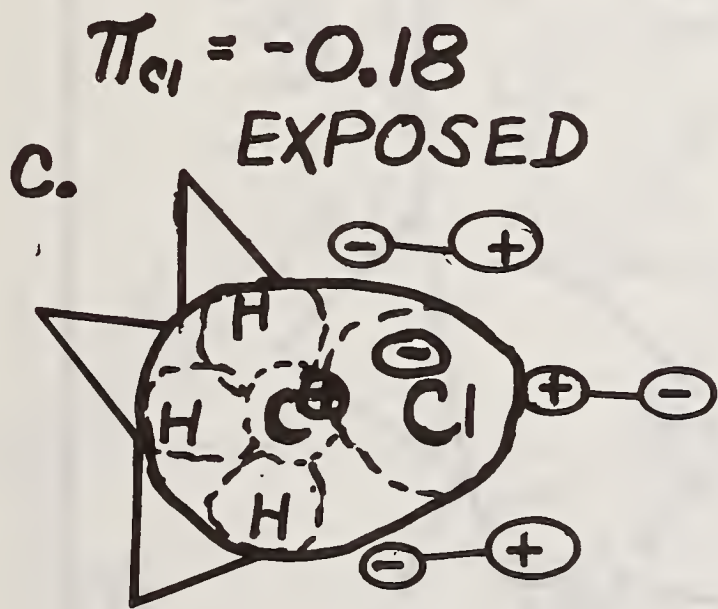
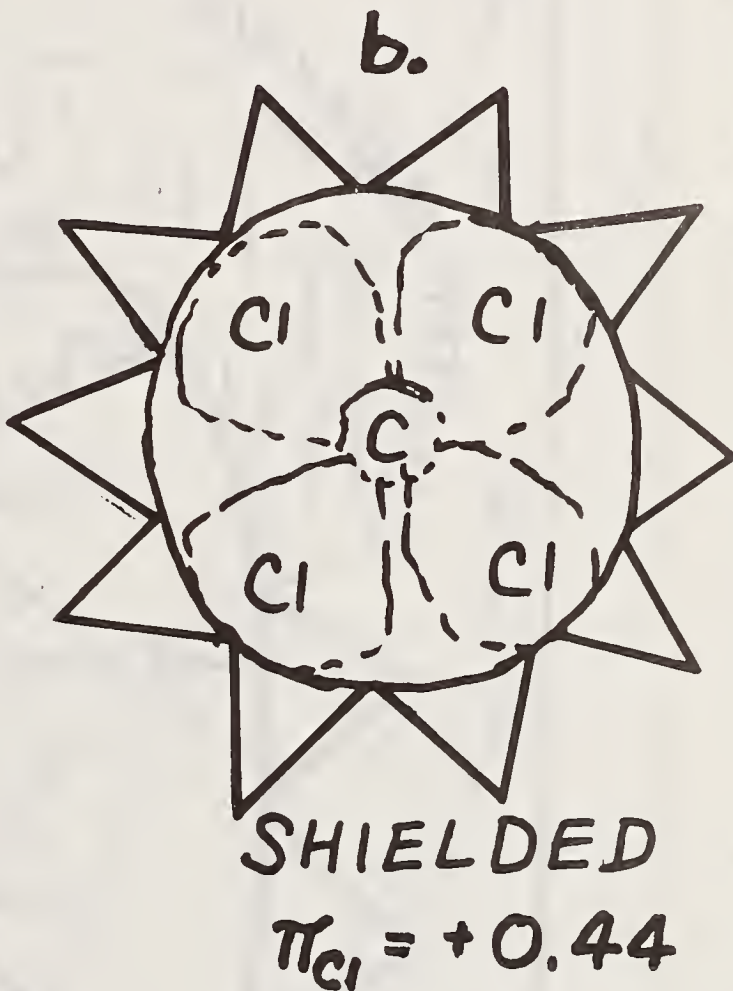
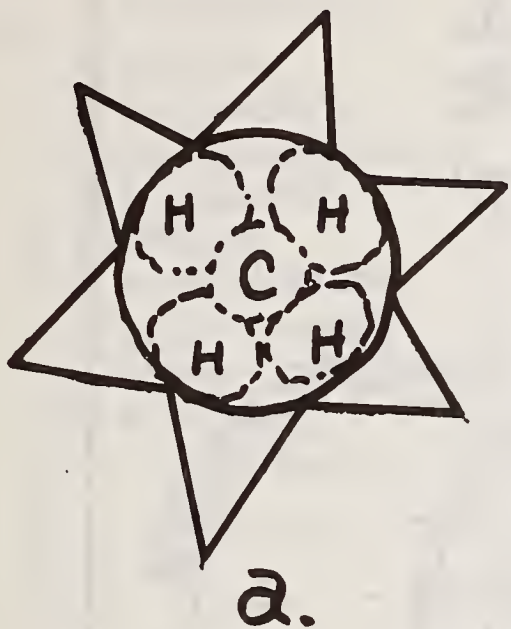


SOLVATION ENERGY AS AFFECTED BY SOLUTE VOLUME AND WATER STRUCTURE

- Cavity in partitioning solvents
- Cavity with solute present
- Solute with polar group
- Solute with hydrogen bonding group

-CONH ₂	-2.18	-1.26	$\begin{cases} f^{1R} = -1.99 \\ f^{X1} = -0.84 \end{cases}$
-NHCONH-	-1.57	-0.82	

¹See text for definition of f^{1R} , f^{X1} , f^{X2} ; Special Fragment Types: for unsymmetrical bi-functional groups, the primary attachment considered that of later WLN symbol; *i.e.*, the *left-hand* bond in structures as shown; the reverse given by $1/\phi$. ²Not affecting H-bonding group.



CHARGE

SEPARATION

FIG. 2.

CHARGE SEPARATION IN ALKYL SOLUTES

- a. No charge
- b. Charge, shielded
- c. Charge, exposed

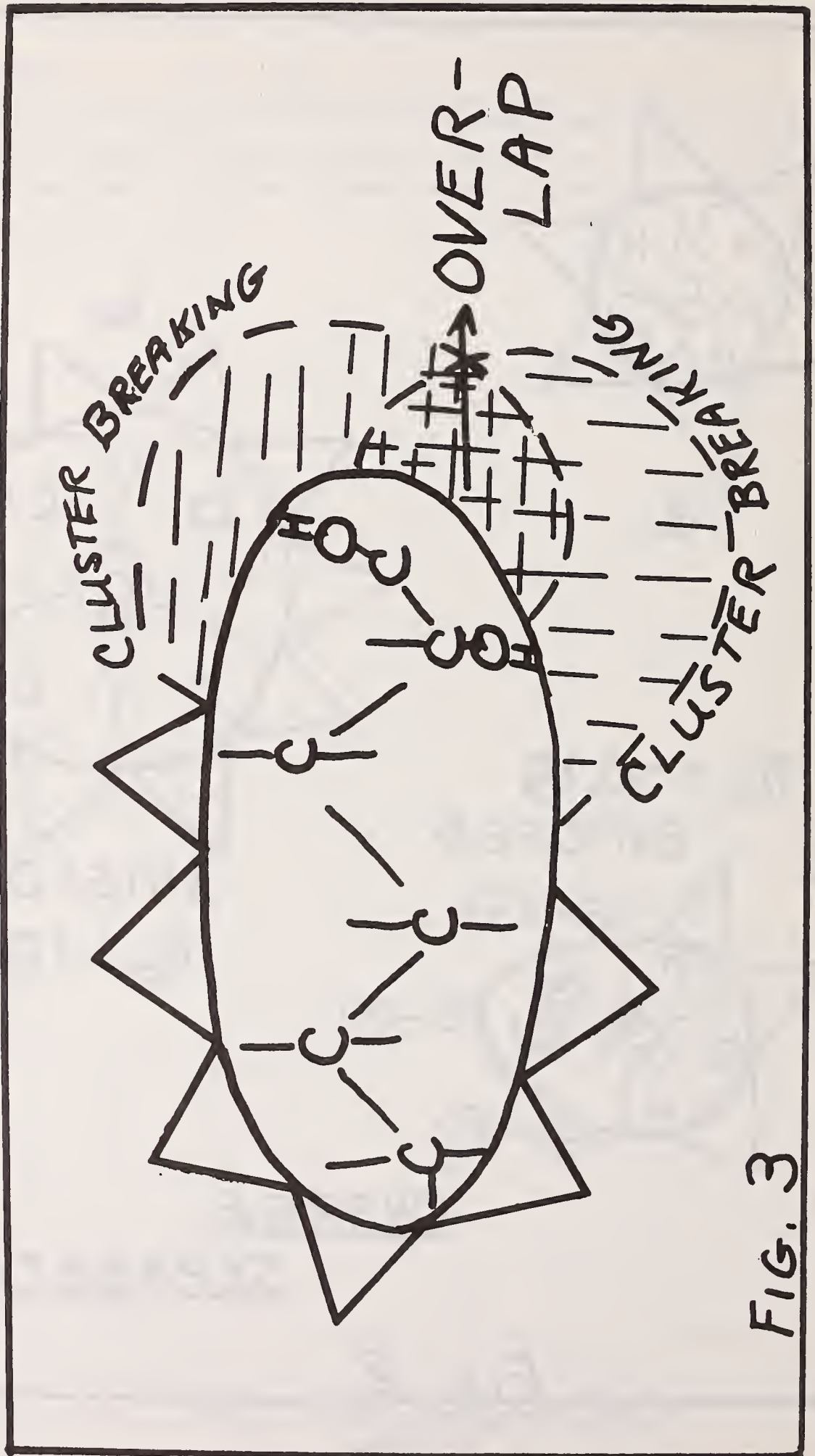
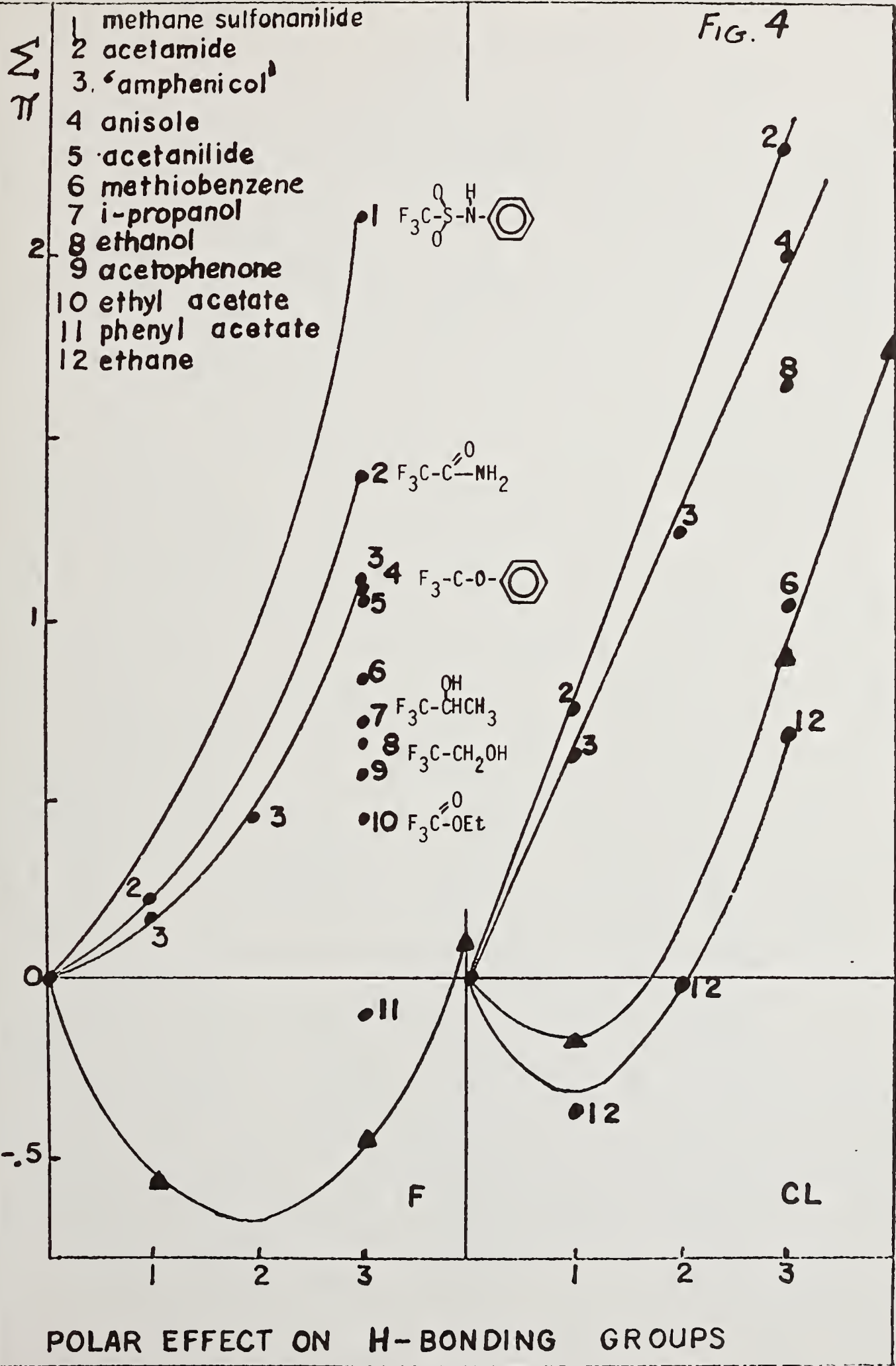


FIG. 3

PROXIMITY EFFECT RESULTING FROM CLUSTER BREAKING OVERLAP

FIG. 4



POLAR EFFECT ON HYDROGEN BONDING EFFECT IN ALKYL STRUCTURES

THE ENVIRONMENTAL PHOTODEGRADATION OF SELECTED ORGANOMETALLIC COMPLEXES

Haines B. Lockhart, Jr.
Health, Safety, and Human Factors Laboratory
Eastman Kodak Company
Kodak Park
Rochester, N.Y. 14650

Introduction

Synthetic chelating agents are being used in agriculture, food and drug processing, photography, and textile and paper manufacturing. The combined United States production of one such chelating agent, the polyamine polycarboxylic acid EDTA, was 64 million pounds in 1972 (1). Any study of the fate of EDTA and similar chelating agents in the environment must be, in fact, a study of the various chelates formed between the common metal ions and the chelating agents. This is a direct result of the concentration of common metal ions in natural waters (2) and the magnitude of the corresponding chelate formation constants (3).

Interaction with sunlight, i.e. photodegradation, may act to remove these chelates from the environment. Previous studies on the photodegradation of Fe(III)-EDTA, one of the most thermodynamically stable EDTA chelates, have identified carbon dioxide (from the carboxyl carbon) formaldehyde (from the acetate carbon), and Fe(II) as products in a 1:1:2 ratio (4,5). Studies on the photodegradation of ferric NTA, an aminopolycarboxylic acid - metal chelate, by Trott *et al.* (6) have identified these same photodegradation products along with iminodiacetic acid (IMDA).

In our studies, we have investigated the rates of photodegradation of buffered aqueous solutions of X(N)-carboxyl- ^{14}C -labeled EDTA in the presence of oxygen and simulated sunlight. Also, the identification of additional ferric EDTA photodegradation products N-carboxymethyl-N,N'-ethylenediglycine [ED3A], N,N'-ethylenediglycine [EDDA-N,N'], N-carboxymethyl-N-aminoethyleneglycine [EDDA-N,N], IMDA, N-aminoethylene [EDMA], and glycine is reported; the structure of these materials is given in Figure 1. These degradation products have been quantified and their generation studied kinetically from pH 4 to pH 8, the pH range of natural waters (6).

Materials and Methods

Static photolysis of X(N)- ^{14}C -EDTA chelates was performed in a modified 50 ml PYREX Erlenmeyer flask. This flask was fitted with a downward curving 3/4" diameter side arm threaded to receive a scintillation vial containing a CO₂ absorber of 1.0 ml of diethanolamine and 0.2 ml of water attached by a threaded TEFLON brand of polytetrafluoroethylene sleeve. The chelate was formed *in situ* at 0 time by adding stoichiometric amounts of the cation chloride and a solution of ^{14}C -EDTA to 50 mM sodium acetate buffer at pH 4.5. All solutions were prepared in sterile water. The final chelate concentration was 1.67 mM. Flasks were sealed with serum stoppers and irradiated at 4000 foot-candles for 100 hours by a 5500 watt xenon arc lamp with a UV transmissive filter. Fresh scintillation vials were attached at appropriate intervals, and 5 ml of 6 N HCl was injected through the stopper at the end of the experiment to release any dissolved carbon dioxide. A scintillation cocktail consisting of toluene and methoxyethanol was added to the vials and the amount of radioactivity volatilized from the flasks was assayed. Triplicate determinations were done in all cases. The EDTA chelates studied in this manner were Na(I), Mg(II), Ca(II), Mn(II), Fe(III), Co(II), Cu(II), Zn(II), Cd(II), Ni(II) and Hg(II). Formaldehyde in flask contents after photodegradation was assayed spectrophotometrically using the chromotropic acid method (7). The photodegradation study of Fe(III)- ^{14}C -EDTA was repeated at pH 4.5, pH 6.9 (50 mM sodium acetate buffer), and pH 8.5 (50 mM ammonium chloride buffer), with eight replicate flasks used for each pH value. Flasks were successively removed over a 96-hour period for analysis of the flask contents for bacteria and the products of photodegradation.

Volatile N-trifluoacetyl-n-butyl esters of EDTA and its photodegradation products

were prepared by the method of Zumwalt *et al.* (8). Standard curves were prepared by gas chromatography for EDTA, ED3A, EDDA-N,N', EDDA-N,N, IMDA, NTA, EDMA, and glycine using 4-aminobutyric acid as an internal standard. Gas chromatographic analysis of these volatile esters was performed on 3% QF-1 on Gas-Chrom Q, programming from 110-260°C at 10°/min.

The N-trifluoroacetyl-n-butyl esters of EDMA and EDDA-N,N as photodegradation products of Fe(III)-EDTA, were identified by fragmentation pattern analysis on GC-MS. The identities of other photodegradation products were determined by comparison to reference materials whose mass spectrometric properties had been established by Belly *et al.* (9).

Results

Of the EDTA chelates surveyed, only those of manganese, iron and cobalt photodegraded at pH 4.5 to produce $^{14}\text{CO}_2$ and formaldehyde. The $^{14}\text{CO}_2$ evolution versus time curve for these three cations is shown in Figure 2.

Some of the results of the in-depth studies on Fe(III)-1- ^{14}C -EDTA are given in Figure 3. Photodecarboxylation was pH dependent, with the greatest amount of $^{14}\text{CO}_2$ evolution occurring at pH 4.5. Similarly, the rate of Fe(III)-EDTA disappearance as determined by gas chromatography was most rapid at pH 4.5, as shown in Figure 3; no Fe(III)-EDTA was detectable after 24 hr of irradiation at pH 4.5 or pH 6.9, and none was detectable after 32 hr of photolysis at pH 8.5. Figure 3 also shows that significant photodecarboxylation was evident even after Fe(III)-EDTA was no longer detectable at all the pH values tested.

ED3A, EDDA-N,N', EDDA-N,N, EDMA, IMDA, and glycine were identified as photodegradation products by GC-MS or by comparison with known materials. Formaldehyde was identified as a photodegradation product at all pH levels studied but was not quantitated since the amounts of formaldehyde in the CO_2 absorbers could not be measured. No NTA was detected during the course of the experiment nor were any other unidentified peaks found on the gas chromatograms. Bacterial counts were insignificant.

After 96 hr of photolysis at pH 4.5 no ED3A, EDDA-N,N', or EDDA-N,N was detectable; EDMA and lesser amounts of IMDA and glycine were the only photodegradation products remaining. All photodegradation products remained after 96 hr of Fe(III)-EDTA photolysis at pH 6.9; at this pH, IMDA and EDMA were found at approximately the same concentrations at the end of the experiment. At pH 8.5, the photolysis of Fe(III)-EDTA gave rise to all the photodegradation products found at pH 4.5 and pH 6.9, but at a slower rate than at the lower pH values. Comparisons of the concentrations of EDDA-N,N' and EDDA-N,N vs. time at any pH value tested indicate that there was no preference for the generation of one of these two EDDA isomers over the other as a photolysis product of Fe(III)-EDTA. The material balance in terms of % nitrogen and % carbon atoms recovered indicates that all major photodegradation products have been identified during these experiments.

Discussion and Conclusions

These studies on the photodegradation of EDTA chelates in aqueous solution have given insight into the fate of EDTA when discharged to the environment. Our results, which indicated a photosensitivity of only the EDTA chelates of Mn(II), Fe(III) and Co(II) out of all of those tested, agree with the findings of Natarajan and Endicott (4), who found the EDTA chelates Fe(III) and Co(II) were photosensitive and those of Cr(III), Ni(II) and Cu(II) were not. These results for Cu(II)-EDTA contrast with those reported for Cu(II)-NTA by Langford *et al.* (10) who reported a significant photodecomposition of this chelate. The production of ED3A, CH_2O and CO_2 from the photolysis of EDTA reported here along with the generation of CO_2 , CH_2O and IMDA as products of Fe(III)-NTA photodegradation reported by Trott *et al.* (6) suggest a similar mechanism may be involved in the photodegradation of these Fe(III) chelates.

The results of Fe(III)-EDTA photodegradation suggest a possible scheme, presented in Figure 4. This is based on the time the various photodegradation products were first de-

tected and on their relative concentrations. As mentioned above, IMDA has been shown to be a product of the photodegradation of Fe(III)-NTA. However, our results indicate that NTA is not a significant photodegradation product of Fe(III)-EDTA, so IMDA generation would appear to be a result of ED3A photolysis.

Although bacterial metabolism was excluded in these experiments, the biodegradation of IMDA, EDMA, EDDA-N,N', EDDA-N,N and ED3A have been recently observed (9). If we base conclusions on the results of these biodegradation studies, the products of the various photodegradation reactions of Fe(III)-EDTA would also be biologically degraded in a natural environment, thus decreasing the probability of photolysis product buildup in natural waters.

It is concluded that photodegradation may play a significant role in the removal of Fe(III)-aminopolycarboxylic chelates such as Fe(III)-EDTA and Fe(III)-NTA from natural waters.

Acknowledgements

The author expresses his appreciation for the synthesis of EDDA-N,N and ED3A by Dr. C. Flynn, and for the GC-MS analyses of photodegradation products by Mr. D. Maier, both Research Laboratories, Eastman Kodak Company.

References

- (1) U.S. Tariff Commission, "Synthetic Organic Chemicals - U.S. Production and Sales, 1972", p. 211, 1974.
- (2) Childs, C.W., 14th Conf., Inter. Ass. Great Lakes Res., Toronto, Canada, April 19-21, 1971.
- (3) Pribil, R., in "Analytical Applications of EDTA and Related Compounds", Pergamon Press, New York, N.Y., 1972.
- (4) Natarajan, P. and Endicott, J., J. Phys. Chem., 77, 2049-54, 1973.
- (5) Carey, J.H. and Langford, C.H., Can. J. Chem. 51, 3665-70, 1973.
- (6) Trott, T., Henwood, R.W. and Langford, C.H., Environ. Sci. Technol. 6, 376-8, 1972.
- (7) Levaggi, D.A. and Feldstein, M.W., J. Air Poll. Control Assn. 20, 312-3, 1970.
- (8) Zumwalt, R.W., Roach, D., Gehrke, C.W., J. Chromatogr. 53, 171-93, 1970.
- (9) Belly, R.T., Lauff, J.J. and Goodhue, C.T., Appl. Micro. 29, 787-94, 1975.
- (10) Langford, C.H., Wingham, M., and Sastri, V.S., Environ. Sci. Technol. 7, 820-22, 1973.

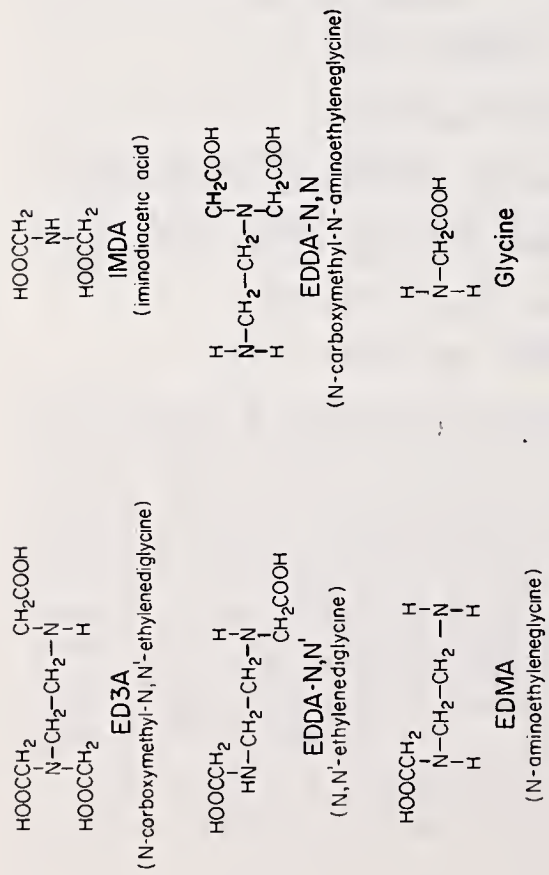


Figure 1
Photodegradation of Products of Fe(III)-EDTA

Concentration of Fe(III)-EDTA and Percent Initial ¹⁴C Volatilized (4000 fc)

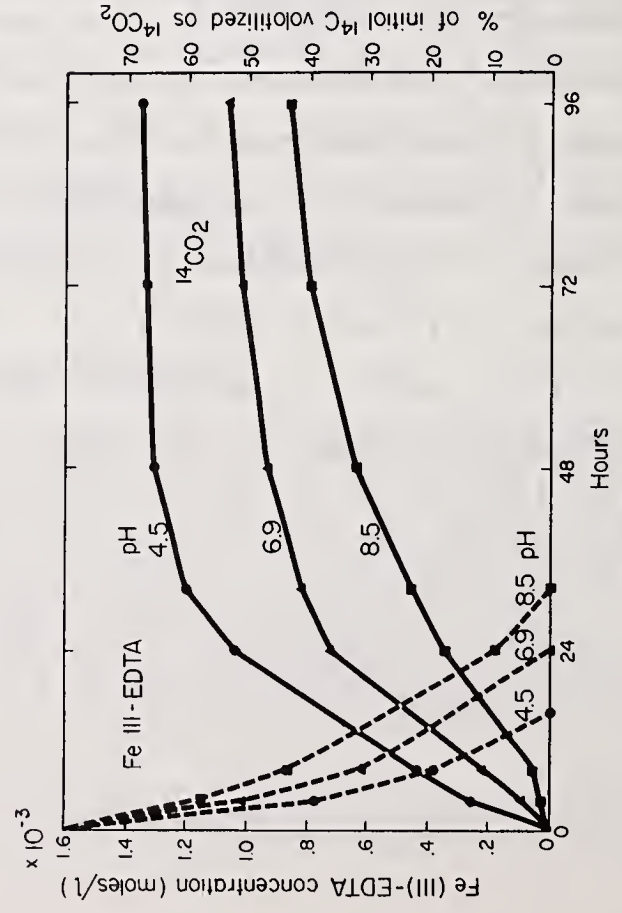


Figure 3
Concentration of Fe(III)-EDTA and Percent Initial ¹⁴C Volatilized (4000 fc)

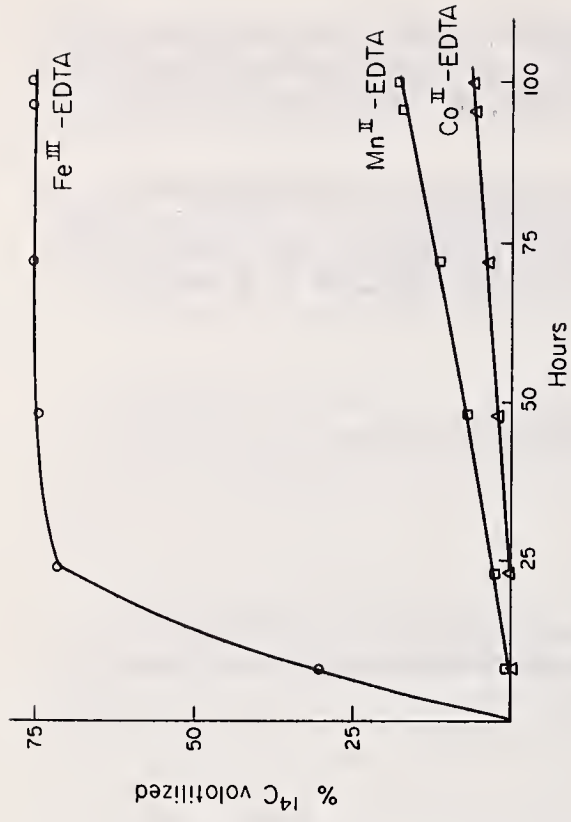


Figure 2
Static Photodegradation of Fe(III)-, Mn(II)-, and

Co(II)-1-¹⁴C-EDTA, pH 4.5, 4000 ft. candles

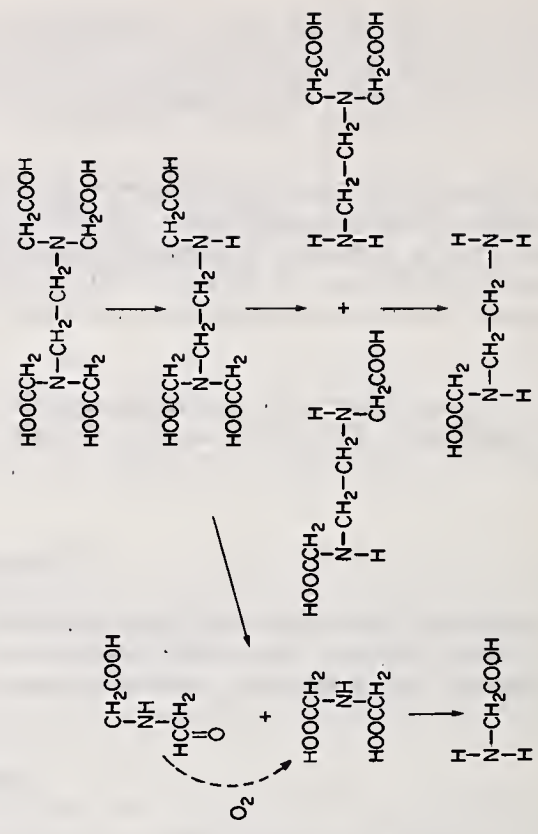


Figure 4
Proposed Photodegradation Scheme for Fe(III)-EDTA

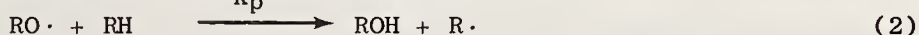
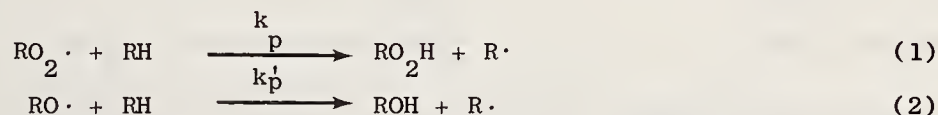
W. R. Mabey and T. Mill
Stanford Research Institute
Menlo Park, CA 94025

A wealth of information is available describing the detailed kinetics of hydrolysis, free radical and photochemical oxidation reactions under controlled and defined laboratory conditions. This knowledge can be used effectively to describe the hydrolytic degradation of organic pollutants in aquatic systems. Almost no detailed information is available, however, on the chemical oxidation reactions that occur in aquatic environments. This paper presents some general features of the kinetics of hydrolysis and free radical oxidations that are applicable toward understanding and evaluating the importance of these reactions in these environmental degradation processes.

Free Radical Oxidation

Oxidation of organic compounds in the environment almost never involves direct reaction of an organic molecule with oxygen; instead the oxidation requires the formation of intermediate radicals and/or excited species.

One of the most common and best understood oxidation processes involves peroxy and alkoxy radical chains (autoxidations) wherein three distinct types of radical processes are recognized: initiation, propagation, and termination. Most of the complications found in autoxidations are readily understood in terms of this chain process in which the two propagation reactions



are mainly responsible for oxidation of the organic substrate. Reactions (1) and (2) are depicted here as H-atom transfer; they can also involve addition of radicals to double bonds such as in vinyl chloride or styrene.

The rate laws for these processes are

$$-\frac{d\text{O}_2}{dt} = R_{\text{ox}} = k_p [\text{RH}][\text{RO}_2 \cdot] \text{ or } k_p' [\text{RH}][\text{RO} \cdot] \quad (3)$$

and for $\text{RO}_2 \cdot$ propagation

$$R_{\text{ox}} = \left(\frac{R_i}{2k_t} \right)^{\frac{1}{2}} k_p [\text{RH}] \quad (4)$$

where R_i is the rate of radical formation and $2k_t$ is the rate constant for radical destruction.

In the environment, oxidation of a substrate (RH) would involve $RO_2\cdot$ or $RO\cdot$ radicals having many different kinds of structures, and the rate of oxidation (R_{ox}) is the sum of the individual rate expressions for oxidation by each kind of radical. If we make the simplifying assumption that all $RO_2\cdot$ or $RO\cdot$ radicals (primary, secondary, and tertiary) have about the same rate constant, k_p or k'_p (a reasonable assumption within a factor of ten), then we can use equation (5) to evaluate the lifetime of a compound in an oxidizing environment.

$$t_{\frac{1}{2}} = \ln 2 / k_p [RO_n\cdot] \quad (5)$$

$$n = 1 \text{ or } 2$$

We have estimated half-lives for a variety of organic compounds using a reasonable value for $[RO_2\cdot]$ of 10^{-8} M, and known values¹ of k_p for the reactive CH bonds at 30° . Table 1 summarizes these values.

Table 1
HALF-LIVES FOR REACTION OF $RO_2\cdot$ WITH C-H BONDS AT $30^\circ C$ ^a

Compound	k_p l/mol sec ^{b,c}	$t_{\frac{1}{2}}$, days
n-Alkanes (CH_2-)	0.00027	3×10^6
Branched alkanes (>CH)	0.0048	1.7×10^5
Olefins (allylic-CH)	0.084	9.5×10^2
Benzyl (CH_2-)	0.10	8×10^3
Dienes (1,4-Allylic)	0.23	3.5×10^3
Alcohols (>CHOH)	0.009	8.9×10^4
Ethers ($-O-CH_2-$)	0.016	5×10^4
Aldehydes ($-CHO$)	3000 ^d	6 hr

^a Calculated from equation (5) using $[RO_2\cdot] = 10^{-8}$ M.

^b For reaction $\underline{t}\text{-BuO}_2\cdot + RH \rightarrow \underline{t}\text{-BuO}_2H + R\cdot$

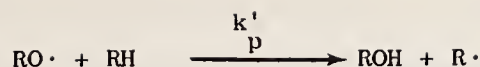
^c Reference 1.

^d For reaction $RC(O)O_2\cdot + RCHO$.

The very long half-lives listed in Table 1 suggest that, for many organic compounds present in the environment, oxidation by $RO_2\cdot$ radicals will be unimportant unless $[RO_2\cdot]$ exceeds 10^{-4} M.

Reaction with Alkoxy Radicals

Although chain oxidation via $RO_2\cdot$ radicals is unimportant under environmental conditions, radical oxidation by $RO\cdot$ radicals is still possible because of their much higher reactivity; values for k'_p for the reaction



are in the range 10^3 - 10^5 liter/mol-sec.¹ Thus, half-lives for reaction of $\text{RO}\cdot$ with organic compounds can be quite short if a continuous source of $\text{RO}\cdot$ radicals is available. Table 2 lists estimated half-lives for different classes of organic compounds assuming $[\text{RO}\cdot] = 10^{-10}$ M.

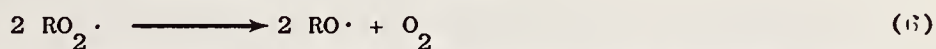
Table 2

HALF-LIVES FOR REACTION OF $\text{RO}\cdot$ WITH ORGANIC C-H BONDS AT 40°C^a

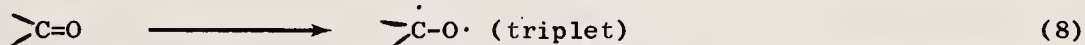
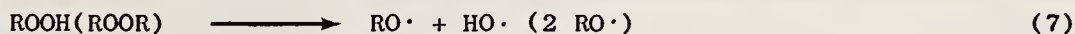
Compound	$k_p' \times 10^{-4}$ l/mol sec ^b	$t_{1/2}$, hours
Alkane ($-\text{CH}_2$)	3.6	52
Branched alkane ($-\text{CH}$)	13	14
Olefin (allylic- CH_2 -)	24	7.2
Benzyl ($-\text{CH}_2$ -)	11	14
Ethers ($-\text{CH}_2$ -)	31	6.1
Ketone ($-\text{CH}_2$ -)	0.6	320
Chlorocarbons- CHCl	0.5	380

^a Calculated from equation (5) using $[\text{RO}\cdot] = 10^{-10}$ M.

However, $\text{RO}\cdot$ and $\text{RO}_2\cdot$ chemistry generally are closely related. Under certain conditions $\text{RO}\cdot$ initiates the $\text{RO}_2\cdot$ chain sequence, and in other situations $\text{RO}_2\cdot$ can be converted to $\text{RO}\cdot$ by the reaction

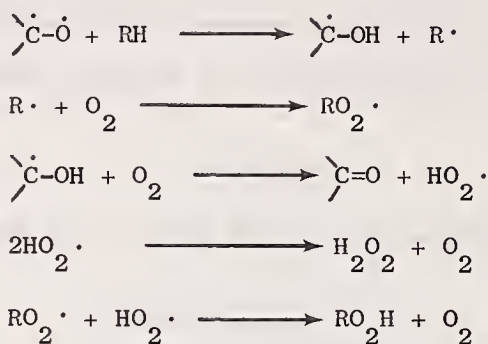


Although reaction (6) may not always be an important source of $\text{RO}\cdot$ radicals, some photochemical and metal-ion-catalyzed reactions could provide high concentrations of $\text{RO}\cdot$ radicals under environmental conditions. Photochemistry is frequently linked to environmental oxidation² and may be the most important general means by which reactive radical species like $\text{RO}\cdot$ are generated.



Reaction (7) is simply homolysis of peroxides formed by radical or singlet oxygen reactions (see below). Although this process is not very efficient in the solar region where peroxides absorb weakly, it can contribute to the radical population. Reaction (8), which proceeds through an excited singlet, could be the most important environmental

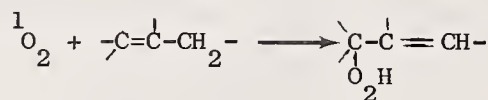
photooxidation reaction* because the triplet diradical has a reactivity similar to that of RO·.³ Reaction with substrate can initiate the oxidation process, and the carbonyl is regenerated for further use by reaction with oxygen:



Peroxides may also be generated by formation of singlet oxygen (¹O₂),⁴



and reaction of ¹O₂ with olefins,⁵



Several transition metal ions, such as Fe and Cu, occur naturally in amounts sufficient to warrant consideration of their possible roles as catalysts for environmental autoxidation. Transition metal ions catalyze autoxidations and peroxide decompositions through the efficient cycle that forms RO· and RO₂⁶⁻⁸



The rates of these reactions depend strongly on the kind of metal-ion complexes present: Fe or Cu phthalocyanine complexes are extremely effective catalysts for peroxide decomposition; FeEDTA is usually inert. In water Fe²⁺ is oxidized rapidly by ROOH, but Fe³⁺ is often nearly inert. In high-pH, aquatic systems where Fe is largely hydrated and insolubilized, its participation in electron transfer reactions may be minimal, but in acidic water Fe or Cu ions could be important in oxidation.

Natural Retarders

A wide variety of natural products can retard or inhibit radical oxidation processes. For example, flavin constituents of pigments (such as quercitol) have phenolic-OH groups

* Oxygen quenching may reduce the efficiency of the process in the environment.⁴

which are very reactive in H-atom transfer to peroxy or alkoxy radicals. In many natural eutrophic waters, the steady-state concentration of inhibitors or retarders present regulates the concentration of $RO\cdot$ or $RO_2\cdot$ radicals through termination (conversion to unreactive radicals). Very likely numerous carotenoid-like molecules are also present that can function as efficient quenchers of 1O_2 .

Hydrolysis

Hydrolysis of organic molecules usually results in introduction of a hydroxyl function (-OH) into a substrate, most commonly with the loss of a leaving group (-X). These reactions



may be catalyzed by acids (k_A) or bases (k_B) or both. The kinetics of hydrolysis of a substrate can be expressed as

$$-\frac{ds}{dt} = R_{\text{hyd}} = k_{\text{obs}}[S] = k_B[OH^-][S] + k_A[S][H^+] + k'_N[H_2O][S] \quad (9)$$

The last term is the neutral reaction with water, and in an aqueous environment $k'_N[H_2O]$ is constant ($= k_N$). With few exceptions hydrolysis reactions are usually first order in substrate. Equation (9) can then be simplified to

$$k_{\text{obs}} = k_B[OH^-] + k_A[H^+] + k_N \quad (10)$$

From the integrated form of equation (9), the half-life for hydrolysis of the substrate, $t_{\frac{1}{2}}$, is calculated.

$$t_{\frac{1}{2}} = \frac{0.693}{k_{\text{obs}}} \quad (11)$$

From equations (10) and (11) it is clear that the half-life will be dependent on the pH when k_B and/or $k_A \neq 0$. From the autoprotolysis water equilibrium,

$$[H^+][OH^-] = K_w \approx 10^{-14} \quad (12)$$

equation (10) may be rewritten

$$k_{\text{obs}} = \frac{k_B K_w}{[H^+]} + k_A [H^+] + k_N \quad (13)$$

The contribution of each term to k_{obs} will depend on the acidity (or pH) of the solution; three regions may be defined:

$$\begin{aligned} \text{Acid} \quad k_A [\text{H}^+] > k_N + \frac{k_B K_W}{[\text{H}^+]} \quad , \quad \log k_{\text{obs}} &= \log k_A + \log [\text{H}^+] \\ &= \log k_A - \text{pH} \end{aligned} \quad (14)$$

$$\begin{aligned} \text{Base} \quad \frac{k_B K_W}{[\text{H}^+]} > k_N + k_A [\text{H}^+] \quad , \quad \log k_{\text{obs}} &= \log k_B K_W - \log [\text{H}^+] \\ &= \log k_B K_W + \text{pH} \end{aligned} \quad (15)$$

$$\text{Neutral} \quad k_N > k_A [\text{H}^+] + \frac{k_B K_W}{[\text{H}^+]} \quad , \quad \log k_{\text{obs}} = \log k_N \quad (16)$$

These expressions implicitly assume that the catalyzed processes are first order in acid $[\text{H}^+]$ or base $[\text{OH}^-]$ concentration. Such behavior is almost always the case in the range of pH 2 to 12 and frequently extends to greater extremes.

From the above discussion it is seen that the observed rate of hydrolysis depends on the relative values of k_N , k_B , and k_A . Within a class of compounds the individual rate constants may vary by several orders of magnitude with the structure and substitution on the molecule. When the acid and base catalyzed mechanisms are operative, the observed rate will also be pH dependent. The hydrolysis rates of carboxylic amides and esters are typically described by acid and base catalyzed mechanisms in their respective regions with a distinct minimum between pH 4 to 7, which indicates no contribution from k_N . Some carbamates are hydrolyzed by all three mechanisms, showing a pH independent rate from pH of about 3 to 7 or 8, with the respective acid and base catalyzed mechanisms being important in the outlying pH regions.¹¹ For many alkyl halides no acid catalyzed mechanism is found, and the hydrolysis rate is pH independent to beyond pH 10 where the base reaction becomes important.¹² Thus, while each class of compounds possesses different reactivity toward hydrolysis, the reaction rates can be expressed in a common analysis that can be used for environmental assessments.

The dependence of the hydrolysis rate on the pH of the solution is conveniently depicted by a plot of $\log k_{\text{obs}}$ as a function of pH.^{10b} From expressions (14), (15), and (16), it is seen that in the pH range where the base catalyzed process is dominant, a slope of +1 is found; a slope of -1 is found in the acid catalyzed region. The neutral hydrolysis is pH independent and shows a slope of zero.

Present knowledge of the theoretical and experimental aspects of hydrolysis reactions makes laboratory studies of hydrolysis rates useful for environmental estimates. Precaution must be taken, however, to ensure that experimental artifacts are not introduced into the kinetic data. The use of buffer salts to maintain a constant pH is a common and acceptable practice, but appropriate experiments should be carried out to demonstrate

the absence of any effects of buffer catalysis or ionic strength. Another problem may arise in the use of organic cosolvents to increase the solubility of the organic substrate in the aqueous solution. Although this practice does expedite the experimental procedures, it can change the rate constant considerably over that found when water is the sole solvent.

For some organic compounds, environmental hydrolysis rates can be estimated from the extensive body of published data not originally intended for environmental relevance. The principal limitations of such data are the frequent use of elevated temperatures and mixed organic-water solvent systems. These conditions can often be corrected for by using the empirical data treatment relationships developed by physical organic chemists in their studies of mechanisms and kinetics of chemical reactions. Although few studies have been carried out at concentrations in the ppm range, the hydrolysis reaction is usually first order in pollutant and the half-life estimates are then not concentration dependent (equations 10 and 11). Half-life estimates for several organic halides and epoxides calculated from literature data are listed in Table 3 and can be quite informative for assessing degradation by hydrolysis processes.¹²

Table 3

HALF-LIVES FOR SELECTED ORGANIC HALIDES AND EPOXIDES TOWARD HYDROLYSIS
AS A FUNCTION OF pH AT 25°C IN WATER

<u>Compound</u>	<u>pH 4</u>	<u>pH 7</u>	<u>pH 10</u>
Methyl bromide	480 hr	→ same	→ same
Methyl chloride	10 ⁴ hr	→ same	→ same
Isopropyl bromide	50 hr	→ same	→ same
Isopropyl chloride	940 hr	→ same	→ same
Allyl chloride	166 hr	→ same	→ same
Benzyl chloride	15 hr	→ same	→ same
Chloroform	32000 yr	3500 yr	3.5 yr
Isobutylene oxide	0.3 hr	106 hr	175 hr
Epichlorohydrin	181 hr	197 hr	197 hr
1,3-Cyclohexadieneoxide	0.42 hr	6 min	53 min

REFERENCES

1. D. G. Hendry, T. Mill, L. Piskiewicz, J. A. Howard, and H. K. Eigenmann, *J. Phys. Chem. Ref. Data*, 3, 937 (1974).
2. (a) D. G. Crosby, Degradation of Synthetic Organic Molecules in the Biosphere (National Academy of Sciences, Washington, D.C. 1972), p. 260.
 (b) J. R. Plimmer, *ibid.*, p. 279.
3. (a) C. Walling and M. J. Gibian, *J. Amer. Chem. Soc.*, 87, 3361 (1965);
 (b) P. J. Wagner and G. S. Hammond, *Adv. Photochem.*, 5, 93 (1968);
 (c) P. J. Wagner, and A. E. Kemppainen, *J. Amer. Chem. Soc.*, 94, 7495 (1972).
4. K. Gollnick, J. Franken, G. Schade, G. Dorhofer, *Ann. N.Y. Acad. Sci.*, 171, 9 (1970).
5. R. Higgins, C. S. Foote, and H. Cheng, *Adv. Chem. Ser.*, 77, 102 (1968).
6. R. Hiatt et al., *J. Org. Chem.*, 33, 1421, 1428, 1430 (1968).
7. G. Sosnovsky and D. J. Rawlinson, Organic Peroxides, D. Swern, ed. (Wiley-Interscience, New York, 1971), p. 153.
8. *Ibid.*, p. 269.
9. P. B. Merkel and D. R. Kearns, *J. Amer. Chem. Soc.*, 94, 1029 (1972).
10. (a) R. P. Bell, Acid-Base Catalysis (Oxford Press, London, 1941), p. 6.
 (b) K. J. Laidler, Chemical Kinetics, 2nd Edition (McGraw-Hill, New York, 1965), p. 450.
11. T. Vontor and M. Vecera, *Collect. Czech. Chem. Commun.*, 38, 516-22 (1973).
12. W. R. Mabey and T. Mill, unpublished work.

notes

PREDICTION OF VOLATILIZATION RATE OF POLLUTANTS IN AQUEOUS SYSTEMS

Donald Mackay and Yoram Cohen
Department of Chemical Engineering & Applied Chemistry
and
Institute for Environmental Studies
University of Toronto
Toronto, Ontario, Canada M5S 1A4

Introduction

For some pollutants volatilization is a significant mechanism of loss from water bodies thus the prediction of the rate of this process is necessary.

Figure 1 gives a diagrammatic representation of this and other processes which may occur. Although the discussion here is primarily about volatilization, the equations developed also apply to the reverse process of direct absorption from the atmosphere.

The rate of volatilization can be expressed by an equation of the form

$$\begin{array}{l} \text{Mass flux} \\ N \text{ (mol/m}^2\text{s)} \end{array} = \begin{array}{l} \text{Mass Transfer Coefficient} \\ K \text{ (m/s)} \end{array} \times \begin{array}{l} \text{Concentration Driving Force} \\ \Delta C \text{ (mol/m}^3\text{)} \end{array}$$

It is suggested that the fundamentally different terms K and ΔC must be considered and quantified separately. The mass transfer term contains kinetic or transport rate information and depends on the local fluid turbulence regime whereas the concentration term is essentially thermodynamic in nature. A knowledge of both is essential. The approach taken here is to review the structure of the flux equation, identify the critical parameters which control K and ΔC , discuss each in turn outlining the present state of knowledge and suggesting methods by which the appropriate data can be determined with a view to using the equation for predictive purposes. Finally, some complications are discussed.

Mass Flux Equation

Diffusion in a single phase is quantified by Fick's Law containing a molecular or eddy diffusivity. In two-phase systems this law may be applied twice and equilibrium assumed at the interface leading to the Whitman two-film theory. This has recently been extensively applied by Liss (1974) to environmental conditions.

The flux equation takes two forms which are mathematically identical, the preferred equation depending on which film controls the mass transfer by offering the greater resistance.

$$N = K_{OL}(C-P/H) \quad \text{where} \quad 1/K_{OL} = 1/K_L + 1/(HK_G/RT)$$

$$\text{or} \quad N = K_{OG}(HC-P)/RT \quad \text{where} \quad 1/K_{OG} = 1/K_G + H/RT K_L$$

where the subscripts on the mass transfer coefficients (K) define them as liquid film (L), vapor film (G), overall liquid (OL) or overall vapor (OG), C is the pollutant concentration in the liquid (mol/m^3), P is its partial pressure in the atmosphere (atm) and H is the Henry's Law constant ($\text{atm}/(\text{mol/m}^3)$) defining the equilibrium by the equation $P = HC$. In most cases one film dominates. Transfer of water soluble pollutants, such as SO_2 (which have high values of H) tend to be gas film controlled whereas less soluble pollutants such as chlorinated hydrocarbons (which have low values of H) tend to be liquid film controlled. It is assumed here that the terms C and P are determined experimentally or alternatively one of them is the object of the modelling exercise. Fortunately, for most pollutants, P is negligible, notable exceptions being some airborne compounds such as sulphur and nitrogen oxides in which ambient levels may be calculated by an appropriate dispersion equation. The ability to calculate the flux N thus depends fundamentally on

a knowledge of the three terms, H , K_G and K_L . These are discussed separately below.

H - The Henry's Law Constant

Henry's Law constant data are readily and reliably available for the common gases and for most reasonably soluble liquids as a function of temperature and often as a function of the concentration of other materials such as electrolytes in aqueous solution. Unfortunately, for certain compounds of environmental interest such as chlorinated hydrocarbons H data are less available and reliable. Thermodynamically, H is an expression of the relative activity of the pollutant in the vapour and liquid phases. Equating the chemical potential or fugacity of the pollutant in each phase leads to an equilibrium equation using the Raoult's Law convention

$$x \gamma P^S = \phi y P_T$$

where x and y are the mol fractions in the liquid, and vapor respectively, γ , the liquid activity coefficient, ϕ , the vapor fugacity coefficient, P^S , the saturation vapor pressure of the liquid pollutant at the ambient temperature and P_T , the total atmospheric pressure.

Fortunately, for most compounds which do not chemically associate in the vapor, ϕ is unity at all environmental pressures. It can be shown that for aqueous systems H is equivalent to $18 \times 10^{-6} \gamma P^S \text{ atm}/(\text{mol}/\text{m}^3)$. Assuming that experimental data for H is not available, it can be estimated from other thermodynamic data although different treatments are required depending on the phase state of the pollutant (Mackay and Shiu, 1975).

There is a tendency to believe that substances which have very low vapor pressures (P^S) will tend to have low Henry's Law constants (H), will therefore be strongly partitioned into the liquid with evaporation then being unimportant. This is certainly true for many compounds, especially ionic species. However, for high molecular weight hydrophobic substances, the low value of P^S is offset by the high activity coefficient γ . This gives a higher Henry's Law constant than is first suspected. Evaporation can therefore be very significant. In addition, although the concentration of these substances is usually low in water bodies even a very low mass flux can have a profound effect on the environmental concentration, significantly depleting the aqueous phase of the contaminant. This was first observed by workers such as Acree et al (1963) in handling solutions of DDT and has been discussed by Mackay and Wolkoff (1973) and Mackay and Leinonen (1975). Coincidentally, these hydrophobic substances may tend to be biologically active because of their preferred partition into lipid phases. The major difficulty in predicting evaporation rates occurs for substances such as poly nuclear aromatics, chlorinated hydrocarbons, or organometallic compounds. These substances have very low vapor pressures (P^S) and the data, when available, may be unreliable and probably exist only for the solid state. They also have high activity coefficients (γ) as evidenced by their low aqueous solubility. The measurement of these low solubilities requires extreme care. It is suggested here that it is better and easier to measure the group γP^S and hence H directly by measuring an evaporation rate under controlled conditions. This has been done recently by Dilling et al (1975) in a discussion of evaporation and reaction rates of chlorinated hydrocarbons from water. Their technique involved exposing a stirred beaker of pollutant solution to the atmosphere and following the concentration decrease. Unfortunately, such measurements give a mass flux which is dependent on the mass transfer coefficient and cannot therefore be used to determine H accurately. A preferable system is to expose the evaporated solution under conditions where the flux rate is independent of the mass transfer coefficient, i.e., the vapor in contact with the liquid is always close to equilibrium. The mass flux rate is then dependent only on the amount of vapor contacted with the liquid and not the exposure conditions. Such an apparatus is shown in Figure 2 in which an air stream is sparged into a liquid. It is believed that the exit vapor achieves > 95% equilibrium with the well stirred liquid. The concentration of the pollutant in the liquid is then monitored as a function of time and the slope of the concentration time curve gives the Henry's Law constant directly. An alternative approach described by Mackay, Shiu and Wolkoff (1975), is to contact a liquid with successive volumes of vapor, extract the pollutant into the vapor and measure the vapor concentration of the pollutant. This vapor phase equilibration approach first proposed by McAuliffe (1971), is applicable only to relatively volatile pollutants of low aqueous solubility.

The environmental contaminants of greatest concern tend to be those which are present in very low concentrations and unfortunately this renders experimental work more difficult due to adsorption on solid surfaces, interference by other substances such as electrolytes and humic acids, the presence of surface active materials, particulate matter and the presence of material in colloidal or micelle form. These difficulties combine to make concentration measurement difficult in laboratory conditions and exceptionally difficult in environmental conditions. There is thus a strong case for obtaining H data from the actual environmental water being studied using a system as described earlier.

K_G the Vapor Phase Mass Transfer Coefficient

Under environmental conditions K_G is of the order of 1 cm/s. Fortunately, there is a considerable body of experience about K_G as a function of wind speed, atmospheric turbulence, and temperature profile and hence on the diurnal variation. Many of these data come from studies of water evaporation. There is a poor understanding of the effect of waves on K_G especially under rough conditions. Ironically, it is under these conditions that fluxes tend to be highest and therefore, quantification of flux rate is probably most important. Experimental measurement is easiest under stagnant or calm conditions when the fluxes are lowest and possibly then of less importance. Actual flux rates under environmental conditions can be measured for some substances for which the resistance lies in the vapor phase by sampling the atmosphere at two levels. This has been done recently for sulphur dioxide absorption into lakes and onto snow surfaces. K_G can also be estimated for a particular environmental situation by evaporating a liquid of known volatility (Mackay and Matsugu 1973).

It must be noted that for many low solubility pollutants the liquid phase controls and the structure of the flux equation renders the flux rate very insensitive to the value of K_G assumed, thus a high degree of accuracy is unnecessary.

K_L the Liquid Phase Mass Transfer Coefficient

There is considerably less understanding of the values of and variations in K_L . Reported values range from 10^{-2} to 10^{-4} cm/s with a typical value of 10^{-3} cm/s or one thousandth of the vapor phase values. The coefficient is very sensitive to the fluid state of the water especially the level of turbulence and the presence of waves. It depends on the surface properties of the solution, on the wind speed and the turbulence below the surface and on the depth of the water body, which may be a river, lake or ocean. A common (and unfortunate) practice is to calculate an equivalent stagnant diffusion layer thickness obtained by dividing the molecular diffusivity (typically 10^{-5} cm²/s) by the mass transfer coefficient thus giving typical values of 0.01 cm or 100 microns. In reality it is likely that eddy diffusion controls the flux except very close to the surface where the mechanism may be unsteady state molecular diffusion into elements of liquid which are periodically moved to and from the surface by hydrodynamic or surface instabilities. The nature of this process is only poorly understood because of the difficulties of measuring and observing them. Again the conditions of greatest interest are those when the fluxes are high, i.e., the water will be turbulent and thus experimentally most difficult and when laboratory conditions are most inapplicable. Some recent measurements of liquid phase transfer coefficients have been reviewed by Weiler (1974).

There has been considerable work on oxygen transfer relating to river aeration and on CO₂ transfer. It is probably essential to measure actual transfer rates in situ, because laboratory techniques are unlikely to simulate environmental conditions adequately. Unfortunately, in situ measurements are extremely difficult although radon diffusion measurements have been used for ocean transfer by Broecker (1971). We have recently used

hydrocarbons for this purpose in the laboratory although in the environment experimental difficulties are introduced by the presence of fast horizontal diffusion and which would force the use of a system to artificially limit horizontal diffusion by some form of corral. The simplest laboratory procedure for measuring K_L is to follow the volatilization of an hydrocarbon from aqueous solution as shown in Figure 3 for a wind-water tank. The slope of the concentration-time curve gives K_L directly. Another approach which we are currently investigating is to measure the dynamic temperature profiles in the upper layers of a water body and from the calculated heat flux deduce the mass flux by analogy between thermal and mass diffusion.

The major areas of inadequate understanding are the dependence of K_L on wind speed, the presence of waves, and on the molecular weight of the pollutant. This latter effect is particularly important when using data for radon or oxygen diffusion to predict flux rates for high molecular weight substances such as PCB^S. There is a real need for a simple method of in situ K_L measurement.

SOME COMPLICATIONS

Most environmental water bodies are covered by a surface microlayer which contains protein material, hydrophobic substances, and surface active agents (Andren et al 1975), which retard mass transfer to some extent and concentrate some pollutants. Most experimental work on microlayers use artificial cetyl alcohol films which may behave quite differently from environmental layers. The effect of these layers is poorly understood.

In quantifying evaporation rates it may be necessary to include terms for the rate associated with bursting bubbles particularly under rough conditions. Direct entrainment of spray particles into the atmosphere is particularly important for transport of ionic compounds. The reverse process of direct deposition can also be quantified by these equations, however, the situation is complicated by the contribution of absorption during rain and snowfall and adsorption of the pollutant on particulate matter which may also settle on to the water body.

Another difficulty arises when the pollutant is present in colloidal or micelle form rather than as a true solution or when it is adsorbed on particulate matter or where other substances such as electrolytes or humic acids influence the activity coefficient and thus H . Many of these contaminants tend to be concentrated in the surface organic microlayer where the immediate chemical environment and hence the physical and equilibrium properties are not well understood.

CONCLUSIONS

For a particular pollutant the prediction of the volatilization rates requires (i) a knowledge of the pollutant concentration in the water body (C) and confidence that it is in true solution and not significantly modified by the presence of other contaminants, (ii) a knowledge of the atmospheric concentration P and (iii) Henry's Law constant data (either literature values or experimentally measured values preferably from laboratory evaporation systems or from estimated solubility and vapour pressure data.) Approximate values of the transfer coefficients K_L and K_G can be obtained and used to estimate the mass flux rate, which will probably be accurate within a factor of about five. This may be sufficient to demonstrate that for a specific pollutant, evaporation is not a major pathway. If it is significant, then accurate determination of the volatilization rate depends on having reliable Henry's Law constant data, reliable mass transfer coefficient data, preferably determined in situ. In most cases the critical quantity is K_L with the value of K_G being required only approximately because the resistance lies mainly in the liquid phase. The two phase resistances are equal when $H = K_L RT / K_G$. K_G data can be obtained from evaporation rate measurements but K_L measurement

and prediction presents a more difficult problem. The inability to predict K_L accurately for a given environmental situation and lack of understanding of the effects of surface microlayer and particulate and dissolved organics on the liquid phase activity represent the most significant gaps in current capability to predict environmental volatilization rates

REFERENCES

Andren, A.W., Elzerman, A.W. and Armstrong, D.E., "Chemical and Physical Aspects of Surface Organic Microlayers in Freshwater Lakes". Paper presented at the IAGLR Symposium on Atmospheric Contributions to the Chemistry of Lake Waters, Geneva Park, Ontario (1975).

Broecker, W.S. and Percy, T.H., *Earth and Planet. Sci. Let.* 11, 99 (1971).

Dilling, W.L., Tefertiller, N.B. and Kallos, G.J., *Env.Sci. and Tech.* 9, 833 (1975).

Liss, P.S. and Slater, P.G., *Nature* 247, 181 (1974).

Mackay, D. and Wolkoff, A.W., *Env. Sci. and Tech.* 7, 611 (1973).

Mackay, D. and Matsugu, R., *Can. J. Chem. Eng.*, 53, 434 (1973).

Mackay, D. and Leinonen, P.J., *Env. Sci. and Tech.*, 9, 1178 (1975).

Mackay, D., Shiu, W.Y. and Wolkoff, A.W., *Water Quality Parameters*, ASTM STP 573, p. 251 (1975).

Mackay, D. and Shiu, W.Y., "Chemistry and Physics of Aqueous Gas Solutions" p. 93, Electrochemical Society, N.Y.

McAuliffe, C., *Chem. Tech.*, 1, 46 (1971).

Weiler, R.R., *J. Fish. Res. Board Canada*, 31, 329 (1974).

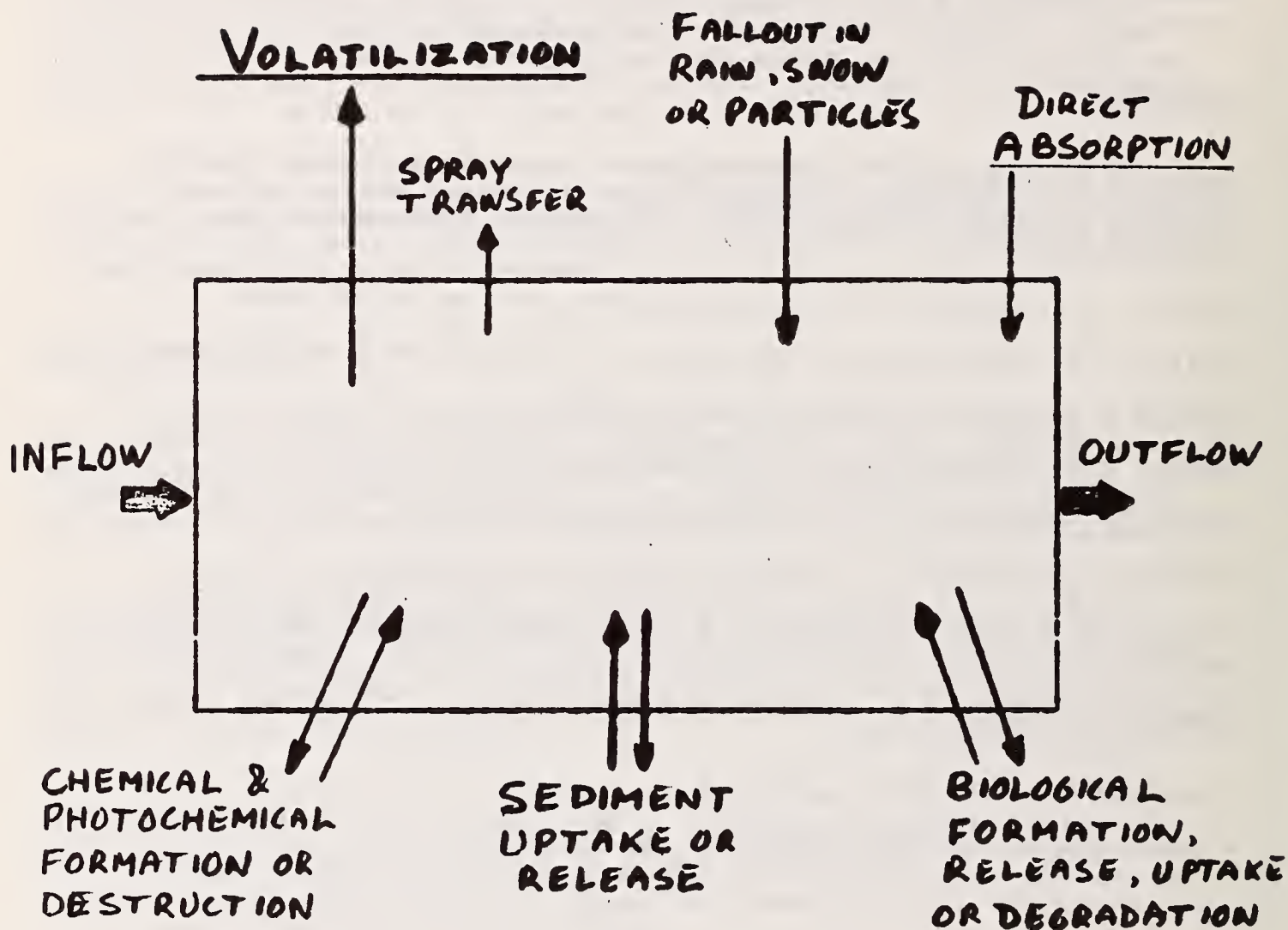


FIGURE 1

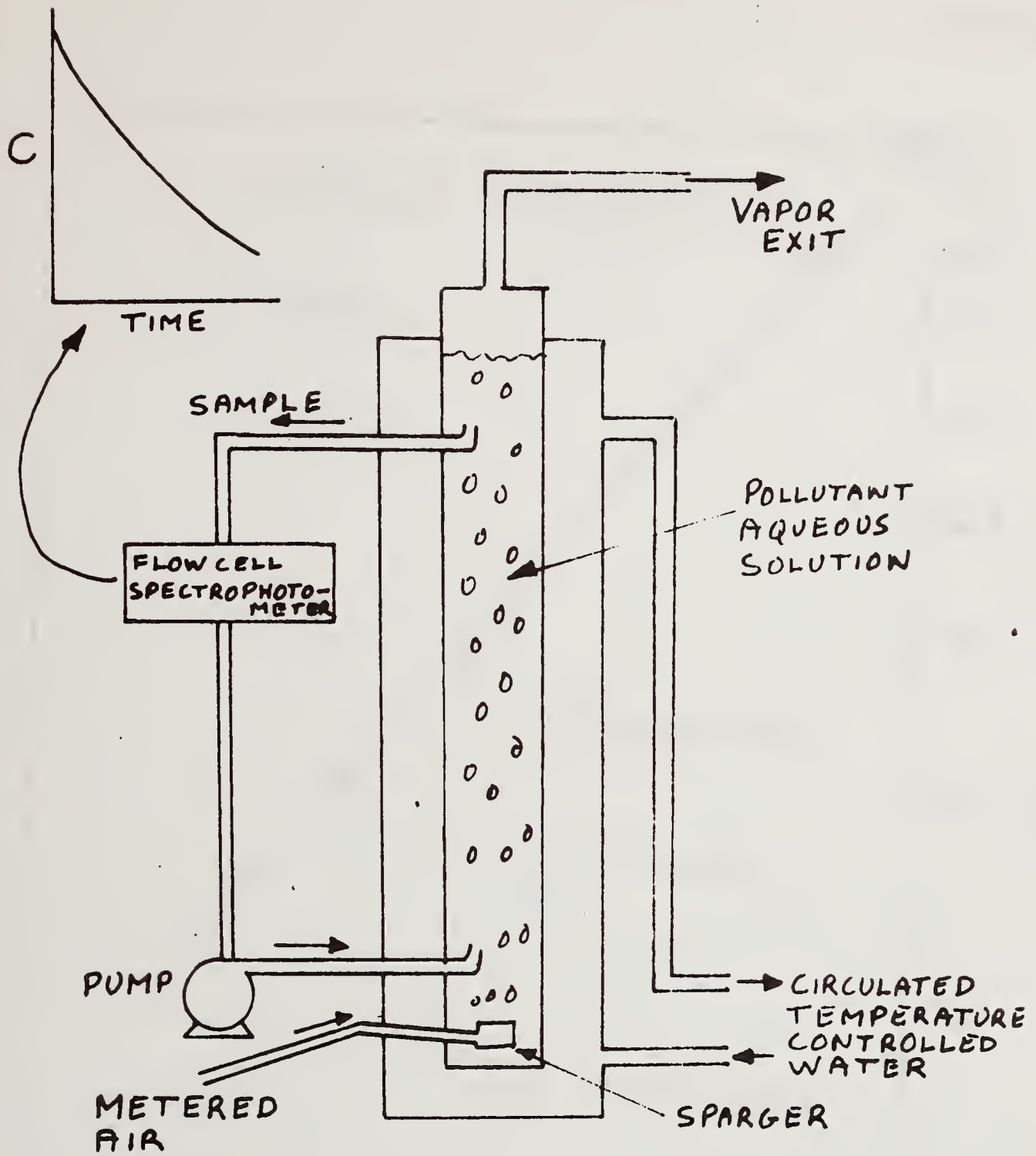
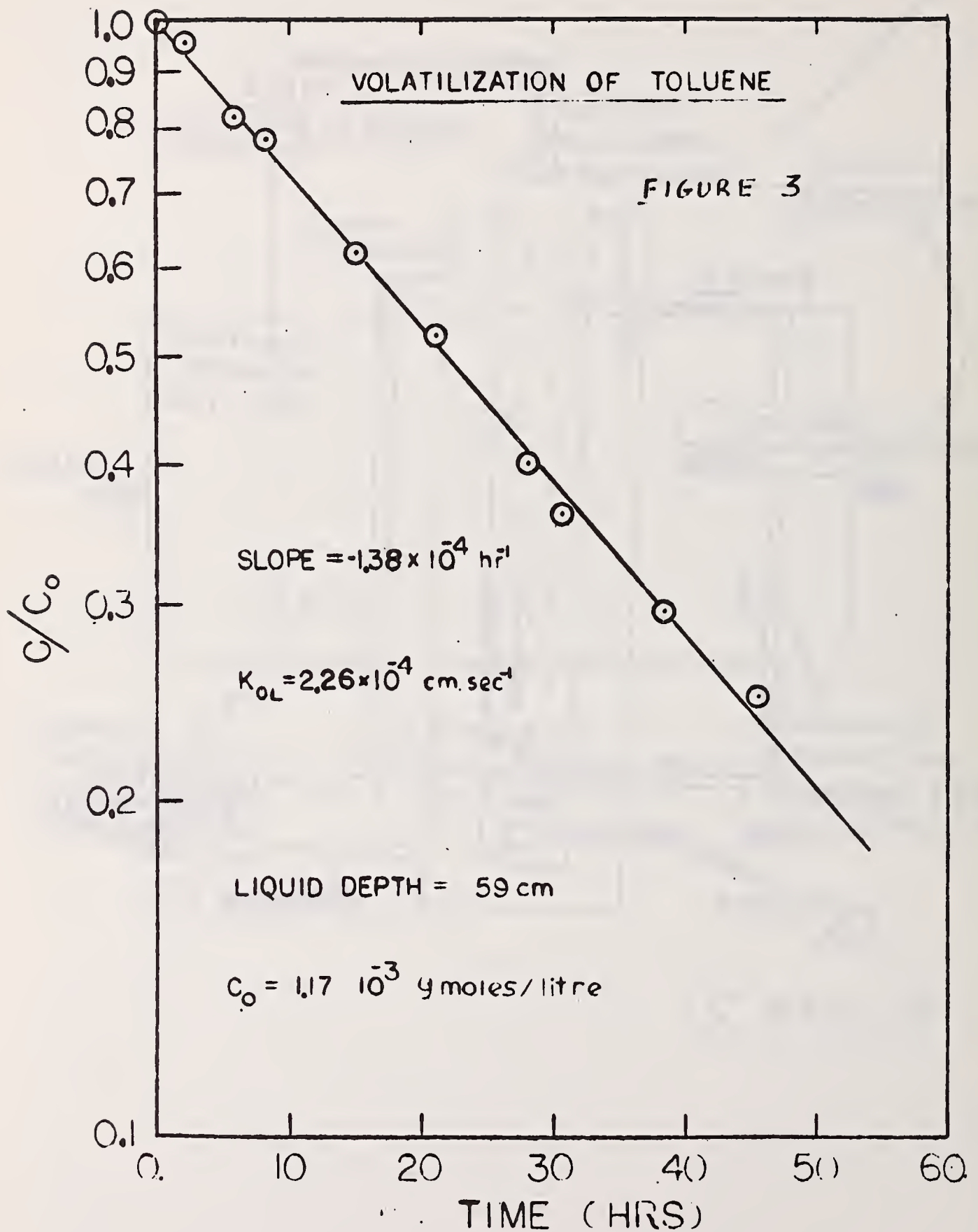


FIGURE 2



notes

COMPLEXATION, PRECIPITATION AND ADSORPTION OF TRACE METALS IN WATER

J. J. Morgan and Jasenka Vuceta
W. M. Keck Laboratory of Environmental Engineering Science
California Institute of Technology
Pasadena, California 91125

Introduction

Metals introduced into fresh water or marine environments in dissolved forms are partially removed to the sediments by precipitation, adsorption onto mineral or organic particles, and incorporation into biological material. Particulate metal inputs may be partially dissolved or desorbed in their travel to the sediments. In fresh water systems, a fraction of each input metal leaves the system in dissolved outflow. This fraction depends upon factors affecting the completeness of adsorption, precipitation, and sedimentation of each metal. Schindler (1975) has proposed a chemical approach, based on adsorption to oxide surfaces, e. g., SiO_2 , to predict the relative residence times of metals in lakes and the absolute residence times in seawater. Among the important physical-chemical factors affecting the driving forces of metal sedimentation via adsorption and precipitation are: (1) pH (acid-base equilibria); (2) complexation of metals by ligands, with the possibility of competition between metals for limited amounts of complexing ligand (Morel, McDuff, and Morgan (1973); Morel and Morgan (1972); Stumm and Morgan (1970)); (3) p_e (redox processes, affecting relative abundances of potential precipitating ligands such as sulfide and oxidation states of metals, e. g., Fe(III) vs. Fe(II)); (4) area of adsorptive surfaces in relation to volume of solution phase; (5) ionic strength, affecting solubilities of pure solid phases and the adsorption tendencies of trace metals on surfaces; (6) temperature.

The strong influence of pH on solubility, adsorption, complexation, and redox equilibria is well recognized. It is necessary to be aware that significant temporal and spatial variation in pH take place in natural water systems, and may account for important alterations in trace metal speciation patterns (Schindler, 1975; Morel, McDuff, and Morgan, 1973).

Complexation by inorganic ligands tends to increase the residence time of metals in natural water systems by impeding adsorption (MacNaughton and James, 1974; MacNaughton, 1973; Schindler, 1975; Vuceta, 1976) or preventing precipitation (Stumm and Morgan, 1970). Metals initially in particulate forms may be "mobilized" (dissolved, desorbed) by complexation or pH alteration, or both.

Thus, it is necessary to consider simultaneously the influences of a number of chemical processes in order to predict the forms, transport, residence time, and fates of trace metals in natural water systems (water and sediments). Needed computational tools are available to describe acid-base, complex formation, solubility, and redox equilibria for model systems of considerable complexity (Morel and Morgan, 1972; McDuff, Morel, and Morgan, 1973; McDuff and Morel, 1973).

Adsorption equilibria for trace metals have been described mathematically by a number of investigators. Extensive reviews and comparisons have been provided by MacNaughton (1973, 1974); Parks (1975); James, Stiglich and Healy (1975); and Vuceta (1976). In the present work we wish to describe interaction of metal adsorption equilibria with acid-base, solubility, complexation, and redox equilibria. We report computations for a number of model systems in which these equilibria interact. We make use of two basically different adsorption models to illustrate expected patterns, (a) an adsorption-hydrolysis, ion-solvent interaction model (AHIS) proposed by James and Healy (1972); (b) a surface complex formation model (SCF) proposed recently by Schindler, Fürst, Dick, and Wolf (1975) for the SiO_2 surface and Hohl and Stumm (1975) for the Al_2O_3 surface, representing a further development of earlier models variously referred to as "ion-exchange," "specific chemical interaction," and "specific adsorption" models. Both the AHIS and SCF models have been found capable of mathematically fitting experimental results on adsorption of metals to certain oxide surfaces as a function of pH and variations in

specific ligands (MacNaughton, 1974; James, Stiglich and Healy, 1975; Vuceta, 1976). Important questions remain to be settled with respect to the fundamental merits of these models as predictive tools.

Adsorption Models

Adsorption of metals from aqueous solutions onto oxide surfaces has been described theoretically in terms of two concepts: (i) electrostatic influences on the distribution of charged species in the vicinity of a charged interface; (ii) specific binding of metal ion species with functional groups on the surface. Electrostatic models include simple charge-dependent ion exchange in the diffuse double layer or the Stern layer (Parks, 1975). Chemical interaction models postulate bond formation to sites on the surface of the solid, i. e., the inner coordination sphere of the adsorbing metal interacts with a ligand on the surface. In a sense, we might characterize the models proposed for metal (or anion) adsorption as either electrostatic models with chemical "corrections," or chemical models with electrostatic "corrections." For hydrolyzable metal ions, which are bound to the protonated hydroxyl ligand in solution, it seems reasonable to expect that these same metals would be bound by similar ligands on the surface of hydrated oxides.

The AHIS model of James and Healy (1972) postulates the adsorption of free and hydrolyzed metal ion species, each with its own free energy of adsorption, resolved into coulombic, solvation, and chemical components:

$$\Delta G_{ads,i} = \Delta G_{coul,i} + \Delta G_{solv,i} + \Delta G_{chem} \quad (1)$$

with

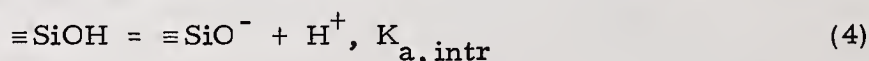
$$\Delta G_{coul,i} = Z_i F \psi_0 \quad (2)$$

and $\Delta G_{solv,i}$ depends upon: Z_i ; the hydrated radius of the adsorbing ion; the ionic radius; and the dielectric constants of the bulk solution, the interfacial region, and the solid. ΔG_{chem} is assigned the same value for each metal ion species. Adsorption is described by a Langmuir isotherm, in which the equilibrium constant for each metal ion species is

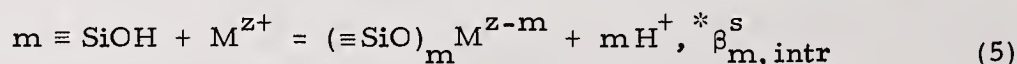
$$K_{ads,i} = \exp(-\Delta G_{ads,i}/RT) \quad (3)$$

and the maximum adsorption density is fixed by the hydrated radius of the metal ion. Total adsorption density of the metal, $\sum \Gamma_i$, is determined by summing over the individually-computed densities for each species. ΔG_{chem} is a fitting parameter in most applications of the model (MacNaughton, 1974); it has been measured directly in certain cases. From a conceptual point of view, the status of ΔG_{chem} in relation to $\Delta G_{solv,i}$ is not obvious. As pointed out by James, Stiglich and Healy (1975), the James-Healy model describes a "physical adsorption" processes. Yet, adsorption of a species such as $\text{Cu}(\text{OH})_2(\text{aq})$ would necessarily involve chemical forces since ΔG_{coul} and ΔG_{solv} would be zero. Similarly, the demonstrated adsorption of any species at $\psi_0 = 0$ demands chemical interaction.

The SCF model for metal ion binding to hydrous oxide employs a framework similar to that developed by Tanford (1961) to describe binding of metal ions to macromolecules with identical protolyzable monomer groups. Intrinsic acid dissociation equilibrium constants and intrinsic metal binding equilibrium constants are defined in the absence of electrostatic effects, and corresponding apparent constants are obtained under specified pH conditions by applying an electrostatic correction function. For the case of the hydrated SiO_2 surface, two types of equilibria are described:



and



The corresponding apparent constants are obtained as

$$k_{a, \text{app}} = K_{a, \text{intr}} e^{z\psi_0/RT} \quad (6)$$

$${}^* \beta_{m, app}^s = {}^* \beta_{m, intr}^s e^{(z-m)\Psi_0/RT} \quad (7)$$

Note the major role played by pH in both the AHIS and SCF models, affecting the adsorption process through Ψ_0 and through hydrolytic equilibria in solution. In the SCF model, hydrogen ions are directly involved in the acid dissociation equilibrium of the binding ligand silanol groups of the surface. For earlier development of SCF-like models see Dugger, et al. (1964) and Stumm, Huang and Jenkins (1970). Recently, Yates, Levine and Healy (1974) put forward a site-binding model of the electrical double layer at the oxide/water interface which introduces formation constants for interfacial ion pairs between $\equiv MO^-$ groups and monovalent cations and includes quantitative consideration of the acid-base behavior of $\equiv MOH_2^+$, $\equiv MOH$, and $\equiv MO^-$ entities on the surface. Such a site-binding model is equivalent to the SCF model (compare equations (4) and (5), above).

Some difficulties in quantitative applications of an SCF model to prediction of behavior in complex systems relate to: (i) questions concerning the functions $\exp(z\Psi_0/RT)$ and $\exp(z-m)\Psi_0/RT$ for obtaining apparent constants; more experimental detail is needed for different ionic strengths, over a pH range from 5 to 9, (ii) questions concerning the independent adsorption of anions, such as sulfate and phosphates in natural systems, and consequent effects on surface charge and potential.

Solution Composition and Adsorption

Adsorption of metals onto surfaces can be viewed as competition between two or more ligands for a fixed total concentration of metal. The distribution coefficient is one way of describing the result of the competition:

$$D = \frac{\text{total surface concentration of metal}}{\text{total concentration of aqueous metal}} = \frac{M_s}{M_{aq}} \quad (8)$$

Let us examine it in terms of the SCF model. From equations (5) and (7)

$$\frac{\{(\equiv SiO)_m M^{z-m}\}}{\{\equiv SiOH\}^m} \cdot \frac{[H^+]^m}{[M^z]} = {}^* \beta_{m, app}^s \quad (9)$$

where { } represents surface concentration of metal complex. For protonated ligands HL_j in the aqueous phase (Schindler, 1975),

$$M_{aq} = [M^z] \left(1 + \sum_j \sum_n {}^* \beta_{jn} [HL_j]^n [H^+]^{-n} \right) \quad (10)$$

Thus,

$$D = \frac{M_s}{M_{aq}} = \frac{\sum_j \{ \equiv SiOH \}^m [H^+]^{-m} {}^* \beta_{m, app}^s}{1 + \sum_j \sum_n {}^* \beta_{jn} [HL_j]^n [H^+]^{-n}} \quad (11)$$

The surface concentration of $\equiv SiOH$ groups depends in turn upon the pH and $pK_{a, app}$ of the acid dissociation. Thus

$$\{SiOH\} = \frac{C^s [H^+]}{[H^+] + K_{a, app}} \quad (12)$$

where C^s is the concentration of unbound (free) surface OH groups.

The quantity of C^s (e.g., moles of groups per unit weight of solid) describes the concentration of unbound surface ligands; C_0^s , the total concentration of surface ligands, is an experimentally determinable quantity through titration procedures (Schindler, Fürst, Dick and Wolf, 1975; Hohl and Stumm, 1975). Thus, C_0^s , $K_{a, app}$, and the ${}^* \beta_m^s$ values are the important properties of the particulate material. The presence of complexing ligands in the aqueous solution, here formally represented as HL_j (e.g., H_2O , HCO_3^- , organic

acids, sulfate, chloride, etc.) increases M_{aq} at the expense of M_s , i.e., the distribution coefficient is lowered. The strong influence of pH is evident in equations (11) and (12). Increasing pH can either increase or decrease adsorption in given pH ranges. The net effect depends upon the magnitude of the equilibrium constants for metal-surface binding and aqueous complexation (including especially hydrolysis), and upon the relative stoichiometrics of surface and aqueous ligands. As reported by MacNaughton and James (1974), aqueous chloro complexes of Hg(II) compete with adsorption to oxide surfaces. Similar distribution coefficients can be constructed for an AHIS model. However, the influence of pH is not as explicitly seen in the AHIS model.

Mixed Ligand Complex Adsorption: Formally, the AHIS model appears as a mixed ligand complex model, if one recognizes that $M(OH)_n$ species are imagined to be bound to the surface by a chemical force (ΔG_{chem}). Additional definitions of ΔG_{chem} for adsorption of such species as $ML(aq)$ or $M(OH)_n L(aq)$ are required to specify adsorption possibilities in media containing complex species other than hydrolysis products. We model non-adsorbable complexes, e.g., CuCITRATE, by imposing large, positive ΔG_{chem} for all such complexes. Favorable ΔG_{chem} values might also be imposed to account for observed enhanced adsorption of certain metals in the presence of specific complexing agents (MacNaughton, 1973).

The SCF models do not describe mixed ligand complexes, i.e., free metal is bound to surface ligands. Such processes as $M L + \equiv SOH = (\equiv SO) M(L) + H^+$ can, however, be envisioned. Experimental data to identify patterns of such possible reactions are not yet available (but again, see MacNaughton, 1973, for some examples).

Illustrative Example Comparing AHIS and SCF Models

Two models were applied to a simple 3-metal (Na^+ , Cu^{2+} , H^+), 2-ligand (Cl^- , OH^-), and one oxide (α - SiO_2) system at 25°C and ionic strength $1 \times 10^{-3}M$. For detailed results, see Vuceta (1976).

The AHIS model employed ΔG_{chem} of $-3.0 \text{ kcal mole}^{-1}$ for Na^+ and $-8.0 \text{ kcal mole}^{-1}$ for all Cu^{2+} species. The ZPC pH for SiO_2 was taken at 2.0, ϵ_{solid} at 4.3. The system surface area was $50 \text{ m}^2/l$ (corresponding in the SCF model to 2.24×10^{-4} moles of silanol groups per liter). Total Cu(II) in the system was $1 \times 10^{-6}M$. For the SCF model we chose (on the basis of experimental data describing adsorption densities vs. pH) the following apparent surface complex formation constants: $\log^* \beta_{1,Cu}^s = -1.8$ and $\log^* \beta_{2,Cu}^s = -3.8$ (mole/liter scale for the system of fixed solid-surface concentrations); $\log^* \beta_{1,Na}^s = -4.2$. At pH 7.0, the following results were obtained:

<u>AHIS</u>	<u>Surface</u>					<u>Aqueous</u>	
	<u>Species:</u>	Cu^{2+}	$CuOH^+$	$Cu(OH)_2$	$Cu(OH)_3^-$	$Cu_2(OH)_2^{2+}$	Cu^{2+}
<u>-log molar:</u>	7.78	6.21	6.46	17.9	12.3	8.27	7.95

$$D^* \cong \frac{10^{-6.21} + 10^{-6.46} + 10^{-7.78}}{10^{-8.27} + 10^{-7.95}} = 59$$

<u>SCF</u>	<u>Surface</u>		<u>Aqueous</u>	
	<u>Species:</u>	$Cu(SiO)$	$Cu(SiO)_2$	Cu^{2+}
<u>-log molar:</u>	7.16	6.04	8.49	8.23

$$D^* \cong \frac{10^{-7.16} + 10^{-6.04}}{10^{-8.49} + 10^{-8.23}} = 108$$

Note: ~ 60% of total SiOH groups in H^+ form; 39% in Na^+ form; 1% in Cu^{2+} form.

Models for Multi-metal, Multi-ligand Systems with Adsorption

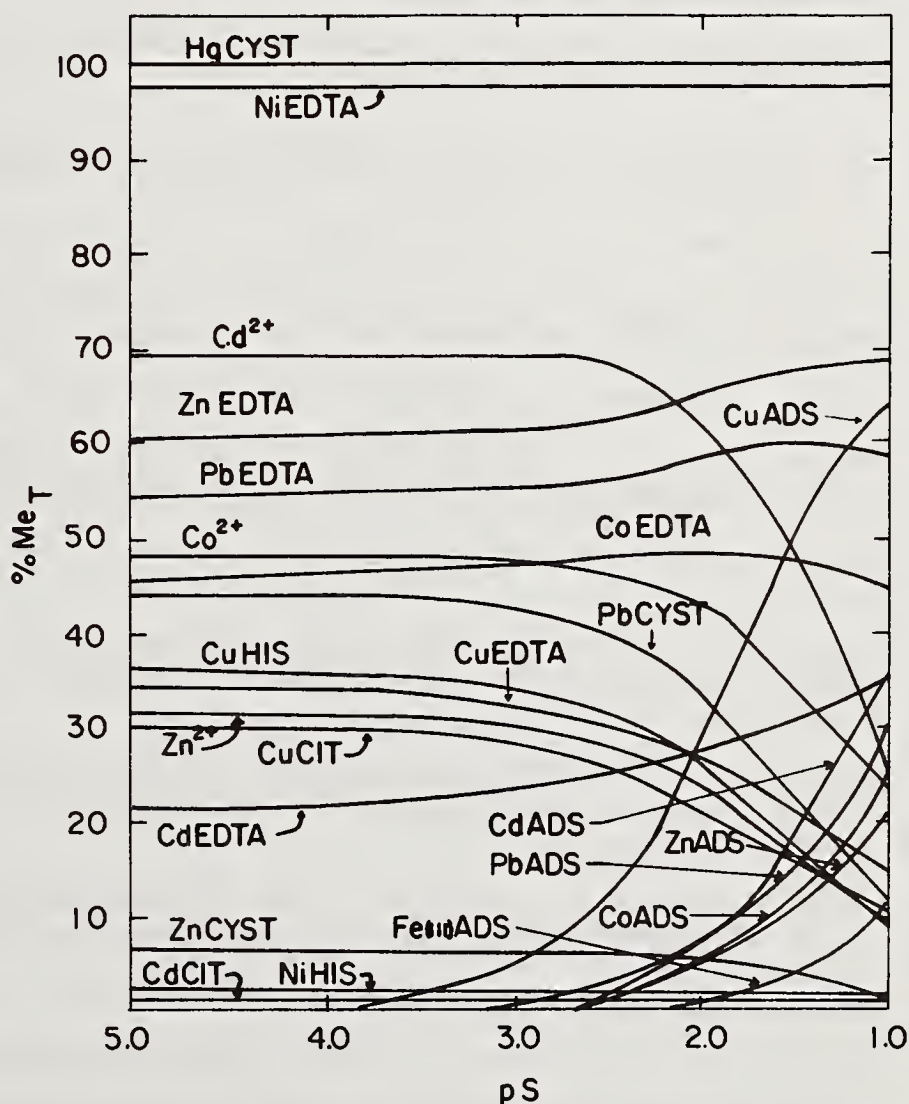
Previous Work: Schindler (1975) has developed SCF models for distribution coefficients of Zn(II) and Cu(II) in fresh water systems (lakes, rivers) in which SiO₂ and TiO₂ are used as model sediments. He has also predicted residence times of 9 elements in the ocean based on SCF models. Agreement with observed data was reasonable in a majority of cases. Guy, Chakrabarti, and Schramm (1975) constructed a laboratory experimental model for Cu(II), Cd(II), and Zn(II), with MnO₂, clay, and solid humic acid as adsorbents. Bicarbonate, tannic acid, and soluble humic acid were used as ligands. The model demonstrated strong influences of pH on the distribution coefficient for particulate vs. aqueous metal. Sibley and Morgan (1976) have carried out computations for a 16-metal, 8-ligand inorganic mixing model of oxic fresh and marine waters. SiO₂ was used as adsorbent in an AHIS model. In fresh water environments, the models showed competition between adsorption and aqueous complexation in determining trace metal speciation. The computations showed low adsorption of trace metals in seawater due to competition from Na⁺, Mg²⁺, and Ca²⁺, and to chloride complexation of a number of metals. These results are somewhat at variance with the findings of Schindler(1975).

In this report we present results of computations for three natural water system models:

I. An AHIS model of an oxic 13-metal, 7-inorganic ligand system, with SiO₂(s) as major adsorbing surface and with MnO₂(s) and Fe(OH)₃(s) as auxiliary adsorbents. Organic ligands (EDTA, citrate, histidine, aspartate, and cysteine) are included to demonstrate influences of strong complexation. Representative results for trace metal speciation as a function of surface area of SiO₂ adsorbent (pS is negative log of surface area expressed as hectare/liter) are given in the accompanying figure.

II. An AHIS model for the components of model I, but under anoxic conditions of the kind encountered in fresh water sediments.

III. An SCF model for aerobic dilute lake waters containing SiO₂ as model adsorbent and the ligands salicylate or citrate as model organic complexing agents. The metals included are: Ca, Mg, Fe(III), Mn(II), Cu(II), Cd, Zn, Ni, and Pb(II); inorganic ligands are carbonate, sulfate, chloride, ammonia, phosphate, silicate, and nitrate. Distributions of species are examined over the pH range from 4 to 8.



Speciation of trace metals in natural fresh waters in the presence of organic ligands (pCIT=pEDTA=pCYST=pHIS=pASP=6.0) as a function of surface area of SiO₂(s) in ha/l.

Detailed results of these three complex-system models will be discussed with respect to the following points: (1) distributions of trace metals as a function of pH; (2) effect of characteristics of different adsorbing surfaces; (3) adsorption in function of surface area; (4) effect of redox environment on the balance of adsorption-complexation-precipitation processes.

References

- Dugger, D. L., et al. 1964. *J. Phys. Chem.*, 68:757.
- Guy, R. D., et al. 1975. *Can. J. Chem.*, 53:661.
- Hohl, H. and W. Stumm. 1975. Interactions of Pb^{2+} with Hydrous $\gamma-Al_2O_3$. 49th Nat. Coll. Sympos., Potsdam, N.Y.
- James, R. O. and T. W. Healy. 1972. *J. Coll. Interfac. Sci.*, 40:65.
- James, R. O., P. J. Stiglich, and T. W. Healy. 1975. Analysis of Models of Adsorption of Metal Ions at Oxide/Water Interfaces. Gen. Disc., Faraday Div. of Chem. Soc. (April).
- MacNaughton, M. G. 1973. Adsorption of Mercury (II) at the Solid-Water Interface. Ph.D. Thesis, Stanford Univ.
- MacNaughton, M. G. 1974. Working Hypothesis and Isotherms for Adsorption of Metal Ions from Water. AGU Sympos., San Francisco (December).
- MacNaughton, M. G. and R. O. James. 1974. *J. Coll. Interfac. Sci.*, 47:431.
- McDuff, R. E. and F. M. Morel. 1973. Description and Use of the Chemical Equilibrium Program REDEQL 2. TR EQ-73-02, Keck Lab., Caltech.
- Morel, F. M. and J. J. Morgan. 1972. *Environ. Sci. Technol.*, 6:58.
- Morel, F. M., R. E. McDuff, and J. J. Morgan. 1973. In Singer, P. C., ed., Trace Metals and Metal-Organic Interactions in Natural Waters. Ann Arbor Science.
- Parks, G. A. 1975. In Riley and Skirrow, eds., Chemical Oceanography, vol. 1, 2nd ed., pp. 214-308.
- Schindler, P. W., et al. 1975. Ligand Properties of Surface Silanol Groups. I. Surface Complex Formation with Fe^{3+} , Cu^{2+} , Cd^{2+} , and Pb^{2+} . 49th Nat. Colloid. Sympos., Potsdam, N.Y.
- Schindler, P. W. 1975. The Regulation of Trace Metal Concentrations in Natural Water Systems: A Chemical Approach. Int. Assoc. Great Lakes Res. Sympos., Geneva PK., Ontario (October).
- Sibley, T. H. and J. J. Morgan. 1976. Equilibrium Speciation of Trace Metals in Freshwater: Seawater Mixtures. Keck Lab., Caltech (January).
- Stumm, W., C. P. Huang, and S. R. Jenkins. 1970. *Croat. Chem. Acta.*, 42:223.
- Stumm, W. and J. J. Morgan. 1970. Aquatic Chemistry, Wiley-Interscience, N.Y.
- Tanford, C. 1961. Physical Chemistry of Macromolecules. Wiley, N.Y.
- Vuceta, J. 1976. Adsorption of Pb(II) and Cu(II) on α -Quartz from Aqueous Solution: Influence of pH, Ionic Strength, and Complexing Ligands. Ph.D. Thesis, Caltech.
- Yates, D. E., et al. 1974. *J. Chem. Soc., Faraday Trans., I.* 70:1807.

notes

ENVIRONMENTAL PHYSICS AND CHEMISTRY OF AQUATIC POLLUTANTS

J. Carrell Morris
Division of Engineering and Applied Physics
Harvard University
Cambridge, Mass.

Classically, the removal or transformation of pollutants in the aquatic environment, -- the so-called "self-purifying" action of natural waters, -- has been ascribed to biochemical activities. Certainly, such activities are of major importance when the principal form of aquatic pollution is domestic wastes. However, as the production and use of synthetic chemicals has increased rapidly in the past few decades, pollution from these materials has become more and more important. Since a widespread characteristic of these anthropogenic substances is resistance to biological oxidation, the role of physical and chemical properties in the transformation and fate of aquatic pollutants is becoming more and more important.

I. PHYSICAL TRANSFORMATIONS

The physical properties that are particularly important in connection with the ultimate fate of polluting materials are volatility, solubility and adsorptive tendency. Since each of these properties is in some way a measure of pressure to escape from the aqueous medium, some correlation of them may be expected and some overlap of their operation in environmental transformations is to be expected.

(a) Volatilization. There seem to be no general quantitative studies on the transfer of volatile polluting materials from the aqueous to the gas phase. Rook and coworkers (1) have noted an overall drop in volatile organic material in the Rhine as indicated by headspace analysis from 1.6 mg per liter at Mannheim to 1 mg. per liter at Wiesbaden, 0.5 mg per liter at Koblenz, 0.3 mg per l. at Dusseldorf, 0.2 mg per l. at Ochten and <0.1 mg per l. at Schoonhoven just before the river reaches the industrial complex of Rotterdam. Because the changes were occurring in materials like benzene, toluene, dichloroethane and octanes, it has been suggested that the major pathway of loss of these compounds is by volatilization. A similar study (2) on water impounded for 20-30 days prior to use for Rotterdam water supply showed losses of 90% in headspace volatiles during the summer period and of approximately 70% in the winter season.

It is difficult with studies like these to be certain that the processes operating are those postulated. Some evidence that the losses are not the result of biological oxidation is provided by the independent studies of Kollé (3) and of Kollé, Koppe and Sontheimer (4). These workers showed, by means of C^{14} measurements, that the organic content of the Rhine shifted gradually from currently photosynthesized materials in the upper reaches to nearly 80% petroleum-derived compounds at Dusseldorf. The dominance of petroleum-based materials served not only to indicate the industrial pollution of the Rhine, but also their persistence against biological oxidation.

The conditions of Rook's studies were such that loss of these small molecules by adsorption was not likely. Some form of photooxidation cannot be ruled out as the mechanism for losses of the materials from aqueous solution, but seems less plausible than volatilization in view of the pattern of the losses.

That the rates of loss of these materials by volatilization is not un-

reasonable is indicated by the laboratory studies of Mackay and Wolkoff (5) Dilling, Tefertiller and Kallos (6) and Mackay and Leinonen (7). The last of these sets of workers showed, in particular, that many organic pollutants of low molecular weight exhibited transport properties giving half-lives for volatilization of 5 to 10 hours for a one-meter depth of water. Dilling and coworkers showed short half-lives also for numerous chlorinated hydrocarbons.

Not all organic compounds of low molecular weight vaporize so readily, however. A classic instance is the tracing of o-nitrochlorobenzene for 1000 miles down the Mississippi River from St. Louis to New Orleans by personnel of the U.S. Public Health Service (8). It may be that volatilization was inhibited in this instance by adsorption of the nitrochlorobenzene onto suspended clay or other mineral particles being transported by the river. In this regard it seems likely that adsorption will often act antagonistically to evaporation.

(b) Precipitation. Particularly when trace pollutants are under consideration, it is difficult to separate direct precipitation from adsorption as transforming mechanisms. Both involve a transfer of material from the aqueous phase to the solid phase, and both will show reductions in aqueous concentration when samples are filtered or allowed to settle. Firm differentiation seems possible only when it can be shown that the aqueous solubility of the pollutant in question is greater than its concentration in the water being examined. Quantitative aqueous solubility data are not generally available, however, for trace pollutants of low solubility.

One series of compounds for which precipitation phenomena may be of importance is the polynuclear aromatic hydrocarbons. These have been found to be principally present in a number of waters in suspended rather than dissolved condition. For example Lewis (9) in his study of 5 polynuclear aromatic hydrocarbons in several British rivers observed that in those samples with total polynuclear aromatic hydrocarbons greater than about 10 mg per l., 50 to 90% of the material was present in the suspended fraction. It could be removed by laboratory filtration or by the standard coagulation-filtration process of water treatment.

Whether the suspended material is clay with adsorbed PAH or precipitated PAH is not certain. Some observations by the Netherlands Government Institute for Water Supply (10) have indicated that the concentration of PAH in rainwater in the vicinity of Rotterdam is several times the concentration in the Rhine, suggesting that the PAH is in suspended particulate form before it reaches the silt-bearing water courses. They may still be adsorbed on soot particles, however. Also, the observation by Borneff (11) that ozonation or chlorination is only partially effective in removing PAH is in accord with the particulate occurrence of much of it in water. Penetration of particulate matter is poor with low concentrations of ozone, especially.

(c) Adsorption. The adsorption of trace pollutants on clay minerals and other particulate matter is probably a major factor in the transport of certain aqueous pollutants into sediments, but is one of the most difficult factors to provide quantitative data for. The variety of potential particulate adsorbents is great, the concentration in any natural body of water may vary greatly and at times quite suddenly, depending on the weather and the adsorptive property for any one pollutant is interactive with those of all other pollutants present. Qualitatively, however, it is clear that much of the transfer of aqueous metallic pollutants and of non-volatile organic substances to the sediments that occurs when rivers are impounded or become quiescent is the result of adsorption.

II. CHEMICAL TRANSFORMATION

Types of chemical reactions that are of general interest in connection with the breakdown of organic pollutants in aqueous solution include hydrolysis, direct oxidation by O_2 , catalyzed oxidations, photolysis, photooxidation and photosensitized oxidations. Other types of reaction are possible, particularly in anoxic waters, but have not been investigated with trace pollutants in sufficient detail to make consideration useful.

All of the types of reactions are likely to be affected in their rates by both temperature and pH, the latter either by its effects on acid-base equilibria of the pollutant or by participation of H^+ or OH^- in the reaction as catalyst or reactant. So, these environmental factors are important parameters in assessing the significance of chemical transformations.

(a) Direct oxidation. Apart from the transformations of simple inorganic materials like Fe^{II} , Mn^{II} and H_2S , direct oxidation by O_2 appears to play a very small role in the oxidation of aquatic pollutants. If an organic pollutant is susceptible to significantly rapid direct oxidation by O_2 it is almost certain to be even more susceptible to biologically mediated oxidation. The latter will generally be dominant in environmental aquatic systems unless some factor is present to maintain sterility in the system.

Rates of direct oxidation are of chief interest to set minimum rates of transformation in material waters for modelling or prediction. In general rates are greater, or duration times less, as a result of biochemical activity.

(b) Catalyzed oxidations. Although direct oxidation of organic pollutants by O_2 is normally slow, the oxidation may be brought about by other oxidants that are subsequently reoxidized by O_2 itself. Thus, Morgan and Stumm (12) and Theis and Singer (13) have discussed the iron-catalyzed oxidation of aqueous phenols by O_2 , in which ferric iron is the actual organic oxidant, with the product ferrous iron being reoxidized by O_2 . It appears that manganese may act similarly.

(c) Photolysis. It has been known for a long time that light may have a strong effect on the transformation of organic substances in water, even though the mechanisms remain obscure. Humic and fulvic acids, the source of the natural stain in water, are strongly resistant to biological degradation as is shown by the persistence of color in natural waters. It has also been noted, for example, that somewhat more than half the total organic carbon remaining in sewage effluents after efficient secondary biological treatment of municipal sewage is humic and fulvic acids (14).

During the first two decades of this century extensive investigation of the behavior of organic color in reservoirs showed that there was a light-induced bleaching of the color that amounted to about 50% per month for the surface layers during New England summers (15). The nature of this photo reaction has not been studied, however, and so the fundamental changes that produce the loss in color are not known.

There are three general types of light-initiated processes that seem to have significance for the transformation of aquatic pollutants:

(a) photolysis, in which light absorbed by the pollutant leads to its decomposition into more reactive fragments. These fragments are considered often to be free radicals that may stimulate considerable oxidation through radical chains; (b) photochemical oxidation, in which excitation of the pollutant by light is followed by formation of singlet oxygen, which then serves as a more active oxidizer than normal O_2 ; (c) photosensitized oxidations, in which the initial step occurs as in (b), but then the singlet O_2 initiates the oxidation of a compound other than the one that was excited initially. All three of these processes may be active in the

light-induced oxidation or transformation of pollutants. Until now, however, studies have not been sufficiently detailed to delineate mechanisms precisely.

Among the compound known to undergo light-induced reactions in dilute aqueous solution are benzo [a] pyrene (16), metallic complexes of nitrilotriacetate and ethylenediaminetetraacetate (17)-(20), 2,4-D esters (21) and pesticides (22) (23). Moreover, Paris, Lewis and Wolfe (24) have described the photosensitized oxidation of malathion in which natural humic acid is the photosensitizer. The half-life for photodecomposition was reduced from 990 hours to 15 hours in the presence of humic acids.

(d) Hydrolysis. Hydrolysis is most significant as a mode of environmental transformation of anthropogenic pollutants for organic esters-- phthalate esters, herbicide esters, phosphates and others. Hydrolysis of these materials is generally acid-base catalyzed so that the times required for hydrolysis are very much dependent on pH. Hydrolysis often leads to complete oxidation or degradation, for the organic acids or alcohols that constitute the hydrolysis products tend to be more readily broken down biologically than the parent esters are.

There are excellent studies on the hydrolysis of 2,4-D esters and Malathion (21) (25). The study on the 2,4-D esters, in particular, is a model of the sort of broad investigation of physical and chemical properties that needs to be conducted for any pollutant if its ultimate environmental fate is to be defined or predicted. The investigation covered not only the hydrolysis reaction as a function of temperature and pH, but also the vaporization process and photooxidation. Other, less significant properties were also considered, though they were not studied as thoroughly. Of the potentially important transformations, only the role of adsorption and transport to the sediments was not covered. All in all, it appears possible now to present a nearly complete picture of the environmental fate of 2,4-D esters. Similarly detailed data for other compounds would be most welcome.

III. SUMMARY

For many conservative or anthropogenic pollutants physical or chemical properties determine environmental transformations and fate. There is a great need for fundamental physical and chemical data that can be related to the behavior of aquatic pollutants under environmental conditions.

REFERENCES

1. J.J. Rook, A.P. Meijers, A.A. Gras and A. Noordsij. Headspace Analyse Flüchtigere Spurensubstanzen im Rhein. Vom Wasser 44, 23-30 (1975).
2. J.J. Rook. Haloforms in Drinking Water. Jour. Am. Water Works Ass'n 68, 168-172 (1976).
3. W. Kölle. Rheinwasser als Rohstoff zur Trinkwasseraufbereitung. Veröffentlichungen der Abteilung und des Lehrstuhls für Wasserchemie Heft 4, 59-87 (1969). Institut für Gastechnik, Feuerungstechnik und Wasserchemie der Universität Karlsruhe (Technische Hochschule).
4. W. Kölle, P. Koppe and H. Sontheimer. Taste and Odour Problems with the River Rhine. Water Trtmt. Exam. 19, 120-135 (1970).
5. D. Mackay and A. W. Wolkoff. Rate of Evaporation of Low Solubility Contaminants from Water Bodies to the Atmosphere.
6. W. L. Dilling, N. B. Tefertiller and G. J. Kallos. Evaporation Rates and Reactivities of Methylene Chloride, Chloroform, 1,1,1-Trichloroethane, Trichloroethylene, Tetrachloroethylene and Other Chlorinated

Compounds in Dilute Aqueous Solution. *Env. Sci. Techn.* 9, 833-838 (1975).

7. D. Mackay and P. J. Leinonen. Rate of Evaporation of Low Solubility Contaminants from Water Bodies to Atmosphere. *Env. Sci. Techn.* 9, 1178-1180 (1975).
8. U.S. Public Health Service. Advanced Waste Treatment Research-I. Summary Report, June 1960-Dec. 1961. SEC TR W62-9.
9. W. M. Lewis. Polynuclear Aromatic Hydrocarbons in Water. *Water Trtmt. Exam.* 24, 243-260 (1975).
10. Rijksinstituut voor Drinkwatervoorziening. Annual Report, 1973, pp. 32-35. Netherlands Ministry of Public Health and Environmental Hygiene, Leidschendam, Neth.
11. J. Borneff and H. Kunte. Carcinogenic Substances in Water and Soil. XVI. Evidence of PAH in Water through Direct Extraction. *Arch. Hyg. (Berlin)* 148, 585-597 (1964).
12. J.J. Morgan and W. Stumm. The Role of Multivalent Metal Oxides in Limnological Transformations, as Exemplified by Iron and Manganese. *Proc. 2nd Int'l Water Poll. Res. Conf., Tokyo*, 103-131 (1964).
13. T. L. Theis and P. L. Singer. Complexation of Iron (II) by Organic Matter and its Effect on Iron (II) Oxygenation. *Env. Sci. Techn.* 8, 569-573 (1974).
14. Anon. Analytical Methods for Organic Compounds in Sewage Effluents. Water Research Centre, Notes on Water Pollution No. 70 (1975) Medmenham, G.B.
15. G. C. Whipple. *The Microscopy of Drinking Water*. John Wiley and Sons, Inc. (1914).
16. M. J. Suess. *Environmental Lett.* 2, 131 (1971).
17. T. Trott, R. W. Henwood and C. H. Langford. Sunlight Photochemistry of Ferric Nitrilotriacetate Complexes. *Env. Sci. Techn.* 6, 367-368 (1972).
18. C. H. Langford, Michael Wingham and V. S. Sastri. Ligand Photo-oxidation in Copper (II) Complexes of Nitrilotriacetic Acid. *Env. Sci. Techn.* 7, 820-822 (1973).
19. H. B. Lockhart, Jr. and Rose V. Blakeley. Aerobi Photodegradation of Fe(III)-(Ethylenedinitrilo)tetraacetate (Ferric EDTA). *Env. Sci. Techn.* 9, 1035-1038 (1975).
20. R. J. Stolzberg and D. N. Hume. Rapid Formation of Immodiacetate from Photochemical Degradation of Fe(III) nitrilotriacetate Solutions. *Env. Sci. Techn.* 9, 654-656 (1975).
21. R. G. Zepp, N. L. Wolfe, J. A. Gordon and G. L. Baughman. Dynamics of 2,4-D Esters in Surface Waters. Hydrolysis, photolysis and vaporization. *Env. Sci. Techn.* 9, 1144-1149 (1975).
22. D.F. Paris and D. L. Lewis. Chemical and Microbial Degradation of Ten Selected Pesticides in Aquatic Systems.

23. R. G. Zepp, N. L. Wolfe, J. A. Gordon, R. C. Fincher and G. L. Baughman. Chemical and Photochemical Transformations of Selected Pesticides in Aquatic Systems. EPA Report (in press).
24. D. F. Paris, D. L. Lewis and N. L. Wolfe. Rates of Degradation of Malathion by Bacteria Isolated from Aquatic System. Env. Sci. Techn. 9, 135-138 (1975).
25. N. L. Wolfe, R. G. Zepp, G. L. Baughman and J. A. Gordon. Kinetics of Chemical Degradation of Malathion in Water. Env. Sci. Techn. (in press).

notes

ENVIRONMENTAL TRANSPORT MODELING OF
POLLUTANTS IN WATER AND SOIL¹

M. R. Patterson, C. L. Begovich
Computer Sciences Division
at Oak Ridge National Laboratory
Union Carbide Corporation, Nuclear Division²

D. R. Jackson
Environmental Sciences Division
Oak Ridge National Laboratory
Oak Ridge, Tennessee 37830

In considering the processes and critical data for evaluation of pollutant transport, one must consider the source of the pollution, how it is injected into the ecosystem, whether the injection of that pollutant is via aerial or terrestrial pathways, whether the origin is of point source nature or area source nature, and whether it is directed toward the surface of the landscape or injected directly into the hydrologic system. The chemical form of the constituent is also of great importance. We will be considering today mainly the transport of solids which can be solubilized or can be transported as particulates. Soluble forms of the heavy metals will be considered to undergo first-order exchange, and other non-exchangeable types of any metal will be transported in particulate form as sediment.

The time scale to be considered in modeling pollutants can vary dramatically from a few seconds to several years. However, for most of those materials of current interest, we think in terms of attempting to simulate time periods on the order of a year. Weathering processes, of course, are natural geologic processes on the time scale of thousands of years. At the other end of the spectrum, kinetic transformations of many very highly reactive substances are such that 99% of the reaction may be complete in the order of a minute. Generally, however, the very short time period transformation reactions are not of interest for pollutant transport because the initial product that is being considered quickly disappears from the system. More persistent chemical forms which last on the order of a year can pose a threat to the health of man or to the environmental health of the ecosystem.

¹Work supported by the National Science Foundation—Research Applied to National Needs—Environmental Aspects of Trace Contaminants Program under NSF Interagency Agreement No. AG-389.

²Prime contractor for the U.S. Energy Research and Development Administration.

Models which address these transport calculations are as varied as is the time scale. Many of these models address an extremely small part of the total ecosystem and are directed at transport in a limited physical space. Such models can be characterized as mathematically interesting and, in certain cases, useful for analysis of the system. However, we have tended overall to study larger geographic areas in order to show interrelationships among a variety of physiographic and environmental processes. We have employed transport models which are oriented toward a watershed basis, in which the area considered varies from one acre through several thousand square miles. These watersheds require the application of models which consider the complete range of environmental processes, starting with infiltration of water through soil, proceeding through evapotranspiration to runoff from the soil surface or runoff in the form of base flow to the stream channel, as illustrated in Fig. 1. Each one of these hydrologic processes is capable of carrying pollutant material in dissolved or particulate form. In fact, within the soil surface the process of evapotranspiration leads to the drying of a toxicant causing it to move from a lower level to a higher level. Further wetting would reverse the flow toward the deeper regions.

Through experience we have found that we need models of the entire hydrologic cycle in order to model the influence of the daily and seasonal variation in precipitation. The model which provided a basis for many of our first studies of toxicant transport was the Stanford Watershed Model of N. H. Crawford and R. K. Linsley [1966], as adapted by D. D. Huff [1968], presently at the Oak Ridge National Laboratory in the Environmental Sciences Division. We called this model the Wisconsin Hydrologic Transport Model [Patterson et al, 1974] and used it to study the transport of a variety of heavy metal ions in the vicinity of fossil fueled power plants. We also studied metal ions emitted as particulates near a lead smelting plant [Patterson et al, 1975]. We have adapted the model further to consider the transport of particulates that are entrained in water by soil erosion processes and by direct deposition into the water. The study of these particulates, for example depleted lead ore, is important because their movement constitutes in some cases the largest mass flow for material we have studied. Particulate transport then provides the main source of material to downstream processes.

Models of the type that we have described require considerable amounts of information in order to be effective; however, even more detailed studies in the near vicinity of structures such as a smelting plant can be effected by using a detailed formulation of the soil moisture equation and its associated transport of soluble material within soil. This type of model has also been studied at ORNL by M. Reeves and J. O. Duguid [1975] who have evolved a finite element code, which is sophisticated in terms of solving the soil moisture equation and is based on the method described by Pinder and Frind [1972]. It is presently limited to the consideration of relatively localized areas of contaminated soil because it requires the conductivity, permeability, and exchange to be the same in each vertical layer of soil. Extensions of this method have been made by Gupta, Tanji, and Luthin [1975]. The finite element is unexcelled in terms of considering the effect of soil type, texture, and permeability on water movement.

We have found that to first order the effect of heavy metal ion mobility in soil can be modeled by a simple exchange coefficient k_d [Begovich and Jackson, 1975]. This exchange coefficient plus considerations for bulk transport and for the initial solubility of the toxicant allow one to establish a budget for the toxicant. The other processes that must be considered in addition to those already mentioned include the sedimentation which occurs when the toxicant reaches the stream channel.

To summarize, the processes that we have found to be important in pollutant transport in terms of transport modeling include the surface flow of a material either as a solute or in bulk form, and the solubilization of the toxicant by incident precipitation, initial infiltration into the soil, the evapotranspiration processes, the subsequent exchange of the cations from the solubilized toxicant, and leaching through soil of the cations which are undergoing transport. The critical data can be inferred from these processes to be the particle size distribution for the toxicants, the solubilities of toxicants, the permeability of the soil horizons involved, and the values of the exchange coefficient k_d . The hydrologic properties that are also critical in determining the entrainment and subsequent transport of the toxicants on a watershed scale can be summarized as streamflow data, that

is data that relates to the streamflow volume, its velocity, the width of the stream, depth, the length of the reaches that make up various segments of the river channel system.

We have used the UTM to study heavy metal transport in the vicinity of a lead smelter in southeast Missouri. In this particular application, four heavy metals including lead, cadmium, zinc, and copper were considered. They are input by atmospheric deposition to the landscape surface. The model used in this simulation was the SCEHM model (Soil Chemistry Exchange of Heavy Metals) which was coupled into the Wisconsin Hydrologic Transport Model to provide input deposition values and to obtain values for precipitation, surface flow, soil moisture content, and soil moisture flux. Figure 2 illustrates various moisture and contaminant fluxes and contaminant exchange within each of the homogeneous soil chemistry layers. Figure 3 shows six years of simulated values for lead in the A1 horizon, which is that part of the soil from 0-3 cm, and in the A2 horizon (3-15 cm) on Crooked Creek Watershed. The exchangeable lead is building up in the soil because of the high soil exchange coefficient (k_d) for lead. Lead continues to accumulate on this watershed because the solubility of the lead is not sufficient for it to be removed from the watershed in surface flow or as the water percolates through the soil profile. In addition, by comparing simulated and experimental results, we have concluded that insoluble lead is infiltrating into the soil in particulate form. In contrast to the build up of lead, we see in Fig. 4 that cadmium in the A1 and A2 horizons is depleted during rainfall events and rainy seasons and that it has gradually built up to asymptotic values in the A1 horizon and has almost reached an asymptotic level in the A2 horizon. Similarly for zinc, in Fig. 5 we see that it also has sufficient solubility and a low enough exchange coefficient to percolate through the soil and lead to the establishment of the steady state concentration value in the surface 3 cm of the soil. Finally in Fig. 6, we see the values for the copper plotted for the six year period of the A1 and A2 horizons and note that copper's behavior is very like that of lead in that it is built up and continues to build up during the six year period. It exhibits slightly more response than lead to rainfall during months of heavy rain.

We believe that this model is most valuable in predicting buildup of heavy metals which remain as free ionic cations after dissolution and during infiltration through the soil. This study points out the different mobilities that can occur from different materials, which may force a different emphasis on the transport model in order to consider that given substance. For example, an extremely mobile compound may require a major emphasis be given to transport in the aquatic system in the stream channel if the compound is not complexed by the soil and if it is readily solubilized. Other conditions could force consideration of the effect of vapor pressure, since vapor pressure of the material can interact very strongly with environmental conditions such as wind speed and turbulence to affect the rate at which the material is dispersed into the environment from terrestrial and aquatic phases. Thus the interaction of the landscape with the aquatic system can lead to formation of a new species, to complexation with the soil, or to passive transport through the pores of the soil and in the aquatic system.

We feel that it is very useful in our studies to have available an integrated transport model such as the Wisconsin Hydrologic Transport Model which allows us to consider a variety of processes that are important in watershed scale transport. We feel that the simplicity of the processes modeled here have aided us in gaining insight into the pathways taken by these toxicants as they flow through the ecosystem. In addition, we have found that we can couple models of plant growth to these transport models and attempt to assess the effect on growth rates due to the entrained toxicant and uptake of that toxicant by the plant. The availability of the general model is useful also because the characteristics of pollutants are variable, and one can study the response of the terrestrial or aquatic system to input of toxicants of varying natures.

REFERENCES

- Begovich, C. L. and D. R. Jackson, *Documentation and Application of SCEHM, a Model for Soil Chemical Exchange of Heavy Metals*, ORNL/NSF/EATC-16 (1975).
- Crawford, N. H. and R. K. Linsley, *Digital Simulation in Hydrology: Stanford Watershed Model IV*, Stanford University Technical Report Number 39 (1966).

- Gupta, S. K., K. K. Tanji, and J. N. Luthin, *A Three-Dimensional Finite Element Ground Water Model*, University of California, Davis, Contribution Number 152 (1975).
- Huff, D. D., *Simulation of the Hydrologic Transport of Radioactive Aerosols*, Ph.D. Thesis, Stanford University (1968).
- Patterson, M. R., J. K. Munro, D. E. Fields, R. D. Ellison, A. A. Brooks, and D. D. Huff, *A User's Manual for the Fortran IV Version of the Wisconsin Hydrologic Transport Model*, ORNL/NSF/EATC-7 (1974).
- Patterson, M. R., J. K. Munro, and R. J. Luxmoore, *Simulation of Lead Transport on the Crooked Creek Watershed*, Proceedings of the 9th Annual Trace Substances Conference, Columbia, Missouri (June 1975).
- Pinder, G. and E. Frind, "Application of Galerkin's Procedure to Aquifer Analysis", *Water Resources Research* 8, pp. 108-120 (1972).
- Reeves, M. and J. O. Duguid, *Water Movement through Saturated-Unsaturated Porous Media: a Finite-Element Galerkin Model*, ORNL-4927 (1975).

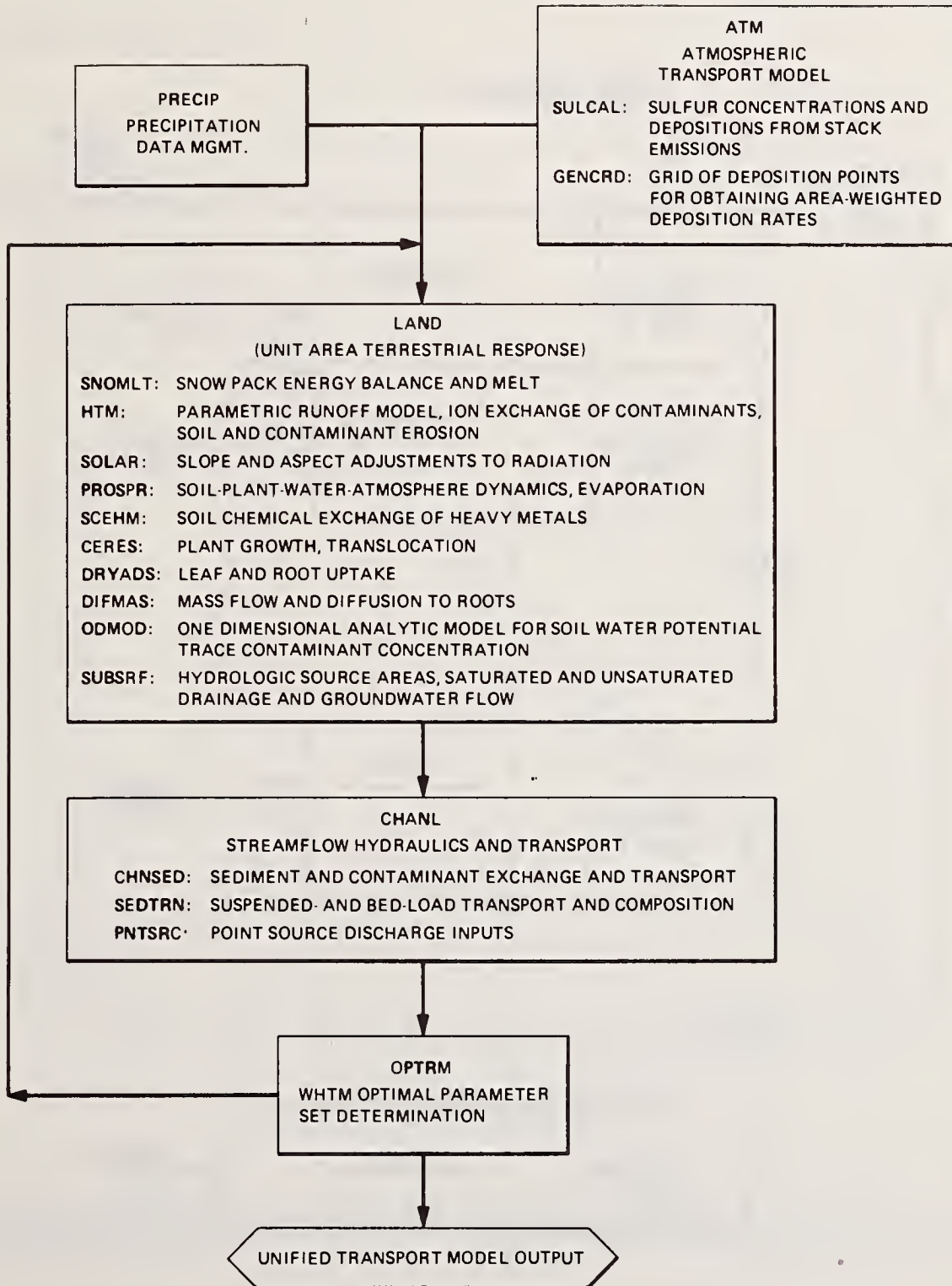


Fig. 1. The Submodels That May Be Linked to Form A Unified Transport Model.

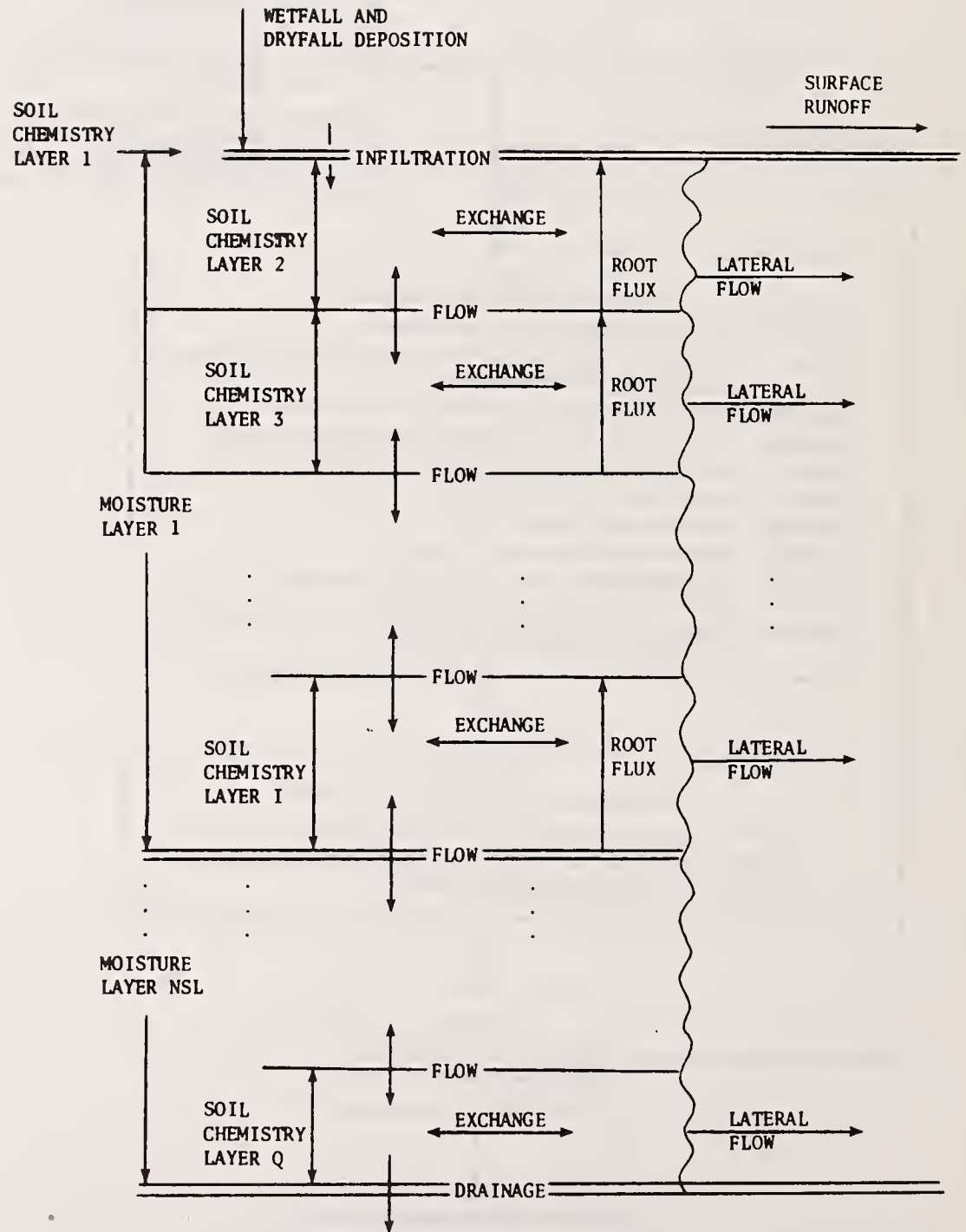


Fig. 2. Schematic of SCEHM.

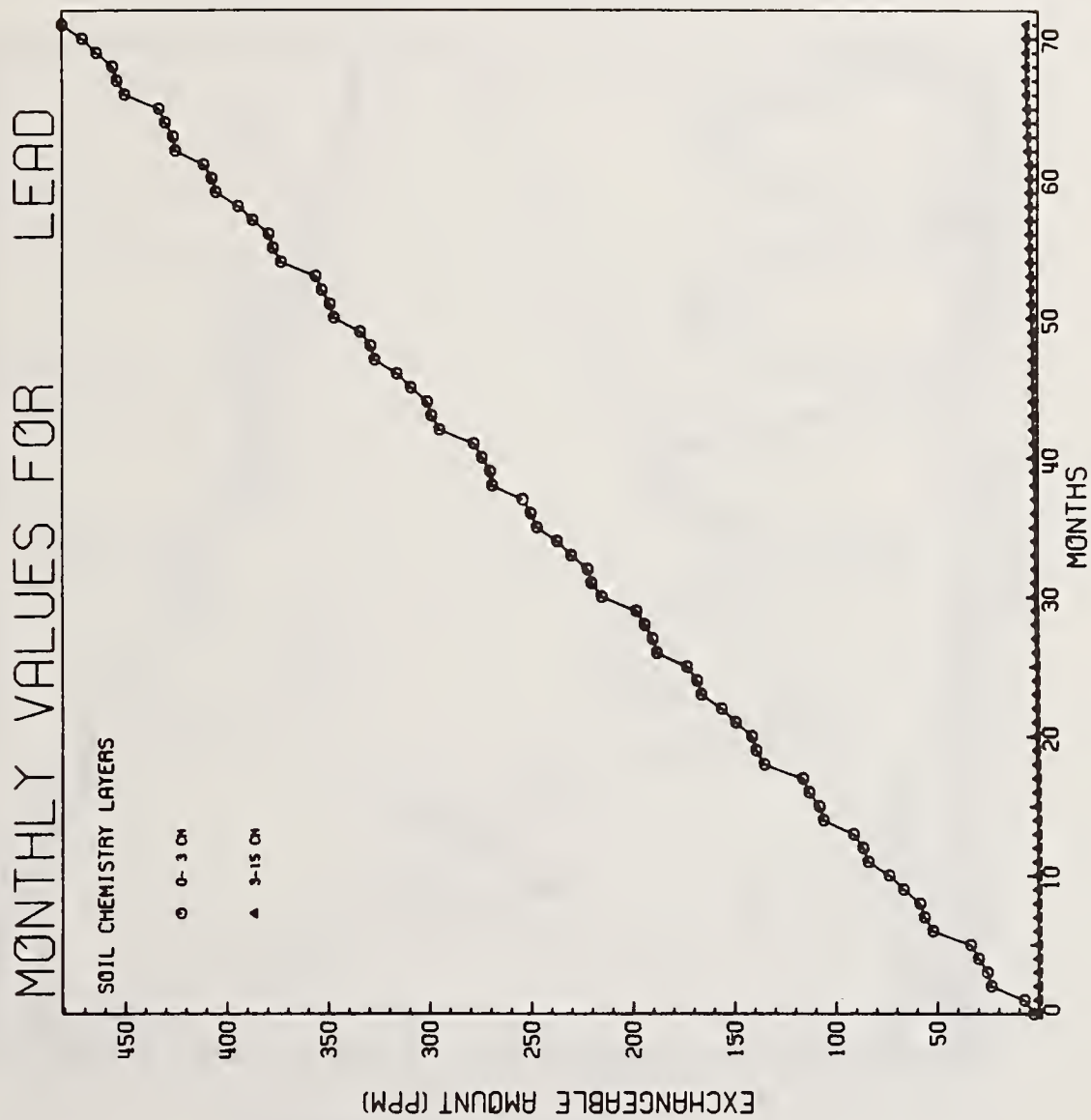


Fig. 3. The Amount of Exchangeable Lead in the A1 (0-3 cm) and A2 (3-15 cm) Horizons for the Six-Year Simulation Run on Crooked Creek Watershed.

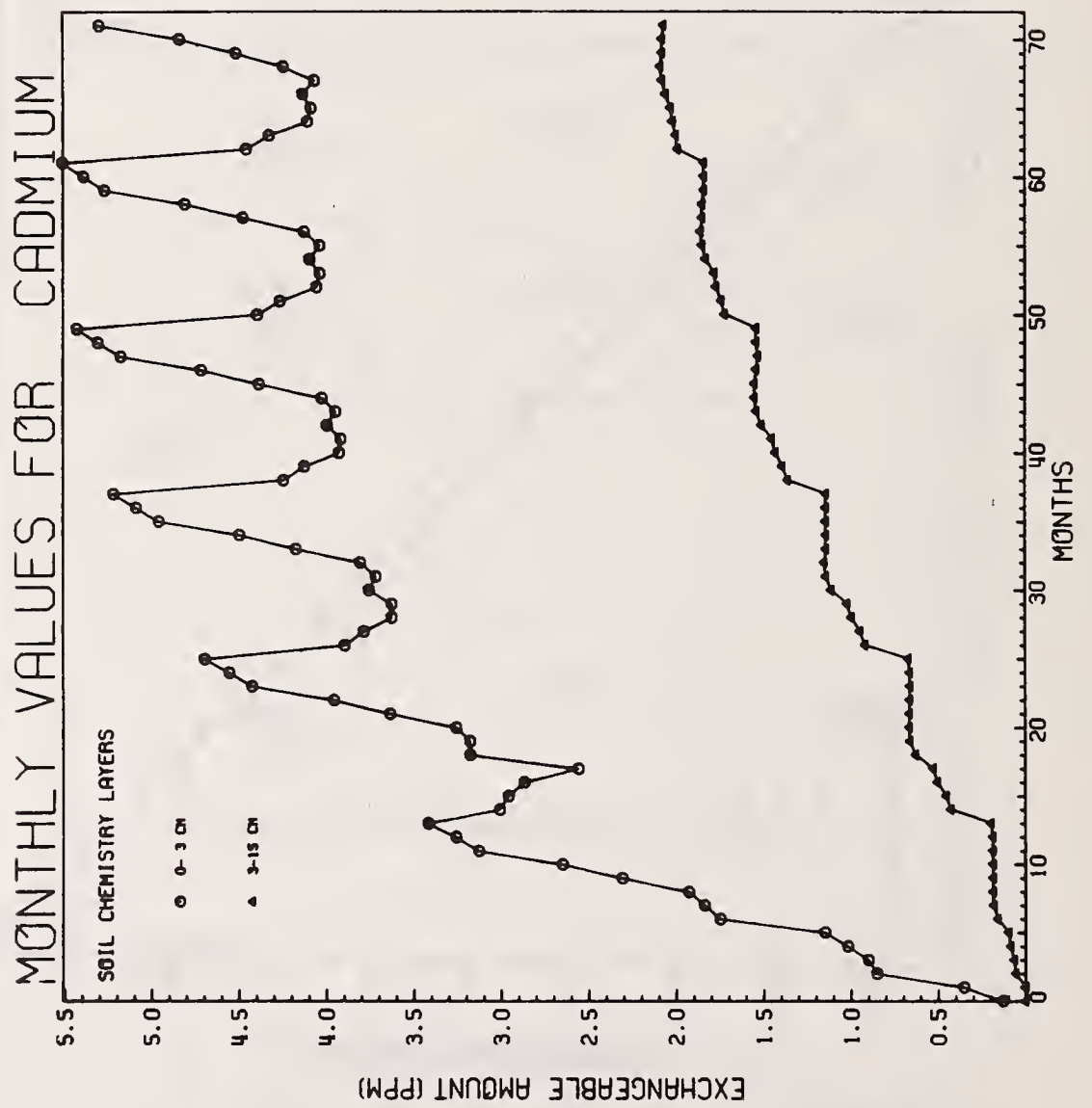


Fig. 4. The Amount of Exchangeable Cadmium in the A1 (0-3 cm) and A2 (3-15 cm) Horizons for the Six-Year Simulation Run on Crooked Creek Watershed.

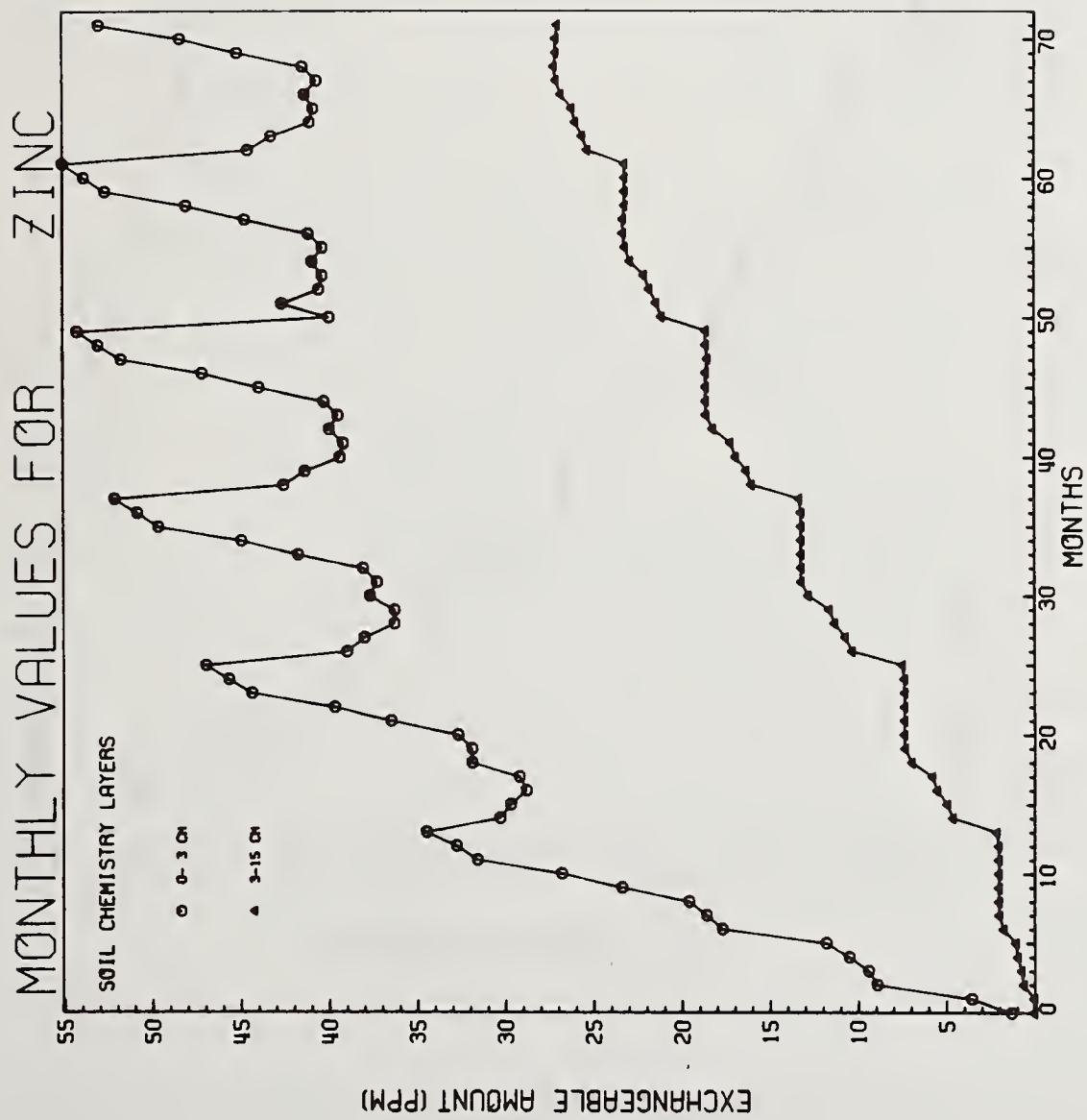


Fig. 5. The Amount of Exchangeable Zinc in the A1 (0-3 cm) and A2 (3-15 cm) Horizons for the Six-Year Simulation Run on Crooked Creek Watershed.

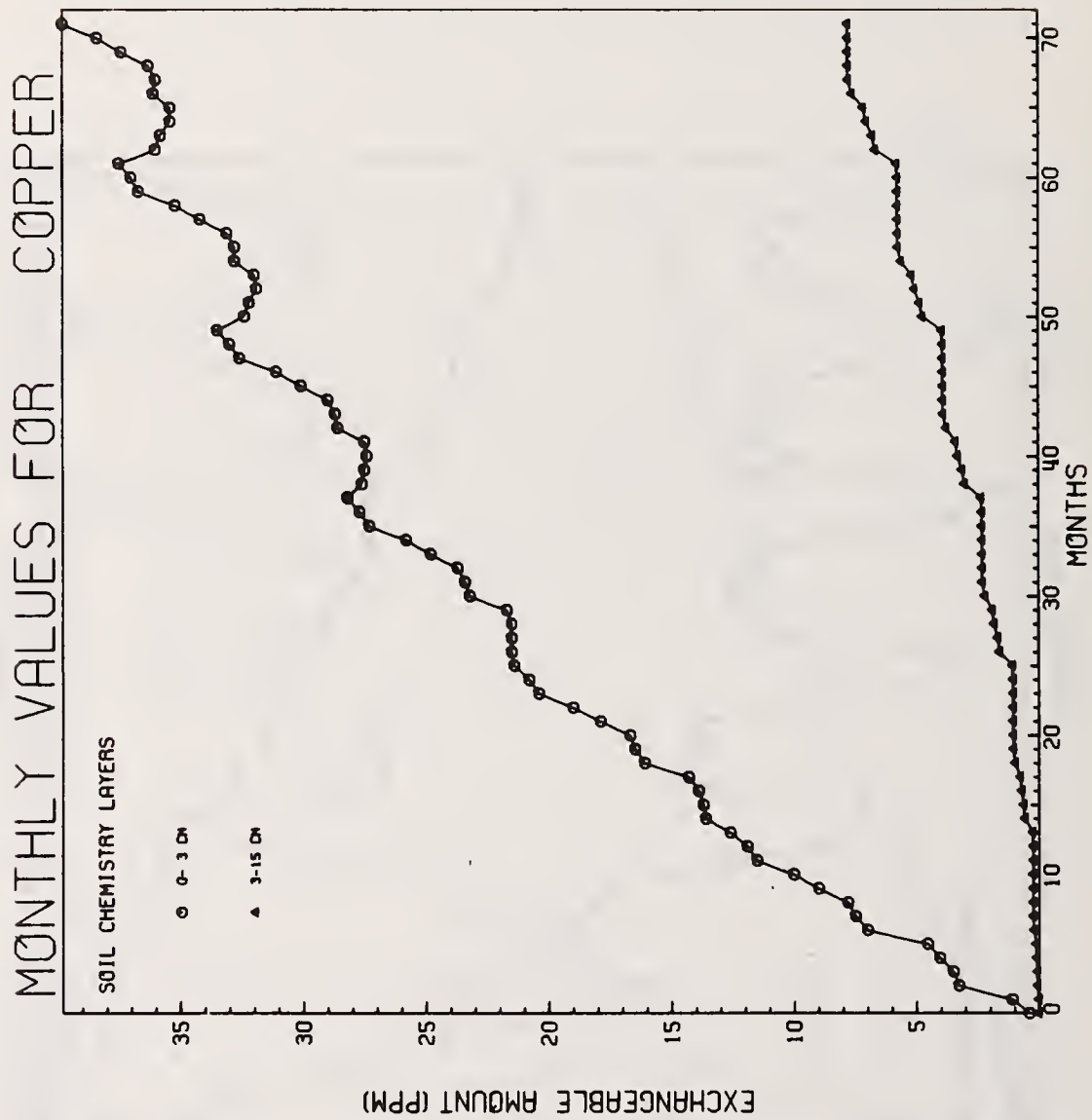


Fig. 6. The Amount of Exchangeable Copper in the A1 (0-3 cm) and A2 (3-15 cm) Horizons for the Six-Year Simulation Run on Crooked Creek Watershed.

notes

OXIDATION AND REDUCTION OF PESTICIDES IN SOILS AND SEDIMENTS

Jack R. Plimmer

Agricultural Environmental Quality Institute,

U.S. Department of Agriculture, Beltsville, Md. 20705

Many pollutants are characterized by their resistance to oxidation, reduction or other chemical reactions. The stability of most pesticides during storage indicates that normally they are quite resistant to chemical decomposition. Nor are suitable conditions for chemical degradation often encountered in the environment and we must regard decomposition by microbial action or by sunlight as primary routes by which degradation of field-applied pesticides occurs. In the absence of quantitative information, however, it is useful to analyze some environmental processes to see whether biological and nonbiological transformations can be distinguished and to what extent they are interdependent.

Soils and sediments are complex media. They contain complex minerals and metal salts intimately associated with organic matter. The heterogeneity and polyfunctional nature of soil macromolecules has made the problem of structure elucidation an arduous task for the organic chemist. The application of modern instrumental techniques and a renewed interest in geochemistry have spurred progress in recent years.

The organic matter content of sediments is about 0.7%. This is largely in the form of insoluble polymeric material known as 'kerogen'. Kerogen is an extremely insoluble, heterogeneous material and it is presumably highly cross-linked. Organic matter in this state is also strongly associated with neighboring molecules through dipolar interaction and hydrogen bonding. It presents a very unattractive proposition for study by the organic chemist. Such organic compounds will be intimately associated with the inorganic fraction and in some cases they may be enclosed in expanded clay lattices.

The aquatic system provides a means for degradation by sunlight irradiation, oxidation, etc. and the organic matter in the sediment may not be typical of that in the biomass above. Eglinton has summarized the situation: "Most organically-rich recent sediments are reducing but there is generally an oxidizing zone in the upper layers of the sediment and the water column above it". Biological activity that results from the introduction of microorganisms and other forms of life makes it difficult to distinguish between organic compounds extracted from the living organisms and those extracted from the non-living components of the sediment. As the depth increases and the sediment is compressed, biological activity falls to zero. Organic matter distribution in recent muds approaches that in ancient shales. Most of the organic matter is an insoluble, polymeric condensed material. Hydrocarbons are present and their composition is indicative of their biological origin. During a relatively short time period molecules may be transformed by biological or nonbiological processes. One major distinction between the two processes is that the former generally involve controlled synthesis or degradation, whereas the latter lack the orientational selectivity and stereochemical specificity that generally characterize enzyme reactions.

Oxidation and reduction reactions in soils and sediments are primarily biological. Microorganisms in soils and sediments are the agents mainly responsible for transformation of pesticides. Soil moisture content, pH, temperature, aeration, and ion exchange capacity influence the nature of the soil microbial population and thus the nature of the metabolic products. In the well aerated upper layers of soil the microbial population consists of aerobic organisms that derive their energy from oxidative reactions. Below a water surface in a sediment rich in organic matter, the microbial population alters as oxygen is depleted. The population of facultative anaerobic microorganisms increases and finally, obligate anaerobic species predominate. These events can be followed in a sedimentary system by measuring the fall in redox potential.

Attempts to make the distinction between chemical and biological reactions in soil media by performing experiments in sterile soils have usually met with much criticism. Autoclaving is normally adequate for sterilizing glassware or equipment contaminated with microorganisms. However, sterilization of soil may affect not only the microbial population but also the chemical and physical structure of the medium. Thus, nonbiological processes may be precluded as a result of such treatment. The use of microbial inhibitors,

fumigants, irradiation, or other methods of reducing microbial activity are equally open to criticism. These techniques often result in substantial changes in soil reactivity or the presence of reactive residues.

Although direct evidence for chemical, as opposed to biological, degradation of a pesticide may be lacking, sometimes we may infer that chemical degradation occurs if we cannot identify soil microorganisms specifically capable of degrading the molecule in question. Degradation of 3-amino-1,2,4-triazole (amitrole) in sterile and nonsterile soils gave carbon dioxide as a product. Degradation in sterile soils occurred when the soil had been sterilized by azide or ethylene oxide, but not when the soil had been autoclaved. Addition of the sodium salt of ethylenediaminetetraacetic acid to nonsterile or ethylene oxide treated soils reduced the rate of degradation. Many unsuccessful attempts have been made to isolate or identify microorganisms capable of degrading amitrole, suggesting either that special conditions are necessary for microbial degradation or that reaction is purely chemical.

The chemistry of the degradation process has been elucidated. Amitrole is resistant to many powerful chemical oxidants, but, in the presence of free-radical generating systems, the ring was ruptured yielding carbon dioxide, cyanamide and urea. These products were also formed when a solution of amitrole in water was irradiated with ultraviolet light of wavelength ca 220 nm. There was no reaction at long wavelengths (> 310 nm) until riboflavin was added to the solution. Reaction with Fenton's reagent gave the same products, indicating that amitrole readily undergoes oxidation by free radicals. Although interesting parallels may be drawn from these observations, the above evidence is no more than circumstantial.

Free radicals are present in soil. Some of these are associated with the humic acid fractions. It has been proposed that their formation and properties are intimately associated with the nature of the silicate environment, since the EPR signal widths vary widely in humic impurities found in different clay types. Other soil components such as lignins, tannins, resins, pigments and antibiotics contain free-radical species. Steelink et al proposed that a model for the radical species in the humic fraction of soil based on an ortho- and para-quinhydrone-containing polymer would account for many of the observed properties.

The role of free radicals in soils remains to be established. They may inhibit one-electron metabolic processes, scavenge halogen-containing compounds or catalyze polymerization reactions.

Although it may be very difficult to distinguish between biological and chemical changes in soils and sediments in most natural situations, a combination of both types is expected. Generally the former take place in aqueous media at ambient temperature and are catalyzed by complex macromolecules, whereas the latter give similar products only under conditions of temperature, acidity or alkalinity unfavorable to life. However, the action of biota on xenobiotic molecules often gives terminal products that result from a combination of biological transformations and thermal reactions. The products of biological reaction are frequently quite reactive and may undergo subsequent chemical reactions spontaneously, following an initial metabolic step. Although these are not strictly 'non-biological' reactions, much of the driving energy for environmental chemical reactions is derived from solar energy or from the proximity of biological systems and such reactions will be significant.

Transformation of organic molecules in plants, vertebrates or higher organisms often involves a complex series of reactions in which the molecule undergoes minor modifications and is ultimately 'conjugated' to yield a compound of high molecular weight. Elimination or 'detoxication' often involves conjugation with water-soluble polar residues of biological origin, such as sugars, amino acids, oligosaccharides, peptides, etc. New functional groups (hydroxylation of aromatic systems, etc.) which favor subsequent conjugation reactions may be formed through the intermediacy of enzymes such as the mixed function oxidases. These routes may also be accompanied by pathways involving more substantial disruption of the molecule. Degradation products containing one or two carbon atoms may be utilized as starting points for the elaboration of biological macromolecules or may be eliminated as carbon dioxide.

By contrast, transformations of complex organic molecules by soil bacteria normally result in degradation to carbon dioxide, water, nitrogen, chloride ions and other inorganic ions as ultimate products. This is referred to as 'mineralization' and there is an optimistic belief that such a self-cleansing process will continue to rid the environment of undesirable compounds. However, complex intermediates formed in some

bacterial processes may subsequently undergo purely chemical reaction to give unanticipated products.

The metabolism of chloroanilines derived from aniline-based herbicides provides an example. In soil, these slowly evolve carbon dioxide, indicating disintegration of the aromatic ring. However, azobenzenes are detected as soil residues and these can only result from the condensation of two molecules of aniline. *Fusarium oxysporum* Schlecht, a fungus present in soil, is capable of effecting the oxidation of a primary aromatic amino group to a phenylhydroxylamine. If 4-chloroaniline is used as a substrate, the rapid formation of 4-chlorophenylhydroxylamine can be demonstrated by color reactions. 4,4'-Dichloroazoxybenzene can be isolated from the medium. (Attempts to isolate 4-chlorophenylhydroxylamine during chemical synthesis by reduction of 4-chloronitrobenzene often result in the isolation of 4,4'-dichloroazoxybenzene, because this product is readily formed by the condensation of two molecules of the reactive hydroxylamine.) 4,4'-Dichloroazobenzene is a further product of metabolism. It is conceivable that condensation of an aniline and a nitrosobenzene represent a chemical route to this compound.

The formation of phenylhydroxylamine represents a major metabolic pathway, but other metabolic routes observed are: hydroxylation of the ring at the ortho position, acetylation or formylation of the aromatic hydroxy and amino groups. Hydroxylation at the ortho position of an aromatic amine is a well-known rearrangement reaction of phenylhydroxylamines. Thus, although we assume that this reaction is mediated by an enzyme system and that direct hydroxylation of the aniline ring occurs, we cannot exclude the possibility that the o-aminophenol is derived through a rearrangement of a phenylhydroxylamine.

Another interesting example is the formation of a triazene from propanil. Propanil (3,4-dichloropropionanilide) is rapidly hydrolyzed to the parent aniline, 3,4-dichloroaniline, in soils. One of its metabolites in soil under special cultural conditions is 3,3',4,4'-tetrachlorotriazene. This compound has three nitrogen atoms. The question of the origin of the third nitrogen atom is important because the only likely source is inorganic nitrite. This must be derived from the soil where its availability depends on bacterial nitrification processes. Synthetically, the triazene is prepared by diazotization of 3,4-dichloroaniline with nitrous acid followed by reaction with 3,4-dichloroaniline in the presence of sodium acetate as a buffer. In soil, the formation of the triazene strongly suggests the intermediacy of a diazo compound that must result from a reaction of aniline with inorganic nitrite. Thus we have a further example of a transformation which may be biological or chemical. If these reactions take place under conditions normally found in soil, N-nitrosation might be a frequent occurrence when appropriate secondary or tertiary amines are present.

Distinctions between 'biological' and 'nonbiological' reactions become extremely subtle as we continue to examine the types of reaction occurring in nature. Two important types of reaction are oxidation and reduction. If we consider an aquatic system containing sedimentary organic material, the upper layer will favor oxidative processes whereas the lower will favor reductive reactions.

The availability of oxygen and nutrients favor growth of biota. Their source of energy is based primarily on the oxidation of organic compounds using oxygen as an electron acceptor. Enzymic systems of microflora are generally capable of accomplishing a variety of oxidative reactions.

Excess oxygen and oxidants will also bring about reactions in the upper layers of an aquatic system. Activated processes of oxygenation such as photosensitized oxidation, oxidation by singlet oxygen, oxidation by transition metals, and radical oxidation processes are conceivable under these circumstances. The absence of oxygen at lower depths will favor microorganisms capable of utilizing other sources of energy and their survival will depend on anaerobic processes, i.e. metabolic reaction sequences will be based on electron acceptors other than molecular oxygen. Thus, reductive processes will predominate. The characteristic property of each depth region is its redox potential. Organic molecules will react as electron acceptors or donors depending on the redox potential of the medium without respect to its origin.

Rates at which reactions occur will depend on the homogeneity of the system, i.e. solubility of the substrate, adsorption of the substrate to interfaces where it is less reactive, and adsorption to interfaces where it is more reactive.

Oxidation

Oxidation is probably responsible for degradation of a substantial fraction of the pollutants present in aquatic systems and soils. Oxidation may occur by microbial action, photooxidation, direct attack of oxygen, or an activated oxidizing species. These factors will be affected by pH, soil type, metal ions, photosensitizers, oxygen content of the sediment, temperature, sunlight, etc. Microbial systems are responsible for many oxidative transformations. A number of complex catalytic systems involving metals can provide models for oxidizing systems. The products are similar to those from biological oxidation and there are close analogies between them in that they both involve the generation of activated species of oxygen.

Photochemical oxidation may also proceed through activated oxygen species. Autoxidation processes involve peroxy and alkoxy radical chains. Photochemical generation of free radicals appears to be one of the most probable sources, although it is suggested that metal ions may catalyze autoxidation reactions. Photochemical reactions may be a source of singlet molecular oxygen (1O_2).³ This is formed by energy exchange between triplet carbonyl and ground state oxygen (3O_2). Singlet oxygen is an extremely active oxidant and it may be produced from oxygen by irradiation in the presence of a wide range of triplet sensitizers. It can also be generated by chemical species. Sensitized photooxidation of amines, sulfides and a variety of organic compounds has been intensively studied.

The role of transition metals as oxidants in aqueous systems requires further investigation. In the presence of complex organic molecules, metal ions may take part in oxidation processes that are closely analogous to biological oxidations mediated by enzymes.

A number of chemical systems mimic the reactions of microsomal oxidases responsible for in vivo oxidation of aromatic compounds and other organic compounds foreign to the organism. These oxidases include drug hydroxylase, demethylase, N-oxidase, etc. and they require TPNH and molecular oxygen together with a metal. The study of chemical model systems has provided some clues as to the nature of activated oxygen species in enzymic reactions. Fenton's reagent (iron salts, hydrogen peroxide and sulfuric acid) is a source of hydroxyl radicals that will hydroxylate aromatic systems or dealkylate amines or ethers. The active species generated is probably the hydroxyl radical. Typical of such model oxidation systems is that containing ferrous sulfate, ascorbic acid and ethylenediaminetetraacetic acid in a buffer. From a study of the hydroxylation of aromatic compounds in the presence of ferric iron together with hydrogen peroxide and catechol it was proposed that the reactive species was not the hydroxyl radical. Hydroperoxy or peroxy radicals seemed unlikely species because they did not react very well with aromatic systems. The formation of an iron-catechol complex was postulated; this complex was then responsible for direct transfer of oxygen to the substrate. This model system bears some analogy to the iron-porphyrin enzymes. Views of the biological mechanism of oxygen activation involve analogous mechanisms in which cytochrome P-450 forms ferric hydroperoxide-type complexes or ferric superoxide-type complexes with a substrate. The proximity of active oxygen to the substrate permits a concerted reaction.

It would be of interest to determine whether humic acids containing metal ions could function as oxygen transfer reagents. The semiquinones of humic acid alone might function as oxidants, but there is little documentation of the role of nonbiological oxidation in soil. The function of metals may be important. Ferrous iron is known to be oxidized to ferric iron and the latter may act as an oxidant in chemical reactions.

There are few examples of nonbiological oxidation of pesticides. The oxidation of amitrole has been discussed. Aldrin is slowly converted to dieldrin in soils and this reaction is considered to be nonbiological. However, documented instances of environmental nonbiological oxidation not mediated by photochemical action are rare. Examples of catalyzed autoxidations occurring in the absence of light are well documented, but the substrates are usually quite different from pesticides in structure. As was pointed out earlier, pesticides are generally quite stable for long periods in storage, whereas labile molecules subject to fairly rapid oxidation are unlikely to become pollutants.

Reductive Transformations

The 'reduction' of organic compounds usually implies such reactions as the saturation or addition of hydrogen to carbon-carbon, carbon-oxygen, or nitrogen-oxygen multiple bonds. The replacement of halogen by hydrogen is a further example that is important in the case

of many pesticide pollutants. In the laboratory, these reactions require vigorous chemical reducing agents or hydrogenation using a metal catalyst. Such conditions are not characteristic of the environment, where reducing reactions must occur under mild conditions. Examples are disproportionation reactions having a low activation energy threshold, or reactions brought about by complex electron-transfer systems. Models for the latter may be constructed if we can postulate the type and role of biological catalysts involved.

Metabolism of toxaphene by rat liver microsomes requires NADPH and anaerobic conditions. Reduced cytochrome P-450 may act as the reducing agent under these conditions. The observation that reduced hematin reacts with toxaphene to cleave C-Cl bonds suggest that iron (II) protoporphyrin systems may provide valuable models for understanding the degradation of some chlorinated hydrocarbons. Mirex also reacted with reduced hematin to give reductive dechlorination products.

Under strongly anaerobic conditions in a flooded soil, toxaphene undergoes extensive alteration and the products appear to be formed by the process of reductive dechlorination.

As stated earlier, the redox potential falls to extremely low values in an anaerobic system and oxidation-reduction potentials as low as -650 mV have been measured. Under these conditions, sulfate is reduced to sulfide and metal salts are reduced. Thus, manganic and ferric salts give manganous and ferrous salts. Subsequent chemical reactions between the metals and hydrogen sulfide give metal sulfides that are stable until they are exposed to oxidizing conditions. Sulfide is then oxidized to sulfate and metal is deposited as oxide or hydroxide.

Reduction of dinitroaniline herbicides proceeds stepwise as the electrode potential is decreased. The sequence proceeds through initial reduction of one nitro group to a phenylhydroxylamine. The second nitro group is then reduced and, after further reduction stages, a *m*-phenylenediamine is the final product. Reduction potentials for a number of dinitroaniline herbicides were found to be dependent on pH by polarographic techniques. Half-wave potentials for the first polarographic wave for trifluralin were -190 mV at pH 1.5, -540 mV at pH 7.4, and -640 mV at pH 9.2. A second polarographic wave was also distinguishable at higher pH's. Dinitramine was more difficult to reduce than other dinitroaniline herbicides. From these observations it was concluded that a nonbiological pathway for degradation of dinitroaniline herbicides is feasible under anaerobic flooded soil conditions.

Clearly these results imply that a study of redox potentials can be extremely valuable in predicting the type and extent of transformations of pollutants that may occur in sediments under anaerobic conditions.

notes

TRANSMISSION OF SUNLIGHT IN NATURAL WATER BODIES

John E. Tyler
Scripps Institution of Oceanography
La Jolla, California 92037

The transmission of sunlight into ocean or lake water is a function of the properties of the impinging radiant energy as well as of the water. The significant properties of any source of light, including daylight, are its magnitude, its wavelength distribution, its polarization, and its directional distribution. The significant properties of the water are its absorption and its directional scattering. It is important to recognize that these properties of the light source are entirely independent of each other and that they will be independently altered by the scattering and absorbing properties of the water body.

Most people have a clear concept of the magnitude, wavelength distribution and polarization of light but the directional distribution does not seem to have been generally accepted as one of its significant properties. In fact, directional distribution is the fundamental measurement of the science of radiometry and it cannot be ignored when dealing with the transmission of daylight into natural waters.

When the exact measurement of radiant energy is the primary objective of a study, the study is referred to as the science of radiometry and here we find the critically defined concepts which deal with the geometrical collection of radiant energy and which have been chosen to fulfill theoretical objectives.

When the primary objective of a study is to apply the science of radiometry to lake and ocean water, the effort is referred to as Hydrologic Optics, or Optical Oceanography, and here again we find the geometrical concepts of radiant energy collection, as well as new concepts which apply to the interaction of radiant energy with scattering-absorbing media.

When the primary objective of a study is to determine the biological response of an animal or plant as a function of the radiant energy which is collected or sensed by the animal or plant, it becomes necessary to deal with new problems. In this case we are faced with a dilemma. On the one hand the detectors used by animals or plants do not necessarily collect radiant energy in accordance with the formal geometrical concepts defined in the science of radiometry and hence these formal methods of collection will not necessarily measure the radiant energy actually sensed by the animal or plant. On the other hand, if we simulate the organic sensor by means of a photoelectric detector that duplicates the collecting properties of some specific animal or plant, we may not be collecting energy in accordance with the established geometry of radiometry, and such measurements may not be suitable for use in existing theory.

The basic concept of radiometry is the concept of radiance, illustrated in Figure 1,

which depicts a measuring device consisting of a photo-detector at the lower end of a long opaque tube. The purpose of the tube is to restrict the field of view of the photo-detector to a fixed solid angle. Radiant energy enters the aperture of the tube along straight lines in the manner illustrated. It can be seen from the figure that if the area of the detector were to be made smaller than illustrated, some of the energy entering the tube would not be detected. The reading obtained with this apparatus is therefore dependent on both the angle of acceptance of the tube and the area of the collector, and the device therefore measures radiant power for a specific solid angle and a specific area. The measurement can be normalized to obtain the radiant power per unit area per unit solid angle and this measurement has been given the name "radiance".

An ordinary camera is a radiance recording device and the image brightnesses formed in its focal plane are proportional to the radiances in the scene.

Measurements of radiance provide an ideal way of examining the details of the underwater light field. For example, Fig. 2 is a photograph taken from a depth of about 10 meters with the camera pointed at the zenith. A 180° wide-angle lens was used and the entire upper hemisphere is consequently compressed onto the film. The horizon is marked by four bright spots around the outside circumference of the exposed area. The picture shows a dark annular ring of nearly uniform density having a width equal to about $1/3$ the radius of the exposed area. Inside the annular ring there is a much lighter circular area which exhibits wave details as well as the bottom of the ship. This bright circle is the Snell circle, so called because it identifies the position of the angle of total internal reflection predicted by Snell's law.

Fig. 3 gives radiance data obtained with a radiance tube (see Fig. 1), which shows details of the Snell circle effect. These data were obtained on an overcast day with calm water surface. Curve A was obtained above the water surface and shows changes in radiance of the terrain and reflection by the water surface. Curve B, obtained at a depth of 2.5 cm, shows an increase in radiance near the zenith direction due to optical compression. At the edge of the Snell circle (48.6°) the radiance drops sharply because the path of sight at this angle is reflected downward into the water at an angle of 48.6° . At greater angles the radiance increases moderately until the horizontal direction is reached and then trails off to lower values. Curves C and D demonstrate the loss of these details due to multiple scattering by the water body as the depth of observation increases.

Fig. 4 gives radiance data as a function of depth obtained on a sunny day for three directions, the sun's direction, the zenith direction, and the nadir direction. Near the surface the sun's direction exhibits much higher radiance than the zenith direction but, again due to scattering, these two directions exhibit the same radiance at 40 meters. At still greater depths maximum radiance is found in the zenith direction. It is also of interest that in the first five meters below the water surface the radiance in the zenith direction increases as a result of scattering by particles in the water.

Fig. 5 is a recording of the radiance distribution in the plane of the sun obtained on an overcast day at a depth of about 43 meters. The values of radiance in the lower hemisphere have been multiplied by 10 in order to show the distribution more clearly. It can be seen that light from the upper hemisphere arrives mainly from the zenith direction whereas light from the lower hemisphere arrives mainly from the horizontal direction.

Fig. 6 compares the magnitude and shape of the radiance distribution in the plane of the sun at two depths. In "A" the maximum radiance value is in the direction of the sun and the distribution is distorted in that direction. In "B" the maximum radiance value is much closer to the zenith direction and the distribution is more nearly symmetrical around the zenith direction. These changes in magnitude and shape of the radiance distribution are due to the water properties only.

In addition to providing a detailed description of the light field, radiance distribution data of this kind can be used to calculate other radiometric quantities which are useful for quantitatively describing the transmission of daylight into natural waters. Figure 7 indicates the mathematical procedure for calculating scalar irradiance h and the vector irradiances $H(+)$ and $H(-)$ from radiance distribution data. The figure also shows the procedure for calculating the irradiance reflectance R and the absorption coefficient a from these irradiances.

Scalar irradiance describes the total radiant energy arriving at a true point. Since it is not possible to make an instrument that will measure at a true point, a substitute measurement of spherical irradiance has been defined, which is directly proportional to scalar irradiance. The concept of spherical irradiance is illustrated in Fig. 8. Its measurement requires a diffuse spherical collector having uniform collecting properties for all directions. Figure 8 illustrates several parallel bundles of radiant energy

impinging on such a sphere from different directions. In a real measurement, bundles such as those shown would be arriving from all directions and the sphere would respond equally to each bundle. Practical collectors of this kind have been built and are in use in research studies dealing with the effect of pollutants on the growth of phytoplankton.

The concept of vector irradiance is illustrated in Fig. 9. This measurement requires a flat collector that collects radiant energy in accordance with the cosine of its angle of incidence on the collector. In Fig. 9 four bundles of radiant energy are shown impinging on such a collector at different angles. Each bundle is accompanied by an equation which indicates the fraction of the bundle that is collected. Practical collectors for determining vector irradiance have been developed and are available commercially.

Measurements of vector irradiance have been used to record the spectral distribution of radiant energy underwater, the spectral reflectance of the radiant energy, and the spectral attenuation of the radiant energy as a function of depth in natural waters.

Figure 10 gives monochromatic measurements of the downwelling irradiance (H-) as a function of depth in ocean water containing a low concentration of phytoplankton. Fig. 11 gives similar data for lake water containing a high concentration of phytoplankton and also decomposition products. Note that the ordinate and abscissa scales are the same in both figures and that in Fig. 10 the depths for measuring downwelling irradiance are at 5m 15m and 25m whereas in Fig. 11 the depths of measurement are for each meter down to a maximum of 10m. The absorption of long wavelengths exhibited in Fig. 10 is largely due to absorption by water. This absorption is also seen in Fig. 11 and in addition Fig. 11 exhibits strong absorption in the blue region of the spectrum due to phytoplankton pigments and soluble decomposition products. Figures 12 and 13 give reflectance data for similar bodies of water.

Figure 14 illustrates the attenuation of irradiance with depth for 5 wavelengths. Except for some local effects that occur near the air-water interface, these data can be described and predicted by an exponential law of attenuation shown in equation 1.

$$\frac{H_2}{H_1} = e^{-K\Delta Z} \quad \dots \quad (1)$$

The experimental fact that the exponential law can be applied to the transmission of daylight into natural waters is of great importance for the ecologist because it provides a way for separating the total attenuation coefficient of ocean or lake water into parts which apply to the separate components found in these waters and this, in turn, makes it possible to determine the quantum efficiency of in situ photosynthesis and the effect of environment on productivity.

The exponential law of attenuation can be written with depth as the only parameter as is done in equation 1 or it can be written to include both depth and concentration as in equation 2.

$$\frac{H_2}{H_1} = e^{-KC\Delta Z} \quad (2)$$

In current research at S.I.O. I have used the exponential law in the form shown in equation 3 where K_w and the coefficients on the right of the equal sign are the attenuation coefficients of the components of ocean water which are of interest. H_1 and H_2 in equation 3 are measurements of irradiance at the upper (H_1) and lower (H_2) surfaces of a selected depth interval ΔZ . K_w is the attenuation coefficient of clean water alone. Since K_w can be evaluated from measurements in clean ocean water, all factors at the left of the equal sign in equation 3 are known.

$$\frac{\ln \frac{H_1}{H_2}}{\Delta Z} - K_w = K_1 C_1 + K_2 C_2 + K_x C_x \quad (3)$$

At the right of the equal sign, $K_1 C_1$ represents the attenuation coefficient per meter of living phytoplankton pigments at a concentration of C_1 ; $K_2 C_2$ similarly represents the attenuation coefficient of the pheopigments (that is, the non-living phytoplankton pigments); and $K_x C_x$ similarly represents the attenuation coefficient of the unidentified absorbing

materials.

To use this form of the exponential law it is necessary to locate ocean water for which $K_x C_x$ is not significant. Figure 15 shows the results of a study made during the S.C.O.R. Discoverer Expedition of 1970 in which the optical density of 10-meter-thick layers of ocean water were measured in situ. In Fig. 15 these densities are plotted against the combined concentrations of living (C_1) and non-living (C_2) plant pigments. In this plot, if the measured density is due only to living and non-living plant pigments at various concentrations, the data will plot along a straight line originating on the ordinate at the density of clean ocean water. If on the other hand the measured density of a 10 meter layer is due in part to a component other than plant pigments the data point will plot higher than the aforementioned line by an amount equal to the excess density over that due only to the plant pigments C_1 and C_2 . The straight line in Fig. 15 starts on the ordinate at the optical density determined for clean ocean water and passes through the data points of minimum density obtained at a number of ocean stations. The equation for this line is given by equation 4,

$$\frac{\log \frac{H_1}{H_2}}{\Delta Z} - K_w = (C_1 + C_2)k \quad (4)$$

where k (the slope of the line) would represent the average attenuation coefficient per meter per unit concentration for the combined living and non-living plant pigments. The analytical determinations of chlorophyll-a and pheopigments for these low density samples showed significant differences in the ratio of these two classes of pigments and made it possible by means of simultaneous equations to evaluate K_1 and K_2 using equation 5,

$$\frac{\log \frac{H_1}{H_2}}{\Delta Z} - K_w = K_1 C_1 + K_2 C_2 \quad (5)$$

on the basis that $K_x C_x$ was insignificant for the low density samples. It was then possible to determine, by difference, the value of $K_x C_x$ in samples which showed high values of optical density due to components other than plant pigments. A second application of the exponential law to the independent computed values of $K_1 C_1$, $K_2 C_2$, and $K_x C_x$ was then used to compute the absorption, per 10 meters of sample thickness, of the independent absorbing components and these values can be normalized to make their sum equal to the total absorption already obtained from measurements.

From these latter calculations the radiant energy absorbed by the viable plant pigments is obtained and this is expressed in quanta absorbed per unit volume per 6 hours of time (noon to sunset). From additional analytical work performed on samples of the same ocean water we have measurements of the carbon-14 fixed by the phytoplankton per unit volume per 6 hours of time (noon to sunset), and from the ratio of these two pieces of data we can calculate the quantum efficiency of photosynthesis by the in situ mixed phytoplankton population.

REFERENCES

The Sea - Ideas and Observations on Progress in the Study of the Seas, M. N. Hill, General Editor. Interscience Publishers, N. Y. Section IV, Chapter 8, Light, by John E. Tyler and R. W. Preisendorfer. pp. 397-451.

The In Situ Quantum Efficiency of Natural Phytoplankton Populations, John E. Tyler. Limnology and Oceanography, vol. 20, #6, pp.976-980. Nov. 1975.

THE CONCEPT OF RADIANCE

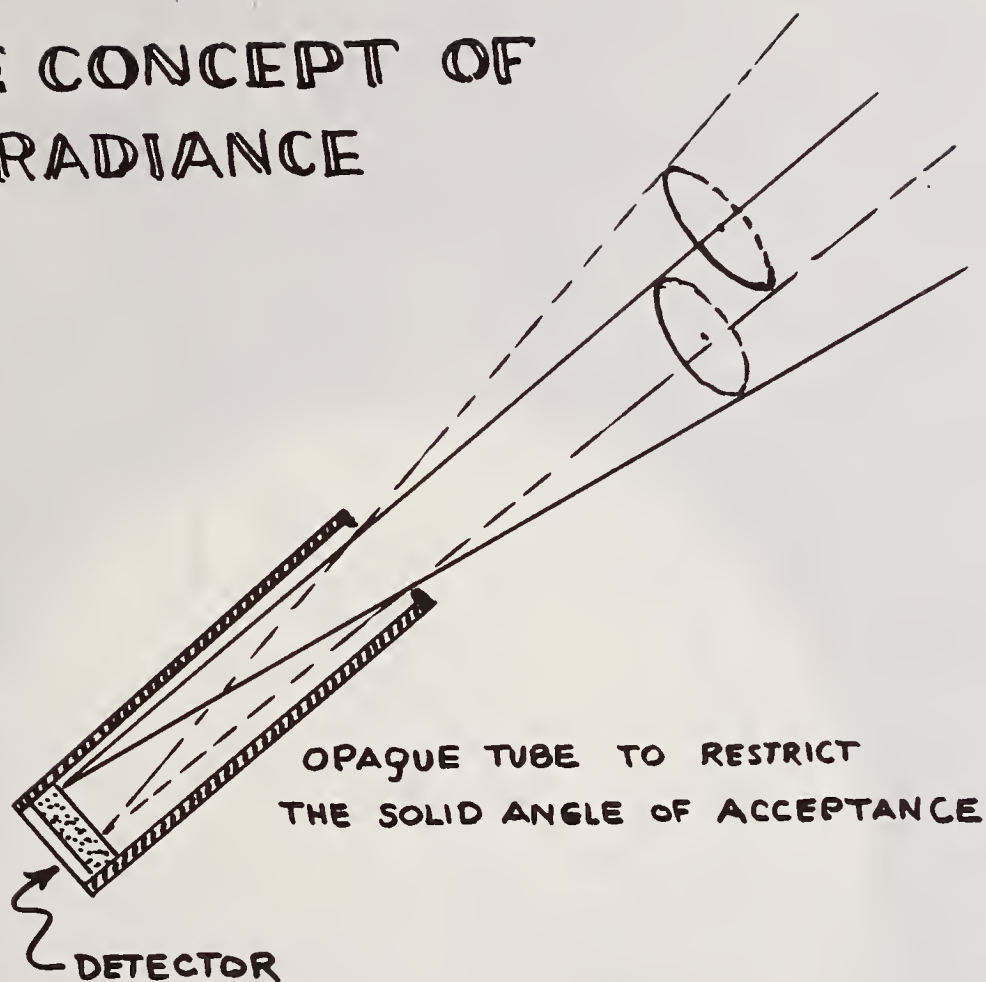


Fig. 1 The figure illustrates the collection of radiant flux from a diffuse source such as the sky. The total radiant flux that can reach the detector depends on the area of the detector and the solid angle of acceptance of the opaque tube.



Fig. 2 Photograph in the zenith direction from 10 meters showing the Snell circle, with details of the ship. The four bright spots separated by 90° mark the horizontal direction underwater.

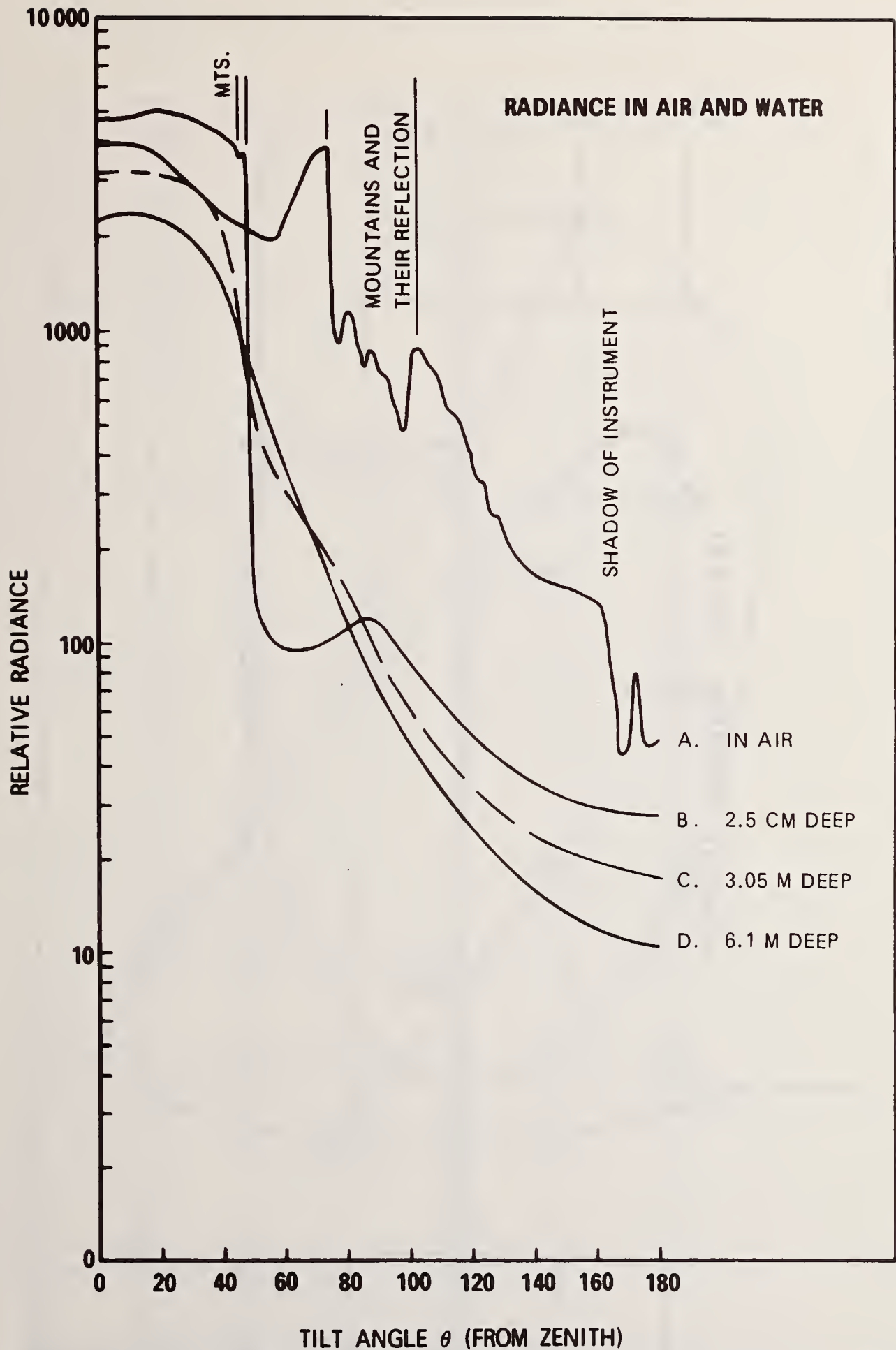


Fig. 3 Scans of radiance vs observation angle with a 6° radiance tube showing the details of the light field above and below the water surface, the latter at different depths. Overcast day.

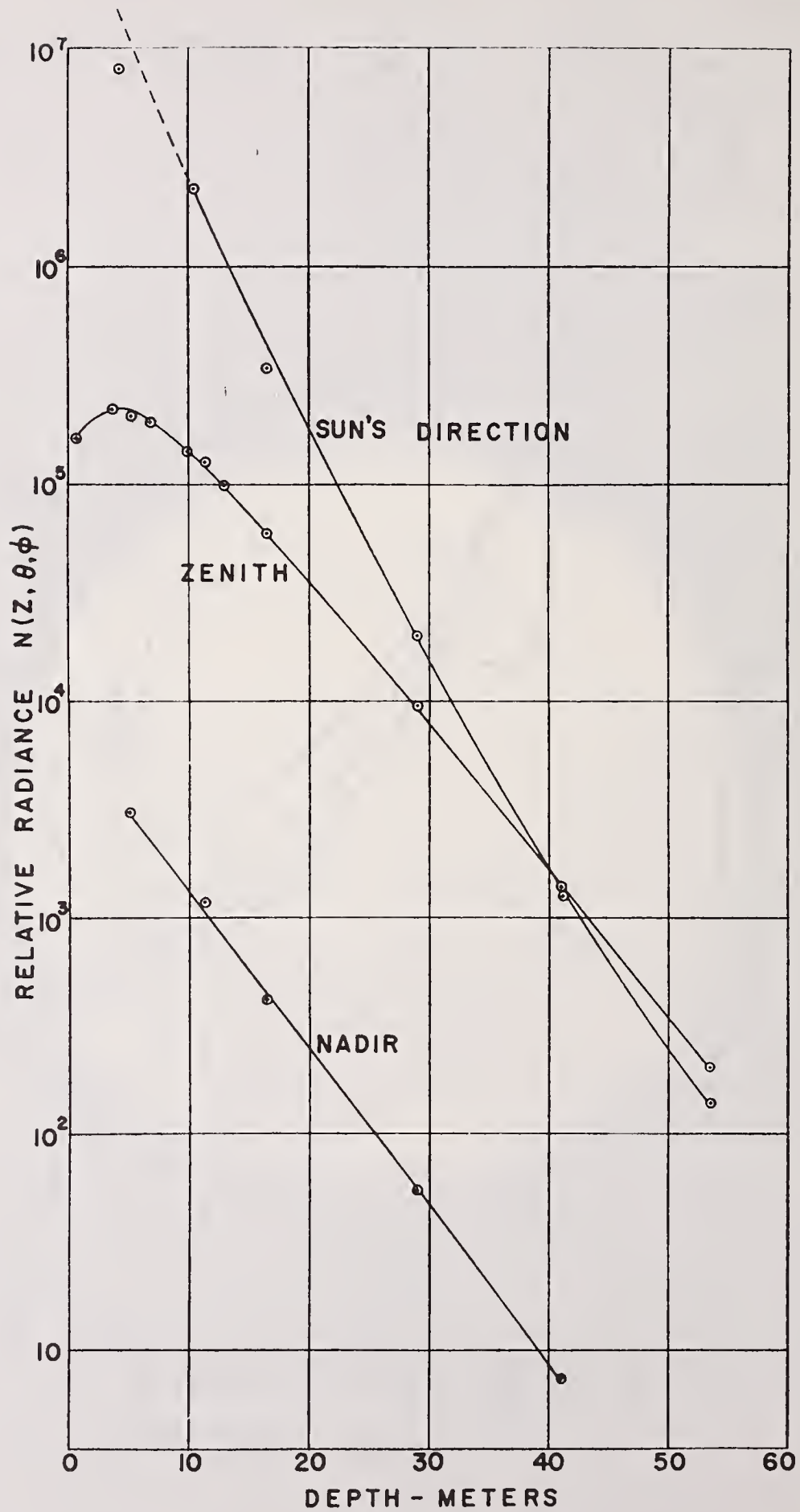


Fig. 4 Scans of radiance vs depth for fixed angles of observation. Sunny day.

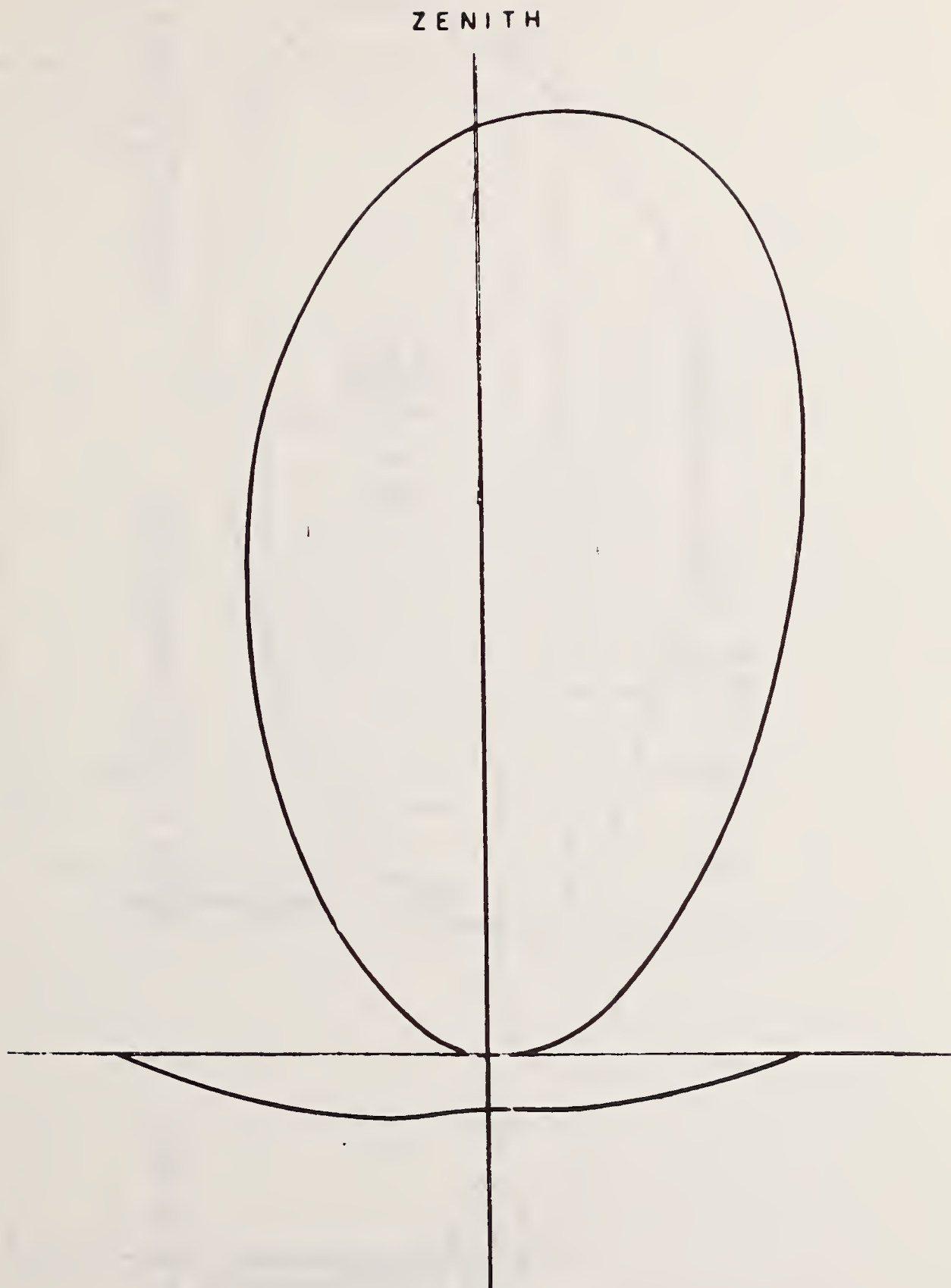


Fig. 5 Relative shapes of the radiance distribution in the upper and lower hemispheres at a depth of 43 meters. Lower hemisphere data has been multiplied by a factor of 10.

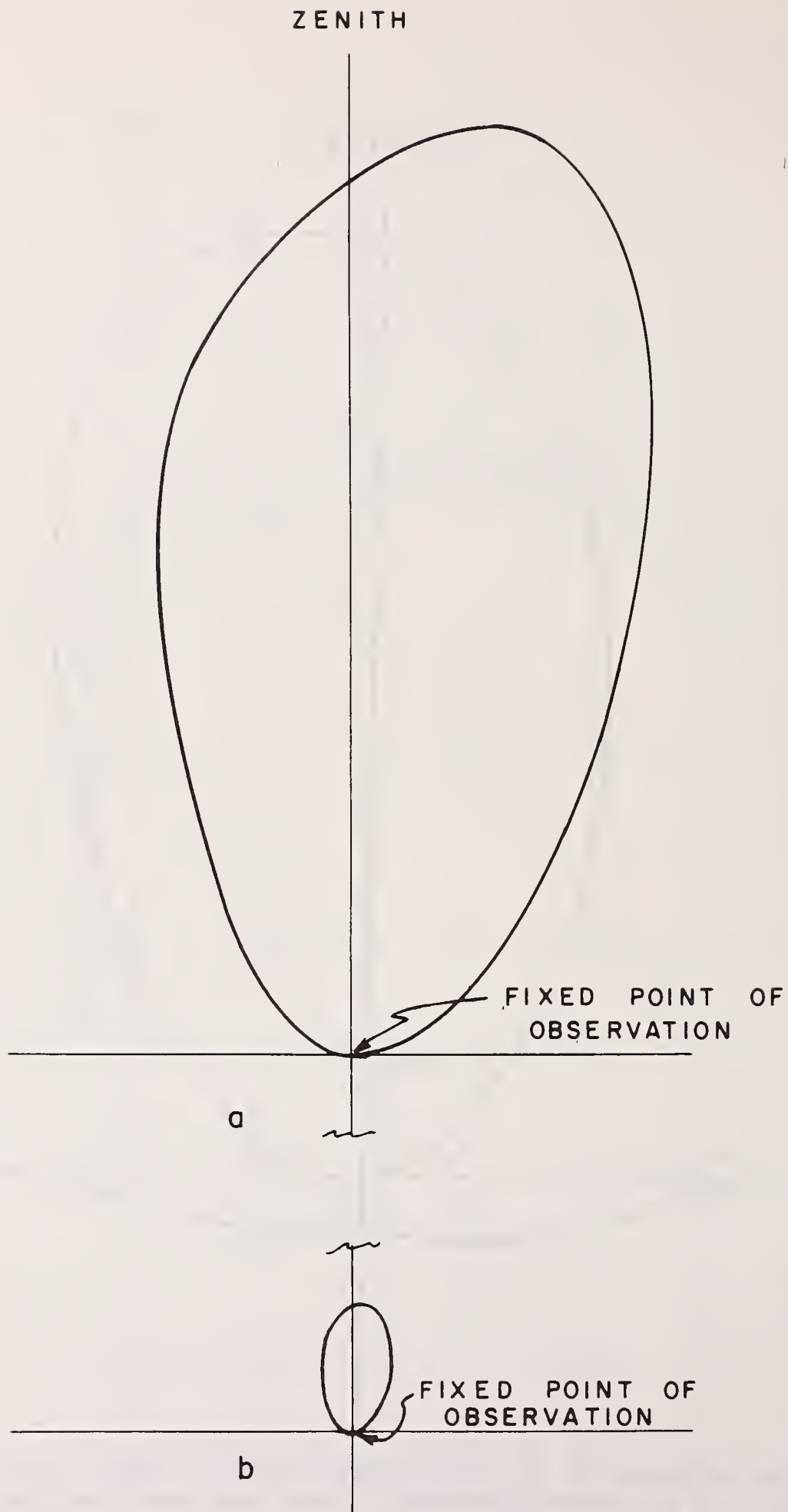


Fig. 6 Radiance distributions at two depths showing changes in shape and in magnitude.

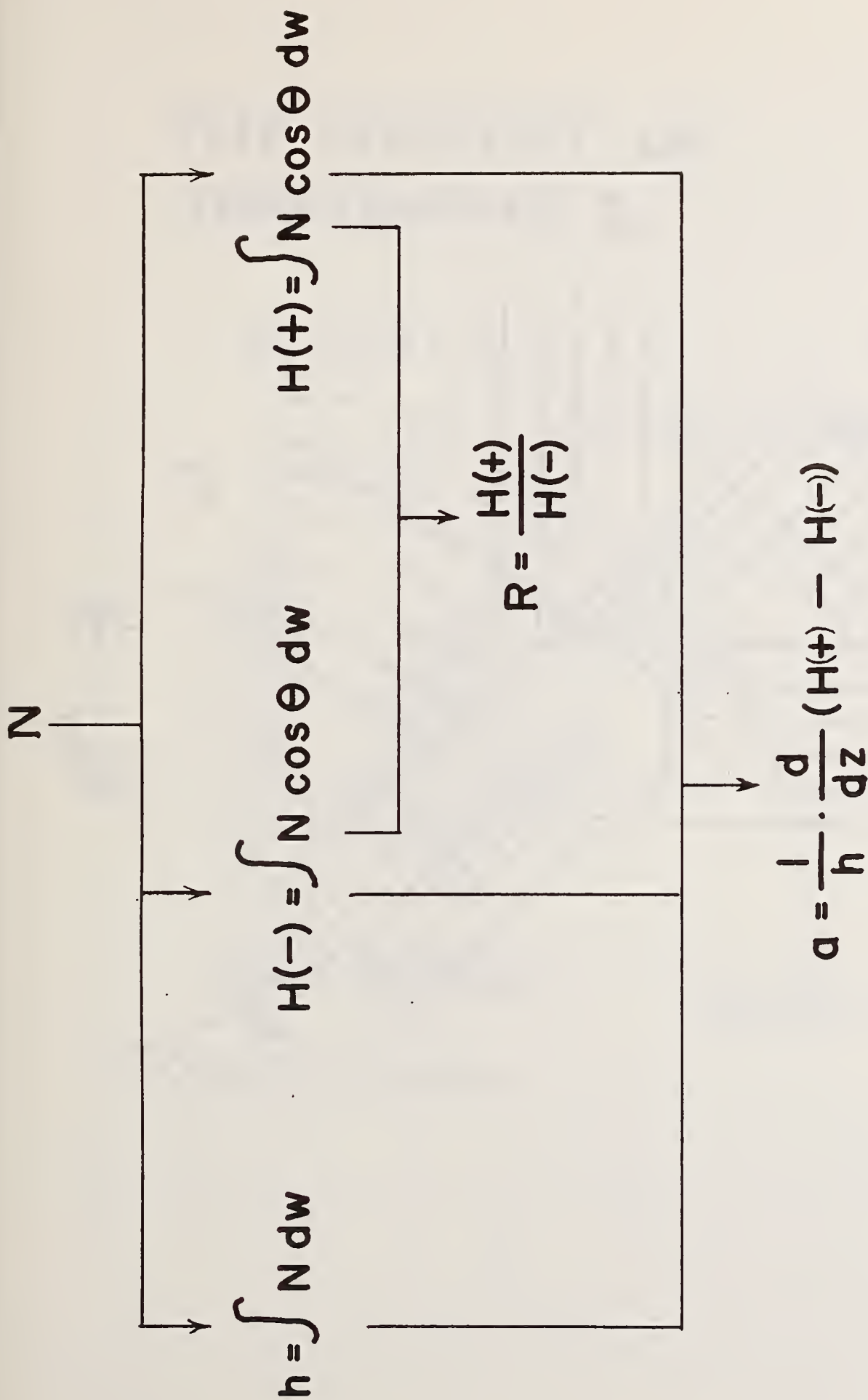
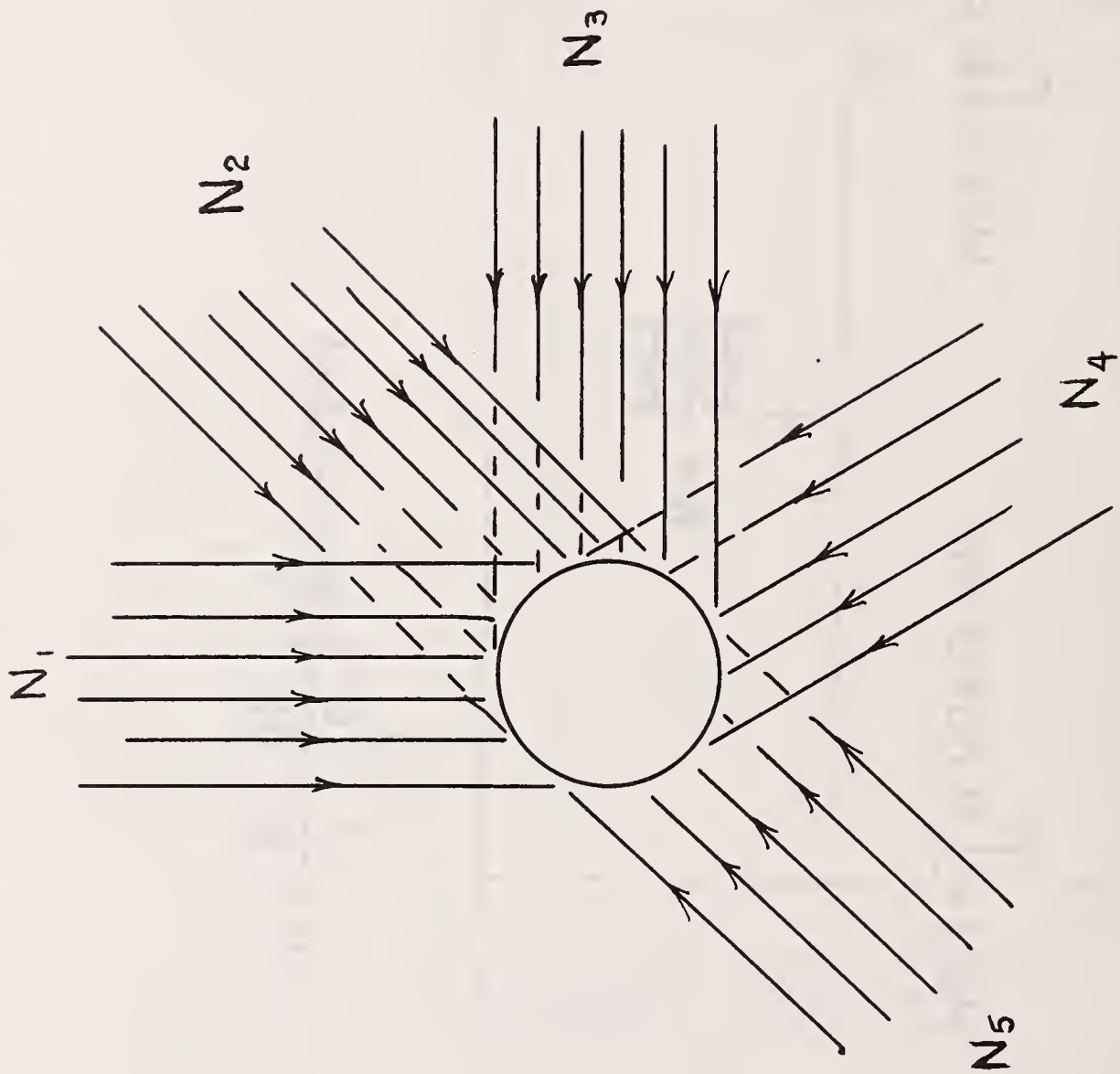


Fig. 7 Computational procedures for computing the irradiances, reflectance and absorption coefficient from radiance data.

THE CONCEPT OF SPHERICAL IRRADIANCE



$$H_{4\pi} = \frac{h}{4}$$

Fig. 8 The figure illustrates the concept of spherical irradiance. The diffusing sphere is designed to collect equally from all directions.

THE CONCEPT OF IRRADIANCE

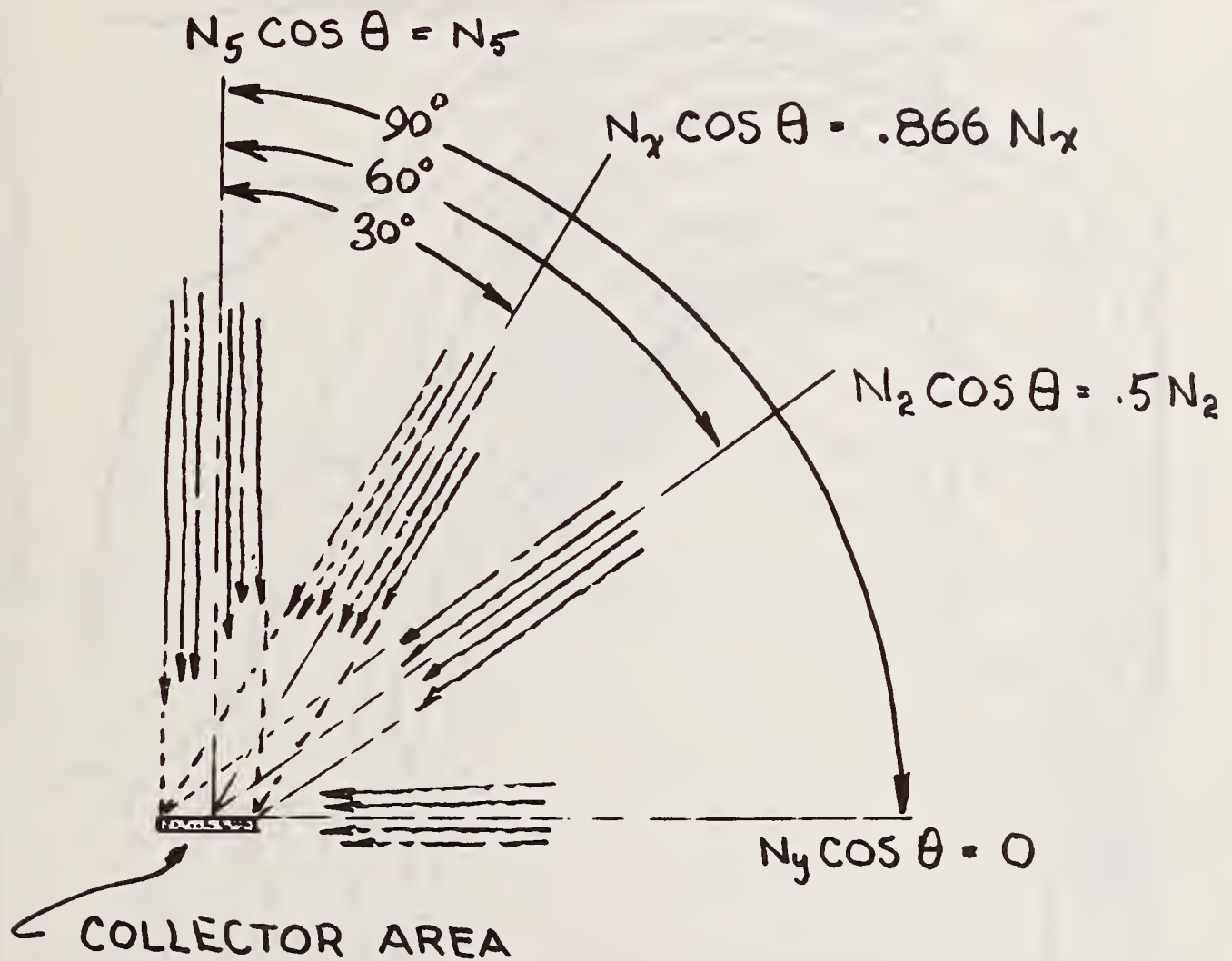


Fig. 9 The figure illustrates the cosine collecting properties of a horizontal collector of fixed mechanical area whose apparent area depends upon the angle of incidence of the bundle of incoming rays.

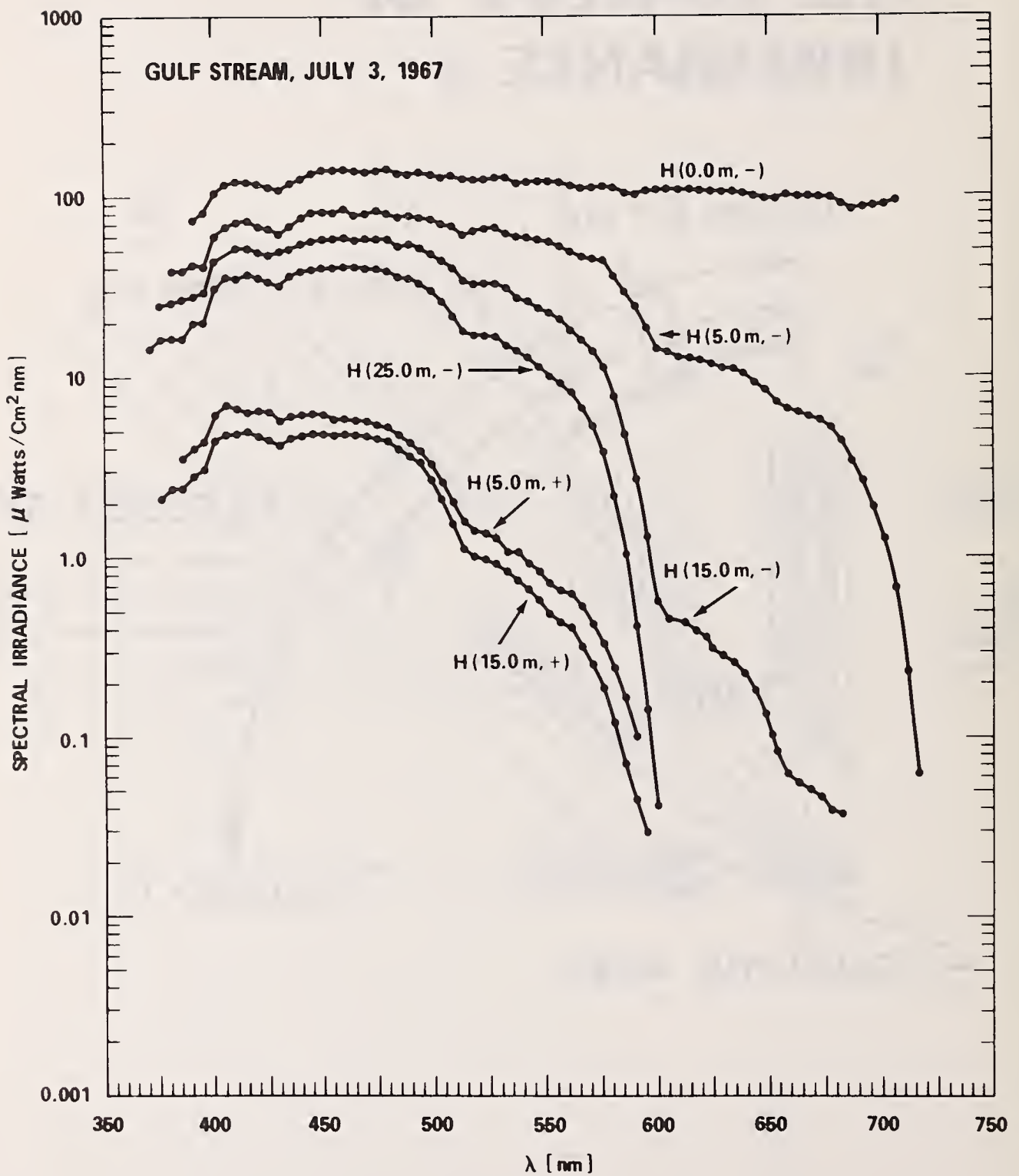


Fig. 10 Irradiance measurements as a function of wavelength in the Gulf Stream.

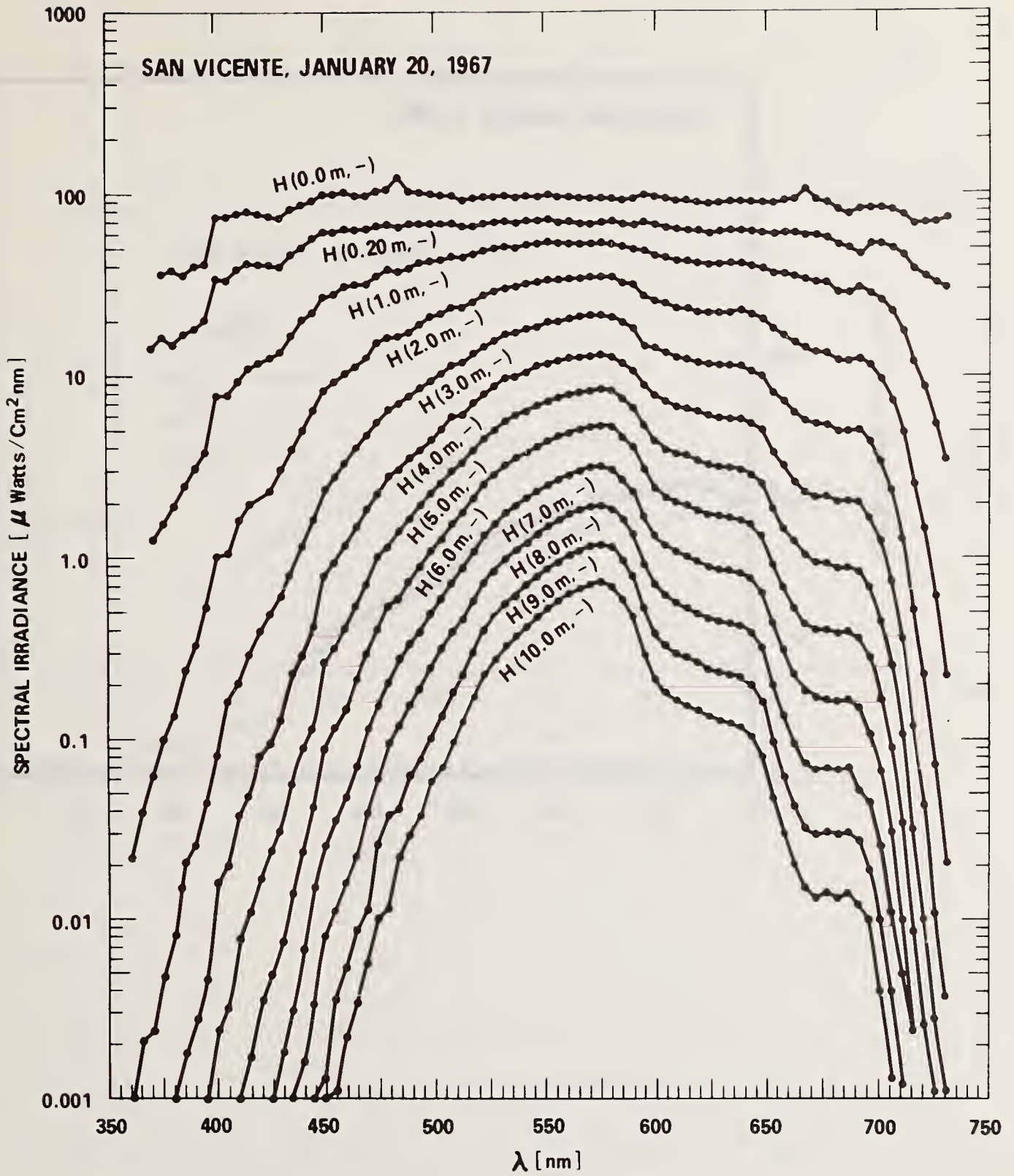


Fig. 11 Irradiance measurements as a function of wavelength in a eutrophic lake.

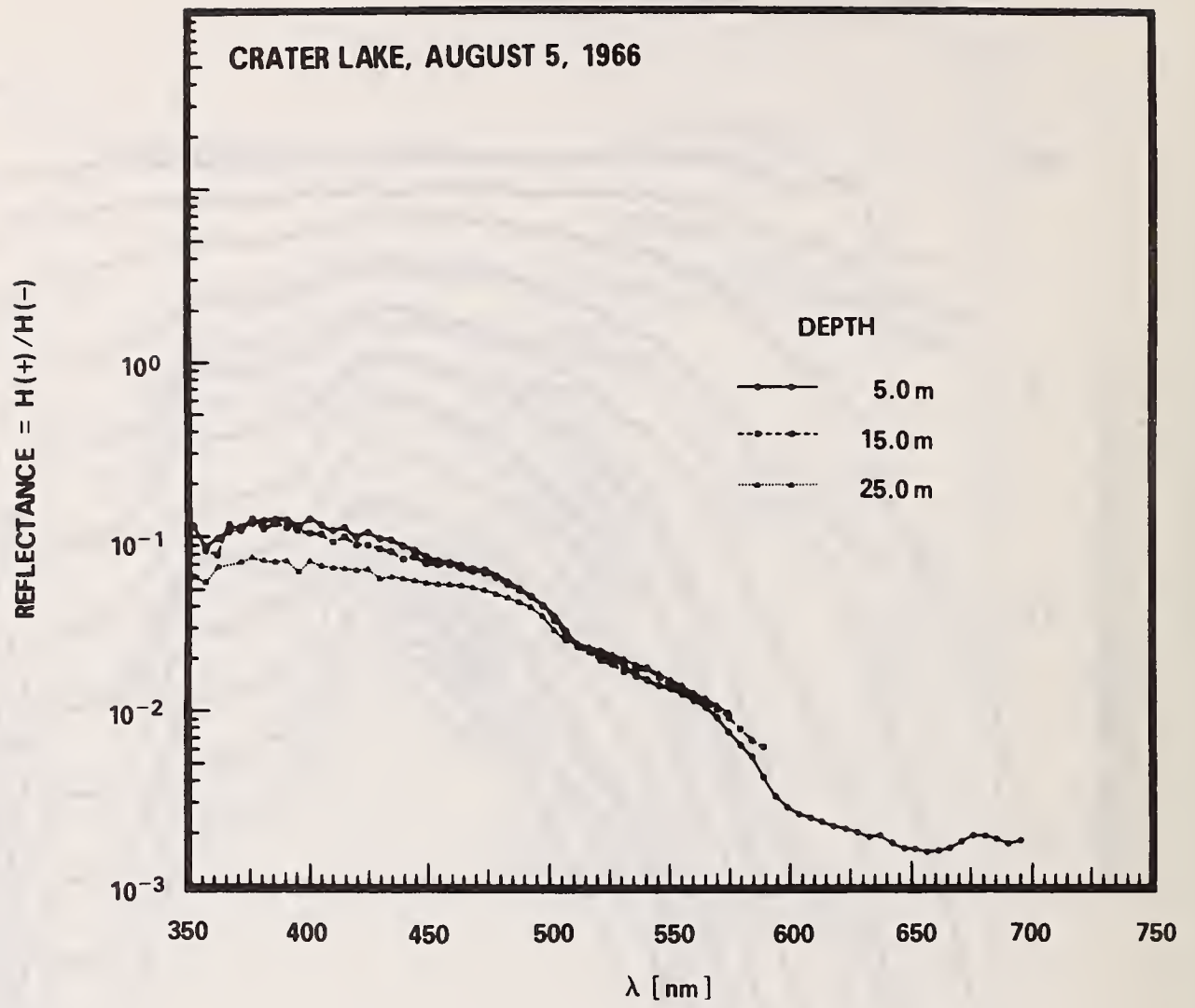


Fig. 12 Reflectance data obtained in Crater Lake, Oregon.

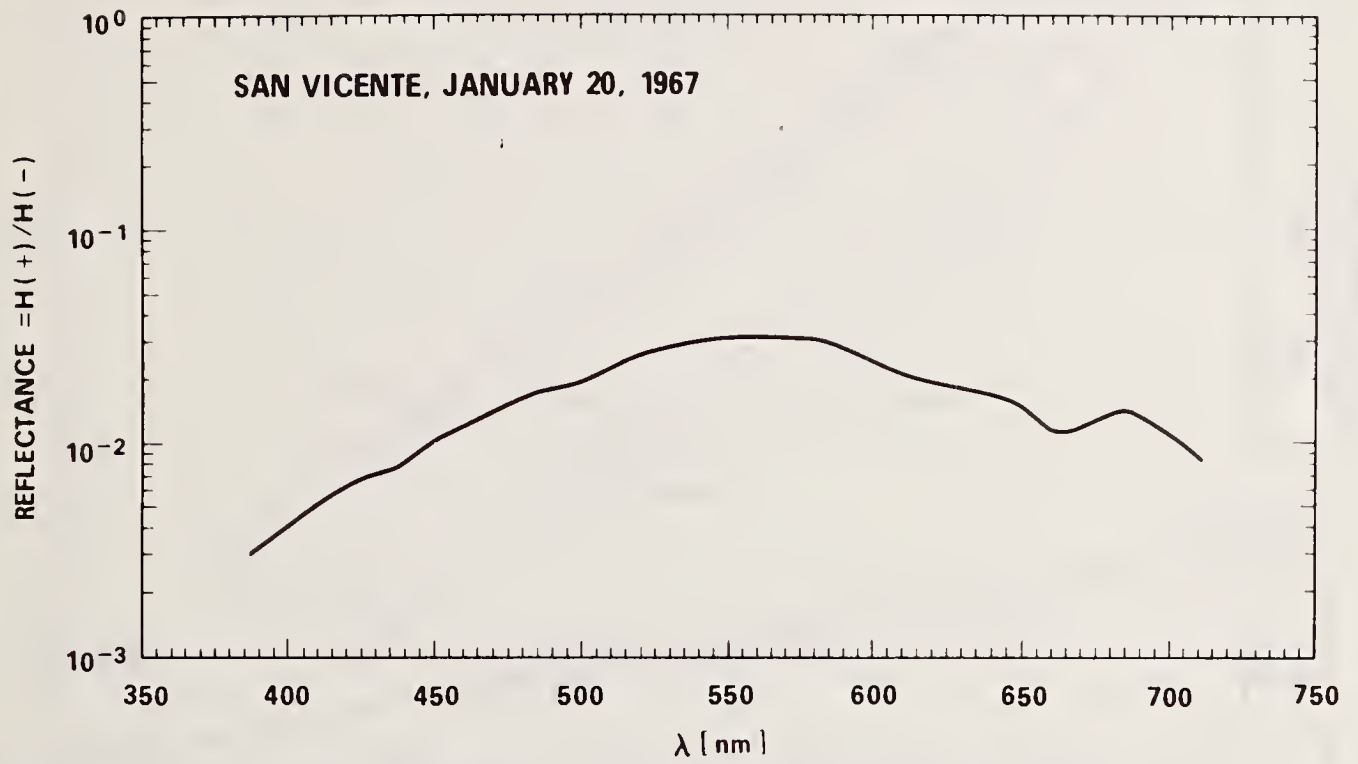


Fig. 13 Reflectance data obtained in a eutrophic lake.

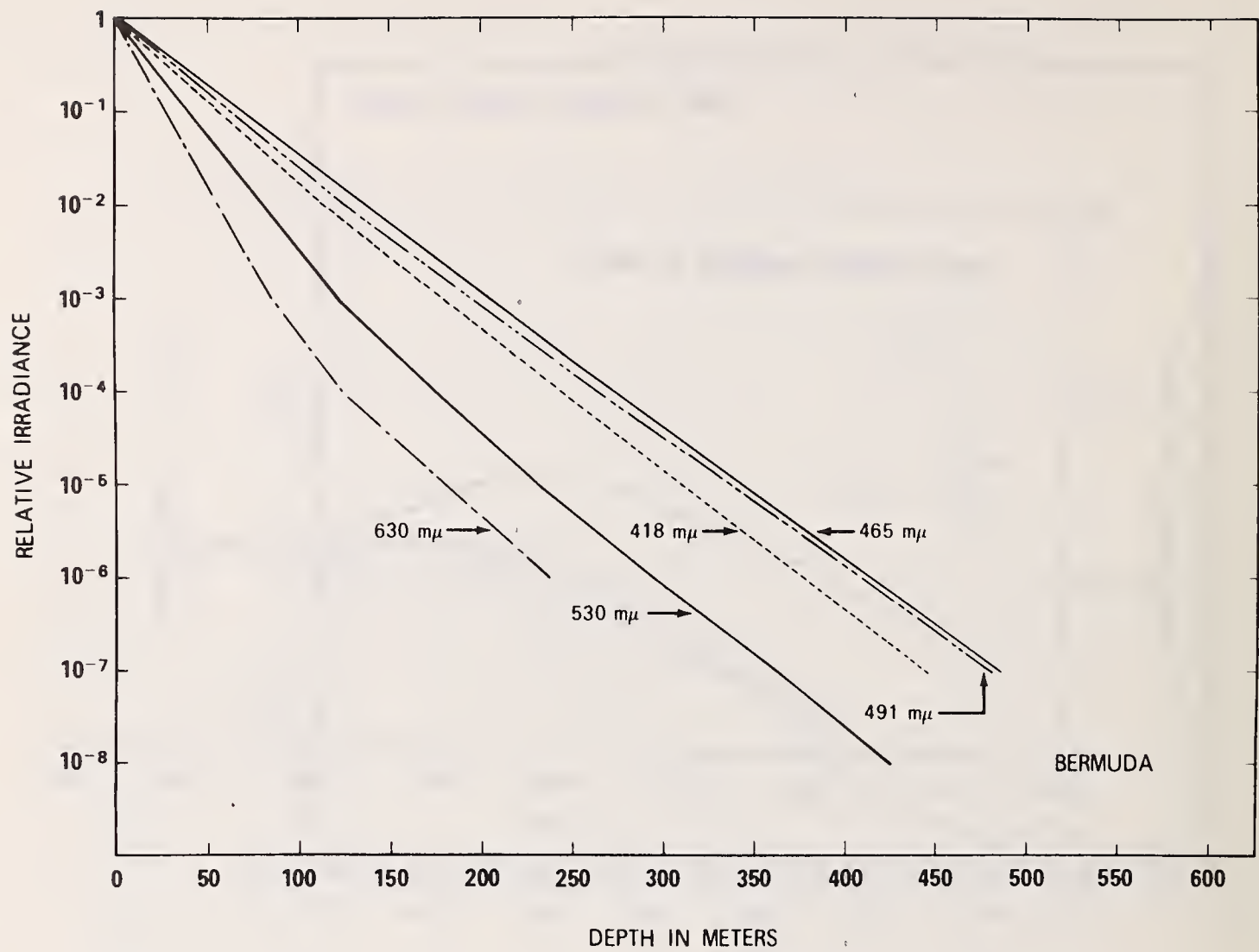


Fig. 14 Attenuation of irradiance with depth for 5 wavelengths in clear ocean water.

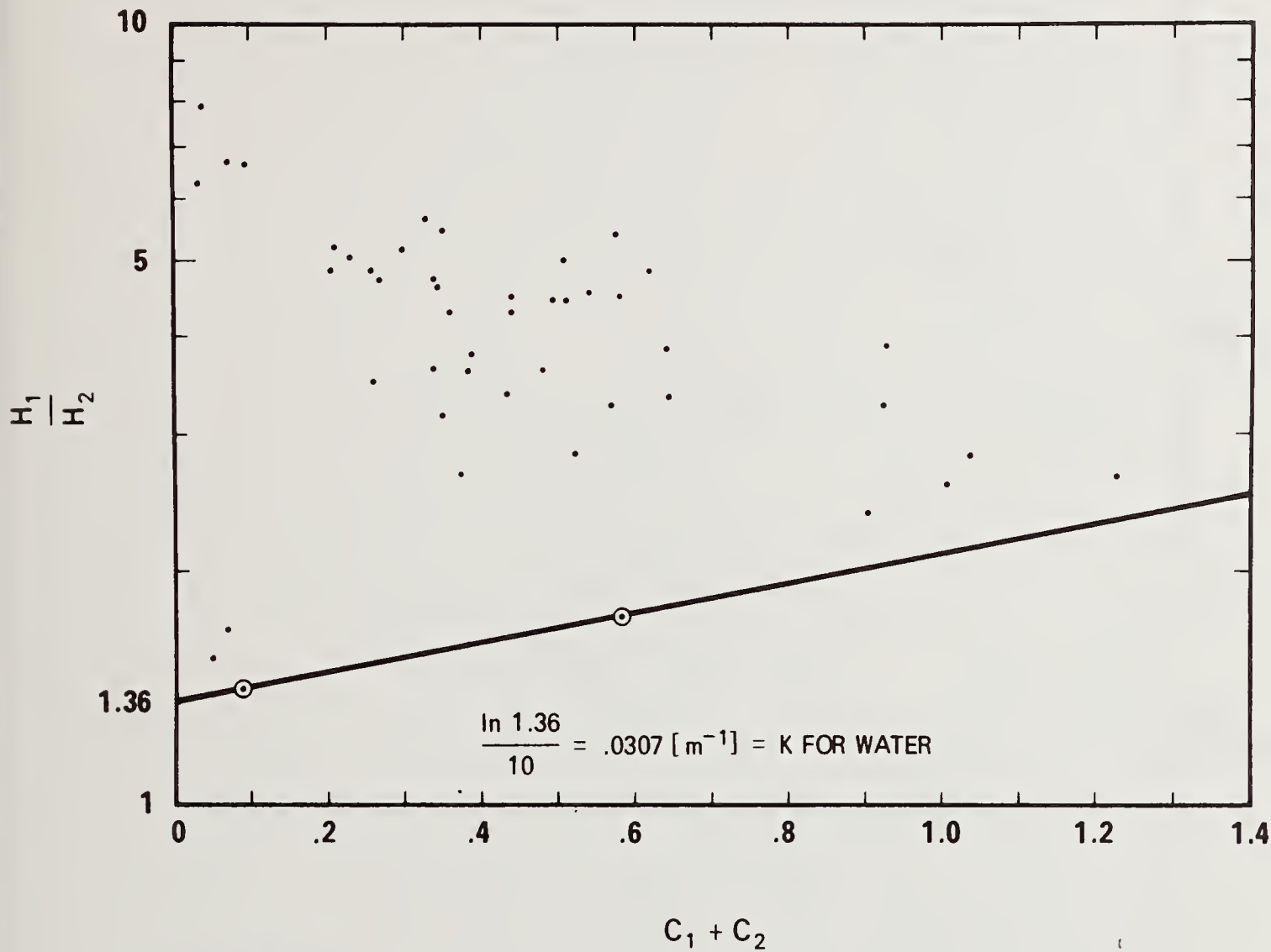


Fig. 15 Plot of optical density of 10-meter layers of ocean water vs the combined concentrations of viable phytoplankton pigments and phaeopigments.

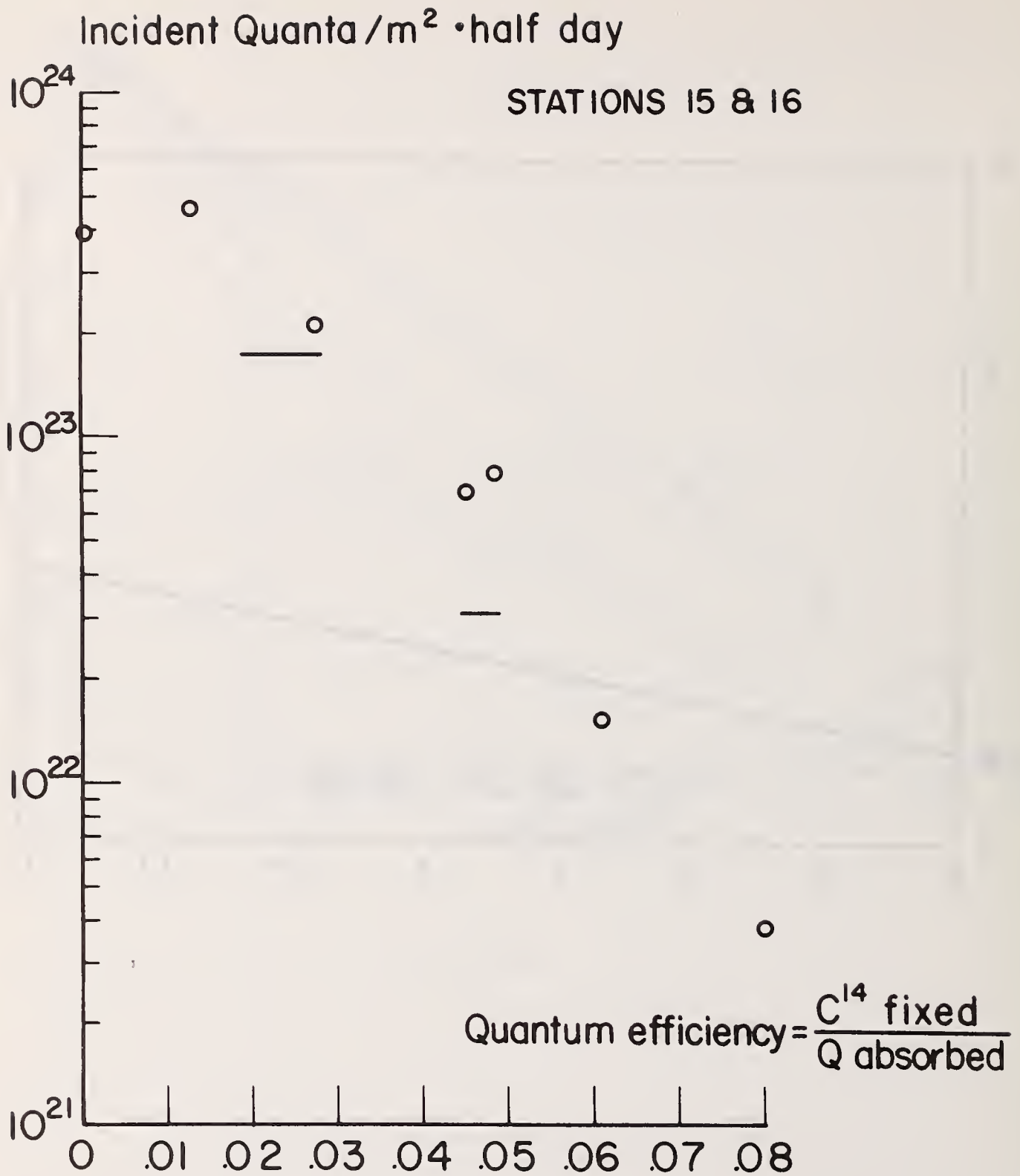


Fig. 16 Plot of the quantum efficiency of photosynthesis in the ocean vs the incident irradiance, the latter determined by the depth of the phytoplankton.

notes

PREDICTION OF ACTIVITIES OF ELECTROLYTES IN NATURAL WATERS

Robert Wood
Department of Chemistry and School of Marine Studies
University of Delaware
Newark, Delaware 19711

The earliest and simplest ways of predicting the properties of mixtures of electrolytes were developed by MacInnes (1919), Harned (1920), and Lewis and Randall (1921). They developed the ionic strength principle which says that the activity coefficient of an ion is a function only of the ionic strength and the mean salt method, which says that the activity coefficient of potassium is the same as that of chloride in KCl. These two approximations are still used in most of the calculations of the speciation of natural waters. Later the Debye-Hückel limiting law (1923) gave the theoretical basis for predicting very dilute solutions. A better method of predicting mixtures was developed by Brønsted (1923), and Guggenheim (1935) who combined the Debye-Hückel limiting law with the assumption that positive ions had uniform interactions with each other. In 1953 T. F. Young and M. B. Smith showed that the ionic strength principle could be improved by applying it to the total solution rather than to partial molal properties. Young's rule states that the change in volume on mixing two components at the same ionic strength is zero. This rule can equally well be applied to heats and free energies and it is far superior to the ionic strength principle. Scatchard (1932, 1961) added triplets and higher terms to the basic assumptions of Brønsted and Guggenheim. Wood and Smith (1965) showed that the interactions of two like charged ions were not uniform and had to be taken into account for accurate calculations. From a knowledge of the important interactions, equations were developed for predicting the properties of charge symmetric mixtures (Wood and Anderson (1966), and Guggenheim (1966)). The way in which these equations were developed shows that they are essentially Young's rule applied to an appropriate set of components of the mixture together with corrections for the like-charged pair interactions and some of the triplet interactions. Following this several different methods were developed for extending the calculations to charge asymmetric mixtures. Reilly and Wood (1969), Scatchard, Rush, and Johnson (1970), Reilly, Wood, Robinson (1971) and Pitzer (1973). These equations are capable of giving accurate estimations of the activity coefficients of mixtures of strong electrolytes even at ionic strengths above 1 molal. Thus they should give accurate predictions of seawater and all natural waters except the very concentrated brines. The success of Reilly, Wood and Robinson equations in predicting the activities of the major components of seawater with as much accuracy as they have been measured is demonstrated.

The equations do not work for mixtures in which the components have strong association and this is the area where current developments are needed. It should prove possible to combine the methods developed for mixtures of strong electrolytes with the normal ion-pairing approach to produce a set of more accurate equations. The possibilities and pitfalls in this procedure are discussed. Another important area for future work is in the development of methods of making measurements of the activities of trace components so that the speciation models being developed can be tested.

U.S. DEPT. OF COMM. BIBLIOGRAPHIC DATA SHEET	1. PUBLICATION OR REPORT NO. NBSIR 76-1130	2. Gov't Accession No.	3. Recipient's Accession No.
4. TITLE AND SUBTITLE PROGRAM & ABSTRACTS, Symposium on Nonbiological Transport and Transformation of Pollutants on Land and in Water: Processes and critical data required for predictive description. May 11-13, 1976		5. Publication Date May 1976	6. Performing Organization Code 151.00
7. AUTHOR(S) L. H. Gevantman, Editor		8. Performing Organ. Report No.	
9. PERFORMING ORGANIZATION NAME AND ADDRESS NATIONAL BUREAU OF STANDARDS DEPARTMENT OF COMMERCE WASHINGTON, D.C. 20234		10. Project/Task/Work Unit No. 1510431	11. Contract/Grant No.
12. Sponsoring Organization Name and Complete Address (Street, City, State, ZIP) National Bureau of Standards, US Department of Commerce Washington, D. C. 20234 Also Environmental Protection Agency, National Science Foundation, Environmental Research & Development Administration		13. Type of Report & Period Covered	
15. SUPPLEMENTARY NOTES		14. Sponsoring Agency Code	
16. ABSTRACT (A 200-word or less factual summary of most significant information. If document includes a significant bibliography or literature survey, mention it here.) Program, abstracts and extended abstracts of 21 papers presented at a symposium on nonbiological transport and transformation of pollutants on land and in water are documented. Most of the extended abstracts are detailed and contain figures and references to pertinent literature on the subject matter discussed at the symposium. The subject matter reviewed deals with the physical and chemical behavior of pollutants including pollutant photochemistry, adsorptive behavior of pollutants, hydrolysis, rates of pollutants, and mathematical models for documenting pollutant behavior in soils and water.			
17. KEY WORDS (six to twelve entries; alphabetical order; capitalize only the first letter of the first key word unless a proper name; separated by semicolons) Adsorption; nonbiological transformation; nonbiological transport; pollutant photochemistry; pollutants; soil pollution; solar spectrum; water pollution.			
18. AVAILABILITY <input type="checkbox"/> Unlimited <input type="checkbox"/> For Official Distribution. Do Not Release to NTIS <input type="checkbox"/> Order From Sup. of Doc., U.S. Government Printing Office Washington, D.C. 20402, SD Cat. No. C13 <input checked="" type="checkbox"/> Order From National Technical Information Service (NTIS) Springfield, Virginia 22151	19. SECURITY CLASS (THIS REPORT) UNCLASSIFIED	21. NO. OF PAGES 177	
20. SECURITY CLASS (THIS PAGE) UNCLASSIFIED		22. Price	

ACKNOWLEDGMENT

The cooperation of the sponsoring agencies is hereby acknowledged. We are grateful to members of the EPA's Environmental Research Laboratory - Athens for their aid in helping organize this Symposium. Special thanks go to Mrs. M. Schlager and the NBS staff for their unflagging efforts in making this meeting a success.

*L. H. Gevantman, Co-Chairman
National Bureau of Standards
Department of Commerce*

*R. G. Zepp, Co-Chairman
Environmental Research Laboratory - Athens
Environmental Protection Agency*

NBSIR 76-1131

A Model Performance Standard for Guardrails

S. G. Fattal, L. E. Cattaneo,
G. E. Turner, and S. N. Robinson

Center for Building Technology
Institute for Applied Technology
National Bureau of Standards
Washington, D. C. 20234

July, 1976

Final Report

“This report is to be incorporated as an appendix in a future publication which will receive general distribution. Please consult the National Bureau of Standards Office of Technical Publications to obtain the proper citation.”

Prepared for
Occupational Safety and Health Administration
Department of Labor
Washington, D. C. 20210

NBSIR 76-1131

A MODEL PERFORMANCE STANDARD FOR GUARDRAILS

S. G. Fattal, L. E. Cattaneo,
G. E. Turner, and S. N. Robinson

Center for Building Technology
Institute for Applied Technology
National Bureau of Standards
Washington, D. C. 20234

July, 1976

Final Report

"This report is to be incorporated as an appendix in a future publication which will receive general distribution. Please consult the National Bureau of Standards Office of Technical Publications to obtain the proper citation."

Prepared for
Occupational Safety and Health Administration
Department of Labor
Washington, D. C. 20210



U.S. DEPARTMENT OF COMMERCE, Elliot L. Richardson, *Secretary*

Edward O. Vetter, *Under Secretary*

Dr. Betsy Ancker-Johnson, *Assistant Secretary for Science and Technology*

NATIONAL BUREAU OF STANDARDS, Ernest Ambler, *Acting Director*

Table of Contents

	<u>Page</u>
Abstract	ii
A.1 Introduction	1
A.2 Structural Safety.	3
A.2.1 Basic Loads.	3
A.2.2 Design Loads	6
A.2.3 Structural Resistance.	8
A.2.4 Foundations	12
A.2.5 Displacement Control	13
A.2.6 Durability and Maintenance	13
A.3 Non-structural Safety.	14
A.3.1 Height of Guardrail.	14
A.3.2 Height in Relation to Width.	16
A.3.3 Size of Openings	17
A.3.4 Passage of Objects Near Floor.	18
A.3.5 Smoothness of Surfaces	18
A.3.6 Projecting Components.	19
A.3.7 Visibility	19
A.3.8 Warning Signs.	20
A.4 Definitions.	21
A.5 References	22
B.1 Examples of Standard Guardrail Designs	23

A MODEL PERFORMANCE STANDARD FOR GUARDRAILS

S. G. Fattal, L. E. Cattaneo
G. E. Turner and S. N. Robinson

Abstract

A model performance standard and design illustrations are presented for the design, construction and evaluation of guardrail systems, which will be used for the protection of employees against occupational hazards. The standard stipulates both structural and non-structural safety requirements. Each criterion includes a commentary section describing the rationale used in its formulation. This rationale is for the most part, based on independent experimental and analytical research investigations conducted at NBS in behalf of OSHA.

Key Words: Design; dynamic loads; guardrails; industrial accidents; non-structural safety; occupational hazards; performance standard; personnel railings; personnel safety; static loads; stiffness; structural safety.

Acknowledgement

The contributions made by Drs. Robert A. Crist and Bruce R. Ellingwood in critically reviewing this Standard are gratefully acknowledged.

A Model Performance Standard
for Guardrails

A.1 Introduction

This Standard documents recommendations for the design, construction and evaluation of guardrail systems which are installed for the purpose of protecting employees from occupational hazards during the conduct of their assigned tasks. The document makes no recommendations as to where or whether guardrails will be required, and is not applicable to situations where the guardrail may be exposed to forces resulting from the impact of power-driven objects or from flagrant abuse.

For the most part, these recommendations draw upon the results of tests and analytical investigations conducted at the National Bureau of Standards (NBS) in behalf of the Occupational Safety and Health Administration (OSHA) and documented in detail in a separate report.* Where a specific recommendation is based on studies conducted elsewhere, the standard identifies the appropriate source in the bibliography** in Section A.5.

The performance approach usually permits the definition of a particular performance attribute without reference to the type of material or construction scheme employed. It is generally less restrictive than materials-oriented prescriptive standards with regard to the utilization of innovative products and design concepts. The terms "conventional" and "non-conventional" have been introduced to distinguish, when necessary, between traditional and innovative applications. Conventional systems or components are built with traditional construction materials (such as steel, aluminum, concrete, masonry and timber), which are deployed in the system in a manner that will constitute a conventional design and construction concept or application. Non-conventional systems or components consist of relatively untried materials or any other materials which are utilized in a manner that would constitute an innovative construction or design concept.

Unless otherwise noted, these recommendations apply to both conventional and non-conventional systems. Conventional systems should, in addition, comply with the appropriate design and construction requirements of the six nationally recognized standards [A.3 - A.8] adopted herein by reference. These standards were judged to have adequate provisions to permit the design of conventional guardrails without the need to prescribe supplementary requirements.

*This report to be entitled "Investigation of Guardrails for the Protection of Employees from Occupational Hazards," by S. G. Fattal, and L. E. Cattaneo, is (as of July 1976) in the final stages of preparation.

**References are indicated by numbers in brackets.

A guardrail system is defined herein as a structural system which is designed and installed in a manner that will inhibit accidental passage of people or objects between the two adjoining regions it separates in the interest of improving the safety of the environment. Guardrails are distinguished from handrails in that handrails are normally installed for the purpose of assisting people in maintaining balance while in the act of walking, climbing and descending stairs, etc. However, in situations where handrails serve the function of guardrails, such as when located along the precipitous edge of a stairway or around elevated landings, they should be designed as guardrails. This Standard includes provisions for the design of guardrails which are specifically called upon to support people or objects during the conduct of an activity. Additional design load requirements are specified for guardrails installed at or near areas where congested peak loading conditions are likely to be encountered in service.

Guardrail systems consist of elements, connections and anchorages. They encompass both temporary and permanent installation. Temporary guardrail systems are used in construction work. Permanent guardrail systems constitute a permanent part of a structure in service. Unless stated otherwise, the provisions of this standard apply to temporary as well as permanent guardrails.

The organization of this document is modeled after a fixed format consisting of Requirement, Criterion, Evaluation and Commentary ranked in that order. The Requirement is a qualitative statement of an expected performance attribute. It is a general statement of what the assembly should be able to do. The Criterion is a quantitative statement giving the level of performance necessary to meet the Requirement. In some cases, several Criteria are associated with each requirement. Evaluation sets forth the method(s) upon which an evaluative judgment of compliance with a Criterion can be based. It states the standards, contract documents, inspection methods, analysis and review procedures, or test methods which may be used in determining whether the system or system components comply with the Criterion. The Commentary provides background information for the reader and presents the rationale behind the Requirement, Criterion and Evaluation.

The Criteria in this standard are identified with one of two categories, namely, structural and non-structural. The structural Criteria specify the types of loads and load combinations to be considered in design, and resistance requirements with regard to strength, safety margins, stiffness properties and deformation tolerances in service. The non-structural Criteria pertain to the geometric configuration of guardrails as governed by the topography and physical characteristics of the surrounding environment and the relationships between perceptual and environmental factors.

A.2 Requirement - Structural safety

Guardrails and all components thereof shall be designed and constructed to support safely all loads anticipated in service.

A.2.1 Criterion - Basic loads

Design loads shall be derived from the following basic loads and their combinations:

- (a) Dead load (D) shall consist of the actual weight of the materials incorporated in the construction and the weight of any appendage or attachment which becomes a permanent part of the guardrail system in service.
- (b) Accidental load (A) shall consist of a concentrated force of 300 lb (1.335 kN) for tributary areas 36 in (91.5 cm) or greater in width, and 200 lb (0.890 kN) for tributary areas 24 in (61 cm) or less in width. For tributary areas between 24 in (61 cm) and 36 in (91.5 cm) in width, the concentrated force shall be determined by linear interpolation.

When combined with other basic loads in accordance with Criterion A.2.2, the point of application and direction of accidental load (A) shall be so determined as to produce the most critical configuration(s) for design.

For calculating local effects, the concentrated force representing accidental load (A) may be uniformly distributed over a 4-in (10.2-cm) length of a beam element or over a 16-in² (103 2-cm²) square area of a plate element.

- (c) Surge load (S) shall consist of a uniformly distributed of 100 lb/ft (1.46 kN/m) applicable to the top of the guardrail at any inclination between and including horizontal and vertical, subject to the following constraints:
- (d) Live load (L) shall consist of any load for which the guardrail is anticipated to provide the means of structural support in service other than dead, accidental or surge load.

A.2.1.1 Evaluation

This Criterion will be evaluated by review of the contract documents (plans, specifications and structural calculations). The width of the tributary area will be measured horizontally as illustrated in figure A.2.

A.2.1.2 Commentary

This Criterion defines the nature and intensity of basic load types, combinations of which are specified for design. It is not the intent of this Criterion to include provisions for abnormal loads or loads resulting from flagrant abuse. Abnormal loads may be attributable to a rare but extreme event such as an explosion or impact by power-driven objects, while deliberate acts such as climbing or bouncing against the guardrail are construed as instances of flagrant abuse.

Unlike larger structures, the weight of the materials comprising the guardrail system will probably be small enough to be negligible in design. However, in some instances it could conceivably increase the calculated stresses by 10 per cent or more and the inclusion of dead load (D) in this Criterion is intended to serve as a reminder that it should not be routinely ignored or overlooked in design. Dead load should include the weight of any object which will become a permanent part of the guardrail in service. The weight of any temporary attachment should be treated as part of the live load (L).

Accidental load (A) represents a force transmitted by the accidental impact of human subjects or objects against guardrails. The 300-lb (1.335-kN) intensity is derived from the results of dynamic load tests using anthropomorphic dummies falling backward against an instrumented mock-up rail from a standing position. The height of the rail and the initial distance of the dummy from it were varied during the tests to measure the influence of these parameters on the magnitude of the impact load. It was observed, for instance, that the maximum load on the midrail was not substantially different from that obtained from top rail tests. This partly explains the rationale for prescribing the same concentrated load at locations other than the top of the guardrail as well. In addition, the Criterion recognizes the need to provide a minimum level of structural resistance against loads resulting from the accidental impact of rolling or sliding objects, or any

equipment other than power-driven objects which may accidentally come in contact with the guardrail. It has been implicitly assumed that the magnitude of such loads would not be appreciably greater than those transmitted by accidental falls of human subjects.

The gradual reduction of the 300-lb (1335-N) force to 200 lb (890N) with the width of the tributary area varying from 36 in (91.5 cm) to 24 in (61 cm) is consistent with the experimentally observed force reduction for falls from an initial heel distance less than 30 in (76.2 cm). In this regard it is assumed that for a given width of tributary area, the maximum possible distance from which the subject can fall on the rail is about 6 in (15.3 cm) less than the width of that area.

No constraints are placed as to the direction of load (A) other than those which can be definitely eliminated by virtue of special characteristics of the environment. For instance, a guardrail without openings, installed to prevent accidental movement from area one into area two, will be subjected to accidental loads from one side only. Where guardrail openings are large enough to permit accidental wedging of humans or objects, forces of unknown intensity will be induced, and thus prudent design practice would select components to have a minimum level of resistance (usually 40 percent of maximum design resistance) in the weakest plane.

Provision A.2.1 (b) makes an allowance for the capacity of the human body to distribute the impact force over a finite length or area which, according to test observations, generally exceeds the specified values when the impact force is in the neighborhood of 300 lb (1.335 kN) or greater. This information is utilized in design to check sectional adequacy (i.e., shear crippling, bearing capacity, local stability etc.) in the vicinity of the applied force.

The provision for surge load (S) recognizes the need to mitigate structural failures under the action of a group of people pushing against the guardrail. Conditions for surge loading could develop as a result of a large number of people simultaneously seeking passage through an exitway or gangway. The 100-lb/ft (1.46-kN/m) uniform load intensity is based on experiments involving measurements of loads transmitted by a group of human subjects, three deep, pushing against an instrumented mock-up guardrail. The mean weight of the subjects selected for this experiment was approximately representative of the weight of the 50 percentile adult male population of the United States.

Live load (L) accounts for a wide variety of imposed loads which the guardrail may be called upon to resist during its service life other than those resulting from surge (S) or accidental impact (A). It is neither feasible nor necessary to identify precisely all the possible loads belonging to this category within the scope of this Criterion. It is possible, however, to identify a given live load with one of two categories: The first category

includes all live loads associated with a specific use or activity for which the guardrail must provide structural support in service. In some cases, the intended structural function of the guardrail includes providing the means of support for workers and/or equipment during the routine conduct of work-related tasks. Specific instances are guardrails used as a bench, or as a lifeline, or for the support of workers and equipment in a tree-spraying operation. The second category includes all live loads which might be anticipated to occur in service as a result of human-environmental factors (other than flagrant abuse) which may generally be construed as guardrail misuse. The source of such imposed loads may not be readily obvious at the design stage. For instance, a guardrail may be exposed to a crowd leaning over it to watch an interesting event several stories below, or it may receive loads from people sitting on a nearby bench and leaning on it. Likewise, a midrail may invite several people to prop a foot or sit on it. Nevertheless, in most instances it is possible for the designer to identify the nature of such imposed loads through consideration of the relevant human and environmental factors inherent to the specific installation. Guidance on the intensities of certain types of imposed loads may be obtained from the experimental results presented in the NBS report to OSHA.*

This Criterion does not advocate the explicit treatment of wind load as a basic load in guardrail design for a number of reasons. It is noted that both accidental load (A) and surge load (S) are peak loads of very short duration and are not likely to occur frequently in service. The probability of wind occurring at the same time and acting in the same direction as one of these loads is so low that it may be disregarded justifiably in design. Furthermore, the combination of wind and dead load alone is not likely to be more critical than the design loads prescribed in Criterion A.2.2, nor are the potential consequences of failure (i.e., risk of injury to workers) under such a combination likely to be as severe as those resulting from failures under the design loads specified by Criterion A.2.2. Nonetheless, it is not the intent of this Criterion to rule out consideration of wind effects in design under unusual circumstances. To cite an example, it is conceivable that a group of people leaning over a guardrail at the edge of an elevated exterior platform may experience and transmit significant wind forces to the guardrail. Such wind-induced forces can be given consideration in design by treating them as part of the basic live load (L) defined in this Criterion. The designer may use engineering judgment to select wind pressures consistent with the type and duration of the anticipated live load. Usually checking for wind in regions experiencing 10-psf (479-N/m^2) or greater wind pressure is a good engineering design practice. In most instances, the wind load provisions of ANSI A58.1[A.1] used in conjunction with the 2-year wind map in reference [A.2] would probably be adequate.

A.2.2 Criterion - Design loads

The following basic load combinations shall be considered in the analysis and design of guardrail systems. These basic loads shall exclude all loads resulting from power-driven objects or from flagrant abuse.

*See footnote on page 1.

- (a) All guardrails shall be designed for load combination U defined by the following relationship:

$$U = c_1 D + c_2 A$$

where D and A are basic loads defined under Criterion A.2.1 and the subscripted letters are load factors specified as follows:

- (1) For conventional systems designed in accordance with the working stress (or allowable stress) concept, $c_1 = c_2 = 1.0$.
 - (2) For conventional systems designed in accordance with the ultimate strength concept, c_1 and c_2 shall be the load factors specified by the applicable code or standard for the load combination U herein defined. The applicable codes and standards are specified in Criterion A.2.3 (a).
 - (3) For non-conventional systems, $c_1 = 1.4$, $c_2 = 1.7$.
- (b) Guardrails installed at or near exitways serving the function of providing the safe and only means of discharge or egress of a tributary population equal to or in excess of 50 persons, shall be designed for the following load combination.

$$U = c_1 D + c_2 S$$

where D and S are basic loads defined under Criterion A.2.1 and load factors c_1 and c_2 are as specified in Criterion A.2.2(a).

- (c) Guardrails used as the means of support of workers and/or objects during the conduct of a work task or any other activity not construed as flagrant abuse shall be designed for the following load combination

$$U = c_1 D + c_2 L$$

where D and L are basic loads defined in Criterion A.2.1 and load factors c_1 and c_2 are as specified in Criterion A.2.2(a). Live load L need not include loads resulting from misuse if the guardrail is designed to meet Criterion A.3.7.

A.2.2.1 Evaluation

This Criterion will be evaluated by examination and review of the contract documents.

A.2.2.2 Commentary

Criterion A.2.2 states design load requirements for guardrails. Requirement A.2.2(a) applies to the design of all guardrails while requirements A.2.2(b) and A.2.2(c) apply to guardrails subjected to surge and live loads, respectively.

Most guardrails will probably need only be designed for load combination A.2.2(a). In the interest of clarity, it should be noted that guardrails required to be designed for more than one loading combination should simultaneously satisfy the design requirements for each loading combination applied independently.

For conventional systems, load factors, c_1 and c_2 are introduced to arrive at design loads which would be consistent with the design approach used by the applicable code or standard. For instance, components designed in accordance with the allowable stress approach would be proportioned to resist the applicable design load of Criterion A.2.2, with the load factors equal to unity, without developing a maximum stress in excess of the allowable stress prescribed by the governing code or standard. On the other hand, a reinforced concrete element which is designed according to the ultimate strength approach prescribed by the ACI Code [A.5] would be proportioned to have a load-carrying capacity (specified by that Code) equal to or greater than the factored total load on the element specified in Criterion A.2.2, with the load factors $c_1 = 1.4$ and $c_2 = 1.7$ (also specified by that Code).

The Criterion requires that all non-conventional systems be designed by the ultimate strength concept. Accordingly, A.2.2(a)(3) prescribes the magnitudes of the load factors to be used in design. The specified dead and live load factors are consistent with those used in conventional design.

It should be noted that Criterion A.2.2(c) does not require consideration of loads resulting from misuse as part of live load(L) if criterion A.3.7 is complied with.

A.2.3 Criterion - Structural resistance

The design load resistance R of the system or any components thereof shall exceed the appropriate design load stipulated in Criterion A.2.2, or

$$R > U$$

where U is the design load specified by Criterion A.2.2.

(a) For conventional guardrail systems, the design load resistance R shall be determined in accordance with the applicable provisions of the latest editions of the following codes and standards:

- (1) Steel: Manual of Steel Construction, American Institute of Steel Construction [A.3].

- (2) Aluminum: Aluminum Construction Manual, Specifications for Aluminum Structures. the Aluminum Association [A.4].
- (3) Concrete: ACI Standard 318-71, Building Code Requirements for Reinforced Concrete, American Concrete Institute [A.5].
- (4) Masonry: Building Code Requirements for Masonry, ANSI A41.1 [A.6] and Building Code Requirements for Reinforced Masonry, ANSI A41.2 [A.7].
- (5) Lumber: National Design Specification for Stress-Grade Lumber and Its Fastenings, National Forest Products Association [A.8].

(b) For non-conventional guardrail systems, the design load resistance R shall be derived from the mean load capacity R_m as follows:

$$R = fR_m c_u$$

where:

f = variability factor which should be such that approximately 95 percent of the system as a whole, or any component thereof, shall exceed fR_m in resistance. If this resistance has a normal probability distribution, $f = 1-1.65v$.

v = coefficient of variation of resistance with respect to R_m .

c_u = coefficient for ductility = $(u + 7)/12$, but not more than 1.0

u = minimum ductility factor under the appropriate design loading condition U defined in Criterion A.2.2.

A.2.3.1 Evaluation

For conventional systems, design compliance will be evaluated by review of contract documents. Construction compliance will be evaluated by field inspection and comparison of construction with the plans and specifications of the contract documents.

When adequate existing test data on the various material properties comprising the non-conventional system and system components are available, evaluation shall be performed using engineering analysis. When adequate test data is unavailable, system components and subsystems shall be evaluated in the laboratory using simulated static load levels consistent with the load combinations specified in Criterion A.2.2.

The ductility factor shall be evaluated as follows: For an ideal elastoplastic (elastic-perfectly plastic) resistance function (plot of applied load as ordinate and deflection as abscissa), the ductility factor is defined as the ratio of ultimate deflection to yield deflection ($u = d_u / d_{ye}$). For a linear resistance function to failure (brittle behavior), the ductility factor is 1.0. For an actual (nonlinear) load-deflection function,

the ductility factor shall be computed from an "effective" function consisting of two straight lines (Figure A.1). The first line is drawn through the origin and a point on the actual function at which the resistance is 60 percent of its maximum load value (P_u). The second line is a horizontal line ending at the ultimate deflection (d_u), which is the abscissa of a point on the descending portion of the resistance function with the corresponding ordinate equal to 95 percent of the maximum load value. The horizontal line is located so that the area under the two lines forming the effective function is equal to the area under the actual function up to the point of ultimate deflection. Effective yield deflection (d_{ye}) is taken as the deflection at the point of intersection of the two lines, which is at a resistance level termed "effective yield resistance." The ductility factor is based on the effective resistance function: $u = d_u / d_{ye}$ [A.9].

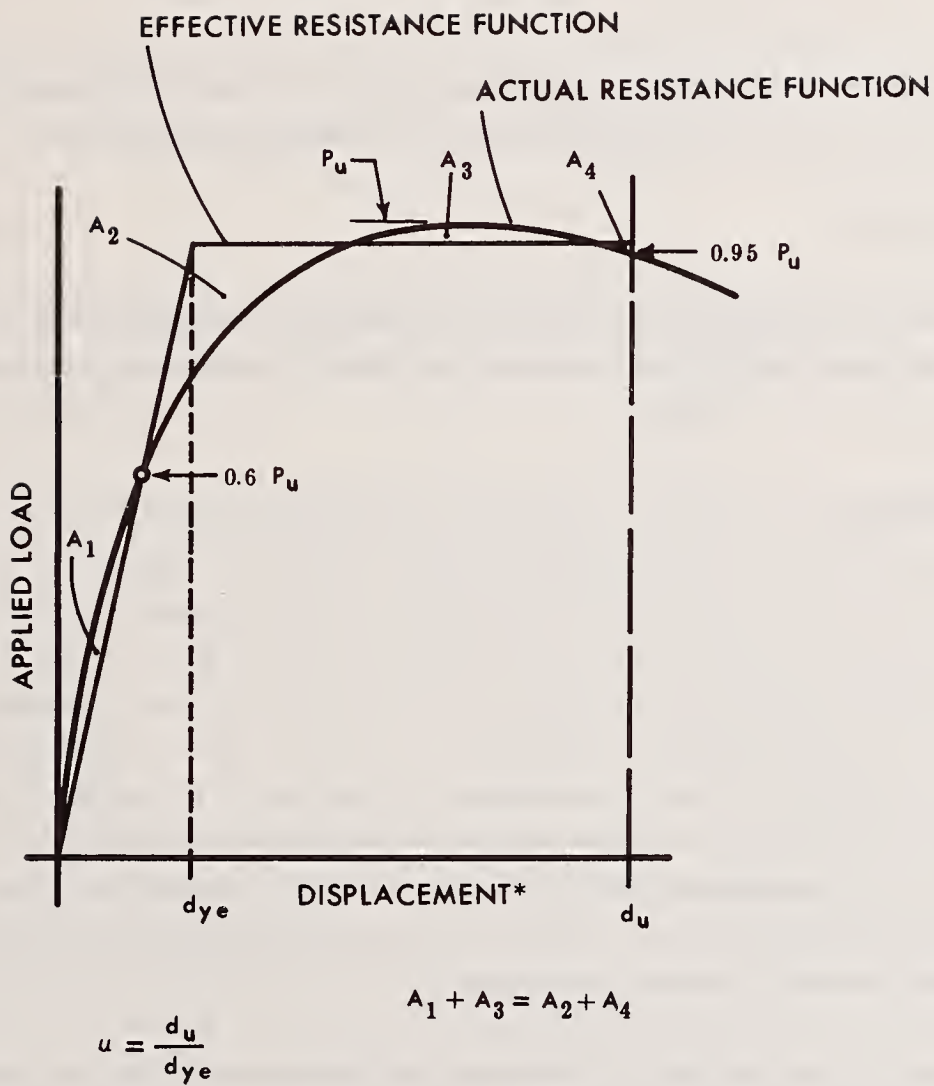
A.2.3.2 Commentary

The intent of Criterion A.2.3(a) is to require, to the extent possible, design and construction compliance with the provisions of nationally recognized codes and standards. Accordingly, Criterion A.2.3(a) gives a specific list of voluntary consensus standards which are judged to be applicable to conventional guardrail systems. The requirements of these standards should be used in conjunction with the design loads stipulated in Criterion A.2.2 and with the provisions of all the other criteria applicable to conventional systems. As a general guide, guardrail systems using structural steel, aluminum, timber, reinforced concrete or masonry do not need overall margins of safety greater than those found in structures designed in accordance with the design standards listed under Criterion A.2.3(a).

The intent of Criterion A.2.3(b), along with Criterion A.2.2, is to provide a minimum level of structural safety against situations which might be anticipated to occur during the service life of the system. The safety margin reflects possible sources of deficiencies such as variations in loading and resistance, as well as assumptions and simplifications made in analysis and design.

The load capacity is reduced from the mean strength value R_m using variability factor f to insure that approximately 95 percent of all systems or components thereof will have at least the required load capacity. The reduction provides for the combined effect of variability in material strength, workmanship, dimensions and quality control.

For relatively untried materials and construction concepts, a reasonable allowance must be made for lack of experience relative to structural response and for variability in material strength. It should be recognized that certain structural materials require a greater margin of safety than others because of either the more critical nature of failure or the greater variability in their strength.



(* Distortional displacement at and in the direction of applied load)

Figure A.1 Determination of the Ductility-Factor

Ductility as well as strength is vital to safety. Adequate ductility allows energy absorption under extreme dynamic or pulse loads, permits redistribution of local concentrations of force from fabrication errors, lack of construction fit or local loadings, and by perceptible inelastic deformations warns users of overloads before load capacity is lost. The coefficient for ductility $c_u = (u + 7)/12$ imposes an extra margin of strength for brittle materials, and becomes 1 at $u = 5$, which is considered representative of ductile structural systems.

A.2.4 Criterion - Foundations

Foundations shall provide the means for attachment of guardrail systems and shall be designed to safely transmit guardrail loads to the supporting structure.

A.2.4.1 Evaluation

The adequacy of the foundation will be determined by inspection and review of contract documents of the supporting structure including details of anchoring devices used for attachment of guardrail to the structure.

A.2.4.2 Commentary

This Criterion provides for the safe support of the guardrail system by the part of the structure to which it is attached. Foundation failures might affect the stability of the entire guardrail system and therefore can be potentially more hazardous in nature than the failure of a single element or connection. A case in point is the premature failures observed in concrete skirts supporting peripheral guardrails at elevated stairway landings attributable to several factors such as insufficient edge distance, shallow embedment of posts and anchors or inadequate reinforcement. The intent of the criterion is to design the supporting foundation to be at least as safe as the guardrail system and thereby reasonably assure against premature failures.

This Criterion also addresses a frequent problem which arises from the inability, on the part of the contractor, to attach guardrails to an otherwise adequate foundation to retrofit sections of a completed structure without exposing his employees to additional risk. This situation is encountered most commonly during the installation of temporary guardrails needed for construction or repair work and there have been instances where the potential risk of accident associated with the erection and removal of such guardrails could not be construed to be less than the risk of accidents attributable to the absence of a guardrail. This criterion therefore stipulates that foundations should be designed and constructed in a manner that would provide a practical and expedient means for the subsequent attachment of guardrails where required by law.

A.2.5 Criterion - Displacement control

Non-conventional systems shall comply with this Criterion. Conventional systems are deemed to satisfy this Criterion.

- (a) With the full dead load 1.0D in place, the maximum displacement of any point on the guardrail due to the applied load of 1.5A sustained for one hour, shall not exceed 4 in (10.16 cm).
- (b) With the full dead load 1.0D in place, the maximum vertical sag of any flexurally non-rigid element as installed shall not exceed 2 in (5.08 cm).

A.2.5.1 Evaluation

Criterion A.2.5 (a) will be evaluated by the physical simulation and laboratory testing of a suitable component or assembly of the system and/or by analysis based on performance data or available test data.

Criterion A.2.5 (b) will be evaluated in the field. The sag is the vertical distance between an imaginary straight line joining the two support points and the lowest point on the element.

A.2.5.2 Commentary

This Criterion introduces displacement limitations deemed necessary to reduce the likelihood of accidental passage of human subject and/or objects over or through the guardrail. Flexible cables such as wire rope will probably need to be maintained under a minimum level of tension in order to comply with Criterion A.2.5 (a). On the other hand, a certain amount of permanent sag may be tolerated in the case of chains which are quite stiff axially once they become taut. It should be noted that any element having the 2-in sag allowed by Criterion A.2.5 (b) will need to have a relatively high axial stiffness in order to meet the displacement limitation of Criterion A.2.5 (a) because the displacement attributable to sag will reduce the permissible displacement due to structural deformation. Additionally, Criterion A.2.5 inhibits the use of non-conventional products exhibiting excessively high creep deformations or low modulus of elasticity which makes them unsuitable for structural applications.

A.2.6 Criterion - Durability and maintenance

- (a) Guardrails exposed to the exterior environment or to chemicals and other corrosive agents and conditions shall be adequately treated to resist the effect of such agents in service.

(b) Guardrails shall be periodically inspected for evidence of excessive wear, damage or understrength. Any element, connection or anchorage exhibiting 20 percent or more degradation in strength and/or stiffness shall be replaced or restored to its initial condition.

A.2.6.1 Evaluation

Durability characteristics and required maintenance will be determined by field inspection and/or testing and engineering analysis. Loss of stiffness can be evaluated in the field by measuring the deflection produced under a given load and comparing it with the deflection of new replicates tested in the laboratory, or, if sufficient test data are available, deflections from field tests may be compared with calculated deflections based on known material properties.

In the absence of an adequate field test method to measure strength degradation, it may be assumed that loss of strength is proportional to loss of stiffness.

A.2.6.2 Commentary

The intent of this Criterion is to insure that a minimum level of structural integrity is maintained during service. In many instances it is possible to identify damage such as dents, cuts, splits, bends, rust, abrasions, etc., by means of visual inspection. Slight shaking of the rail with the hand may reveal slack in the system and help identify loose connections or anchorages.

A.3 Requirement - Non-structural safety

A guardrail system separating two adjoining regions shall prevent and control the accidental passage of workers and objects from one region into the other.

A.3.1 Criterion - Height of guardrail

Except as permitted by Criterion A.3.2, the minimum height H of the guardrail system relative to the adjacent floor or walking surface shall be 42 in (106.68 cm) except if the top rail is flexurally non-rigid H shall be 44 in (111.76 cm).

A.3.1.1 Evaluation

Height H will be measured within a tolerance of 1 in (2.54 cm) in the direction normal to the adjacent floor or walking surface as defined in figure A.2. Where any object large enough to be stood over is located on the floor adjacent to the guardrail, or where a layer of debris has accumulated on the floor adjacent to the guardrail, the effective height H will be measured relative to the top of such object or layer.

Note. Definition of tributary width applies to Criterion A.2.1 (b)

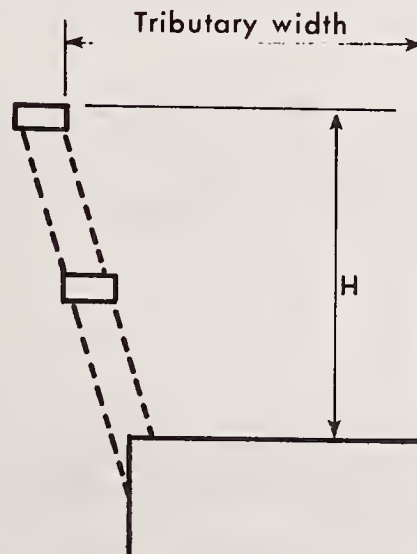
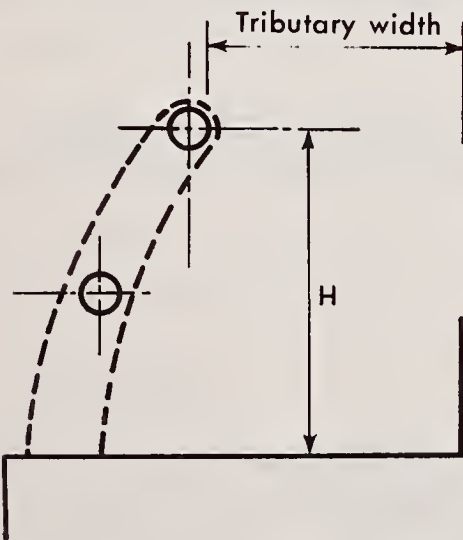
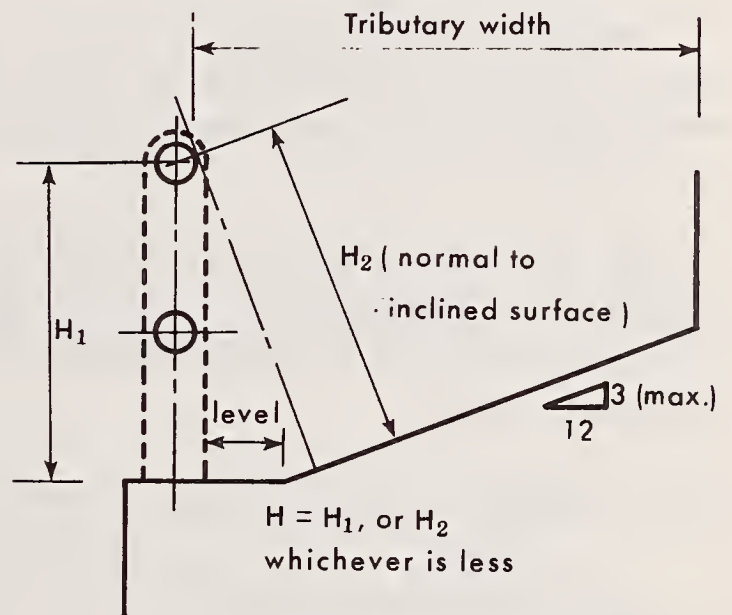
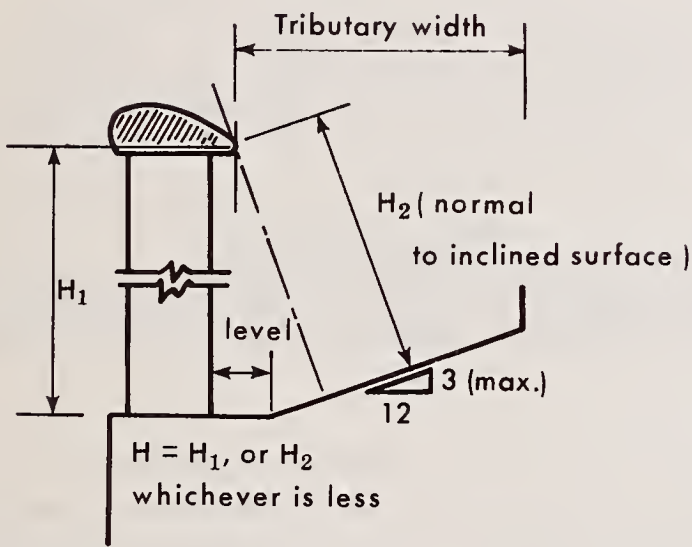
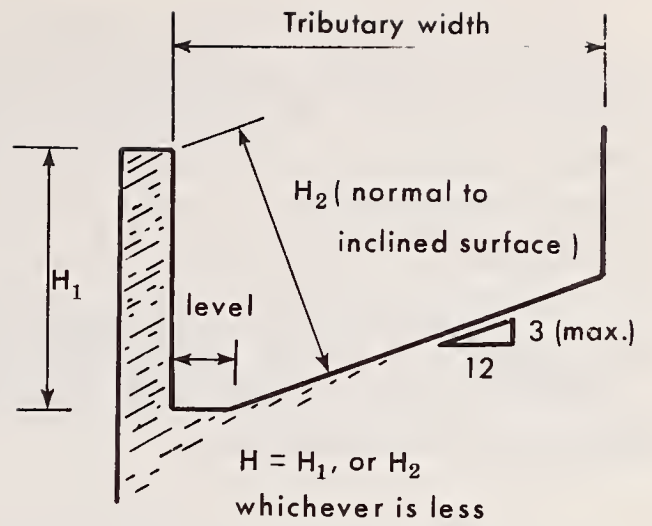


Figure A.2 Definition of guardrail height H

A.3.1.2 Commentary

The rationale for the height requirement is to inhibit accidental passage of the human body over the guardrail. The prescribed height of the guardrail system is set approximately equal to the height of the centroid of the 95 percentile composite adult male population in the United States [A.10]. The centroidal height of the subject is measured with the subject in a straight posture standing on a level surface. Tests using anthropomorphic dummies and mock-up guardrails have indicated that the chances of the dummy going over the guardrail increase rapidly when the top rail is positioned at heights lower than the centroid of the dummy. These tests involved simulation of various postures of human subjects leaning against the guardrail as well as human subjects moving at normal or brisk walking speeds and squarely impacting against the guardrail.

The increased height prescribed for flexurally non-rigid top rails such as tensioned cables or draped chains recognizes the need to compensate for height loss due to generally larger displacement of these elements relative to other top rails under the same anticipated service loads.

The 1-in tolerance specified under section A.3.1.1 is considered necessary to allow for the possible deviation from the prescribed 42-in height that may be anticipated to occur as a result of materials imperfections, settlements, creep, warping and miscellaneous other aging effects.

A.3.2 Criterion - Height in Relation to Width

The height requirement stipulated in Criterion A.3.1 may be relaxed under the following conditions:

- (a) If the top surface of the guardrail is horizontal and has a width greater than 6 in (15.24 cm), and the floor surface of the interior adjoining region is level, the minimum height H of the guardrail shall be not less than,

$$H = K_1 - B$$

where B is the minimum width of the top surface of the guardrail and K_1 is 48 in (121.92 cm). However, in no case shall the minimum height be less than 30 in (76.2 cm).

- (b) If, in addition to the conditions stipulated in (a) above, the projection of any part of the human body beyond the exterior edge of the top surface of the guardrail brings it in contact with a hazardous substance, the minimum width B of the top surface of the guardrail shall be not less than

$$B = K_2 - 2C$$

where C is the vertical distance of the boundary of the hazardous region below the exterior edge of the top surface of the guardrail and K_2 is 36 in (91.44 cm). However, in no case shall the minimum width be less than 24 in (60.96 cm).

A.3.2.1 Evaluation

Compliance will be determined by measurements and inspection in the field after installation. Height H and width B will be evaluated within a tolerance of 1 in (2.54 cm).

A.3.2.2 Commentary

The minimum height of 30 in (76.2 cm) is 9 in (22.86 cm) above the kneecap height of the 95 percentile adult male subject in the United States, measured from the floor where the subject is in straight standing posture on level surface. The 9-in (22.86 cm) distance permits the human subject to exercise leverage, assuming adequate ground friction, against overturning following his accidental backing onto the guardrail. In addition, tests have indicated that, at a guardrail height of 30 in (76.2 cm), the 95 percentile human male subject does not gain reach advantage when he assumes a climbing posture (with one foot on the floor and the other on top of the rail) as opposed to his reach when both his feet are on the floor.

The equation prescribed in Criterion A.3.2 (a) is based on 95 percentile dummy tests which indicate that a height less than 30 in (76.2 cm) increases the likelihood of total passage to the other side of the guardrail following an accidental fall. The minimum width of 24 in (60.96 cm) stipulated in Criterion A.3.2 (b) is likewise based on the same tests using the 95 percentile dummy.

A.3.3 Criterion - Size of openings

Any opening in the guardrail system shall reject passage of a spherical object 19 in (48.3 cm) and greater in diameter.

A.3.3.1 Evaluation

This Criterion will be evaluated by field measurement after installation using a 19-in (48.3-cm) spherical object. In the case of flexurally non-rigid elements with sag, the object should be forced only to the extent needed to take up the slack or to make such elements taut but without stretching them.

A.3.3.2 Commentary

The rationale for this criterion is to inhibit accidental passage of the human body through guardrail openings. The dimension given for the spherical object is slightly more than the shoulder width of the 50 percentile U.S. adult male population [A.10]. In this regard, it is noted that the chest depth for the 5 percentile U.S. male (which is less than the corresponding size of the 5 percentile U.S. female) is approximately 8 in (20.3 cm). Therefore, it is implicitly assumed that the subject will be capable of grabbing the guardrail or wedging himself by some other means and prevent his complete passage to the exterior after such passage is accidentally initiated.

A.3.4 Criterion - Passage of objects near the floor

Guardrails shall reject the passage of spherical objects 0.5 in (1.27 cm) and greater in diameter, up to a height of 5 in (12.7 cm) from the adjacent floor surface. This Criterion may be waived if it can be satisfactorily established that no risk of injury to personnel arises as a result of said waiver.

A.3.4.1 Evaluation

This Criterion will be evaluated by field inspection after installation. The 5-in (12.7-cm) height will be measured normal to the adjacent floor surface in a manner similar to measurement of guardrail height (refer to figure A.2).

A.3.4.2 Commentary

The rationale for this criterion is to prevent the shod foot, hand tools and miscellaneous small debris from falling, sliding or rolling under the guardrail. The 5-in (12.7-cm) minimum height dimension is approximately based on the ankle pivot height of the 95 percentile U.S. male wearing heavy winter footwear [A.10]. It is assumed that this height will be sufficient to prevent passage of hand tools and debris.

The specified waiver is predicated on the condition that no risk of injury to employees exists on either side of the guarded area by virtue of such omission. It is recommended that compliance with this criterion be required for all inclined work surfaces protected by guardrails installed on the downhill side, to provide an obstacle against, and thereby inhibit, accidental slippage of subjects under the guardrail. It is likewise recommended that compliance with this criterion be required in all cases where the risk of injury to employees exists as a result of loose objects accidentally leaving the guarded area.

A.3.5 Criterion - Smoothness of surfaces

The surfaces and edges of guardrail systems shall be smooth and void of characteristics that can capture clothing or cause cuts, snags, abrasions, or other injuries to the hands and other parts of the body as a person comes in contact with the guardrail while standing or conducting a work activity next to it.

A.3.5.1 Evaluation

Inspection and/or field testing after installation. Field testing will be conducted using one layer of a wet, commercially available chamois skin wrapped around a gloved hand. The chamois skin will be run along surfaces or edges exposed to body contact and observed for substantial cuts, tears, punctures or other major destruction to the surface. Any evidence of such destruction may be interpreted as failure of compliance with this Criterion.

A.3.5.2 Commentary

The intent of this Criterion is to reduce the potential risk of injury resulting from contact with rough surfaces. To satisfy this Criterion, surfaces should be void of sharp projections (screws, nails, threaded ends of bolts), substantial delaminations having sharp edges or points (cracked wood or metal skins), etc.

Although the field test suggested is rather crude (see reference [A.11] for additional information), it may be used together with visual inspection to provide an indication of relative roughness of surfaces. This test may be rendered more effective by specifying standards for the materials used (chamois skin and glove), the applied force, the contact area and the speed of the movement. For better control, a standard padded object may be used in lieu of the gloved hand.

A.3.6 Criterion - Visibility

The color or intensity of the guardrail system or the minimum dimension of any guardrail element shall be such that it can be readily seen at any distance from the guardrail up to 25 ft (762 cm) away.

A.3.6.1 Evaluation

This Criterion will be evaluated by analysis or by field inspection if deemed necessary. The minimum required dimension of any guardrail component will be determined according to the viewing distance formula [A.12, A.13]

$$t = 0.0025 d_v$$

where t is the minimum dimension of the guardrail component and d_v is the viewing distance.

Field inspection will be conducted during the period when employees are on duty and under adverse environmental conditions (i.e., early morning or late afternoon, overcast skies, time of the year with short daylight, etc.).

A.3.6.2 Commentary

The intent of this Criterion is to provide for early visual perception of the guardrail and guardrail components (particularly the top rail) by prescribing a safe viewing distance. A commonly accepted value for human reaction time is 3/4 second (driver's handbooks, U.S. Bureau of Public Roads tests on average stopping distance of cars, etc.). The 25-ft (762 cm) distance includes a reaction distance of approximately 10 ft (304.8 cm) and an assumed stopping distance of 7 ft (213.36 cm) for a person running at a speed of 10 mph (16.1 km/hr). This allows him to stop 8 ft (243.84 cm) short of the guardrail.

The minimum dimension of guardrail components will probably be greater than 0.75 in (1.905 cm) when determined by the viewing distance formula in section A.3.7.1, with the exception of wire rope which might have a diameter less than 0.75 in (1.905 cm) as determined by structural design requirements. In the latter case, this Criterion can be met by attachment of signs of the appropriate size and at such intervals along the element that will make them visible from anywhere within the 25 ft (762 cm) viewing region.

In instances where the visually handicapped are required to come in contact with the guardrail, or in situations where the task being performed would prevent seeing the guardrail prior to contact with it, acoustic, tactile, and/or other cues should be provided.

A.3.7 Criterion - Warning signs

Warning signs stating that the guardrail is not to be sat on, stood on, used as a tool, or otherwise misused shall be applied to the guardrail in locations along its length where it is first encountered and at regular intervals elsewhere, and shall be legible at a viewing distance of 10 ft (305 cm). Guardrails designed to support all loads stipulated in Criterion A.2.2(c) including live loads attributable to misuse need not comply with this Criterion.

A.3.7.1 Evaluation

This Criterion will be evaluated by analysis using the viewing distance formula given in section A.3.6.1, and, if deemed necessary, by field inspection as specified under section A.3.6.1.

A.3.7.2 Commentary

This criterion attempts to eliminate, or at least limit, those loading situations for which the guardrail was not designed.

A.4 Definitions

Anchorage - component of guardrail used for securing guardrail system to a foundation.

Basic Loads - types of loads and their intensities in terms of which design loads are specified.

Component - unit used in assembly of guardrail system.

Connection - component of guardrail system used for attachment of guardrail elements.

Design Loads - specified combinations of basic loads used in the design of guardrail systems and their foundations.

Element - component or structural unit of guardrail system other than connection or anchorage.

Foundation - component of a structure providing support to guardrail system.

Guardrail - same as "Guardrail System."

Guardrail System - structural system serving the function of impeding accidental or inadvertant passage of humans and objects between two adjoining areas it separates.

Midrail - longitudinal element located at intermediate level between top of guardrail and floor.

Structural Systems - assembly of components serving a structural function.

Subsystem - assembly of portion of guardrail system consisting of more than one element and one or more connections and/or anchorages.

System - assembly of components serving a specified function. Same as "guardrail system" unless specified otherwise.

Toprail - longitudinal element located at top of guardrail.

Tread Surface - working surface adjacent to guardrail.

A.5 References in Model Performance Standard

- A.1 Building Code Requirements for Minimum Design Loads in Buildings and Other Structures, ANSI A58.1-1972, American National Standards Institute, New York, New York, 1972.
- A.2 Thom, H.C.S., New Distributions of Extreme Winds in the United States, Proceedings, Journal of the Structural Division, American Society of Civil Engineers, New York, New York, July, 1968.
- A.3 Manual of Steel Construction, American Institute of Steel Construction, Inc., 101 Park Avenue, New York, New York 10017, 1973.
- A.4 Aluminum Construction Manual, Specifications for Aluminum Structures, The Aluminum Association, 420 Lexington Avenue, New York, New York 10017, November, 1967.
- A.5 Building Code Requirements for Reinforced Concrete, ACI 318-71, American Concrete Institute, Detroit, Michigan, 1971.
- A.6 Building Code Requirements for Masonry, ANSI A41.1-1953 American National Standards Institute, New York, New York, 1970.
- A.7 Building Code Requirements for Reinforced Masonry, ANSI A41.2-1960, American National Standards Institute, New York, New York, 1970.
- A.8 National Design Specification for Stress-Grade Lumber and Its Fastenings, National Forest Products Association, Washington, D.C., 1973.
- A.9 Newmark, N.M., and Hall, W.J., Procedures and Criteria for Earthquake Resistant Design, Workshop Proceedings on Building Practices for Disaster Mitigation, Wright, R., Kramer, S., and Culver, C., Editors, BSS-46, Building Science Series, National Bureau of Standards, Washington, D.C., February, 1973.
- A.10 Diffrient, Niels, Tilley, Alvin R., and Bardagjy, Joan C., Humanscale 1/2/3, the MIT Press, Massachusetts Institute of Technology, Cambridge, Massachusetts, 1974.
- A.11 Synthetic Skins for Automotive Testing, SAE J202, SAE Handbook, Vol. II, Society of Automotive Engineers, Inc., 1975.
- A.12 Woodson, Wesley E., and Conover, Donald N., Human Engineering Guide for Equipment Designers, Second Edition, University of California Press, Berkeley, California, 1973.
- A.13 Safety Color Code for Marking Physical Hazards, ANSI Z53.1-1971, American National Standards Institute, New York, New York, 1971.

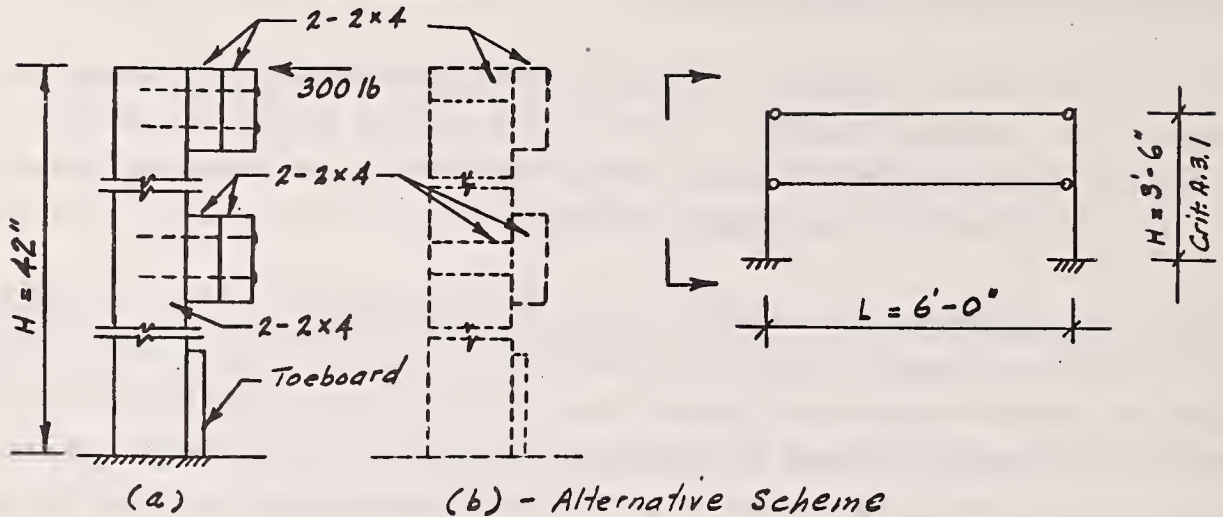
B.1 Examples of Standard Guardrail Designs

This section presents numerical illustrations of standard design conforming with provisions of the foregoing Criteria. Included are designs of guardrails consisting of (a) nominal 2 x 4 wood sections (figure B.1), (b) aluminum pipe sections (figure B.2), and (c) single standard size steel angles (figure B.3).

The standard guardrail used in these illustrations consists of a top rail, intermediate rail and two posts anchored to the floor but not built continuous with the rails. This configuration produces conservative designs since no advantage is taken of the continuities between adjoining spans of systems with more than two posts. In each of the examples, the members are proportioned using the 300-lb (1335-N) concentrated accidental load (A) specified in Criterion A.2.1 for tributary areas equal to or greater than 36 in (91.4 cm) in width. The direction of this load is governed by the most critical stress condition it produces in the individual elements. The maximum deflections under a load of 1.5A are calculated and compared with the values stipulated in Criterion A.2.5.

The use of section standardization throughout a particular type of guardrail installation is usually governed by economic considerations and local availability of common stock items. The sizes used in these examples have been selected arbitrarily and therefore, are not necessarily those most readily available.

Wood Guardrail System



Design Conditions

- Two posts + top rail + midrail
- Posts fixed at base, rails simply supported
- Southern pine, construction grade (19% max. m.c.)
- 300 lb accidental load (A).

Reference

NFPA table 1
Crit. A.2.2

Top & Mid Rails

Assume $L = 6'-0"$, $M = PL/4 = 300(72)/4 = 5400 \text{ in-lb}$

$F_b = 1050 \times 2 \text{ (impact)} \times 1.1 = 2310 \text{ psi}$

Try 2-2x4, Layout (a) above

$S_{req'd.} = M/F_b = 5400/2310 = 2.34 \text{ in}^3$

Assume no integral action betw. 2x4's (conserv.)

$S_{suppl'd.} = 2^{No.} \cdot (1.5)^2(3.5)/6 = 2.62 \text{ in}^3 > 2.34 \text{ in}^3 \text{ OK}$

Check for 300 lb acting downward

$S_{suppl'd.} = 1.5(3.5)^2/6 = 3.06 \text{ in}^3 > 2.34 \text{ in}^3 \text{ OK}$

Posts

$M = PH = 300(42) = 12,600 \text{ in-lb}$

$S_{req'd.} = M/F_b = 12,600/(1050)(2) = 6.0 \text{ in}^3$

$S_{suppl'd.} = 2^{No.} \cdot (1.5)(3.5)^2/6 = 6.12 \text{ in}^3 > 6.0 \text{ in}^3 \text{ OK}$

NFPA table 1 &
figure H-1

Check Deflection

$I_{rail} = 2^{No.} \cdot (3.5)(1.5)^3/12 = 1.97 \text{ in}^4$, $I_{post} = (3)(3.5)^3/12 = 10.7 \text{ in}^4$

$\Delta_{rail} = PL^3/48EI = (300 \times 1.5)(72)^3/48(1.4^6)(1.97) = 1.27 \text{ in}$

$\Delta_{post} = (P/2)H^3/3EI = 225(42)^3/3(1.4^6)(10.7) = 0.37 \text{ in}$

$\Delta_{total} = 1.27 + 0.37 = 1.64 \text{ in} < 4 \text{ in allow. OK}$

Crit. A.2.5

Crit. A.2.5

Figure B.1 Design of wood guardrail system

Design Conditions

- Two posts + Top Rail + Mid Rail
- Posts Fixed, Rails Simply Supported
- No Welds
- Use 6063-T6 Pipe (40 schedule):

Reference

$$F_{ty} = 25 \text{ ksi}, \quad F_{tu} = 30 \text{ ksi} \quad \dots \quad \text{ACM Table 3.3.1a}$$

$$n_y = 1.65, \quad n_u = 1.95 \quad \dots \quad \text{ACM Table 3.3.3}$$

$$F_{b1} = 1.17 F_{ty} / n_y = 1.17(25) / 1.65 = 17.73 \text{ ksi} \leftarrow \text{Use} \quad \text{"}$$

$$F_{b2} = 1.24 F_{tu} / n_u = 1.24(30) / 1.95 = 19.08 \text{ (not govern)} \quad \text{"}$$

Use $L = 6'-0"$

$$M_{1/2} = 300(6 \times 12) / 4 = 5400 \text{ in-lb} \quad \dots \quad \text{Crit. A.2.2}$$

$$S_{req'd.} = M / F = 5400 / 17.730 = 0.305 \text{ in}^3$$

Use Nominal $1\frac{1}{2}" \phi$ pipe (Schedule 40) Top & Mid rail

$$M_{post} = 300(42) = 12,600 \text{ in-lb} \quad \text{Crit. A.2.2}$$

$$S_{req'd.} = 12600 / 17730 = 0.710 \text{ in}^3 \quad \text{\& A.3.1}$$

Use Nominal $2\frac{1}{2}" \phi$ pipe (Sch. 40) Posts @ 6'-0" o.c.
($S_{supplied} = 1.06 \text{ in}^3 \approx 0.710 \text{ in}^3$ OK)

Max. Deflections:

$$I_{rail} = 0.310 \text{ in}^4, \quad I_{post} = 0.666 \text{ in}^4$$

$$\Delta_{rail} = \frac{PL^3}{48EI} = \frac{(450)(72)^3}{48(10.1^6)(0.310)} = 1.12" \quad \text{Crit. A.2.5}$$

$$\Delta_{post} = \frac{(7/2)H^3}{3EI} = \frac{(225)(42)^3}{3(10.1^6)(0.666)} = 0.83"$$

$$\Delta_{TOT.} = 1.95"$$

$$(< 4" \text{ allowed, } \therefore \underline{\text{OK}})$$

Crit. A.2.5)

Figure B.2 Design of aluminum pipe guardrail system

A. Using Angle Sections

Design Top & Mid Rails:

Try 1 - $2\frac{1}{2} \times 2\frac{1}{2} \times \frac{3}{8}$ L, A36 Steel

Wt. = 5.9 lb/ft

$$A = 1.73 \text{ in}^2, r_z = .487", I_z = Ar_z^2 = .410 \text{ in}^4$$

$$S_{\text{tens.}} = .410 / .955 = .429, S_{\text{comp.}} = .41 / 1.078 = .380 \text{ in}^3 (\text{min.})$$

$$\text{Use } L = B' = 96", M_{L/2} = 300(96)/4 = 7200 \text{ in-lb}$$

$$f = M / s_{\text{min}} = 7200 / .38 = 18,950 \text{ psi} < 22,000 \text{ psi} \quad \underline{\text{OK}}$$

Design of Posts:

$$M = 300(42) = 12,600 \text{ in-lb}, I_x = .984 \text{ in}^4$$

$$S_{\text{tens.}} = .984 / .762 = 1.29 \text{ in}^3, S_{\text{comp.}} = .984 / 1.738 = .566 \text{ in}^3 (\text{min.})$$

$$b = 1.738", b/t = 1.738 / .375 = 4.63$$

$$76 / \sqrt{F_y} = 76 / \sqrt{36} = 12.7 \gg b/t, \text{ way } \underline{\text{OK}} \quad (\text{AISC 19.1.2 \& App. C})$$

$$f_b = M / s_{\text{min}} = 12,600 / .566 = 22,261 \approx 22,000 \text{ allow.} \quad \underline{\text{OK}}$$

Check $M_{\text{wt.}} = 5.9(8)^2(12)/8 = 566.4 \text{ in-lb}$

DL: $f_{DL} = M / S_x(\text{tens.}) = 566.4 / 1.29 = 439 \text{ psi}$

$$\therefore f_b(\text{combined}) = 18,950 + 439 = 19,389 < 22,000 \quad \underline{\text{OK}}$$

\therefore Use $2\frac{1}{2} \times 2\frac{1}{2} \times \frac{3}{8}$ L for all members

Check Deflections:

Top rail, @ z-axis:

$$P = 450\# @ L/2, \theta = 45^\circ$$

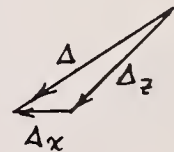
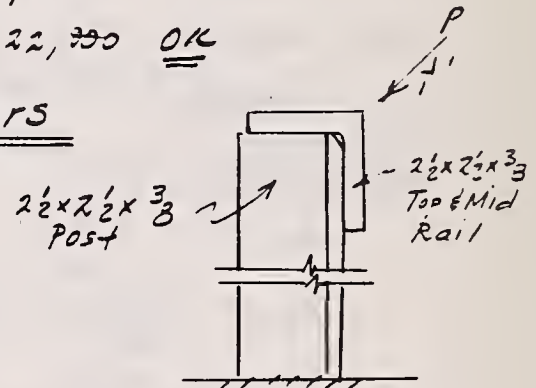
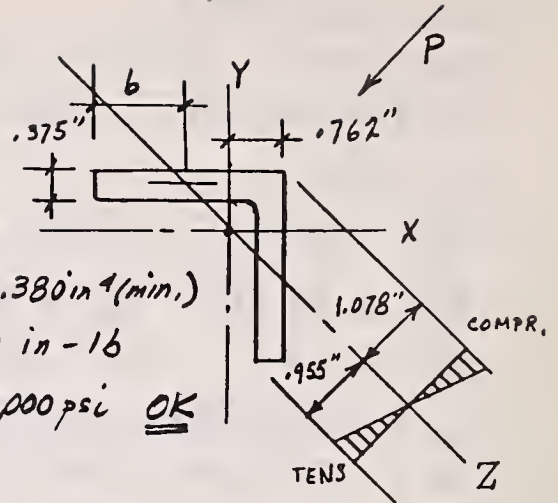
$$\Delta_z = \frac{450(96)^3}{48(29 \times 10^6)(.410)} = 0.70 \text{ in}$$

$$\text{Post load: } 0.5P / \sqrt{2} = 450(.5) / \sqrt{2} = 159\#$$

$$\Delta_x = \frac{PH^3}{3EI_x} = \frac{159(42)^3}{3(29 \times 10^6)(.984)} = 0.21 \text{ in}$$

$$\Delta = \{ [(0.70/\sqrt{2}) + 0.21]^2 + [0.70]^2 \}^{1/2} = .99"$$

$\ll 4"$ allowed, way OK



B. Using steel Pipe

Calculations similar to fig. B.2 lead to following sections:

Top & Mid Rails: $1\frac{1}{2}$ " ϕ standard pipe (sched. 40, A36 steel)

Posts: 2" ϕ standard pipe (sched. 40, A36 steel) @ 3'-0" o.c.

Figure B.3 Design of steel guardrail systems

U.S. DEPT. OF COMM. BIBLIOGRAPHIC DATA SHEET	1. PUBLICATION OR REPORT NO. NBSIR 76-1131	2. Gov't Accession No.	3. Recipient's Accession No.
4. TITLE AND SUBTITLE A Model Performance Standard for Guardrails		5. Publication Date July 1976	
		6. Performing Organization Code	
7. AUTHOR(S) S.F. Fattal; L.E. Cattaneo; G.E. Turner and S.N. Robinson		8. Performing Organ. Report No.	
9. PERFORMING ORGANIZATION NAME AND ADDRESS NATIONAL BUREAU OF STANDARDS DEPARTMENT OF COMMERCE WASHINGTON, D.C. 20234		10. Project/Task/Work Unit No. 461 2471	
		11. Contract/Grant No.	
12. Sponsoring Organization Name and Complete Address (Street, City, State, ZIP) Occupational Safety and Health Administration Department of Labor Washington, D.C. 20210		13. Type of Report & Period Covered Final Report	
		14. Sponsoring Agency Code	
15. SUPPLEMENTARY NOTES NBSIR to sponsor to be incorporated in BSS Report containing analysis of experimental data basis; and augmented by NBSIR containing additional background material.			
16. ABSTRACT (A 200-word or less factual summary of most significant information. If document includes a significant bibliography or literature survey, mention it here.) A model performance standard and design illustrations are presented for the design, construction and evaluation of guardrail systems, which will be used for the protection of employees against occupational hazards. The standard stipulates both structural and non-structural safety requirements. Each criterion includes a commentary section describing the rationale used in its formulation. This rationale is for the most part, based on independent experimental and analytical research investigations conducted at NBS in behalf of OSHA.			
17. KEY WORDS (six to twelve entries; alphabetical order, capitalize only the first letter of the first key word unless a proper name; separated by semicolons) Design; dynamic loads; guardrails; industrial accidents; non-structural safety; occupational hazards; performance standard; personnel railings; personnel safety; static loads; stiffness; structural safety.			
18. AVAILABILITY <input checked="" type="checkbox"/> Unlimited <input type="checkbox"/> For Official Distribution. Do Not Release to NTIS <input type="checkbox"/> Order From Sup. of Doc., U.S. Government Printing Office Washington, D.C. 20402, SD Cat. No. C13 <input checked="" type="checkbox"/> Order From National Technical Information Service (NTIS) Springfield, Virginia 22151		19. SECURITY CLASS (THIS REPORT) UNCLASSIFIED	21. NO. OF PAGES
		20. SECURITY CLASS (THIS PAGE) UNCLASSIFIED	22. Price

NBSIR 76-1132

Personnel Guardrails for the Prevention of Occupational Accidents

S. G. Fattal, L. E. Cattaneo
G. E. Turner, S. N. Robinson

Center for Building Technology
Institute for Applied Technology
National Bureau of Standards
Washington, D. C. 20234

July 1976

Final Report

Prepared for
Occupational Safety and Health Administration
Department of Labor
Washington, D. C. 20210

NBSIR 76-1132

PERSONNEL GUARDRAILS FOR THE PREVENTION OF OCCUPATIONAL ACCIDENTS

S. G. Fattal, L. E. Cattaneo
G. E. Turner, S. N. Robinson

Center for Building Technology
Institute for Applied Technology
National Bureau of Standards
Washington, D. C. 20234

July 1976

Final Report

Prepared for
Occupational Safety and Health Administration
Department of Labor
Washington, D. C. 20210



U.S. DEPARTMENT OF COMMERCE, Elliot L. Richardson, *Secretary*

Edward O. Vetter, *Under Secretary*

Dr. Betsy Ancker-Johnson, *Assistant Secretary for Science and Technology*

NATIONAL BUREAU OF STANDARDS, Ernest Ambler, *Acting Director*



TABLE OF CONTENTS

	Page
Abstract	1
1. Introduction--Objectives and Scope	2
2. Review of Existing Standards and Technical Literature	4
3. Anthropometric Data	12
4. Field Survey of Guardrail Installations	25
5. A Conceptual Model of Safety	53
6. An Analysis of Guardrail Accidents	60
7. Summary	76

PERSONNEL GUARDRAILS FOR THE PREVENTION OF OCCUPATIONAL ACCIDENTS

S. G. Fattal, L. E. Cattaneo,
G. E. Turner and S. N. Robinson

Existing information is compiled which would assist in determining structural and non-structural safety requirements for guardrails used for the protection of employees against occupational hazards. Critical aspects of guardrail safety are identified through exploratory studies consisting of field surveys of prototypical installations, reviews of existing standards and industrial accident records, and compilation of relevant anthropometric data. These exploratory studies will be utilized to design an experimental program which will consist of structural tests to determine design loads and non-structural tests to determine geometric requirements for guardrail safety.

Key Words: Anthropometric measurements; guardrails; industrial accidents; non-structural safety; occupational hazards; performance standard; personnel railings; personnel safety; structural safety.

1. Introduction - Objectives and Scope

This report documents the first phase of research studies conducted at the National Bureau of Standards (NBS) in response to a request by the Occupational Safety and Health Administration (OSHA) for technical assistance in developing performance standards and design guidelines for guardrails which will be used to protect employees against occupational hazards. Under the Occupational Safety and Health Act of 1970, OSHA exercises a mandate over employee safety regulations including prescriptive requirements for all guardrails that are installed in areas where employees conduct work-related activities. The general lack of technical literature to support the existing OSHA guardrail regulations, and, for that matter, guardrail provisions of other mandatory or voluntary standards, has been one of the principal motivating factors behind the research program. The two principal objectives of the project were the development of basic technical information through research and the utilization of this information to prepare performance-oriented recommendations for the design, construction and evaluation of guardrail systems which come under the jurisdiction of OSHA.

The scope of this project was established by mutual agreement between OSHA and NBS participants. It was agreed that NBS research should apply to temporary and permanent guardrails used for the protection of employees against occupational hazards, and therefore, should only consider factors associated with guardrail use by adult personnel during the conduct of their assigned tasks. It was further stipulated that NBS research should exclude consideration of guardrail loading situations arising through flagrant abuse or through the impact of power-driven vehicles or other heavy mobile objects propelled by people. In addition, it was agreed that NBS research need not be concerned with investigations of whether or where the installation of guardrails will be required.

The types of guardrail installations given high research priority by OSHA included the following, listed in the order of decreasing priority: (1) elevated walkways (2) erected and swinging scaffolds, (3) balconies and mezzanines, (4) hot-dip galvanizing operations, (5) roofing operations, (6) cast-in-place concrete construction, (7) petro-chemical towers, (8) mobile equipment, (9) elevated work or storage areas, and (10) marine dry docks. It was understood that as many of these installations as possible should be examined within the specified project resources without diluting the credibility of the end product. NBS researchers examined eight of these installations, the excluded ones were chemical towers and mobile equipment.

At the beginning of this project it was reasoned that if the principal factors contributing to the safe functioning of guardrails could be identified in some systematic fashion, the task of developing an effective approach to meet the specified project objectives would be simplified. Accordingly, one of the earlier tasks was to devise a

conceptual model which considers both human and environmental factors and their interactions with respect to safety and to proceed to study guardrails within the framework of this model. (See Section 5).

Using the guidelines of the safety model, a two-phase approach compatible with the stated project objectives was formulated. The first phase was exploratory in nature and was necessitated by almost a total lack of rational basis behind existing guardrail design provisions. It was aimed towards such studies as the prevailing modes of guardrail use in service, the adequacy of present design and construction practices, factors influencing human-guardrail interaction, and the principal agents of potential hazards. Specifically, the scope of the first phase included the following disciplinary studies which are documented in this report for the benefit of researchers and analysts concerned with guardrail safety.

- (1) A literature search of available technical information and a study of the provisions of existing guardrail design standards (Section 2).
- (2) A compilation of existing statistical data on the anthropometric and kinematic characteristics of the human body relevant to guardrail analysis (Section 3).
- (3) A field survey of prototypical guardrail installations (the eight types mentioned above), to become familiar with current practices and, if possible, to identify safe and unsafe employee activities and environmental characteristics (Section 4).
- (4) An analysis of employee accident records compiled by various agencies to determine the frequency and nature of those accidents which appear to be guardrail-related (Sections 5 and 6).

In phase two, the results presented herein will be used in the preparation and subsequent conduct of an experimental-analytical program. It is expected that these exploratory studies will prove valuable in designing experiments to measure the static and dynamic loads induced on guardrails during simulated accident situations, and in developing a data base from which the essential safety features of guardrails can be established. On the basis of information acquired from the above, performance-oriented recommendations and a guide for the design and evaluation of guardrails will be prepared.

The implementation of this project was carried out through the cooperative efforts of NBS research investigators from the structural, architectural and psychological disciplines. For convenience in recovering the original sources and data, a reference list for each of the four tasks identified above is appended to the end of the appropriate section.*

*Citations of references are indicated by numbers in brackets.

2. Review of Existing Standards and Technical Literature

This section presents a summary of existing guardrail provisions of some of the major codes and standards that are widely used throughout the United States and Canada. For ease of reference, these provisions are presented in tabular form (table 2.1) consisting of entries of prescribed horizontal and vertical design loads, required height of guardrail, and notes related to these entries. The first entry gives the code references and the pertinent sections from which the listed data have been excerpted. The references from which table 2.1 has been prepared and the sequence in which they have been listed, (which is arbitrary) are as follows:

- (1) Uniform Building Code [2.10]
- (2) The BOCA Basic Building Code [2.11]
- (3) Building Code of the City of New York [2.12]
- (4) Southern Standard Building Code [2.13]
- (5) The National Building Code [2.14]
- (6) National Building Code of Canada [2.5]
- (7) Canadian Construction Safety Code [2.16]
- (8) Occupational Safety and Health Standard, Part 1910 [2.2]
- (9) Construction Safety and Health Regulations, Part 1926 [2.1]

An examination of the information compiled in table 2.1 reveals a general lack of consistency and uniformity between load and height requirements. Some base their load requirements on the number of occupants while others specify loads according to guardrail location. In cases where two or three different loadings are specified, it is not always clear whether these loads are intended to be applied simultaneously or individually in design. Quite often, certain critical decisions are left to the designers with such terms as "substantial guardrails shall be provided. . ." or "openings should restrict climbing." The requirements of some of the codes are much more stringent than others. Certain codes and regulations give standard member sizes and dimensions. Sometimes there are ambiguities with regard to whether the specified loads are factored or unfactored (ultimate strength design vs working stress design).

The wide diversity of guardrail practices as evidenced by the foregoing study is principally attributed to the paucity of technical information needed to develop a rational

and unified engineering approach to guardrail analysis and design. Specifically, it points out the need for experimental research to establish criteria for guardrail loads induced by human subjects either accidentally or through normal usage, and for guardrail geometry to inhibit accidental falls resulting from geometric inadequacies such as insufficient height and/or width, or excessively large openings.

In an attempt to utilize available technical knowledge and at the same time avoid the possibility of research duplication, a computerized research of published literature on the general subject of guardrails was carried out using the Engineering Index and the Government Reports Index (NTIS). This search identified more than 100 publications on experimental and analytical research investigations of highway guardrails and other vehicular crash barriers; however, no document related directly to personnel guardrails could be located. Subsequently, a selected number of these publications were acquired and examined for technical content for possible application to the analysis of personnel guardrails. However, some of these documents proved to be of little utility because they dealt with investigations of the response of guardrails under vehicular impact, which is fundamentally different from that produced by the human body. A number of other publications dealt with the evaluation of automotive safety devices through tests using human subjects and anthropomorphic dummies. Some of these publications, [2.3, 2.4, 2.22] provide information on the energy absorption characteristics of the simulated human body. A number of other publications compiled anthropometric and engineering data on the human body [2.5-2.9, 2.23-2.28].

Table 2.1 Summary of Guardrail Provisions of Existing Building Codes and Safety Standards

Ref. Sect.	Horiz. Load	Vert. Load	Height in	Notes
1) UBC/1716 /3305(i) /Table 23-C			42	Guardrails & stair railings Interm. rail req'd. Max. opening = 9 in.
			30-34	Stair handrails
	50 plf 20 plf	--		Occupancy > 50 Occupancy < 50
2) BOCA/417.5.5 /615.2 /616.5.1 /616.5.2 /709.4 /870.5			23-36 30-33	Railings - public assembly Handrails on ramps
	200 lb any pt. & dir.		30-34	Handrails - stairways
			42	Guards - floors, mezzs., landings Balusters: 6 in max. spa. Interm. rails: 10 in max. spa. Other: mesh, grill, walls
	50 plf or 200 lb any pt. & dir.	20 plf		Railings - other than public assembly 50 plf & 20 plf not concurrent
	50 plf	100 plf		Railings - publ. assembly 50 plf & 100 plf concurrent
	Engineering Design			Guardrails - Fl. & wall openings Toeboard req'd.
3) NYC/503.4 /503.8 /604 /604.13 /709.5 /710.6 /MDL Sec. 62 /902.3 /1903.2 /1907.9			42	Guard: rails, fence or parapet
			120	Guards - roof recreation
			36	Railings - skylight
			30-34	Handrails - stairs
			32	Handrails - fire escapes
			36	Guards - landings Max. opening = 5 in.
			42	Guards & parapets - roof vehicular parking areas
			8	Guards - vehicle wheels
			42	Guards & railings - perimeter of interior flr. openings.
			42	Guard railings & parapets: wire (mult. dwell.)
	40 plf	50 plf	42	Railings - non-publ. assembly; H & V simultaneous
	50 plf	100 plf	42	Railings - public assembly
	20 plf	20 plf	42	Railings - 1 & 2-family dwellings
	or 200 lb any pt. & dir.			
	40 plf	50 plf		Rails: intermediate & bottom; H & V simult. (not for post and anchor design).
	20 psf	--		Solid panels of railings
	300 plf or 2500 lb (the >)	--		Vehicular, applied at 20-in ht.
		42	Guardrails & solid enclosures - perim. of excavations	
		36-42	Guardrails (standard) - construction toprail: 2 x 4 midrail: 1 x 4 posts: 2 x 4 at 8 ft. altern: 1 1/4-in Std pipe; 2 x 2 x 1/4 angles	

Table 2.1 (cont.)

Ref. Sect.	Horiz. Load	Vert. Load	Height in	Notes
7) Canadian Construction Safety /3.5.22 /3.11.5			42	Guardrails + toeboards - shaft openings
			36-42	Guardrails: 5-in min. ht. toeboard w/ 2 x 4 on 2 x 4 at 8-ft. spacing; midrail 3-in wide on inside of posts or Taut 1/2-in wire cable with 2-in wide vert. separators at 8 ft spacing
			48	or Snow fencing: 4-ft vert. wood strips (1 1/2 in wide x 3/8 in thick at 3 1/2-in spac.) tied with specif. taut strands.
8) OSHA (Occupational Safety) /1910.23			42	Railings: 2 x 4 top and mid; on 2 x 4 at 6-ft spac.; or 2 perp. 1 x 4's top on 2 x 4 at 8 ft spac. (2 x 4 mid) or 1 1/2-in pipe top and mid. on posts at 8-ft spac.
				or 2 x 2 x 3/8 angles top and mid. on posts at 8-ft. spac.
		200 lb any pt. & dir.	30-34	Handrails: 2-in diam. wood; 1 1/2-in pipe mounted at 8-ft spac.
		200 lb any pt. & dir. except up		
/1910.28			36-42	Guardrails - scaffold: 2 x 4 top; 1 x 4 mid; supported at 10 ft. (or equiv.) (1 x 6 mid. for single pt. suspens.)
9) OSHA (Constr. Safety) /1926.500	200 lb any pt. & dir. except up.		42	"Standard railing: 2 x 4 top; 1 x 6 mid; 2 x 4 posts at 8-ft spac. or 1 1/2-pipe top, mid, posts or 2 x 2 x 3/8 top, mid, posts or Equivalent
			30-34	Stair railing (plus standard rail req.)
10) HUD-MPS/402-8			42	Railings - balc. & roof decks Max. opening = 5 in.
	/601-7	50 plf	100 plf	Railings: Not clear if H & V concurrent. Anchors: should not fail under twice specified loads.

References

- 2.1 Construction Safety and Health Regulations, (Federal Register Part 1926), Occupational Safety and Health Administration, U.S. Department of Labor, Washington, D.C., June 24, 1974.
- 2.2 Occupational Safety and Health Standards, (Federal Register Part 1910), Occupational Safety and Health Administration, U.S. Department of Labor, Washington, D.C., October 8, 1972.
- 2.3 Walunas, J. B., and Miller, J. S., An Evaluation of Dynamic Performance Characteristics of Anthropometric Test Devices, Volume 3, DOT HS-800 863, National Highway Traffic Safety Administration, U. S. Department of Transportation, Washington, D. C. 20590, May, 1973.
- 2.4 Ross, H. E., Jr., White, M. S., Young, R. D., and Lammert, W. F., Vehicle Exteriors and Pedestrian Injury Prevention, Volume IV-Drop Test of Dummies on a Mock Vehicle Exterior, DOT HS-801-544, National Highway Traffic Safety Administration, U. S. Department of Transportation, Washington, D. C. 20590, May 1975.
- 2.5 Weight, Height, and Selected Body Dimensions of Adults, United States 1960-1962, U.S. Department of Health, Education and Welfare, Washington, D. C., June 1965.
- 2.6 Diffrient, N., Tilley, A. R., and Bardagjy, J. C., Humanscale 1/2/3, MIT Press, Massachusetts Institute of Technology, Cambridge, Massachusetts, 1974.
- 2.7 Roebuck, J. A., Jr., Kroemer, K. H. E., and Thomson, W. G., Engineering Anthropometry Methods, John Wiley & Sons, New York, N. Y.
- 2.8 McCormick, E. J., Human Factors Engineering, McGraw-Hill Book Company, New York, N. Y., 1970.
- 2.9 Handbook of Human Engineering Data, Tufts College Institute for Applied Experimental Psychology, 1951.
- 2.10 Uniform Building Code, International Conference of Building Officials, 1973.
- 2.11 The BOCA Basic Building Code, Building Officials and Code Administrators International, Inc., Chicago, Ill., 1975.
- 2.12 Building Code of the City of New York, Volumes 1, 2, 1972.
- 2.13 Southern Standard Building Code, Southern Building Code Congress, Birmingham, Alabama, 1973.

- 2.14 The National Building Code, American Insurance Association, New York, N. Y. 1967.
- 2.15 National Building Code of Canada, National Research Council of Canada, Ottawa, Canada, 1975.
- 2.16 Canadian Construction Safety Code, National Research Council of Canada, Ottawa, Canada, 1975.
- 2.17 Minimum Property Standards, U.S. Department of Housing and Urban Development, Washington, D.C., 1973.
- 2.18 Building Construction and Facilities, Volume 4, National Fire Codes, National Fire Protection Association, Boston, Massachusetts, 1973-1974.
- 2.19 Floor and Wall Openings, Railways, and Toeboards, American Standards Association, New York, N. Y., May, 1932.
- 2.20 American Standard Safety Code for Building Construction, American Institute of Architects, National Safety Council, New York, N. Y., June 1944.
- 2.21 Safety Requirements for Floor and Wall Openings, Railings, and Toeboards, ANSI A12.1-1973; Safety Requirements for Personnel Hoists, ANSI A10.4-1973; Safety Requirements for Dredging, ANSI A10.15-1974; Safety Requirements for Concrete Construction and Masonry Work, ANSI A10.9-1970; Safety Requirements for Scaffolds, ANSI A10.8-1969, American National Standards Institute, New York, N. Y.
- 2.22 LeFevre, R. L. and Silver, J. N. Dummies - Their Features and Use, Proceedings, Automotive Safety Seminar, General Motors Training Center, Warren, Michigan, June 1973.
- 2.23 Swearingen, J., Determination of Centers of Gravity of Man, Project 62-14, Civil Aeromedical Research Institute, Oklahoma City, Oklahoma, 1962.
- 2.24 Kromer, K., Push Forces Exerted in Sixty-Five Common Working Positions, AMRL - TR - 68 - 143, Aerospace Medical Research Lab, Wright-Patterson Air Force Base, Dayton, Ohio, 1969.
- 2.25 Croney, J., Anthropometrics for Designers, Van Nostrand Reinhold Co., New York, New York, 1971.
- 2.26 Van Cott, H. P., Human Engineering Guide to Equipment Design, American Institute for Research, Washington, D. C., 1972.

2.27 Singleton, W. T., Fox, J. G., and Whitfield, D., Measurement of Man at Work: An Appraisal of Physiological and Psychological Criteria in Man-Machine Systems, Van Nostrand Reinhold Co., New York, New York, 1971.

2.28 Woodson, W. E. and Conover, D., Human Engineering Guide for Equipment Designers, University of California Press, Berkeley, California, 1973.

3. Anthropometric Data

3.1 Introduction

The objective of this section is to compile general anthropometric data on human subjects for application in the formulation of design requirements for guardrails. For instance, the kinematic aspects of the human body could be utilized to estimate the nature and intensity of human-induced loads on guardrails. Body measurements might be relevant in specifying certain geometric aspects of guardrails such as the maximum size of openings to prevent passage of people into hazardous areas. Anthropometric studies could also assist in establishing relevant hypotheses requiring experimental verification such as the relationship between the height of the guardrail and the centroidal height of the human subject to the inhibit accidental falls.

The anthropometric information presented herein consists of four categories of data broken down according to sex and percentile levels. The first category compiles various height measurements where the subject is in a standing or sitting posture. The second category consists of dimensions and weights of the human body and the heights of convenient reference points on the body for locating other measurements such as the whole-body centroid. The third category specifies the displacement bounds of the body centroid when the subject assumes various postures with and without a 20-lb (89-N) backpack. The fourth category of data provides information on the maximum intensities of forces human subjects are capable of exerting on the guardrail. Measurements reported herein are categorized for the 97.5, 50, and 2.5 percentile levels. Percentiles are values representing the percentage of people at or below a certain measurement. They can delineate an upper or lower bound for a specific characteristic. With regard to body height, for example, the 98th percentile designates the height at which 98 percent of the sample are shorter and 2 percent of the sample are taller.

The 50th percentile in a group of measures is called the median. It is the score that divides the ranked measures such that one half of the measures are larger than the median, and the other half are smaller. Similarly, the 97.5 percentile can represent the larger body measurements and the 2.5 percentile can refer to the smaller body measurements. Although the median value for either male or female, does not exactly represent the arithmetic average or mean, it is a close enough approximation for the purposes of this report. The average adult is the arithmetical mean between the median male and median female. All data are for U. S. adults.

The anthropometric data presented herein have been excerpted primarily from three different publications [3.1, 3.2, 3.3]. In addition, four other sources were consulted for general background information [3.4 through 3.7].

3.2 Anthropometrics Relatable to Guardrail Height

Criteria upon which proper guardrail height may be determined focus on the necessity of guardrails to be easily seen and to be capable of keeping an individual from a hazardous area. The following heights may influence the determination of proper guardrail heights:

(1) Standing height: distance from floor to vertex of head, measured from either front or back when subject is standing erect with heels together.

(2) Eye height: distance from floor to inner corner of eye when subject is standing erect with heels together.

(3) Shoulder height: distance from floor to uppermost point on the lateral edge of shoulder when subject is standing erect with heels together.

(4) Elbow height: distance from floor to the depression at elbow formed where bones of the upperarm and forearm meet, when subject is in standing erect with heels together.

(5) Crotch height: distance from floor to crotch when subject is standing erect with heels together.

(6) Seat height: distance from floor to horizontal seat reference plane measured when subject is in sitting posture.

(7) Kneecap height: distance from floor to top of kneecap when subject is standing erect with heels together.

Figure 3.1 gives a schematic illustration of the heights defined above and table 3.1 compiles their magnitudes for the 97.5, 50 and 2.5 percentile U. S. male and female adults. These data were prepared from various recent civilian and military samples [3.1].

Guardrails could serve as a visual as well as physical barrier for most situations. In cases where visual barriers are of primary importance, guardrail heights could be related to eye height. In instances where a guardrail need not serve as a visual barrier but as a physical barrier and where there is little threat of individuals climbing the rail, a top rail height just above the body centroid might prove to be sufficient. Guardrails of elbow height are easy to lean on and could serve as work counters. Guardrails of lower heights would not present a barrier too high to cross, but could still adequately isolate individuals by defining hazardous areas.

3.3 Anthropometrics Relatable to Guardrail Height and Strength

The centroid of a body may be visualized as the point at which the resultant of the distributed gravitational body forces acts. Other factors being equal, the stability of an object is dependent on the location of its centroids above the ground. Stability generally decreases as the height of the centroid relative to the ground increases and vice versa. Consequently, it may be conjectured that a person coming in contact with a guardrail either by leaning on it or inadvertently walking into it might be less likely to go over it if the top of the rail is close to his centroid. In this case, the anthropometric value relevant to guardrail height would be the centroidal height of the human subject.

Certain guardrail strength requirements, may be established on the basis of static loads transmitted by human subjects in any one of a variety of stationary body postures such as leaning or sitting, as well as dynamic loads generated by the impact of moving human subjects. Anthropometric data relevant to estimating such body forces would be quantitative information on the weights of the body and individual body segments. In addition, anthropometric data on shoulder and hip width, for instance, can help in establishing lengths or areas over which body forces may be distributed.

The following anthropometric measurements excerpted from ref. [3.1] are sketched in Figure 3.2 and compiled in table 3.2 for the 97.5, 50 and 2.5 percentile U. S. male and female adult.

- (1) Whole-body centroidal height: distance from floor to the centroid of the body when the subject is standing erect with heels together.
- (2) Ischium height: distance from floor to the top of the lowermost of the three sections of the hip bone when the subject is standing erect with his heels together. The ischium is used as a reference point for location of other points in the body such as the centroid.
- (3) Shoulder width: maximum horizontal distance across the shoulder muscles when subject is in erect sitting posture with upper arms touching his sides.
- (4) Standing hip width: maximum horizontal distance across the hips when subject is in erect standing posture with heels together.
- (5) Sitting hip width: maximum horizontal distance across the hips when subject is in erect sitting posture.
- (6) Body weight: total body weight of the subject without clothing.

It should be pointed out that data on the centroidal height of the U. S. adult female is not available. However, Swearingen [3.2] notes that in spite of the wide variety of

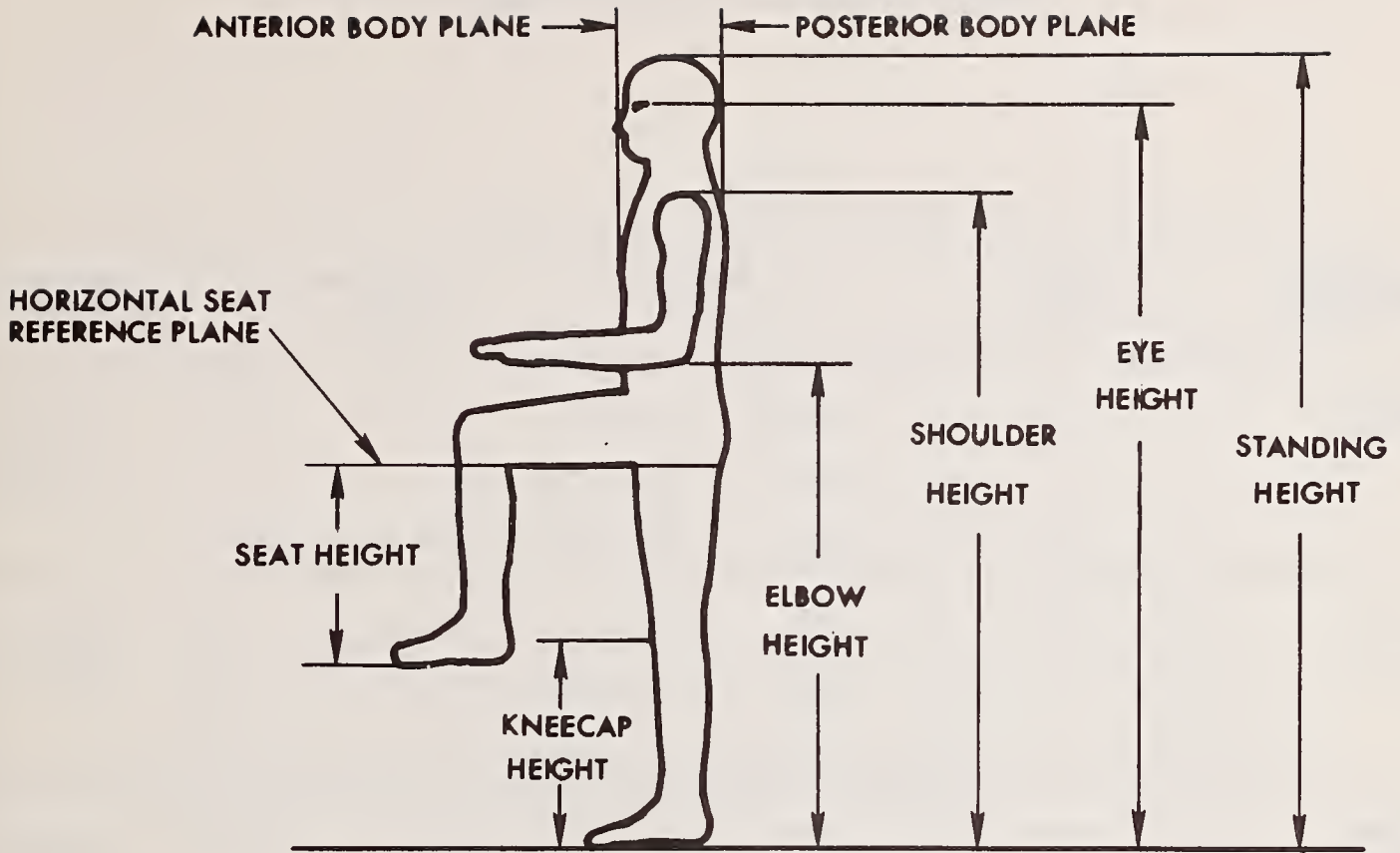


Figure 3.1 Body measurements related to guardrail height (cf. table 3.1).

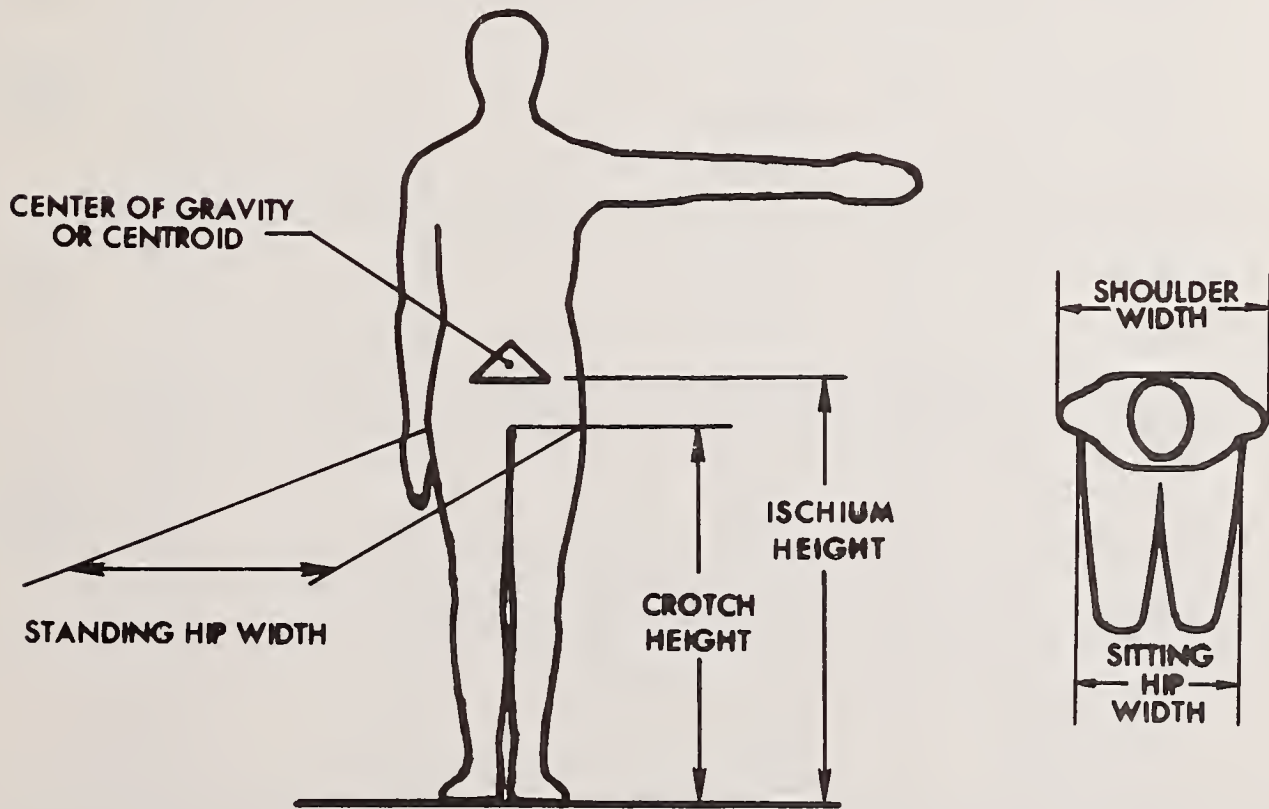


Figure 3.2 Body measurements related to guardrail height (cf. table 3.2).

Table 3.1 Height measurements from the floor level with human subjects in standing or sitting posture.

Type of Measurement	Percentile Level %	Male inches (cm)	Female inches (cm)	Average Adult inches (cm)
Standing Height	97.5	74.0 (188.0)	68.5 (174.0)	66.2 (168.1)
	50	68.8 (174.8)	63.6 (161.5)	
	2.5	63.6 (161.5)	58.7 (149.1)	
Eye Height	97.5	69.3 (176)	64.1 (162.8)	62.0 (157.5)
	50	64.4 (163.6)	59.6 (151.4)	
	2.5	59.6 (151.4)	54.7 (138.9)	
Shoulder Height	97.5	61.4 (156.0)	56.2 (142.7)	54.2 (137.7)
	50	56.6 (143.8)	51.9 (131.8)	
	2.5	51.9 (131.8)	47.8 (121.4)	
Elbow Height	97.5	45.3 (115.1)	41.8 (106.2)	40.3 (102.4)
	50	42.0 (106.7)	38.6 (98.0)	
	2.5	38.6 (98.0)	35.2 (89.4)	
Crotch Height	97.5	35.3 (89.7)	36.2 (91.9)	32.9 (83.6)
	50	32.5 (82.6)	33.3 (84.6)	
	2.5	29.6 (75.2)	30.4 (77.2)	
Seat Height	97.5	18.5 (47.0)	16.9 (42.9)	16.7 (41.4)
	50	17.0 (43.2)	15.6 (39.6)	
	2.5	15.6 (39.6)	14.3 (36.3)	
Kneecap Height	97.5	21.4 (54.4)	19.6 (49.8)	18.9 (47.8)
	50	19.7 (50.0)	18.0 (45.7)	
	2.5	18.0 (45.7)	16.5 (41.9)	

Table 3.2 Measurement of heights, widths and weight of human subject in standing or sitting posture.

Type of Measurement	Percentile Level %	Male inches (cm)	Female inches (cm)	Average Adult inches (cm)
Whole Body Centroid Height	97.5	41.2 (104.6)		
	50	37.9 (96.3)		
	2.5	34.6 (87.9)		
Ischium Height	97.5	39.5 (100.3)	36.2 (91.9)	
	50	36.4 (92.5)	33.3 (84.6)	34.9 (88.6)
	2.5	33.3 (84.6)	30.4 (77.2)	
Shoulder Width	97.5	19.4 (49.3)	17.7 (45.0)	
	50	17.7 (45.0)	16.0 (40.6)	16.9 (42.9)
	2.5	16.0 (40.6)	14.4 (36.6)	
Standing Hip Width	97.5	14.9 (37.8)	16.7 (42.4)	
	50	13.1 (33.3)	13.8 (35.1)	13.5 (34.3)
	2.5	11.7 (29.7)	11.5 (29.2)	
Sitting Hip Width	97.5	15.8 (40.1)	17.7 (45.0)	
	50	13.9 (35.3)	14.6 (37.1)	14.3 (36.3)
	2.5	12.4 (31.5)	12.3 (31.2)	
Body Weight*	97.5	192 (854)	157 (699)	
	50	172 (765)	145 (645)	159 (708)
	2.5	151 (672)	133 (592)	

*1b or (N)

body sizes and mass distributions there is surprisingly little variation in the location of the whole body centroid of U. S. men for any given posture when measured from a reference point on the pelvis (i.e.: ischium), with the centroid of at least 90 percent of the adult male population falling within a sphere of 2 in (5.08 cm) in diameter. Based on the premise that this will more or less be true in the case of U. S. females, the differences between the centroidal and ischium heights of the U. S. males may be added to the ischium heights of the corresponding percentile levels of female population to arrive at generally conservative (high side) but sufficiently accurate estimates of the centroidal heights of U. S. females. This procedure together with the appropriate data in table 3.2 yields centroidal heights of 37.9 in (96.3 cm), 34.8 in (88.4 cm) and 31.7 in (80.5 cm) for the 97.5, 50 and 2.5 percentile female population, respectively.

3.4 Location of Centroid for Selected Body Postures

The heights, weights, and widths of body components are of limited value in calculating static force vectors if the direction of those vectors cannot be determined. The whole-body centroid can serve as a reference point for these static force vectors. Since the centroid varies with the positions of the body and its extremities, it is necessary to identify the various locations of the whole-body centroid with respect to those body postures that approximate guardrail use. Swearingen has measured centroid variation relative to body position in subjects chosen to represent a wide range of body sizes and weights [3.2]. Data which appear to be of relevance to guardrail use and design are excerpted from this reference and presented in tables 3.3 through 3.6. A further discussion is presented in reference 3.2.

3.5 Peak Forces Exerted by People on Guardrails

If an individual has proper auxiliary support and can push against a guardrail thereby causing it to collapse, then a possible anthropometric criterion of maximum guardrail strength might be the maximum strength of an individual. Strength in this sense refers to the muscular capacity to exert force under static conditions. Kroemer [3.3] has measured the strength of 45 male college students. Subjects pushed against a force plate as shown in Figure 3.3. For those infrequent instances where this loading condition is felt to govern guardrail design, reference 3.3 should be consulted to obtain the required load magnitudes.

3.6 Analysis of the Anthropometric Data

The intent of the anthropometric survey was to incorporate within the body of this report a condensed and expedient source of information to assist in the evaluation of the possible effect of human body characteristics on guardrail design rather than provide an exhaustive study on the subject. Although human body characteristics alter with time, the rate of change is so slow as to be insignificant, design-wise over relatively long periods.

Table 3.3 Displacement of body c.g. by anterior movements.

Body Position	Location of Av. C. G.	Horizontal & Vertical Range For Subjects
A. Body standing straight	(4, 5%)	± 7/8"
B. Head forward	(4 1/2, 5%)	± 7/8"
C. Both arms extended forward	(5 1/4, 7)	± 3/4"
D. Head and trunk forward	(5 1/2, 4)	± 1 1/2"
E. Both legs straight forward	(9, 11)	± 1 1/4"
F. All body parts in maximum anterior position	(12, 10%)	± 1 1/2"

Table 3.4 Displacement of body c.g. by posterior movements.

Body Position	Location of Av. C. G.	Horizontal & Vertical Range For Subjects
A. Standing, body straight	(5 1/4, 6)	± 1 1/8"
B. Head back	(5 1/2, 5%)	± 1"
C. Arms back	(5 1/4, 6 1/4)	± 1"
D. Head & trunk back	(7 1/4, 5%)	± 1 1/4"
E. Legs back	(6 1/2, 7%)	± 1"
F. All body parts in maximum posterior position	(9%, 6%)	± 1 1/4"

Table 3.5 Displacement of body c.g. by lateral movements.

Body Position	Location of Av. C. G.	Horizontal & Vertical Range For Subjects
A. Standing, body straight	(0, 5%)	± 7/8"
B. Head flexed to side	(1/2, 5%)	± 3/4"
C. One arm extended laterally	(1/2, 6%)	± 5/8"
D. One arm extended across chest	(3/4, 6%)	± 3/4"
E. Head and trunk in lateral flexion	(1 1/4, 5%)	± 3/4"
F. One leg abducted	(1 1/2, 6%)	± 3/4"
G. Maximum lateral movement of both legs	(1%, 6%)	± 3/4"
H. All body parts moved laterally	(4%, 7%)	± 1 1/8"

Table 3.6 Displacement of c.g. by 20-lb back pack in sitting and standing positions (c.g. of pack 18 5/8 in above ischium, 6 in back).

Body Position	Location of Av. C. G.	Horizontal & Vertical Range For Subjects
A. Sitting without pack	(8%, 9%)	± 1 1/8"
B. Sitting with pack	(7%, 10%)	± 1 1/8"
C. Standing without pack	(5, 5%)	± 7/8"
D. Standing with pack	(3%, 7%)	± 7/8"

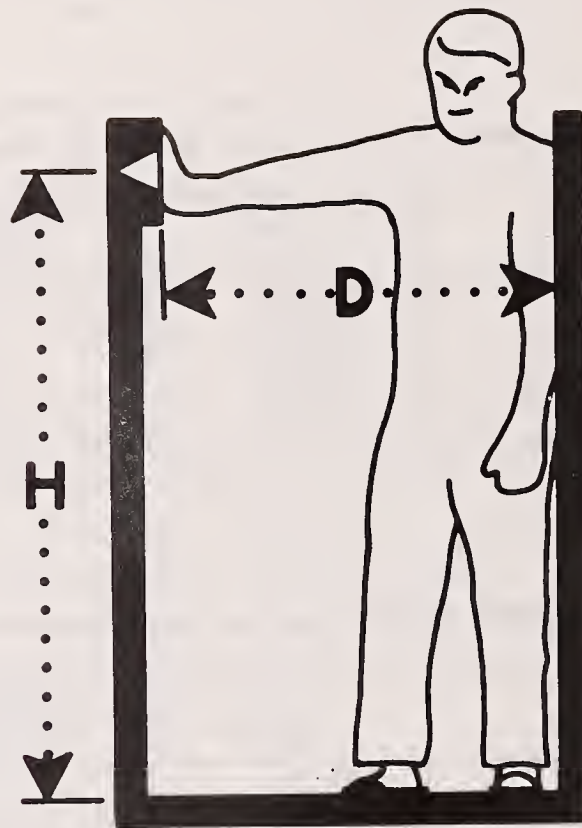


Figure 3.3 Laterally braced push with the preferred hand. Force plate adjusted to a height (H) of 100 % of each subject's acromial height, and to a distance (D) of 80% of his lateral thumb-tip reach.

Percentiles can be used in design to delineate the bounds for a particular characteristic measurement. The design of equipment or structures normally accommodates 95 percent of the sample population by specifying an upperbound, a lower bound or both. In the latter case, the data can be utilized directly to include 95 percent of a group having a particular body characteristic falling within the 2.5th and 97.5th percentile values shown. In guardrail design, however, the value of interest is more likely to be a maximum or a minimum. For instance, if the guardrail height were to safely accommodate 95 percent of the population (i.e., inhibit people from accidentally falling over it), then the measurement of interest would be the centroidal height of the 95th percentile subject. Similarly, to impede the accidental passage through the guardrail, the size of openings would probably have to relate to the head, shoulder or chest dimension of the 5th percentile subject.

The statistical data compiled in tables 3.1 and 3.2 exclude measurements for the 5th and 95th percentile subject required in guardrail analysis. Intermediate percentiles of body characteristics may be retrieved by making use of the fact that anthropometric measurements generally tend to adhere to the normal probability law. Figures 3.4 and 3.5 were developed from the measurements listed in tables 3.1 and 3.2. The ordinates in these charts represent the magnitudes of the given measurements and the abscissa represents the percentage of population whose corresponding measurements are less than the specified values. The scale of the abscissa is such that the plot of a normally distributed function would appear as a straight line. Note that in most instances the points representing the 97.5th, 50th and 2.5th percentile levels of a particular measurement are collinear. This indicates that the distribution is symmetric but not necessarily normal. Connecting these points with a straight line for the purpose of interpolation indicates that a normal distribution is being assumed to describe the variable in question.

Figures 3.4 and 3.5 provide an expedient means of extracting the 5th and 95th percentile body characteristics of both male and female subjects. The percentile characteristics of a mixed sample may be estimated with a reasonable degree of accuracy by averaging the corresponding measurements of the male and female subjects. With regard to the interpretation of body weights, however, a word of caution is in order. Curves A in figure 3.4 give the average body weights of male and female subjects corresponding to respective standing height percentiles specified by curves A in figure 3.5. The average weight of a man having the 95th percentile height, (see curve A of figure 3.4), for instance, is less than that of a man having the 95th percentile weight.

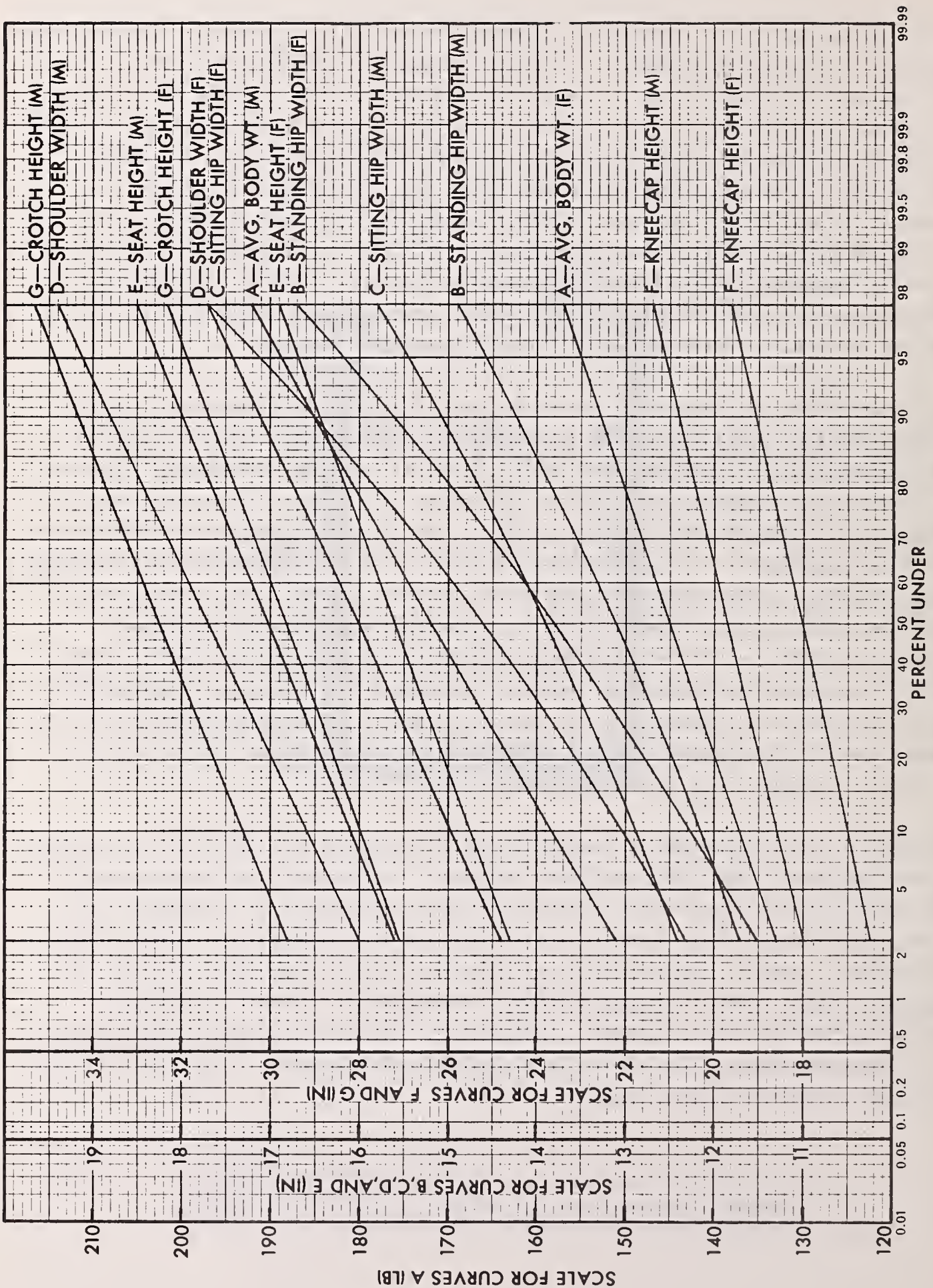


Figure 3.4 Body measurements of U.S. adult male and female subjects according to percentile levels.

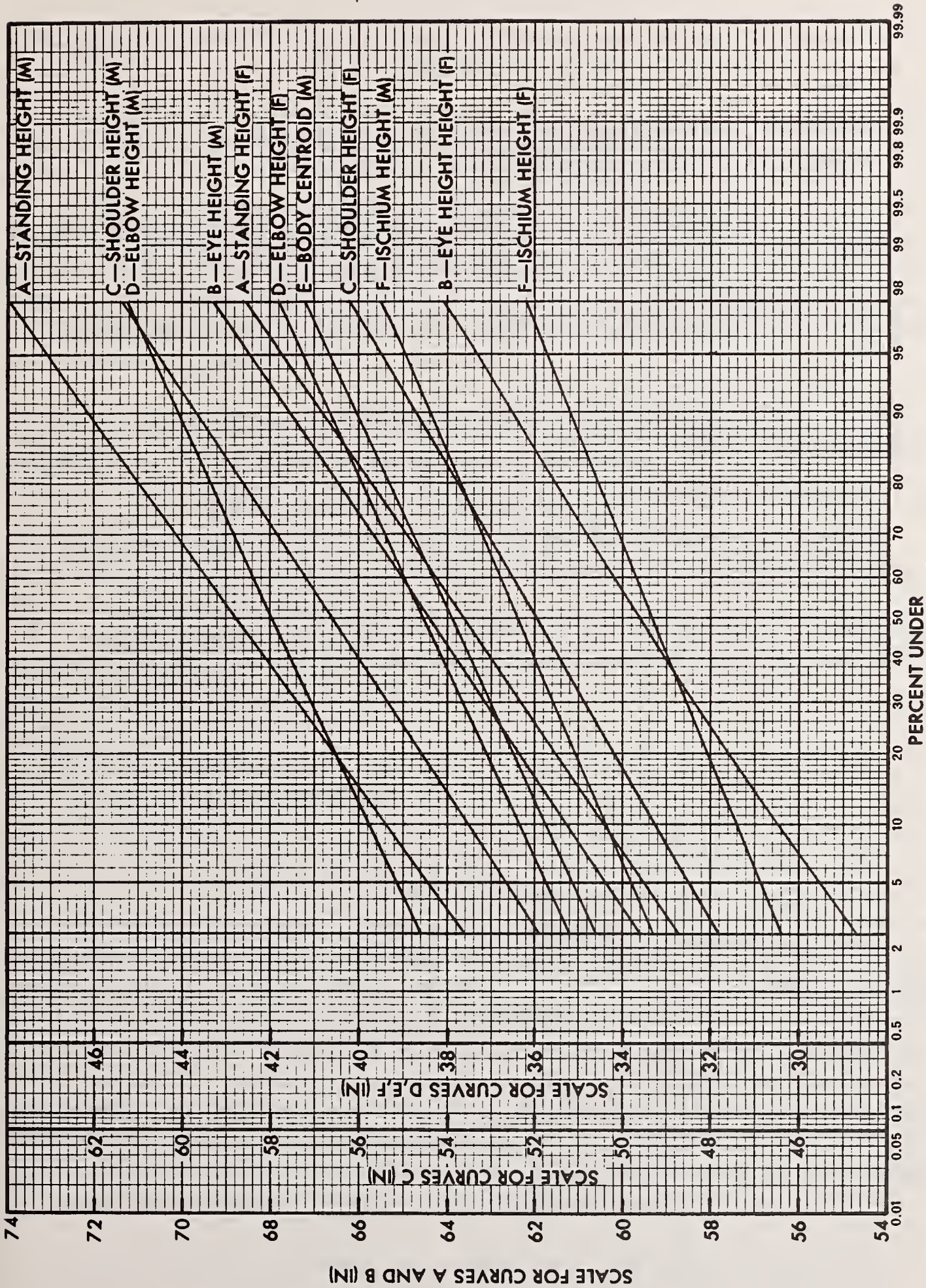


Figure 3.5 Body measurements of U.S. adult male and female subjects according to percentile levels.

References

- 3.1 Diffrient, N. Tilley, A., and Bardagjy, J. Humanscale 1/2/3, MIT Press, Massachusetts Institute of Technology, Cambridge, Massachusetts, 1974.
- 3.2 Swearingen, J., Determination of Centers of Gravity of Man, Project 62-14, Civil Aeromedical Research Institute, Oklahoma City, Oklahoma, 1962.
- 3.3 Kromer, K., Push Forces Exerted in Sixty-Five Common Working Positions, AMRL - TR - 68 - 143, Aerospace Medical Research Lab, Wright-Patterson Air Force Base, Dayton , Ohio, 1969.
- 3.4 Croney, J., Anthropometrics for Designers, Van Nostrand Reinhold Co., New York, New York, 1971.
- 3.5 Van Cott, H. P., Human Engineering Guide to Equipment Design, American Institute for Research, Washington, D. C., 1972.
- 3.6 Singleton, W. T., Fox, J. G., and Whitfield, D., Measurement of Man at Work: An Appraisal of Physiological and Psychological Criteria in Man-Machine Systems, Van Nostrand Reinhold Co., New York, New York, 1971.
- 3.7 Woodson, W. E. and Conover, D., Human Engineering Guide for Equipment Designers, University of California Press, Berkeley, California, 1973.

4. Field Survey of Guardrail Installations

4.1 General

This section presents a general overview of the types and locations of guardrails in the work environment based on information acquired through a field survey.

The objective of the site visits was to gain familiarity with current practices of prototypical guardrail installations and their use. Field examination of the various guardrail types helped identify safe as well as unsafe situations due to inadequacies in design and construction, exposure to corrosive agents and other detrimental environmental conditions, and, in some instances, the inadequacy of the physical environment to permit the installation of appropriate safety barriers.

Prior to the field survey, ten different types of guardrail installations in public and industrial settings were identified by OSHA to be of primary concern. These installations are listed in the approximate order of decreasing priority as follows:

- (1) Elevated walkways
- (2) Scaffolds and staging platforms
- (3) Balconies and mezzanines
- (4) Hot-dip galvanizing operations
- (5) Roofing operations
- (6) Cast-in-place concrete construction
- (7) Petro-chemical towers
- (8) Mobile equipment
- (9) Elevated work and storage areas
- (10) Marine dry docks

Eight of these installations were included within the scope of the field survey. The excluded ones were petro-chemical towers and mobile equipment. In addition, in a series of "by chance" encounters, other miscellaneous types of guardrail installations were observed to be used for the purpose of restricting human movement in a variety of extremely hazardous to slightly hazardous areas. In all but one of the locations visited during this survey the purpose of the guardrail was to prevent falls from a higher elevation to a lower elevation. The one location which differed was a hot-dip galvanizing plant where the "guardrail" was used to prevent movement or falls into the hot-dip kettle containing molten zinc at a level above the working surface. Because the barrier has considerable width in addition to height, both of these geometric features contribute to the prevention of workers from accidentally coming into contact with the zinc.

Visits occurred during working hours on week days. A member of the staff of the facility being visited served as a guide for the team of NBS observers. Observations

during each visit were recorded on a checklist supplemented by photographs. The majority of the visits to both public and private organizations were prearranged.

The checklist was categorized to include observations not only of guardrails, but also other aspects of their environment. This method provided an ordered and overall view of accident safety and a basis for developing the second phase tasks of the project. The sources of the data were: (1) comments supplied by the guide, (2) impressions of the NBS observers, and (3) dimensional measurements and material descriptions of the guardrails. The information gathered consisted of: (1) the general location and function of the guardrail within the installation, (2) types of employee activities near the guardrail, (3) environmental characteristics of the area in the immediate vicinity of the guardrail as well as the general topography of the background, and (4) a physical description of the guardrail.

4.2 Elevated Walkways

4.2.1 Shopping Center, First Site

The first guardrail installation examined was located on the second level of an enclosed shopping center. The area was an elevated walkway which provided access to a variety of retail stores. The guardrail functioned as a barrier restricting movement or accidental falls into a series of large wells opening to the ground level (figure 4.1).

Several types of employee activities were observed in the vicinity of the guardrail. Human traffic to and from various locations typically occurred during the hours that the center was open. Surveillance and monitoring of the ground floor by security employees occurred intermittently during which time the guardrail was used for casual leaning and watching events at the lower level. Maintenance activities near the guardrail involved cleaning of carpets, benches and ashtrays and emptying waste receptacles.

The guardrail was well defined relative to the background and highly visible from all points of entry into the region aided by uniform electric and natural lighting through skylight openings in the roof. The surfaces adjacent to the guardrail were carpeted floors with rubber tile in areas around benches.

The top rail was made of aluminum tubing material and was located 41.75 in (106 cm) above the tread. The steel posts of tubular section were spaced at 5 ft (152.4 cm) on centers and the tubular steel toeboard was approximately 2 in (5.08 cm) high. There were no intermediate rails but rather 0.5-in (1.27cm) round steel balusters placed 5 in (12.7 cm) on centers. As indicated in figure 4.1, several of these balusters were bent out of shape creating a potentially hazardous situation for accidental passage of children through guardrail openings. However, consideration of such a concern is not within the scope of these studies which are addressed to the guardrail needs of adult personnel.

4.2.2 Shopping Center, Second Site

The second guardrail installation examined was located at the edge of an elevated walkway at the exterior of the same shopping center (figure 4.2). The walkway was used for delivery of merchandise to the stores and removal of trash. The guardrail served as a barrier to prevent falls into a sodded area one story below.

Three types of employee activities were observed occurring on the walkway: (1) routine use of the walkway to gain access to either the stores or the parking area, (2) pulling or pushing hand trucks filled with merchandise, and (3) carrying boxes, packages, and other miscellaneous discarded objects.

No extreme environmental characteristics were observed. The temperature and lighting were natural, the sound level was produced by light vehicular traffic. The walkway was 5.9 ft (1.8 m) wide and consisted of a cast concrete slab supported by steel framing cantilevered from the building.

The guardrail was a solid wall made of 8-in nominal concrete masonry units (7.5 in or 19 cm in actual thickness) and precast concrete capping. The top of the guardrail was 43 in (109.2 cm) above the tread surface.

4.3 Scaffolds and Staging Platforms

4.3.1 Library Structure

The guardrails examined at this site were located around scaffolds erected on two sides of a seven-story library building (figure 4.3). The scaffold was being used for the purpose of applying masonry facing to this building. The function of these temporary construction guardrails was to prevent accidental falls to a concrete plaza one to seven stories below.

Work-related employee activities near the guardrail involved bending, stooping, crouching and standing to perform the masonry work necessary in the marble-facing operation. Other activities such as walking towards exit points and delivery of materials to locations along the scaffold occurred periodically.

Visibility of the guardrails was generally good. The flooring of the scaffolds consisted of aluminum planks. The two adverse environmental conditions observed were the presence of materials and equipment stored along walking and working surfaces and the occurrence of intermittent wind gusts particularly at the higher elevations.

The top and intermediate rails were aluminum angles or pipe sections located at a height of 39 in (99.1 cm) and 21 in (53.3 cm) from the tread surface, respectively.

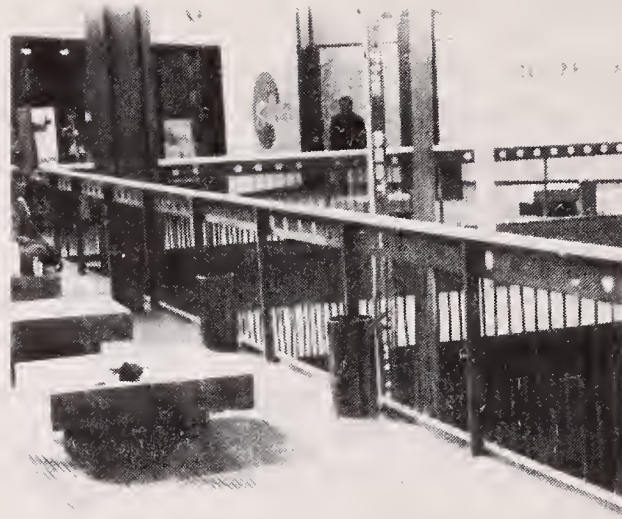


Figure 4.1 Guardrail location within enclosed shopping center.

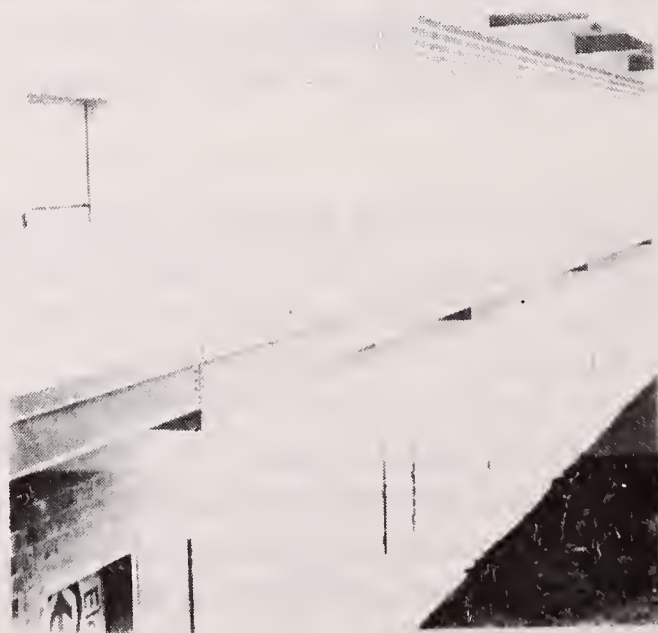
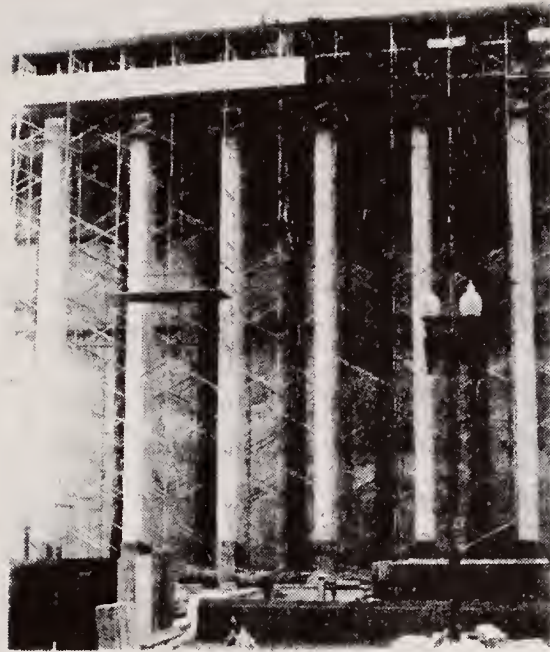
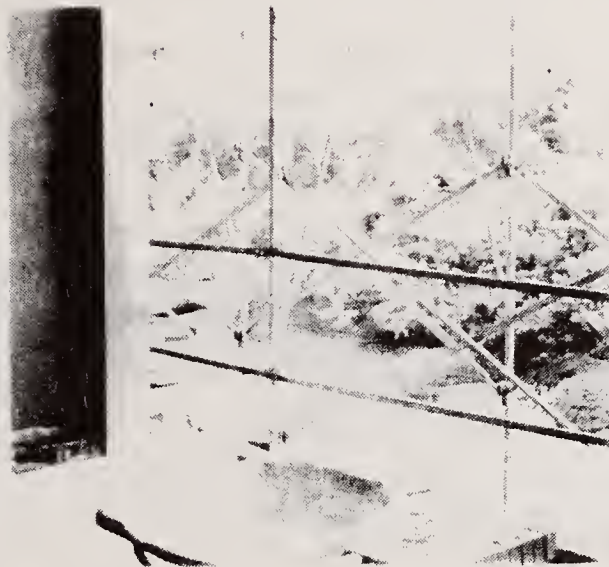


Figure 4.2 Guardrail location outside shopping center.



(a)



(b)

Figure 4.3 Temporary guardrails used during construction of a multi-story library building.

Toeboards were frequently absent. When used, they were made of 1-in by 4-in (2.54-cm by 10.16-cm), nominal, wood board. Guardrail elements were connected by bolts or miscellaneous clamping devices.

4.3.2 Pharmaceutical Supply Co.

At this location, the guardrail was attached to a suspended scaffold being used in the application of fascia materials to the building (figure 4.4). The intended function of the guardrail was to prevent inadvertent falls to the ground three stories below.

The employee task near the guardrail was the application of bolts to the concrete facade. The activity involved bending and standing. The workmen were wearing safety belts with rope lanyards attached to the wood top rail which was being used to serve as a lifeline as well as a safety barrier.

The work was being performed on the exterior of the building and there were no unusual characteristics observed with respect to lighting or temperature. The floor of the scaffold was made of aluminum planks. A potentially hazardous characteristic observed was the presence of power tools and extension cord attachments on the floor of the scaffold.

The top rail was a 2-in by 6-in (5.08-cm by 15.24-cm), nominal wood board, about 42 in (106.7 cm) above the tread. Although this rail was intended to serve as a lifeline as well as a barrier, it appeared to be structurally quite inadequate to support the impact load of a falling human subject transmitted through the lanyard. The wood toeboard was 1 in by 4 in (2.54 cm by 10.16 cm), nominal. There were no intermediate rails. Suspended from the roof by a counterweight device mounted on wheels (figure 4.4 b), the scaffold could be moved easily along the building perimeter. Roofers were working at the same time as the men on the scaffold and the perimeter guarding system for the roofers was either removed or being laid down to allow the mobile scaffold support system to move along the building edge. This was the first observation of a conflict between a safety requirement for one trade and the construction method of another.

4.3.3 Miscellaneous Suspended Scaffolds

Two sites of suspended scaffolds were examined while passing buildings where construction activity was occurring (figure 4.5). For one instance, the scaffold was being used by bricklayers (figures 4.5 a). It was constructed entirely of wood. The guardrail consisted of plywood boards attached to vertical wood posts joined by horizontal members at the top. The second scaffold was located at the site of a building being remodelled (figure 4.5 b). It appeared to have a metal plank floor and no guardrails at the ends or at the side nearest the building. At the far side, the wood guardrail consisted of top and intermediate rails and a toeboard, all supported by two end posts estimated to be at least 20 ft (6.1 m) apart. This spacing was judged to be excessive in relation to the apparent size of the

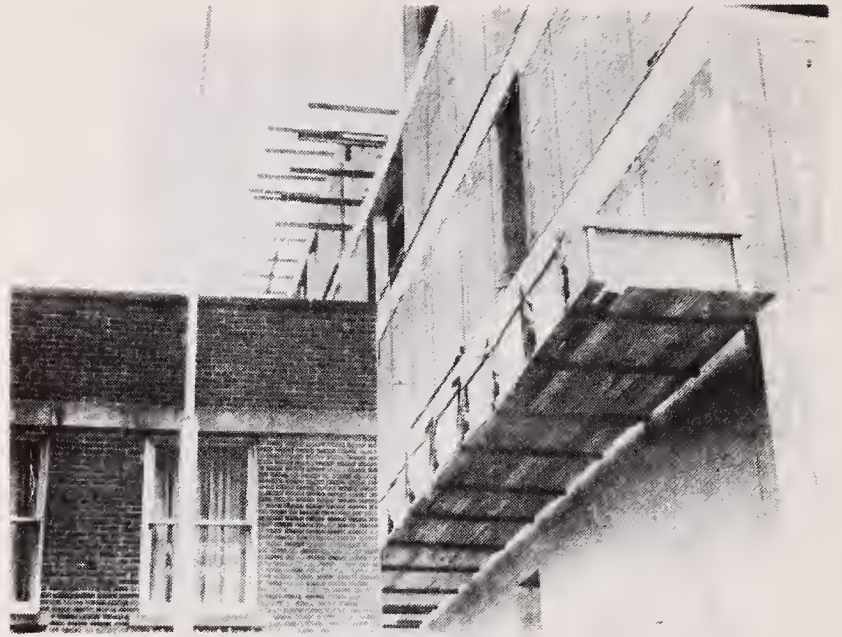


(a)



(b)

Figure 4.4 Temporary guardrails on scaffolds or staging platforms used during construction of pharmaceutical building.



(a)



(b)

Figure 4.5 Examples of temporary guardrails on suspended scaffolds used in construction, maintenance or renovation of buildings.

top rail to prevent a structural failure in the event of an accidental fall of the employee against the guardrail.

4.4 Balconies and Mezzanines

4.4.1 Hotel Structure, First Site

The first guardrail installation examined was located at the edges of the balconies of the guest rooms of a hotel. The guardrail served as a barrier to prevent falls from heights of one to six stories above grade (figure 4.6).

Cleaning the sliding glass doors and windows from the balcony was the principal employee activity identified at this site.

The temperature and lighting were natural. The balcony slab was cast-in-place concrete. The walls were either glass panels or brick veneer. The balcony was about 31 in (78.74 cm) wide.

All guardrail components appeared to be made of aluminum. The top rail was a 2-in wide by 4-in deep (5.08-cm by 10.16-cm) rectangular tube, the top of which was 42 in (106.7 cm) above the tread. There were no toeboards or intermediate rails but rather, 0.75-in (1.9-cm) square tubular balusters 6 in (15.2 cm) on centers between the top rail and a 1-in. (2.54-cm) square tubular bottom rail 6.5 in above the tread. The posts were 2-in (5.08 cm) square tubular sections at 52-in (132 cm) intervals. Each post was fitted into the sleeve of a base plate and attached to it by two screws driven from opposite sides. The rail components were connected by welds and screws. The square base plate was attached to the concrete slab with four anchor bolts and nuts which were not galvanized. As a result, evidence of severe corrosion was observed at several locations. In addition, many of the nuts had become loose or completely detached.

4.4.2 Hotel Structure, Second Site

The second guardrail installation examined was located within the lobby of the same building. The lobby served as an access to various hotel service areas and as a sitting lounge. On each side of an open stairway, a guardrail served as a barrier to prevent falls to the ground level one story below (figure 4.7).

The employee activities occurring near the guardrail were routine walks from one location to another and cleaning operations of floors.

The light level was high because of a nearby window wall. In addition, the window wall produced a significant amount of reflected glare in the location adjacent to the guardrail.



(a)



(b)

Figure 4.6 Permanent guardrail installations on balconies of multi-story hotel structure.



(a)



(b)

Figure 4.7 Permanent guardrails used in lobby of hotel structure.

The guardrails were quite similar in materials, layout and sectional configuration to those installed at the balconies (section 4.4.1) except the top rail was a 2-in wide by 4-in deep (5.08-cm by 10.16-cm) finished wood board. Since these guardrails were located indoors, no evidence of corrosion at the anchorages was anticipated and none was observed.

4.5 Hot-Dip Galvanizing Operations

4.5.1 Galvanizing Plant, First Site

The first location examined was a galvanizing kettle containing molten zinc equipped with an overhead conveyor system (figure 4.8). In this case the walls of the kettle above the work surface served as a barrier (guardrail) to keep the employees from accidentally coming in contact with the zinc. The top shelf of the wall served as a support for hand tools used by the employees working at the kettle.

Routine work-related employee movements included walking, standing next to and leaning over the barrier to skim the zinc surface with a wooden paddle and tapping the galvanized objects with long implements as they were retrieved from the kettle.

The lighting around the work area was generally much dimmer than in a typical office. The concrete floor surfaces adjacent to the kettle were generally cluttered with debris.

The top of the wall barrier was 31 in (78.7 cm) above a 7-in high by 34-in wide (17.8-cm by 86.4-cm) platform (tread surface) located on the working side of the kettle. The width of the wall was 28 in (71.1 cm) at the top. This surface was made of welded steel plates. A typical sectional configuration of the barrier is shown in Figure 4.8 b.

4.5.2 Galvanizing Plant, Second Site

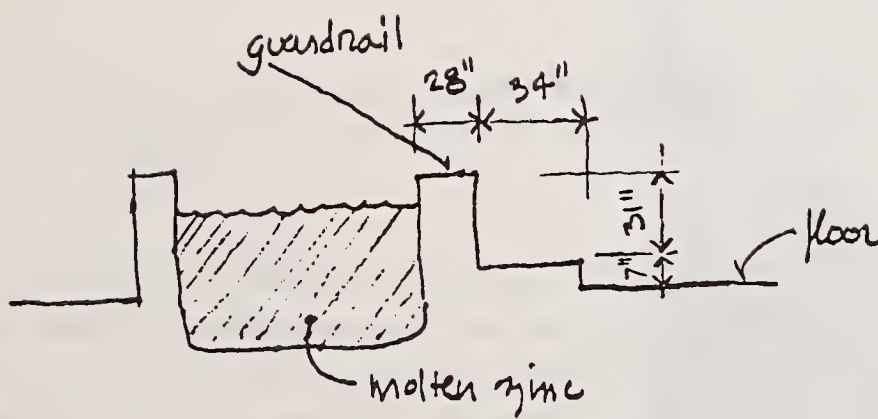
The galvanizing kettle examined at this location was similar to the first one except the kettle walls were shallower and there were no raised work platforms (figure 4.9). As before, both the height and width of the kettle walls served as barriers to restrict employees from coming in contact with the molten zinc. The top of the wall was used as a shelf for various tools and as a means to gain leverage in maneuvering the galvanized objects with metal implements.

In addition to the work activities observed at the first site, the employees were engaged in manipulating and aligning a large suspended appliance. This involved pulling cords, pushing and tapping the appliance with hand implements, and jacking it with long rods using the shelf of the wall as pivot.

The environmental characteristics were similar to those observed earlier. The accumulation of substantial debris on the floor adjacent to the exit side of the kettle



(a)



(b)

Figure 4.8 First example of wall barrier around molten zinc kettle used in galvanizing operations.

(the foreground area shown in Figure 4.9 b) caused a reduction in the wall height at that location and consequently in its effectiveness to function as a safety barrier.

The sectional configuration of the wall barrier was rectangular as shown in figure 4.9(c), the height and width being 26 in (66cm) and 24 in (60.1 cm), respectively. The walls consisted of an assembly of welded steel plates.

4.5.3 Galvanizing Plant, Third Site

At this location the galvanizing was carried out by using manually controlled chain and pulley equipment (figure 4.10) as opposed to the use of conveyor systems observed at the first two locations (figures 4.8 and 4.9). As before, the walls of the kettle functioned as barriers to prevent accidental body exposure to molten zinc and as support for the hand tools used by the employees working at the kettle.

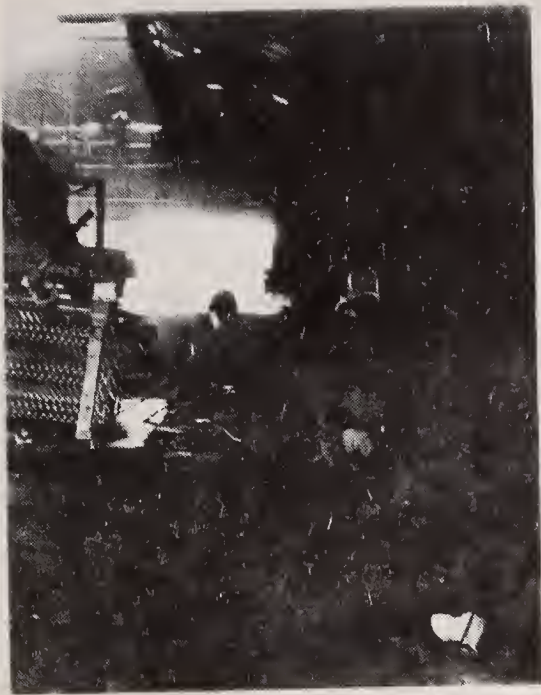
Besides the activities noted earlier, this operation required manipulation of the chain-pulley assembly to lower or raise the objects being galvanized. The kettle was equipped with a ledge which provided a bearing surface for the foot to facilitate pulling the object out of the vat. However, the ledge reduced the effective height of the barrier and encouraged hazardous postures, for the purpose of gaining reach advantage, such as shown in Figure 4.10 c.

Visibility and other environmental factors were similar to those observed at the other two locations. The concrete tread surfaces near the kettle were likewise littered with various objects and debris.

The barrier was 25 in (63.5 cm) high on all four sides and had an 11-in high by 10-in wide (27.9-cm by 25.4-cm) ledge or projecting shelf on the working side, thereby reducing the effective height of the barrier above it to 15 in (38.1 cm). The 31-in (78.7-cm) width of the barrier was in excess of those at the other two locations. The surfaces were made from welded steel plates. The line drawing in figure 4.1 (d) shows the cross sectional configurations of the kettle.

4.6 Roofing Operations (Retail Merchandise Distribution Center)

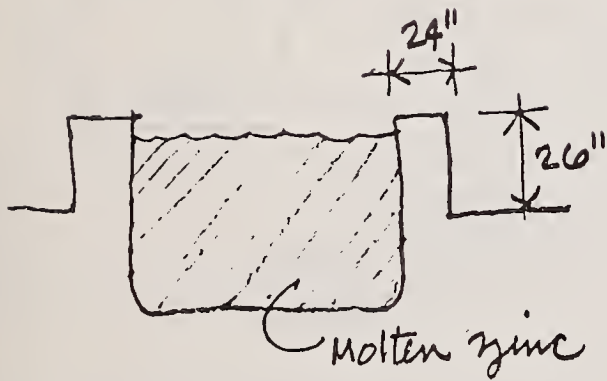
The purpose of this visit was to examine the perimeter-guarding installations used during a large built-up roofing operation on a warehouse having approximately 46 acres of (18.63 ha) storage area. The roof was approximately 30 ft (9.1 m) above grade and the roofing operations were at various stages of completion (figure 4.11 and 4.12). The guardrails at this site were symbolic rather than physical barriers, placed at a distance from the edge of the roof to alert workers of the potential hazards of the region beyond the demarcation line. These rails were not in compliance with the existing perimeter



(a)



(b)



(c)



(d)

Figure 4.9 Second example of wall barrier around molten zinc kettle used in galvanizing operations.



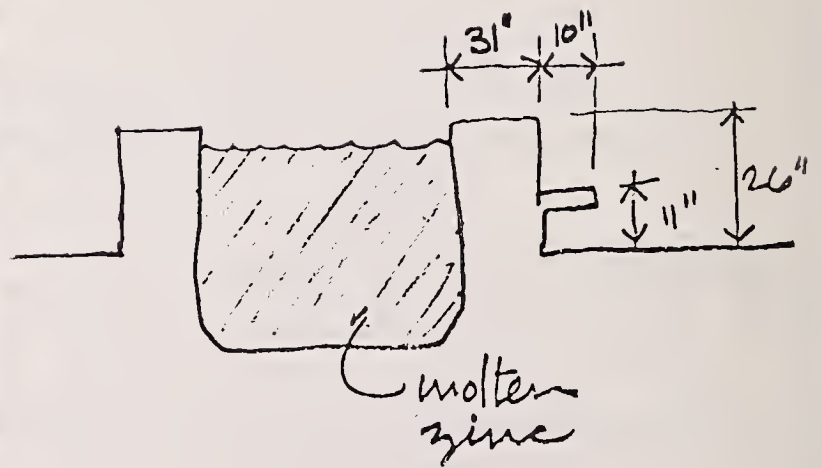
(a)



(b)



(c)



(d)

Figure 4.10 Third example of wall barrier around molten zinc kettle used in galvanizing operations.

guarding regulations of OSHA. However, because of an absence of construction provisions, prior to the roofing operations, for the attachment of compliant guardrail systems, the roofing contractor had been given a variance by OSHA to use the portable symbolic guardrails shown, subject to specific restrictions governing the movement of workers within defined hazard zones at the periphery of the roof.

The primary activities for installing the roofing were pushing and pulling machines while applying layers of felt or tar, bending to place installation, or standing and shovelling gravel. At one time or another, the application of each layer required the employees to get close to the edges. Operations and application of roofing to the edge required the joint effort of 2 to 3 workers whose movements included standing, walking leaning and crouching.

Extension of the facade beyond the top of the roof provided about a 12-in (30.5-cm) high ledge at its periphery. This served the (unintended) function of a toeboard and provided some measure of safety for employees when conducting their work tasks in a crouched posture. The roofing consisted of a corrugated steel deck on open web steel joists, and layers of rigid insulation boards, tar-coated roofing felts and gravel. At times the 1/4-in (0.6-cm) wire rope warning rails were not readily discernible against the background terrain (figure 4.11 a) and in some instances the light brown gravel surface merged with the clay-colored terrain 30 ft (9.1 m) below making it difficult to visually discriminate the drop beyond the roof edge. The presence of equipment and various materials on the walking surfaces near the edges required a certain level of alertness on the part of the observers to avoid tripping. Also very hazardous, was the slippery corrugated metal deck surface when wet.

The symbolic guardrail consisted of two 1/4-in (0.64-cm) wire ropes clamped to steel posts attached to 40-lb (178-N) cast concrete blocks at the base. Trials were being made to increase the lateral stability of the posts through adhesion of stick clips with the tar surface (figure 4.12 b). Without such adhesion, a 6 lb. (26.7N) horizontal force applied to the top of the post would cause it to overturn.

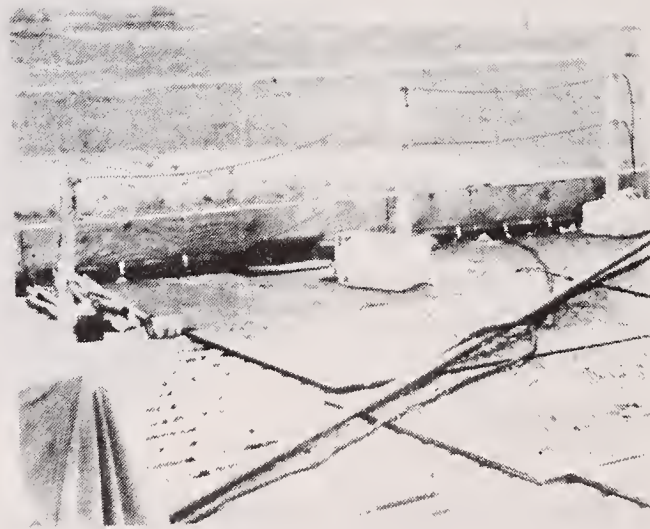
4.7 Cast-In-Place Concrete Construction

Two types of guardrails which were used in cast-in-place concrete construction work were examined while passing sites where construction was occurring. At the first site, the guardrail was being used to prevent falls from a walkway work platform adjacent to the concrete forms around the buildings (figure 4.13 a). The walkway appeared to be used by carpenters during the preparation of the wood formwork, by workers placing the steel reinforcement inside of the forms, and by workers casting and curing the concrete.

The guardrails were assembled in a manner to permit quick dismantling and reassembly for use in construction of additional floors of the building. They consisted of 2-in



(a)



(b)

Figure 4.11 Symbolic guardrails used in built-up roofing operations.



(a)



(b)

Figure 4.12 Additional exhibits of built-up roofing operations.

by 4-in (5.08-cm by 10.16-cm), nominal, wood, top and intermediate rails and vertical supports spaced approximately 8 ft (2.44 m) on centers. The rails were fitted into the slots of plywood gusset plates nailed to the posts. The platform guardrail assembly was supported by equally-spaced 4-in (10.16-cm) square, nominal, wood beams wedged between the exterior concrete floor beam and 4-in (10.16-cm) square, nominal, spliced wood shoring posts below, and by diagonal members fastened to the same shoring posts. No guardrail toeboards were observed at this site.

At the second site visited (figure 4.13 b and c), the concrete had already been cast and the forms removed. The guardrails were placed at the edge of the concrete slabs to prevent accidental falls of workers engaged in concrete curing and finishing operations. The guardrails consisted of modular steel pipe framing units joined together by a wood top rail. The assembly was seated on the concrete slab but not attached to it.

4.8 Elevated Work or Storage Areas

4.8.1 Library Building, First Site

The guardrails examined at this site were located in construction work areas around large central openings inside the building (figure 4.14) to prevent accidental falls of workers from 12-ft to 72-ft (3.66-m to 21.95-m) high elevations.

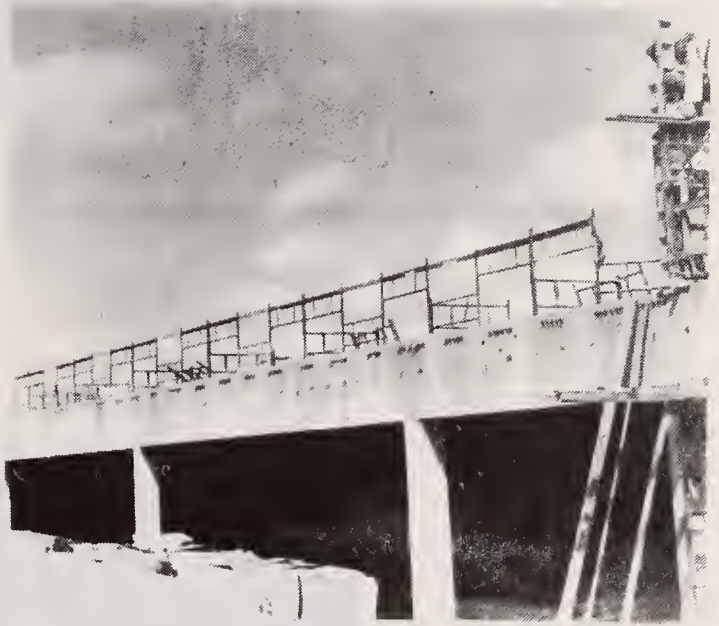
The only employee activity observed was the routine movement of walking past the guardrails. Other construction-related activities are likely to occur near the rails where the interior finishes are applied and permanent guardrails are installed at the same location before the building is put in service.

The lighting around the guardrail area was generally dim. As a result, the cable rails and sometimes the wood rails as well, tended to merge with the background and were not always readily visible. Another hazardous situation was the presence of miscellaneous construction materials and debris on the concrete floor adjacent to the rails.

There were two types of guardrails installed around the opening. One was constructed of wood (figure 14.a) with a 42-in (106.7-cm) high top rail and 24-in (61-cm) high intermediate rail. The spacing of the vertical posts varied from 5 ft to 7 ft (1.5 m to 2.1 m) on centers and the toeboard height varied from 4 in to 10 in (10.16 cm to 25.4 cm). The wood members were typically 2 in by 4 in (5.08 cm by 10.16 cm), nominal, and were fastened together with nails. The second type (figure 14.b) used 1/2-in (1.27-cm) wire rope top and intermediate rails, 43 in (109.2 cm) and 22 in (558 cm) from the tread, respectively. The vertical wood supports were spaced between 5 ft to 7 ft (1.5 to 2.1 m) on centers. The wood toeboard was 6 in (15.2 cm) high. The wire ropes were looped around and tied to concrete columns located along the periphery of the openings. They were kept taut by means of turnbuckles.



(a)

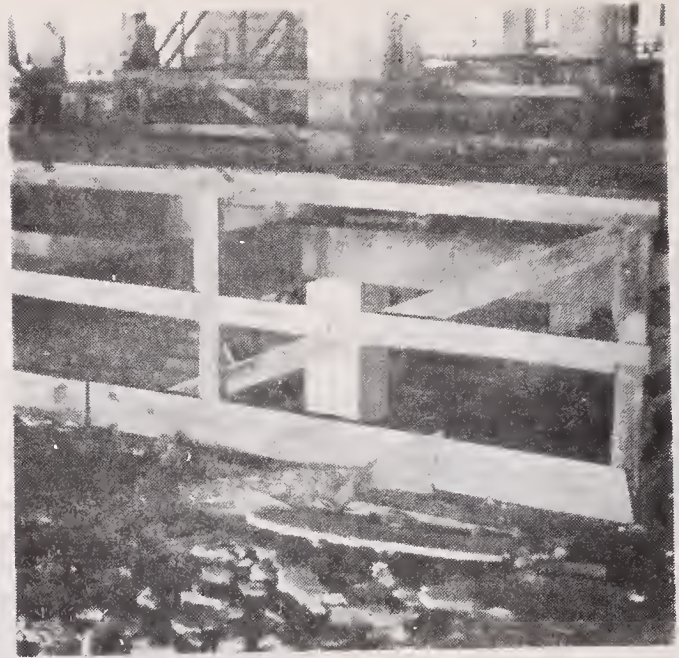


(b)

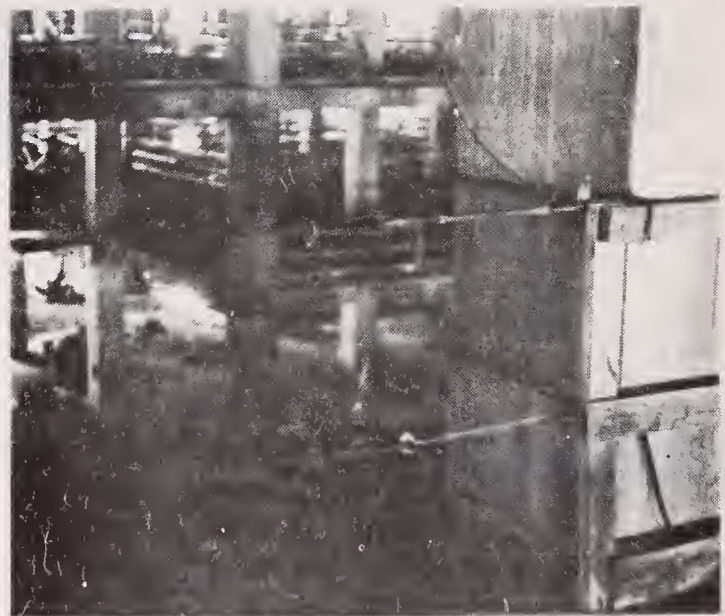


(c)

Figure 4.13 Miscellaneous types of temporary guardrails used in cast-in-place concrete building construction.



(a)



(b)

Figure 4.14 Temporary guardrails installed around openings during construction of multi-story buildings.

4.8.2 Library Building, Second Site

The second location observed was a materials storage area adjacent to a large opening in the exterior wall of the building (figure 4.15). The location served as a storage area for bricks and as an access point to the exterior scaffolding. The guardrail was symbolic and served the purpose of alerting workers to the opening approximately 10 ft (3 m) away.

The only employee activity observed was the routine movement of walking past the guardrail. It was assumed that the use of hand and motorized vehicles for carrying brick occurred near the rail.

The concrete floor surface adjacent to the rail was littered with wood remnants and other miscellaneous debris.

The guardrail consisted of two wire ropes loosely attached to two of the building columns approximately 30 ft (1.4 m) apart. The top rail was 35 in (89 cm) high and the intermediate rail was 14 in (35.6 cm) high. There were no toeboards.

4.8.3 Post Office Building

The guardrails examined were located in the mail sorting and routing areas of a large post office. They were installed around platforms used for the maintenance of conveyor belts and other machinery (figure 4.16). The platforms were approximately 12 ft (3.66 m) high and the rails served as barriers to prevent falls (figure 4.16).

While no employee activities were observed during the visit, the guide noted that cleaning, repair and maintenance work of motors and other pieces of equipment were the primary type activities on the work platforms.

The lighting on the platforms was adequate to distinguish between small objects. The working surface was made of steel grating.

The top rail on the first type of platform was 41 in (104.1 cm) high with a 20-in (50.8-cm) high rail and a 3-in (7.62-cm) high toeboard. Vertical supports were located at 5.25-ft (1.6-m) intervals. The top rail, intermediate rail, and toeboard were made of steel angles connected with bolts, and welds. On the second type of platform, the top rail was 41 in (104.1 cm) high, the intermediate rail was 21 in (53.3 cm) high, and the toeboard was 3 in (7.62 cm) high. Vertical supports were spaced at approximately 3 ft (91.4 cm) on centers. The rails were steel pipe sections and the toeboard was a steel angle. All connections were welded joints. On the third type of platform the top rail was 36 in (91.4 m) high, intermediate rail was 18 in (45.7 cm) high, and the toeboard was 4 in. (10.16 cm) high. Vertical supports were spaced at approximately 5.75 ft (1.75 m) on centers. The rails were steel pipe sections and the toeboard was a steel angle. All connections were welded joints.

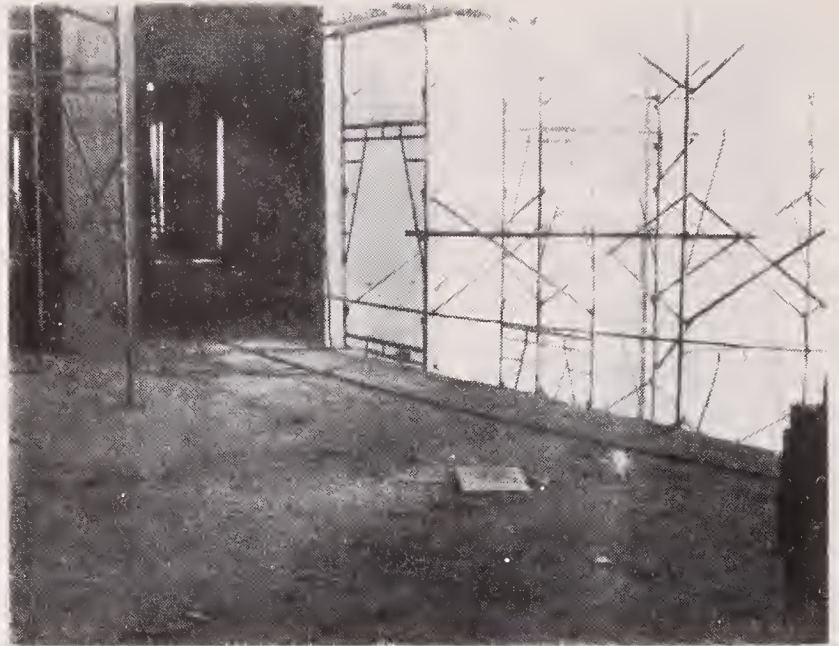


Figure 4.15 Temporary guardrails around storage area used during construction of multi-story building.

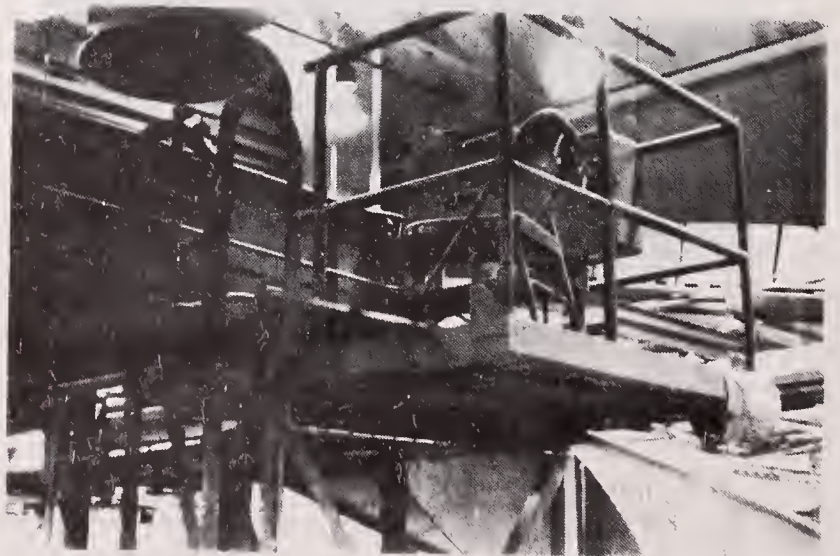


Figure 4.16 Guardrails installed around platform used for maintenance of machinery.

4.9 Marine Dry Docks

4.9.1 Ship Yard, First Site

The guardrails examined at this site were located around a dry dock for the maintenance and repair of ships (figure 4.17). Judging from a posted sign warning people not to lean against them, these guardrails were intended to be symbolic rather than physical barriers to prevent falls to a concrete surface approximately 50 ft (15.2 m) below.

The warning signs were not always effective in discouraging employees from leaning against the guardrail to observe activities in the dry dock area (figure 4.17 b). There were no other activities observed except employees walking past the guardrail.

The guardrail was visible at all locations visited. There was evidence of corrosion which is probably aggravated by the proximity of a large body of water as well as by rain and humidity. Another potentially hazardous condition experienced was the occurrence of high wind gusts in the general vicinity of the guardrail.

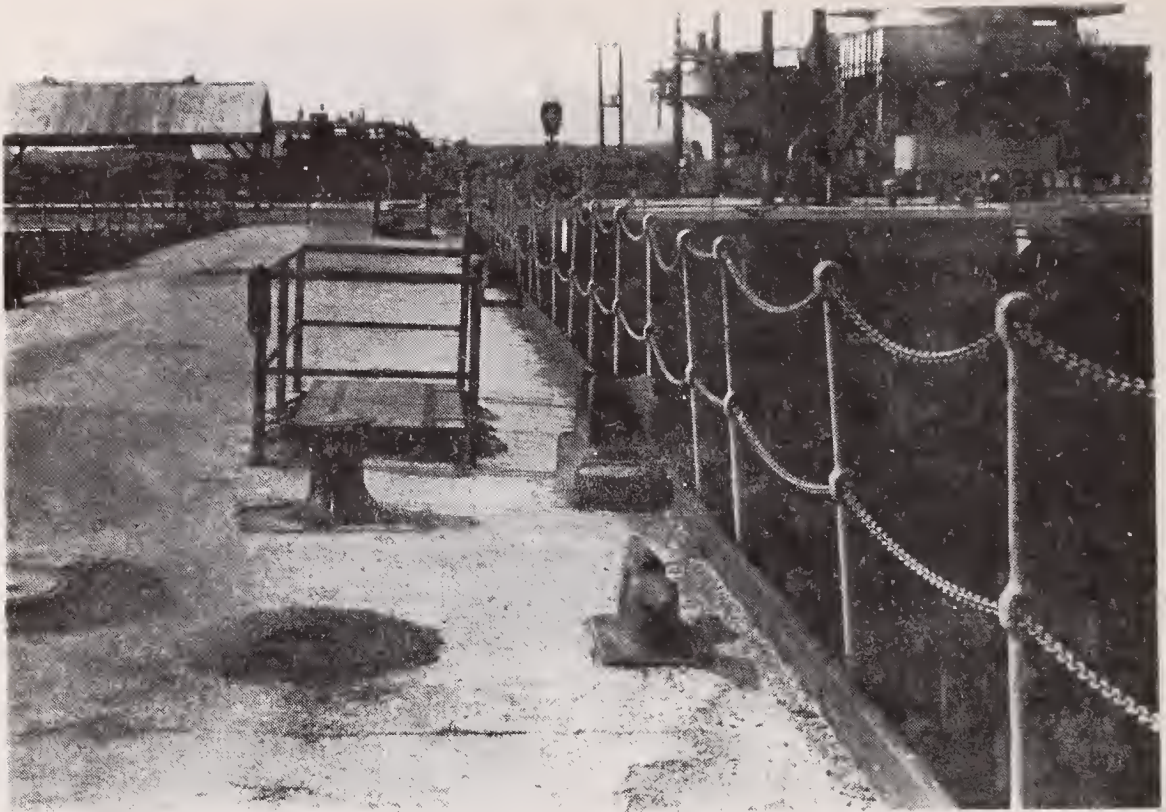
The guardrail consisted of cast steel posts spaced at 7.25 ft (2.2 m) on centers, a set of 2 or 3 steel chain rails passing through slots in the posts and occasionally, a 7-in (17.8-cm) high concrete curb or metal toeboard (figure 4.17). Despite the warning sign, at first glance the guardrail could convey the false (and dangerous) impression of being structurally sturdier than it actually is. This is partly due to the fact that the chains are installed with a built-in slack and are not constrained from sliding through the slots. Consequently, a force applied to the rail will cause it to sag excessively by taking up the slack from the adjacent spans as in figure 4.17(b). It also appeared that some of the post anchorages would not be capable of transmitting lateral forces to the foundation because of either loose fittings, or insufficient edge distance.

4.9.2 Ship Yard, Second Site

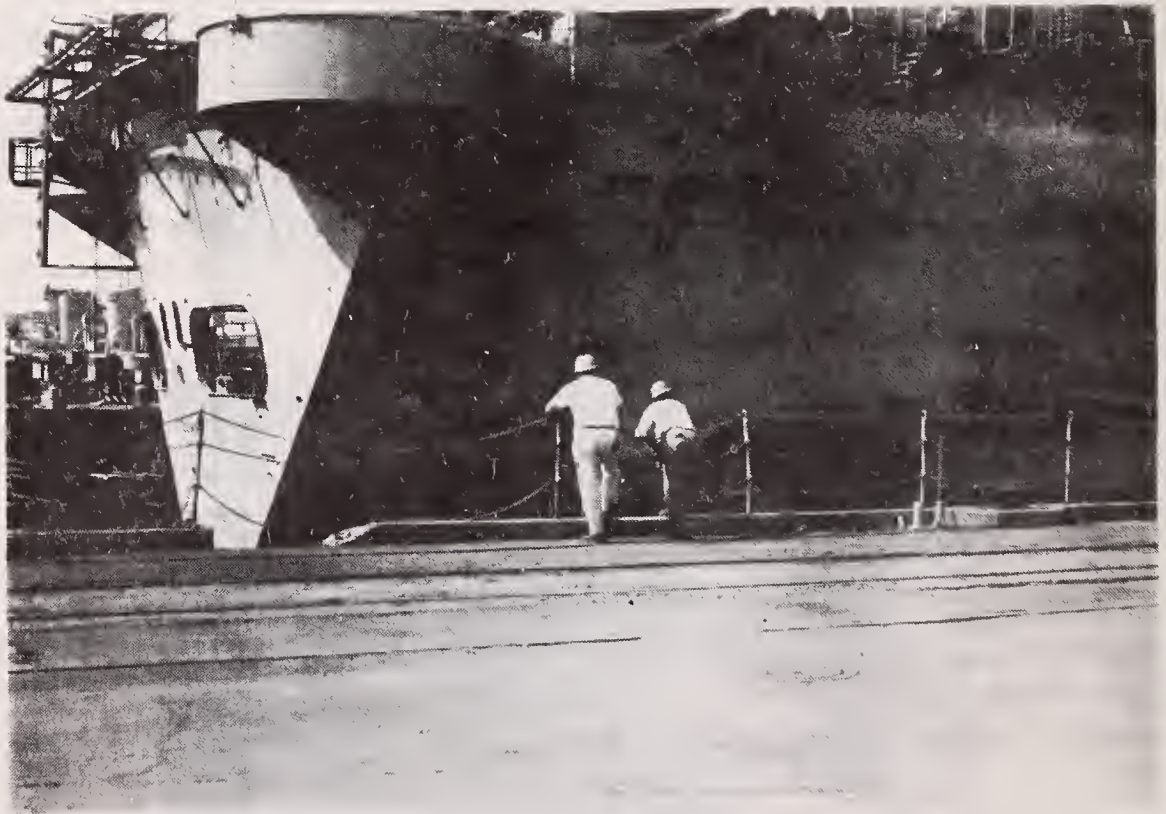
At this site the guardrail was located around a marine railway catwalk (figure 4.18). The marine railway is used for the maintenance and repair of submarines. The guardrail functioned as a barrier to prevent falls into water or onto a wood deck or concrete surface approximately 50 ft (15.2 m) below.

While no employee activities were observed during the visit, the guide noted that the catwalk was used only as a walkway.

The surface around the guardrail was a wood plank floor. The catwalk was 42 in (106.7 cm) wide. The characteristics considered potentially hazardous were excessive projections of the anchoring devices into the walkway and the occasional gusts of wind.



(a)



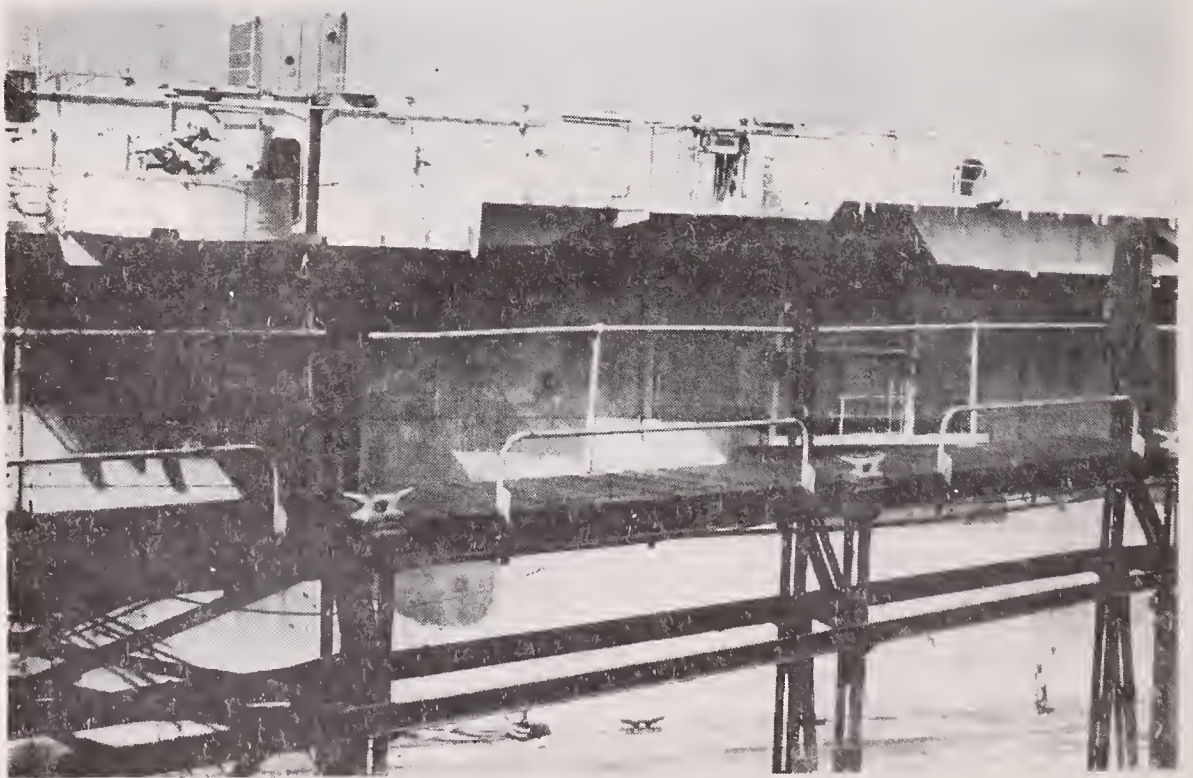
(b)

Figure 4.17 Permanent symbolic guardrails installed at marine dry dock facility.

There were different guardrails on each side of the walkway. On the outside (the side away from the ship being worked on), the top rail was 37.5 in (95.2 cm) high with vertical supports at 5 ft (1.5 m) on centers (figure 4.18 a). There was no intermediate rail or toeboard. The top rail and vertical supports were made of steel pipe connected by bolts and welded joints. On the side adjacent to the ship, the guardrail was a series of sections of steel pipe 17.5 in (44.4 cm) high by approximately 6 ft (1.83 m) long (figure 4.18 b). The sections were spaced approximately 4 ft (1.22 m) apart. Connections were made by bolts and welded joints. The size and design of the rail appeared to provide little protection from falls.



(a)



(b)

Figure 4.18 Permanent guardrails on elevated catwalks.

5. A Conceptual Model of Safety

5.1 Introduction

Safety research attempts to identify methods by which accidents and their consequences can be eliminated or mitigated to insure an acceptably low level of risk of injury or death. Since guardrails are intended to prevent people from entering or falling into hazardous areas, they may be treated as units within a broader framework of a safety system consisting of human and environmental factors. This framework can then serve as a qualitative guide in the preparation of safety requirements for guardrails.

A number of conceptual models have been developed which attempt to identify causes of accidents [5.2, 5.3]. Although most of these descriptions have assisted in further exploration and understanding of accidents and the accident development process, their practical usefulness in designing safe environments or determining safe behavior are limited. This is largely due to the fact that accident research, in general, attempts to identify the causes of accidents post hoc, based on accident data which is seldom adequate. On the other hand, safety research is focused on the prevention and control of accidents through the specification of the requirements for safe environments and procedures. Another deficiency of accident research models is that they emphasize either human causes of accidents or environmental causes of accidents. Safety is a result of complex interactions between both sets of variables, however, and can best be developed and maintained through a simultaneous treatment of both.

The safety model presented in this section attempts to systematize a decision-making process that has heretofore been subjective and often incomplete. Since it is based on fundamental notions of safety originally formulated by Gibson [5.1], a brief introduction to Gibson's ideas is presented first. This is followed by a detailed description of the safety model.

5.2 Gibson's Margin of Safety Concept

Gibson proposes that a margin of safety exists between an individual and an accident. By behaving recklessly an individual overextends his margin of safety and increases the likelihood of an accident; conversely, he may behave very cautiously and decrease the likelihood of an accident. Safe behavior is that which falls within an individual's margin of safety.

According to Gibson, individuals overextend their margin of safety in two ways. The first is by misperceiving danger in the environment (i.e., perceptual failures), the second is by reacting inappropriately to a perceived danger (i.e., behavioral failures). In short, "an individual may suffer harm from a failure to perceive or a failure to act." Perceptual

and behavioral failures are often due to the absence of the environmental characteristics which indicate danger (as in a dark surrounding), or due to unreliable environmental characteristics (such as seats that look sturdy but are not). Perception may fail even when environmental characteristics are present and reliable. This may occur because of (a) defects in the sensory apparatus; (b) immaturity of the sensory apparatus; (c) temporary incapacity from drugs or illness; (d) untrained discrimination; (e) inattention. Behavior may likewise fail even though the environment provides cues to safety performance. This may occur because of defective, inadequate untrained, or temporary incapacities of behavior. As with perceptual failures the solutions to these performance failures most often involve training and education.

5.3 A Conceptual Framework of Safety

The conceptual safety model displayed in figure 5.1 extends Gibson's fundamental notions of safety by taking into account additional human and environmental factors and their interrelationships. First, accidents occur in social as well as physical environments. Safety is often a function of interpersonal activities or cultural attitudes. Safe individual behavior may do little to prevent an accident if others are behaving carelessly. Similarly, in many settings safety is a matter of management policy or the social norms of a community.

Second, safe physical environments as well as social environments can be considered in more detail. In addition to failures in the most immediate (proximal) environment, accidents may be caused by failures in the distal environment. The extent of fire damage to a building, for example, is often related to the inaccessibility of firefighting equipment or units. To be complete in specifying safety requirements then, any conceptualization must include characteristics of distal as well as proximal environments.

Third, Gibson's approach appears to account only for perceptual and behavioral failures as it does not specifically address individual characteristics and abilities. Accidents, however, are often caused by structures or equipment whose design does not incorporate the body measurements (anthropometric) of their users, or by the lack of physical or mental ability of an individual to perform the proper activity, as in the case of the elderly.

Fourth, by focusing on the prevention of accidents, Gibson considers only part of the total accident sequence. A more complete analysis might apply Gibson's principles not only to the human (behaviors, abilities, and anthropometrics) and environmental (social and physical, proximal and distal) factors preceding an accident, but also to those factors which contribute to the continuation of the accident and factors which prevent or impair recovery from an accident. By including such factors, safety practitioners can identify the safety requirements for the control of and recovery from accidents, as well as for accident prevention.

Finally, by suggesting that the margin of safety concept is focused on behavior, Gibson precludes many of the factors that originate in the environment. Not only do individuals cause accidents by perceptual failures, behavioral failures, etc., but environments cause accidents by failing to provide proper or adequate information which supports behavior.

The model shown in figure 5.1 incorporates the foregoing factors and provides a schematic illustration of the interactive process. As indicated in the figure, human factors that contribute to accidents may be related to an individual's physical characteristics, abilities, or activities. Physical characteristics include body measurements (anthropometric data) and body structure (mechanical properties); abilities include physical and mental abilities; and activities include perceptual and motor behaviors. Environmental characteristics can originate from either the social or the physical environment. Physical environmental factors are found in either the proximal or distal environments. In particular, guardrails can be considered as physical factors located in the proximal environment, as shown by the shaded elements in figure 5.1.

Table 5.1 summarizes the analysis step of the safety model. In this step, each human and environmental factor is analyzed to identify how they may contribute to an accident. Human factors may contribute to accidents by being defective, inadequate, temporarily incapacitated, or untrained (or underdeveloped). Environmental factors can contribute to accidents by being absent or unreliable. In addition, the safety model reveals that human factors may conflict with environmental factors to cause accidents, as when an elderly individual attempts to climb a set of stairs that are dimly lit or do not have a handrail. In other instances, anthropometric characteristics may conflict with proximal environmental characteristics, as when guardrails with top rails set below the human body centroid height make it physically easier for an individual to fall over them. Also, individual activities may be in conflict with proximal environmental characteristics as in the case of welders working on skyscrapers. The model, then, provides a framework for the qualitative statement of safety requirements. Table 5.2 illustrates how this may be achieved. For example, besides training, developing, educating or selecting abilities, the safety practitioner might accommodate or incorporate the physical characteristics or activities of the user into the design of the environment.

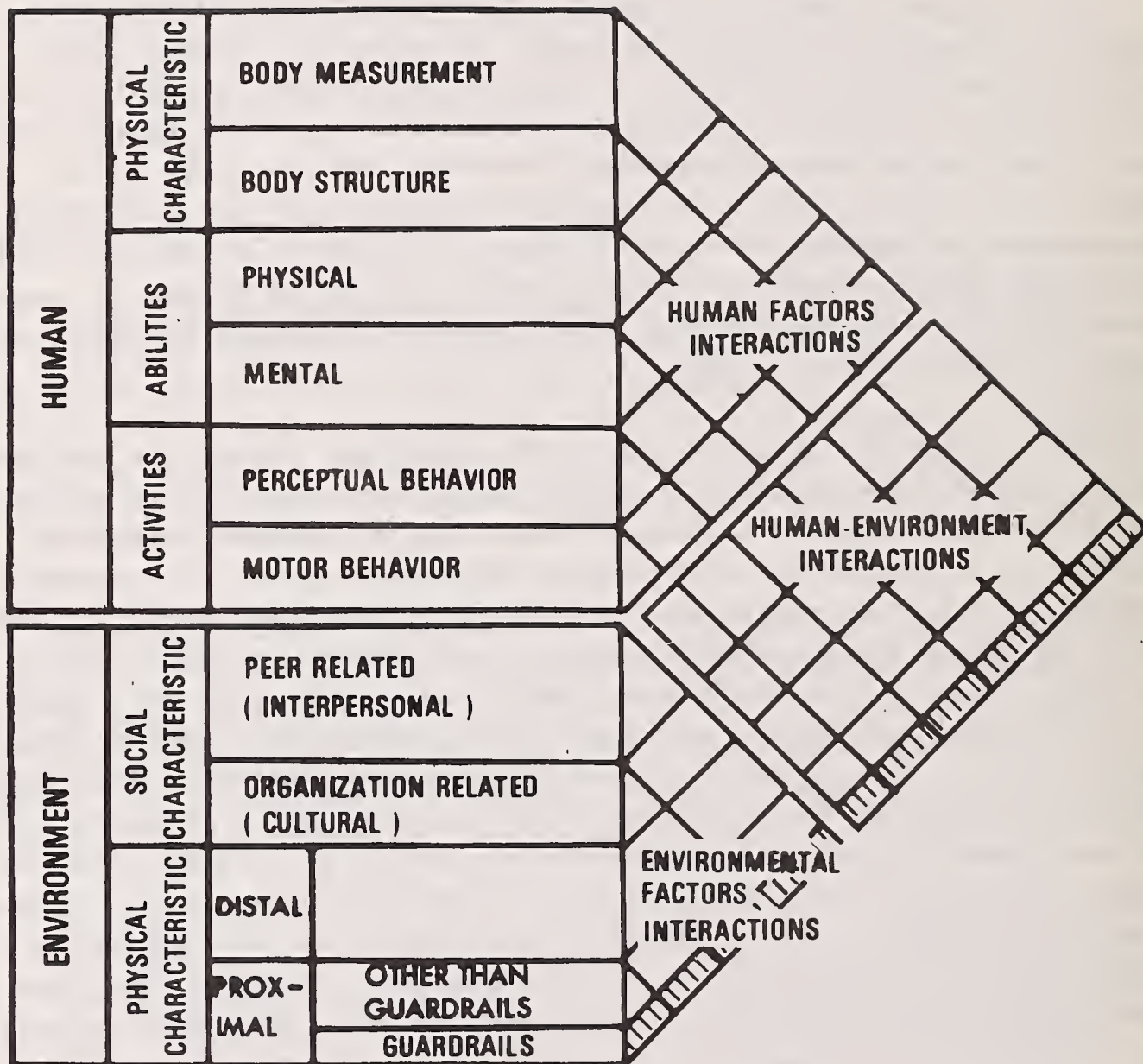


Figure 5.1 The conceptual model of safety.

Table 5.1 Application of the conceptual safety model to safety analysis.

ENVIRONMENTAL FACTORS		HUMAN FACTORS			
		PHYSICAL CHARACTERISTICS	ABILITIES	ACTIVITIES	SOCIAL CHARACTERISTICS
TYPES OF FACTORS	BODY MEASUREMENT	BODY STRUCTURE	PHYSICAL	PERCEPTUAL	PEER OR INTERPERSONAL
			MENTAL	MOTOR	CULTURAL OR SOCIAL
CONDITIONS OF FACTORS		<ol style="list-style-type: none"> 1. DEFECTIVE 2. INADEQUATE 3. TEMPORARILY INCAPACITATED 4. UNTRAINED (UNDERDEVELOPED) 			
		<ol style="list-style-type: none"> 1. ABSENT 2. UNRELIABLE 			

Table 5.2 Performance requirements derived from the safety model.

HUMAN FACTORS				ENVIRONMENTAL FACTORS					
TYPES OF FACTORS	PHYSICAL CHARACTERISTICS		ABILITIES	ACTIVITIES		SOCIAL CHARACTERISTICS	PHYSICAL CHARACTERISTICS		
	BODY MEASUREMENT	BODY STRUCTURE		PHYSICAL	MENTAL		PERCEPTUAL	MOTOR	PROXIMAL
REQUIREMENTS OF FACTORS	1. SELECT	2. ACCOMMODATE	3. INCORPORATE	4. TRAIN	5. DEVELOP	6. EDUCATE	1. PROVIDE	2. MAKE RELIABLE	3. EMPHASIZE

References

- 5.1 Gibson, James J., The Contribution of Experimental Psychology to the Formulation of the Problem of Safety, a Brief for Basic Research, Behaviorial Approaches to Accident Research, Association for the Aid of Crippled Children, New York, New York, 1961.
- 5.2 Johnson, W. G., Sequences in Accident Causation, Journal of Safety Research, National Safety Council, Chicago, Illinois, June 1973.
- 5.3 Surry, Jean, Industrial Accident Research, A Human Engineering Appraisal, Labor Safety Council, Ontario Ministry of Labour, Toronto, Ontario, 1974.

6. An Analysis of Guardrail Accidents

6.1 Introduction

Industrial accident reports are analyzed within a conceptual framework which considers guardrails as units within a safety system (section 5). Included is information on the location of guardrail accidents, the work tasks and activities of the employee at the time of the guardrail accident, the injuries resulting from the guardrail accident, and the sequence of events that led to the guardrail accident. A clear understanding of effective as well as ineffective guardrail performance is important. The analysis of guardrail accidents reported herein attempts to identify activities associated with guardrail misuse or failure.

This section consists of three main sub-sections. The first describes the approach used in the analysis of guardrail accidents in industrial settings based on the conceptual safety model. The second presents an analysis of industrial accident investigations collected from a major source of accident reports: the National Safety Council (NSC). The third section presents a statistical analysis of causes of industrial accidents collected from two sources of industrial accident statistics: the New York Department of Labor and the United States Bureau of Labor Statistics.

6.2 Systems Approach to Guardrail Safety

The interaction between guardrail factors and guardrail user (employee) factors that contribute to guardrail accidents are shown in table 6.1. Each employee/guardrail interaction creates one of four work situations (i.e., accident, incompetence, victimization or emergency) each of which varies in the degree of safety present. Incompetence situations arise from an employee exhibiting unsafe behavior near a safe guardrail, such as sitting or standing on the top rail. An employee working near the edge of an unguarded, elevated surface represents a victimization situation. Accident situations occur "for no apparent reason," that is, when an employee is apparently exhibiting safe behavior near a safe guardrail. Emergency situations occur when an employee is acting carelessly near an unsafe guardrail.

Each work situation suggests guidelines which may rectify the unsafe conditions. These are shown in table 6.2. Incompetence situations suggest the specification of human performance guidelines to promote safe conditions. Victimization situations suggest the specification of design and construction guidelines to promote safe conditions. Emergency situations suggest the adherence to design and construction guidelines previously specified by the incompetent and victimization situations. Accident situations suggest the specification of new or improved design, construction or user performance criteria. In addition, each unsafe situation suggests the need to implement prevention, control, and recovery

Table 6.1 Employee/guardrail interactions and the four levels of safety situations that they create.

HUMAN/ENVIRONMENT INTERACTIONS FOR GUARDRAILS		GUARDRAIL FACTORS	
		Safe guardrail factors	Unsafe guardrail factors
EMPLOYEE ACTIVITIES	Safe employee activities	ACCIDENT SITUATIONS	VICTIMIZATION SITUATIONS
	Unsafe employee activities	INCOMPETENCE SITUATIONS	EMERGENCY SITUATIONS

Table 6.2 Safety guidelines and safety countermeasures suggested by work situations.

WORK SITUATION	SAFETY GUIDELINES	SAFETY COUNTERMEASURES
ACCIDENT SITUATION	New design guidelines New construction guidelines New human performance guidelines	Prevention countermeasures Control countermeasures Recovery countermeasures
INCOMPETENCE SITUATION	Human performance guidelines	
VICTIMIZATION SITUATION	Design guidelines Construction guidelines	
EMERGENCY SITUATION	Adherence to: Design guidelines Construction guidelines Human performance guidelines	

countermeasures. Prevention countermeasures decrease the probability of occurrence of unsafe situations. Control countermeasures either control the unsafe condition or mitigate the severity of the consequences. Recovery countermeasures alleviate the nature, extent, or severity of personal injury or property damage. Table 6.2 indicates that prevention, control and recovery countermeasures all may interact with design, construction, and user performance guidelines.

6.3 Analysis of Guardrail Accident Reports

The National Safety Council (NSC) volunteered 5,467 reports on accidents of various types for analysis. These data were originally collected in 1974 by the NSC for the American Society for Testing and Materials (ASTM) during a project which was focused on identifying areas of need for occupational safety and health standards [6.1, 6.2]. Since the companies were assured that they would remain anonymous, no names will be reported in this review.

The sample represents 80 establishments employing a total of about 40,000 workers in the following eight, industries: automotive, steel, mining, building materials, construction, meat packing and leather, retail, and chemical.

The NSC revision of the OSHA Form 101 titled "Supplementary Record of Occupational Injuries and Illnesses," was used in the project. It combines the standard narrative reporting along with a precoded feature helpful in computer analysis. The narrative statements proved to be most useful in identifying major types of guardrail accidents, and these were analyzed following documented procedures [6.3, 6.4].

The analysis of the accident reports revealed six major types of guardrail-related accidents, (1) guardrail failure, (2) guardrail misuse, (3) guardrail as cause of injury (guardrail absent), (4) walking surface accident (guardrail absent), (5) platform accident (guardrail absent), (6) fall from high elevation. A composite of each accident type is described below. Included in each description is information as to where the accident occurred (Location), the task that the employee was performing at the time of the accident (Task), the activity that the task necessitated (Activity), the injury that resulted from the accident (Injury), and a brief description of the sequence of events of the accident (Sequence of events). Following the third and sixth accident types, guidelines and countermeasures are suggested that might rectify the unsafe situations.

6.3.1 Accident Type #1, Guardrail Failure

Location: Within a specified work area.

Task: Performing specific work tasks.

Activity: Walking, bending, reaching, pulling, pushing, etc.

Injury: Broken bones and concussions.

Sequence of events: Many times objects would fall from one elevation and injure an employee working below. Other times, an employee would trip on debris or a rough or slippery floor surface, fall toward a guarded edge, and over a low guardrail.

User-environment interaction: A common demoninator of these accidents is that they could have been controlled or prevented through safe guardrail design or construction practice. With respect to the above examples, toeboards would prevent objects from sliding under guardrails and higher guardrails would prevent individuals from falling over them. Similarly, individuals would be prevented from falling through guardrail openings if the space between the rails was minimized. Since the employees appear to exhibit safe behavior in these instances, the accidents may be mostly attributed to unsafe guardrail factors and as such would fall under "victimization" work situations (table 6.1). It was noted, however, that with respect to other accident types, these accidents seemed to occur somewhat less frequently.

6.3.2 Accident Type #2, Guardrail Misuse

Location: On the job, in the plant or work area.

Task: Operating equipment or handling materials.

Activity: Reaching, climbing, or jumping.

Injury: Sprained ankle, leg, arm or back.

Sequence of events: Employee misuses guardrail to climb upon, or over, and often to circumvent a more time consuming or difficult action. As a result, the guardrail fails to protect the employee from a hazardous area or dangerous fall.

User-environment interaction: This type of accident represents an "Incompetence" situation in which the user of the guardrail does not exhibit safe behavior (see table 6.1). The only difference between this type and Accident Type #1 is that the guardrail structure does not fail under misuse, although, they both involve static forces applied by the employee.

6.3.3 Accident Type #3, Guardrails as Causes of Injury

Location: On the job, in the plant or work area.

Task: Operating or servicing equipment.

Activity: Walking from one location to another in a work area while performing task.

Injury: Bruise or fracture of leg, arm, or hand.

Sequence of events: Employee often falls upon or impacts against the guardrail. The cause of the fall is often not related to the guardrail; however, the guardrail is usually the cause of the injury. In some cases, proper placement of the guardrail could have averted the accident.

User-environment interaction: Since guardrail factors are safe and the employee usually exhibits safe behavior, this accident type is categorized as an "accident" situation (table 6.1).

6.3.4 Suggested Guidelines and Countermeasures for Unsafe Situations in Which Guardrails Were Present but Were Either Misused or Caused Injury

Accident types #2 and #3 could have been mitigated had the employees not misused the guardrails and if the guardrails were designed properly. Improved design, construction and behavioral guidelines, though, could better control the accident situation and to some extent even the incompetence situation. First, guardrails may be designed and constructed to withstand a limited amount of misuse. Studies by Kromer (see Section 3.5) identified maximum forces that an individual can exert against a guardrail-type barrier. These accident data provide some support for using push-force information in designing and constructing guardrails that are strong enough to withstand forces exerted by employees using them as supports. A second set of guidelines might focus on dynamic forces that falling people could transmit to guardrails. Furthermore, many accident situations indicate that guardrails which are more noticeable than others are less likely to cause injury. These accident data suggest countermeasures that would make guardrails more noticeable and less likely to be bumped into or fallen upon. Such measures might involve new construction materials as well as height or placement guidelines. Finally, type #1 accident situations could be controlled and/or prevented by guardrail designs which complement employee activities.

6.3.5 Accident Type #4, Guardrail Absent: Walking Surface

Location: In the plant but not on the job. Often in a public area or hallway.

Task: Employee is usually not performing a work task at the time of the accident.

Activity: Walking or standing.

Injury: Bruise or strained back or leg. Lacerations of the hand, leg or arm are also common.

Sequence of events: Employee slips or trips and falls on walking surface while walking from point A to point B on company property. Common accident agents are slippery floors, holes or cracks in the sidewalk, protruding equipment or stock. In many instances the victim does not fall but strains himself while restoring his balance. Other times, the employee hits his head on overhanging equipment or cuts his hand or leg on protruding stock or machinery.

User-environment interaction: This type of accident can be categorized as a "victimization" situation since the employee is exhibiting safe behavior in the environment but an unsafe guardrail factor (unguarded area) causes the accident (table 6.1).

6.3.6 Accident Type #5, Guardrail Absent: Fall from an elevation

Location: On the job, in the plant or work area.

Task: Maintenance and materials handling.

Activity: Walking, standing, climbing, or reaching.

Injury: Back and head injuries.

Sequence of events: Employee is often working around an unguarded area, loses his balance and falls from one elevation to another. He is often performing a maintenance task of some kind in which he subjects himself to some degree of risk.

User-environment interaction: Due to the absence of guardrails, the environment must be considered unsafe in most cases. As long as the employee is not engaged in reckless behavior the unsafe situation can be considered one of "victimization."

6.3.7 Accident Type #6, Guardrails Absent: Platforms

Location: On the job, in the plant or work area.

Task: A variety of job tasks ranging from operating equipment and hand tools, to clerical work in an office or stock area.

Activity: These accidents predominantly occur while the employee is stepping down, stepping off or stepping onto a raised platform of some sort.

Injury: Twisted ankles or knees.

Sequence of events: Employee twists his/her ankle while stepping off an unguarded platform.

User-environment interaction: Inasmuch as a guardrail, properly placed, might have prevented the individual from leaving or entering the platform at the hazardous area (an area on which a twist is more likely than not), this situation is categorized as "victimization." Obviously, this does not apply to cases in which the platform was merely a stool or a bench. This categorization does apply to low platforms where guardrails would designate safe areas to enter or exit.

6.3.8 Suggested Guidelines and Countermeasures From Unsafe Situations in Which Guardrails Were Absent and Employees Were Injured as a Result of Falls on Walking Surfaces, From Platforms, or From One Elevation to Another

All the accident types relevant to the guardrail-related falls reported above represent "victimization" situations in which the lack of guardrails led to an injury. This implies that the presence of guardrails might have prevented the fall or at least controlled it well enough to minimize injury. Guidelines for the proper placement of guardrails might prevent death resulting from a fall into an open pit as well as a twisted ankle resulting from a fall off a low platform. These data emphasize that the placement and function, as well as the design and construction of guardrails, are components in a complex building safety system in which guardrails contribute to the prevention and control of accidents.

6.4 Statistical Analysis of Guardrail Accidents

6.4.1 New York Department of Labor Data

The predominance of guardrail-related falls revealed in the accident analysis suggested that an assessment of fall-related accidents in industry might identify those industries most affected by the lack of guardrails or inadequate guardrails. The New York report, "Characteristics and costs of work injuries in New York State, 1966-70" was obtained from the New York State Department of Labor and was analyzed with respect to work-surface accidents [6.5] involving scaffolds and stagings, platforms and ramps, and roofs, since the previous accident analysis suggested that these might be guardrail-related settings. Data from the thirteen industries with the highest percentages of injuries from guardrail-related, work-surface falls to a different elevation are summarized in table 6.3. Also shown for each industry are the total number of injuries, total number of injuries due to unsafe work-surface, the total number of injuries involving falls to a different elevation, and the amount of compensation for injuries involving falls to a different elevation (Rows 7-10).

It is of importance to note in table 6.3 that at least 13 of the industries in New York State had injury rates of 48% or greater for injuries involving falls to a different elevation due to unsafe work-surfaces and that the total compensation for just fall injuries in these industries was over 50.8 million dollars.

Table 6.3

A Summary of Information from New York State
Workman's Compensation Claims for 13 Industries

INJURIES	INDUSTRY	Painting & Decorating	Roofing & Sheet Metal Work	Carpentry & Wood Flooring	Special Trade Contractors	General Building Contractors	Structural Steel Erection	Electrical Contracting	Masonry & Stone Work	Plumbing, Heating and Air Conditioning	Concrete Work	Retail Trade: Building Materials	Retail Trade: Building Materials	Misc. Repair Services	Heavy Construction (Non-Highway)
% of all injuries due to unsafe work-surfaces		48	33	31	32	30	33	31	30	24	28	18	15	17	
% of work-surface injuries due to scaffolds & staging platforms & ramps, & roofs.		26	43	29	35	30	20	12	41	12	22	15	8	16	
% of work-surface injuries due to scaffolds & staging, platforms & ramps, & roofs involving falls to a different elevation.		96	88	91	87	90	86	84	88	84	90	82	79	85	
% of all injuries involving falls to a different elevation.		38	27	22	23	20	22	20	19	14	16	15	1	12	
% of falls to a different elevation due to unsafe work-surfaces		78	76	68	66	60	59	57	57	54	49	48	48	48	
% of falls to a different elevation due to scaffolds & staging, platforms & ramps, & roofs		31	46	38	43	40	26	16	57	18	35	16	11	20	
# all injuries		5,722	2,520	2,661	2,040	16,970	2,127	2,758	3,016	7,008	3,007	1,955	2,749	4,797	
# work-surface injuries		1,204	827	832	660	5,051	1,438	898	898	1,686	847	343	408	837	
# of falls to a different elevation		866	673	585	475	3,385	460	891	569	1,098	480	288	232	585	
Amount of Compensation for fall injuries \$K		5,722.9	3,818	2,257	2,240	17,118.5	3,460.7	2,788.5	2,630	3,075.5	2,947	1,003	561.7	3,202.5	

In these industries injuries due to unsafe work-surfaces ranged from 15% to 48% and injuries involving falls to a different elevation ranged from 1% to 38% of the total. A significant portion of work-surface injuries (8%-43%) were due to scaffolds and stagings, platforms, and ramps, or roofs (i.e., guardrail-related). Of these guardrail-related, work-surface injuries, 79%-96% involved falls to a different elevation. Although a good portion, 4%-21%, of the guardrail-related, work-surface injuries did not involve falls to a different elevation, these data suggest that proper placement and construction of guardrails on scaffolds and stagings might have prevented or controlled many of those injuries that did. Similarly 48%-78% of injuries involving falls to a different elevation were due to unsafe work-surfaces and of these 11%-57% were due to scaffolds and stagings, platforms and ramps, or roofs. Since many injuries (at least 43%) involved falls to a different elevation that were not due to scaffolds and stagings, platforms and ramps, or roofs, there remains a sizeable number of accidents from falls that might have been prevented or controlled through the proper placement of guardrails.

To summarize these results, about 25% of work-surface accidents seem to be guardrail-related with 87% of these involving falls to a different level. About 60% of the injuries involving falls to a different level are due to unsafe work-surfaces and at least 30% of these seem to be guardrail-related. One conclusion that is suggested by these data is that most guardrail-related accidents involve inadequate protection from falls to a different elevation, and thus, guardrails might most effectively prevent and control accidents through proper placement, design and construction.

6.4.2 Bureau of Labor Statistics Data

The analysis of industrial accidents suggested that placement and function of guardrails were of critical importance to their effectiveness in preventing and controlling falls in industrial settings. A statistical analysis of industrial accidents was conducted to find evidence to further support or reject this implication. Data were obtained from sixteen independent reports on work injuries and accident causes gathered by the Bureau of Labor Statistics for different intervals during 1941-1966 [6.6 to 6.21]. Industries represented are listed below:

Water-Supply Utilities

School Lunchrooms

Fabrication of Structural Steel and Architectural Metalwork

Concrete Brick and Block

Hotel

Hospital

Longshore

Shipyards

Textile Dyeing and Finishing

Clay Construction Products

Plumbing Operations
Carpentry Operations
Paperboard Containers
Warehousing Operations
Boilershop Products

Data from selected industries regarding work injuries due to inadequate guarding and/or lack of guardrails are summarized in tables 6.4 thru 6.6. Work injury frequencies were converted to percentages of all work injuries to allow across-industry comparisons. Weighted mean percentages were calculated from frequencies and percentages as general indicators of trends. Conclusions as to the relative importance of one major category (column) to another should be made with caution since no tests of significant differences have been performed. There is little reason to believe, however, that when large differences are evident, they do not represent "real" differences in trends and can therefore serve as general, though rough, indicators. Weighted mean percentages of the data suggest that injuries due to improperly guarded agencies occur with moderate frequency in relation to those injuries due to other hazardous conditions. Also, the category "inadequate guarding" may include machine mechanism guards as well as guardrails and should be interpreted in that light. Finally, industries that were "selected" for each table, were selected solely on the basis of availability of data.

Table 6.4 This table shows work injuries due to lack of guardrails and inadequate guarding (includes machine-mechanism guards) by type of accidents for selected industries. Although a variety of accident types are indicated with respect to inadequate guarding, only falls are consistently important with respect to lack of guardrails. Also indicated is a preponderance of falls to a different level.

Table 6.5 This table identifies various activities recorded previous to accidents due to inadequate guarding and lack of guardrails. Consistent weighted mean percentages indicate manual handling, walking and using hand tools as most common. The high average for operating power equipment under "inadequate guarding" is inconsistent with the low average under "lack of guardrails" and is therefore probably due to inadequate machine guards as opposed to a lack of guardrails.

Table 6.6 This table specifies the causes of guardrail-related accidents. Inconsistencies in magnitude and direction of weighted mean percentages suggest that most accidents due to the lack of guardrails involve machines or work surfaces.

The accident analysis of Bureau of Labor Statistics data suggests that when guardrails are absent work injuries occur from falls to a different level onto work surfaces or machinery while the employee is walking. Falls through or over guardrails (guardrail failures) are not indicated as a significant cause of work injuries due to inadequate

Table 6.4

Work injuries due to the lack of guardrails and inadequate guarding by type of accident for selected industries. (ref. 6.6 - 6.21)

INDUSTRY	TOTAL # (%)	STRIKING AGAINST # (%)	STRUCK BY			FALLS			CAUGHT IN, OR BETWEEN # (%)	TEMPERATURE EXTREMES # (%)	ABSORPTION # (%)	OTHER # (%)
			Total # (%)	Falling Objects #	Thrown Objects #	Total # (%)	To a different level #	On the same level #				
Lack of guardrails												
Carpentry operations	382 (4)	--	10 (3)	--	--	365 (96)	347	18	--	--	7 (1)	
Clay construction products	65 (1.1)	1 (2)	2 (3)	--	--	52 (80)	46	6	4 (6)	--	6 (9)	
Concrete brick & block	10 (1)	--	--	--	--	10 (100)	10	--	--	--	0 (0)	
Weighted mean %	(3.52)	(2)	(3)			(94.15)			(0)		(4.7)	
Inadequate Guarding												
Carpentry operations	1350 (14.9)	480 (35.5)	19 (25)	56	56	485 (36)	464	21	21 (1.5)	7 (1)	17 (1)	
Clay construction products	388 (6.8)	43 (11)	47 (25)	25	25	64 (16)	55	9	142 (37)	9 (2)	18 (5)	
Concrete brick & block	119 (10)	7 (6)	5 (18)	16	16	12 (10)	10	2	64 (54)	4 (3)	9 (7)	
Plumbing operations	162 (5.9)	3 (3)	38 (23)	2	2	70 (43)	67	3	36 (22)	--	9 (5)	
Structural steel & metalwork	214 (14.8)	16 (7)	129 (60)	11	11	26 (12)	24	2	29 (14)	--	14 (7)	
Paperboard containers	356 (24.4)	50 (14)	22 (6)	6	6	25 (7)	23	2	251 (70)	--	3 (1)	
Water-supply utilities	196 (11.4)	2 (1)	98 (50)	9	9	41 (21)	32	9	34 (17)	--	6 (3)	
Boiler shop products	294 (14.6)	39 (13)	119 (40)	29	29	37 (13)	32	5	80 (28)	--	5 (1)	
Hotels	129 (33)	90 (69)	6 (5)	--	--	7 (5)	7	--	6 (5)	--	3 (3)	
School lunchrooms	140 (7.8)	93 (67)	35 (25)	--	--	6 (4)	5	1	6 (4)	--	0 --	
Weighted mean percentages	(13.38)	(38.06)	(33.83)			(30.4)			(45.41)		(1.85)	(4.14)
									(6.84)			

Table 6.5

Work injuries due to the lack of guardrails or inadequate guarding by activity for selected industries. (ref. 6.6 - 6.21)

Industry	Total # (%)	Materials Handling # (%)	Using Handtools # (%)	Operating Power Equipment # (%)	Walking # (%)	Standing # (%)	Climbing # (%)	Stepping # (%)	Running # (%)	Other # (%)
<u>Lack of Guardrails</u>										
Concrete brick & block	10 (.8)	7 (70)	1 (10)	--	--	--	--	--	--	2 (20)
Water-supply utilities	55 (3.2)	8 (14.5)	19 (34.5)	2 (4)	20 (36)	2 (4)	4 (7)	--	--	
Carpentry operations	382 (4.2)	39 (10)	35 (9)	4 (1)	30 (8)	--	2 (1)	5 (1)	4 (1)	263 (69)
Structural steel & metalwork	24 (1.7)	2 (8)	3 (12)	1 (5)	11 (46)	--	--	--	--	7 (29)
Hospitals	438 (1.4)	385 (87)	43 (10)	--	--	--	--	--	--	10 (3)
WEIGHTED MEAN PERCENTAGES	(2.68)	(78.2)	(14.32)	(2.14)	(24)	(4)	(5)	(5)	(5)	(65.32)
<u>Inadequate guarding</u>										
Concrete brick & block	119 (10)	17 (14)	23 (19)	52 (44)	--	--	--	--	--	27 (23)
Water-supply utilities	196 (11.4)	45 (23)	91 (46)	16 (8)	23 (12)	15 (8)	5 (2.5)	--	--	1 (.5)
Carpentry operations	1350 (14.9)	51 (4)	56 (4)	807 (60)	35 (2.5)	--	22 (1.5)	8 (.5)	8 (.5)	363 (27)
Structural steel & metalwork	214 (14.8)	12 (6)	33 (15)	118 (55)	--	--	--	--	--	51 (24)
Boilershop products	294 (14.6)	44 (15)	59 (20)	125 (42.5)	25 (8.5)	--	--	--	--	41 (13)
Hotels	129 (3.3)	2 (1)	14 (11)	87 (67)	3 (3)	--	--	--	--	23 (18)
Hospitals	766 (2.5)	533 (70)	49 (6)	--	--	--	--	--	--	184 (24)
Plumbing operations	79 (3.9)	19 (24)	16 (20.5)	--	20 (25.5)	--	--	--	--	24 (30)
School lunchrooms	140 (7.8)	10 (7)	15 (11)	103 (73.5)	--	--	--	--	--	12 (8.5)
WEIGHTED MEAN PERCENTAGES	(10.57)	(54.63)	(20.96)	(58.13)	(10.33)	(8)	(1.69)	(.5)	(.5)	(24.56)

Table 6.6

Work injuries due to the lack of guardrails and inadequate guarding by agency of accidents for selected industries.
(ref. 6.6 - 6.21)

INDUSTRY	Total Cases # (%)	Stock & Materials # (%)	Handtools # (%)	Machines # (%)	Work Assemblies # (%)	Working Surfaces # (%)	Vehicles # (%)	Other # (%)
LACK OF GUARDRAILS								
Structural steel & metal	24 (1.7)	-- (--)	-- (--)	1 (1)	-- (--)	12 (50)	6 (25)	5 (21)
Carpentry operations	382 (4.2)	-- (--)	-- (--)	-- (--)	-- (--)	333 (87)	-- (--)	49 (13)
Concrete brick & block	10 (0.8)	-- (--)	-- (--)	1 (10)	-- (--)	4 (40)	5 (50)	0 (0)
Paperboard containers	29 (2.0)	-- (--)	-- (--)	4 (14)	-- (--)	17 (59)	1 (3)	7 (24)
Clay construction products	65 (1.1)	-- (--)	-- (--)	3 (5)	1 (2)	31 (48)	-- (--)	30 (46)
Water-supply utilities	27 (1.5)	-- (--)	4 (15)	7 (26)	-- (--)	-- (--)	2 (7)	14 (52)
Warehousing operations	59 (4.4)	13 (22)	-- (--)	1 (2)	4 (6)	19 (32)	11 (19)	11 (19)
Hospitals	438 (1.4)	-- (--)	-- (--)	397 (91)	-- (--)	3 (.5)	3 (.5)	35 (8)
WEIGHTED MEAN PERCENTAGES	(2.6)	(22)	(15)	(87.89)	(5.2)	(78)	(14.37)	(23.32)
INADEQUATE GUARDING								
Structural steel & metal	214 (14.8)	27 (13)	16 (7)	60 (28)	11 (5)	13 (6)	13 (6)	74 (35)
Concrete brick & block	119 (10)	-- (--)	6 (5)	62 (52)	15 (13)	4 (3)	26 (22)	6 (5)
Carpentry operations	1350 (14.9)	-- (--)	379 (28)	446 (33)	-- (--)	333 (25)	-- (--)	192 (14)
Paperboard containers	356 (24.4)	-- (--)	-- (--)	296 (83)	-- (--)	18 (5)	10 (3)	32 (9)
Clay construction products	388 (6.8)	21 (6)	19 (5)	148 (38)	32 (8)	38 (10)	47 (12)	83 (21)
Water-supply utilities	196 (11.4)	-- (--)	20 (10)	14 (7)	-- (--)	82 (42)	13 (7)	67 (34)
Warehousing	165 (12.4)	13 (8)	8 (5)	32 (19)	15 (9)	29 (17)	36 (22)	32 (20)
Hospitals	766 (2.5)	-- (--)	-- (--)	512 (67)	-- (--)	3 (1)	49 (6)	202 (26)
Boilershop products	294 (14.6)	2 (1.5)	41 (14)	110 (37)	2 (1.5)	15 (5)	2 (1.5)	122 (41)
Plumbing operations	162 (6.0)	-- (--)	3 (1)	-- (--)	-- (--)	43 (27)	-- (--)	116 (72)
Shipyards	106 (16.2)	-- (--)	-- (--)	5 (5)	-- (--)	70 (66)	1 (1)	30 (28)
Textile dyeing & finishing	711 (9.6)	166 (23)	10 (1)	419 (59)	-- (--)	29 (5)	1 (0)	86 (12)
Hotels	129 (3.3)	-- (--)	-- (--)	91 (70)	-- (--)	7 (6)	-- (--)	31 (24)
School lunchrooms	140 (7.8)	-- (--)	-- (--)	127 (90)	-- (--)	5 (4)	-- (--)	8 (6)
WEIGHTED MEAN PERCENTAGES	(11.25)	(19.22)	(23.26)	(56.6)	(8.95)	(27.41)	(12.25)	(29.16)

guarding. This would imply that placement of guardrails is at least just as significant a factor in preventing or controlling accidents as guardrail design.

6.5 Conclusions

The results of the accident analysis suggest that guardrail accidents could be better prevented and controlled by the proper placement of guardrails, by making guardrails more noticeable, and by determining guardrail design criteria with respect to how guardrails are used and who uses them. Many of the accidents resulting from structural inadequacies of guardrails can be prevented by determining guardrail strength criteria with respect to guardrail use. Similarly, accidents resulting from non-structural inadequacies could be prevented through proper height, size of openings and placement of guardrails and by environmental cues to alert an employee to the presence of a hazardous area sooner and thereby decrease the severity of the guardrail accident.

References

- 6.1 Kelley, Doug, Joint NCS/ASTM Project Points Way to More Effective Standards Development, National Safety News, National Safety Council, Chicago, Illinois, 1975.
- 6.2 Kelley, Doug, A New National Safety Council Member Service...Computerized OSHA Reporting and Analysis Service, National Safety News, National Safety Council, Chicago, Illinois, 1974.
- 6.3 Festinger, L. and D. Katz, Research Methods in the Behavioral Sciences, Holt, Rinehart and Winston, New York, New York, 1966.
- 6.4 Selltitz, C., Johoda, M., Deutsch, H., and Cook, S. Research Methods in Social Relations, Holt, Rinehart, and Winston, New York, New York, 1959.
- 6.5 Characteristics and Costs of Work Injuries in New York State, Special Bulletin No. 243, New York State Department of Labor, New York, New York, December 1972.
- 6.6 Injuries and Accident Causes in Water-Supply Utilities, BLS Report No. 166., Bureau of Labor Statistics, Washington, D.C., 1953.
- 6.7 Injuries and Accident Causes in the Fabrication of Structural Steel and Architectural Metalwork, BLS Report No. 266., Bureau of Labor Statistics, Washington, D.C., 1962.
- 6.8 Work Injuries and Accident Causes in School Lunchrooms, BLS Report No. 316., Bureau of Labor Statistics, Washington, D.C., 1967.
- 6.9 Work Injuries and Accident Causes in the Concrete Brick and Block Industry, BLS Report No. 317., Bureau of Labor Statistics, Washington, D.C., 1967.
- 6.10 Work Injuries and Accident Causes in Hotels, BLS Report No. 329., Bureau of Labor Statistics, Washington, D.C., 1967.
- 6.11 Work Injuries and Accident Causes in Hospitals, BLS Report No. 341., Bureau of Labor Statistics, Washington, D.C., 1968.
- 6.12 Injuries and Accident Causes in the Longshore Industry, 1942, Bulletin No. 764., Bureau of Labor Statistics, Washington, D.C., 1944.

- 6.13 Fatal Work Injuries in Shipyards 1943 and 1944, Bulletin No. 839., Bureau of Labor Statistics, Washington, D.C., 1945.
- 6.14 Injuries and Accident Causes in Textile Dyeing and Finishing, Bulletin No. 962., Bureau of Labor Statistics, Washington, D.C., 1949.
- 6.15 Injuries and Accident Causes in the Manufacture of Clay Construction Products, Bulletin No. 1023., Bureau of Labor Statistics, Washington, D.C., 1951.
- 6.16 Injuries and Accident Causes in Plumbing Operations, Bulletin No. 1079., Bureau No. 1079., Bureau of Labor Statistics, Washington, D.C., 1952.
- 6.17 Injuries and Accident Causes in Carpentry Operations, Bulletin No. 1118., Bureau of Labor Statistics, Washington, D.C., 1953.
- 6.18 Injuries and Accident Causes in the Manufacture of Paperboard Containers, Bulletin No. 1139., Bureau of Labor Statistics, Washington, D.C., 1953.
- 6.19 Injuries and Accident Causes in Warehousing Operations, Bulletin No. 1174., Bureau of Labor Statistics, Washington, D.C., 1955.
- 6.20 Injuries and Accident Causes in the Boilershop-Products Industry, Bulletin No. 1237., Bureau of Labor Statistics, Washington, D.C., 1958.
- 6.21 Shipyard Injuries and Their Causes, 1941, Bulletin No. 722., Bureau of Labor Statistics, Washington, D.C., 1943.

7. Summary

This report presents results of the phase one study at the National Bureau of Standards consisting of existing information compiled in order to assist in determining structural and non-structural safety requirements for personnel guardrails. The literature search and study of existing guardrail design provisions revealed a general lack of consistency between load, height and strength requirements, and a paucity of quantitative test data and analysis procedures upon which such requirements could be based. The anthropometric data indicate those body measurements which might be significant to human-guardrail interaction. This is of value not only in determining non-structural requirements such as minimum guardrail openings, toeboard heights, etc., but also in establishing the range of guardrail sizes over which load testing should be planned for the phase two effort to follow. The field survey provided a valuable perspective by showing the broad range of usage of guardrails in service, while the analysis of guardrail-related accidents revealed that the placement of the guardrail may be as significant a factor in accident prevention as the actual design of the guardrail.

It is apparent from this study that a lack of knowledge of realistic service loads is a major obstacle to the ability to develop rational guardrail design criteria. In addition, a quantitative description of the relations between certain anthropometric data and guardrail measurements remains obscure. Accordingly, the phase two effort will consist of an experimental-analytical program which will seek to measure, among other things, static and dynamic loads on guardrails resulting from simulated accident situations. On the basis of the above information, phase two will conclude with a performance-oriented guide and criteria for the design and evaluation of personnel guardrails.

8. Acknowledgements

The contributions made by Drs. Robert A. Crist and Bruce R. Ellingwood in critically reviewing this report are gratefully acknowledged.

The authors also express their appreciation to the many organizations which made available their records and facilitated field observations of guardrails in service to provide the necessary information for this report.

U.S. DEPT. OF COMM. BIBLIOGRAPHIC DATA SHEET		1. PUBLICATION OR REPORT NO. NBSIR 76-1132	2. Gov't Accession No.	3. Recipient's Accession No.
4. TITLE AND SUBTITLE Personnel Guardrails for the Prevention of Occupational Accidents			5. Publication Date November 1976	6. Performing Organization Code
7. AUTHOR(S) S. G. Fattal, L.E. Cattaneo, G.E. Turner, S. N. Robinson			8. Performing Organ. Report No.	
9. PERFORMING ORGANIZATION NAME AND ADDRESS NATIONAL BUREAU OF STANDARDS DEPARTMENT OF COMMERCE WASHINGTON, D.C. 20234			10. Project/Task/Work Unit No. 4612471	11. Contract/Grant No.
12. Sponsoring Organization Name and Complete Address (Street, City, State, ZIP) Occupational Safety and Health Administration Department of Labor Washington, D. C. 20210			13. Type of Report & Period Covered Final Report	14. Sponsoring Agency Code
15. SUPPLEMENTARY NOTES				
16. ABSTRACT (A 200-word or less factual summary of most significant information. If document includes a significant bibliography or literature survey, mention it here.) Existing information is compiled which would assist in determining structural and non-structural safety requirements for guardrails used for the protection of employees against occupational hazards. Critical aspects of guardrail safety are identified through exploratory studies consisting of field surveys of prototypical installations, reviews of existing standards and industrial accident records, and compilation of relevant anthropometric data. These exploratory studies will be utilized to design an experimental program which will consist of structural tests to determine design loads and non-structural tests to determine geometric requirements for guardrail safety.				
17. KEY WORDS (six to twelve entries; alphabetical order; capitalize only the first letter of the first key word unless a proper name; separated by semicolons) Anthropometric measurements; guardrails; industrial accidents; non-structural safety; occupational hazards; performance standard; personnel railings; personnel safety; structural safety.				
18. AVAILABILITY <input checked="" type="checkbox"/> Unlimited <input type="checkbox"/> For Official Distribution. Do Not Release to NTIS <input type="checkbox"/> Order From Sup. of Doc., U.S. Government Printing Office Washington, D.C. 20402, SD Cat. No. C13 <input checked="" type="checkbox"/> Order From National Technical Information Service (NTIS) Springfield, Virginia 22151		19. SECURITY CLASS (THIS REPORT) UNCLASSIFIED	21. NO. OF PAGES 79	
		20. SECURITY CLASS (THIS PAGE) UNCLASSIFIED	22. Price \$5.00	

